

Fluid Transients in Systems



E.B. Wylie , V.L. Streeter

ematics)--Mathematical models.
mathematical models. 3. Pumping
Mathematical models. I. Streeter,
III. Tide.

91-40426
CIP

UMPHREY
n and
DeLORENZO
NICO
RENS
DICKEY
WORKIN

fall, Inc.
ation Company
ver, NJ 07458

this book may be
any means,
rom the publisher.

is book have used their best efforts in preparing this book. These efforts include the
ing of the theories and programs to determine their effectiveness. The authors and
any kind, expressed or implied, with regard to these programs or the documentation
hors and publisher shall not be liable in any event for incidental or consequential damages
ut of, the furnishing, performance, or use of these programs.

America

934423-3

UK) Limited, London
y, Limited, Sydney
ronto
ana, S.A., Mexico
e Limited, New Delhi
kyo
Ltd., Singapore
al, Ltd., Rio de Janeiro



KNJIŽNICA UL FGG

J 532
WYLIE E. B.
Fluid



020140560

COBISS ©

UNIVERZA V LJUBLJANI

ISBN 0-19-934423-3



Contents

PREFACE NOMENCLATURE

1 FLUID TRANSIENT FLOW CONCEPTS

- 1-1 Classification of Flow: Definitions 1
- 1-2 Arithmetic Derivation of Transient Flow Equation 2
- 1-3 Effects of Air Entrainment 9
- 1-4 The Cause of Transients: Role of Valving 11
- 1-5 Column Separation: Gas Release 12
- 1-6 Methods of Analysis 13
- 1-7 Scope and Range of Problems in Unsteady Flow 16

2 BASIC DIFFERENTIAL EQUATIONS FOR TRANSIENT FLOW

- 2-1 Equation of Motion 20
- 2-2 Continuity Equation 23
- 2-3 Wave Propagation Velocities 26
- 2-4 Forms of the Equations for Special Purposes 31
- 2-5 The Continuity Equation for Highly Deformable Tubes 33

ix
xi

1

20

iii

3 SOLUTION BY CHARACTERISTICS METHOD	37		
3-1 Characteristics Equations	37	6-9 Dynamic Check Valve	133
3-2 Finite Difference Equations	39	6-10 Controllers	136
3-3 Basic Boundary Conditions	42	6-11 Adjacent Nonpipe Elements in Systems	137
3-4 Single-pipeline Applications	46		
3-5 Series, Branches, and Other System Facilities	50		
3-6 General Systems	56		
3-7 High Friction, Attenuation, and Frequency Dependence	61		
3-8 Localized Column Separation	66		
3-9 Algebraic Method	69		
4 THE COMPLETE EQUATIONS	80		
4-1 Nonsimplified Equations	80		
4-2 The Method of Characteristics	81		
4-3 Steady-State Solution	84		
4-4 The Numerical Method: Interpolations	84		
4-5 The Characteristics Grid	91		
5 OTHER METHODS OF SOLUTION	95		
5-1 Rigid Water Column Theory	95		
5-2 Graphical Method	98		
5-3 Implicit Method	105		
5-4 Finite Element Method	109		
6 COMPLEX SYSTEMS WITH MULTPIPE AND NONPIPE ELEMENTS	113		
6-1 Wave Transmission and Reflection	113		
6-2 Infinite Pipeline	121		
6-3 Lumped Elements	122		
6-4 Air Chamber or Accumulator	125		
6-5 Other Surge Devices	127		
6-6 Cooling-Water Condenser	129		
6-7 Air-Inlet Valve	130		
6-8 Spring-Mass Systems	132		
		7 TRANSIENTS CAUSED BY TURBOMACHINES	143
		PUMPS AND PUMPING SYSTEMS	143
		7-1 Sequence of Events During Power Failure	144
		7-2 Dimensionless-Homologous Turbopump Characteristics	144
		7-3 Head Balance and Speed-Change Equations	149
		7-4 Pumping Station with Single Pump	151
		7-5 Pumping Station with Multiple Pumps	154
		7-6 Considerations in Analysis of Pumping Systems	159
		7-7 Pump Startup	161
		GOVERNED TURBINES	162
		7-8 Turbine and Governor Equations	162
		7-9 Transients in Governor-Turbine-Hydraulic System	164
		7-10 Stability	169
		8 TWO-COMPONENT AND SINGLE-COMPONENT TWO-PHASE TRANSIENT FLOWS	177
		8-1 Liquid-Gas Mixtures in an Elastic Pipe	178
		8-2 Discrete Free-Gas Cavity Model	184
		8-3 Two-Component Two-Phase Experimental Comparisons	188
		8-4 Column Separation in Liquids with No Free Gas; Isolated Cavities	192
		8-5 Mechanics of Distributed Vaporization	196
		8-6 Additional Vaporization Examples	204
		8-7 Air Trapped in Piping Systems	208
		9 VALVE STROKING	215
		9-1 Initiating and Stopping Flow in Systems	216
		9-2 Frictionless Valve Stroking for a Single Pipe	219

9-3	Control of Single Pipeline in Specified Time	222	13 ANALYSIS OF OSCILLATORY FLOW IN SYSTEMS	317
9-4	Control with Pressure Constraint	228	FREQUENCY RESPONSE ANALYSIS	317
9-5	Systems with Control Elements Other than Valves	232	13-1 Applications of Impedance to Hydraulic Systems	317
9-6	Series, Branching, and Parallel Systems	234	13-2 Additional Hydraulic Elements	322
9-7	Experimental Comparisons	238	13-3 Applications of Transfer Matrix Method	325
9-8	Valve Stroking Applied to Pump Failures	241	13-4 Multiforcing Functions and Nonharmonic Forcing Functions	332
10 METHODS FOR CONTROLLING TRANSIENTS		246	13-5 Impulse Response Method	334
10-1	Wavespeed Reduction Methods	247	13-6 Reciprocating Pumps	343
10-2	Air Chamber or Accumulator	247	FREE VIBRATION ANALYSIS	348
10-3	Surge tanks	249	13-7 Analysis of Complex Systems	349
10-4	Check Valves	252	13-8 Discussion of Mode Shapes and System Frequencies	356
10-5	Flow-Control Methods and Valving	255		
10-6	System Geometrical Design Changes	257		
11 MULTIELEMENT SYSTEMS AND TRANSMISSION LINES		260	14 NATURAL GAS PIPE TRANSIENTS	363
11-1	Steady-State Flows in Systems	260	14-1 Equation of State	364
11-2	Schematization of Complex Systems	261	14-2 Equation of Continuity	364
11-3	Simplified Treatment of Adjacent Nonpipe Elements	265	14-3 Equation of Motion	365
11-4	Transmission Pipelines	267	14-4 Steady-State Equations	366
11-5	Flying Switching in Long Oil Pipelines	271	14-5 Method of Characteristics Solution	367
11-6	System Simulation for Operation, Control, and Leak Detection	273	14-6 Evaluation of Inertial Multiplier α	370
12 CONCEPTS OF OSCILLATORY FLOW AND RESONANCE		287	14-7 Boundary Conditions: Compressors, Valves, and Storage Fields	372
12-1	Introduction	287	14-8 Computer Program for Gas Flow	373
12-2	Unsteady Flow Equations for Use in Linear Methods	289	14-9 Other Examples	375
12-3	Impedance Method and Transfer Matrix Method	293		
12-4	Frequency Response Analysis	296		
12-5	Free-Vibration Analysis	298		
12-6	Consideration of Frequency-Dependent Factors	303		
12-7	Resonance	305		
15 OPEN-CHANNEL TRANSIENT FLOW			15 OPEN-CHANNEL TRANSIENT FLOW	380
15-1	Differential Equations for Unsteady Open-Channel Flow	380	15-1 Differential Equations for Unsteady Open-Channel Flow	380
15-2	Solution by Method of Characteristics	382	15-2 Solution by Method of Characteristics	382
15-3	Solution by Implicit Method	388	15-3 Solution by Implicit Method	388
15-4	Gate Stroking to Control Unsteady Channel Flow	392	15-4 Gate Stroking to Control Unsteady Channel Flow	392
16 SPECIAL TOPICS			16 SPECIAL TOPICS	400
16-1	Nonprismatic Sections and Distributed Lateral Flows	400	16-1 Nonprismatic Sections and Distributed Lateral Flows	400

16-2	Application of the Characteristics Method in Soil Dynamics	403
16-3	The Energy Equation	410
16-4	Fuel Injection Systems	414
16-5	Two- and Three-Dimensional Fluid Transients	419

APPENDIX A SI AND ENGLISH CONVERSIONS AND CONSTANTS

431

APPENDIX B PROPERTIES OF MATERIALS

432

APPENDIX C DISCHARGE COEFFICIENTS FOR VALVES

434

APPENDIX D REFERENCE COMPUTER PROGRAMS

435

INDEXES

- Author Index 457
- Subject Index 457

Preface

Three books have been published on this topic by the authors prior to this title: *Hydraulic Transients*, McGraw-Hill Book Co., New York, 1967, *Fluid Transients*, McGraw-Hill Book Co., New York, 1978, and *Fluid Transients*, FEB Press, Ann Arbor, Michigan, 1982. Significant changes were incorporated in the second version over the first, minor corrections in the third, and now a serious revision to bring the material to the current state of the art. Professor Streeter's role in this latest manuscript is less than previously, but his presence will forever be felt whenever anyone addresses this topic. It is my belief that his singularly unique and thoughtful contributions to this specialized science exceed the originality of all the rest of us combined. The addition of Dr. Lisheng Suo on the title page of this version is evidence of his assistance in its production, and of the mutual respect developed during his years at Michigan. His contributions appear mostly in Chapters 12 and 13, but his influence may be noted in a number of other locations.

The book, devoted primarily to unsteady confined fluid flow, presents methods for analyzing a broad range of fluid transient conditions, and for the design of facilities to cope with problems that may develop. Emphasis is placed on numerical methods, but not at the expense of fundamental understanding, the former just being a means with which to handle complicated systems. Fundamental concepts are developed and emphasized throughout. The method of characteristics is the solution procedure of choice for analysis and design of systems, and it appears in almost every chapter. Frequency-domain studies are recommended for special problems. Other methods are included for the sake of completeness, including the graphical approach, which is recommended for visualization and understanding. Examples and problems to aid in gaining a better understanding of the material are included where

appropriate, and comparisons with experimental results from laboratory and prototype conditions are shown where available.

The coverage is intended for practicing engineers and for use in academic instruction. The contents provide the primary source of material for a two-semester course sequence in transient flow at the University of Michigan, and the material has been a basic part of an annual continuing engineering education course offered at a number of locations over an extended time period.

As in earlier editions, the contributions of the many investigators in this field have been incorporated and acknowledged to the best of our knowledge. We apologize if we have failed to appropriately recognize individual contributors. It is unwise to mention individual names, as some will be missed, but clearly those who have been associated with the University of Michigan as graduate students, primarily in fluid transients, have left an indelible mark on the field. These include Chintu Lai, D. N. Contractor, R. A. Baltzer, D. C. Wiggert, W. Zielke, T. P. Propson, M. A. Stoner, J. L. Caves, M. E. Weyler, W. Yow, B. Petry, M. F. El-Erian, C. N. Papadakis, C. P. Liou, R. Henke, D. A. Goldberg, A. R. Simpson, and L. Suo. Their contributions are evident throughout.

E. B. Wylie

Nomenclature

A	Area of pipe
A_e	Equivalent area
A_G	Area of opening of a valve
A_m	Amplitude of the m th harmonic
A_n, A_P	Nozzle area; area of piston in reciprocating pump
A_S	Area of surge tank
A_T	Penstock area; total area
A_{TH}	Minimum surge tank area
a, a_e	Speed of pressure pulse; equivalent wavespeed
a', a_s	Wavespeed with free gas; speed of shock front
a_n	Dimensionless nozzle area
a_1, a_2	Constants to describe pump head-discharge curve
B	Width of rectangular section; width of open channel bottom
B	Isothermal wavespeed
B	Allievi constant, $aV_0/(gH_0)$, or pipeline characteristic impedance, a/gA
B'	Dimensionless Allievi constant
B_M, B_P	Known constants in compatibility equations
C	Pipeline capacitance = gA/a^2
C^+, C^-	Name of characteristic equations
C_D, C_d	Orifice discharge coefficient
C_K	Proportionality factor
C_M, C_P	Known constants in compatibility equations
C_M, C_T	Constant in Manning formula; constant in turbomachine torque equation

C_v	Number of piston displacement volumes; specific heat at constant volume	K	Minor loss coefficient; bulk modulus of elasticity
C_v	Valve coefficient	K'	Combined modulus of elasticity of fluid and container
c	Wavespeed in open channel; isentropic wavespeed	K_s, K_p	Equivalent bulk modulus; proportional control constant
c	Loss coefficient for simple surge tank	K_s, K_h	Spring constant; heat transfer coefficient
c_p, c_1	Specific heat at constant density; dimensionless parameter that describes the effect of pipe constraint condition on the wavespeed	k	Entrance loss coefficient; dimensionless head in turbine stability
D	Subscript for downstream end of pipe; depth of rectangular section	k	Ratio of specific heats
D	Pipe diameter; characteristic dimension of turbomachine	L	Pipe length; pipeline inertance = $1/gA$
E	Energy; modulus of elasticity; collection of variables in energy equation	L_{cav}	Length of cavity
E_m	Exponent of τ -equation	L_1, L_2	Identification of continuity and momentum equation in characteristics method
E_R	Modulus of rigidity of rock or concrete	l	Pipe length
e	Pipe wall thickness	M	Number of harmonics used in an harmonic analysis to describe a periodic motion; number of pumps in parallel pump system; mass
F	Pressure wave traveling in the $-x$ direction in the pipe; linearized resistance factor; Coulomb frictional force	M	Slope of head-discharge curve; mass rate of flow of gas
F	Transfer matrix	MOC	Method of characteristics
f	Pressure wave traveling in the $+x$ direction in the pipe	m	Mass; integer identifying a particular harmonic in a Fourier series; thickness of confining soil layer; exponent of diameter in friction term; isothermal Mach number
f	Darcy–Weisbach friction factor	\dot{m}	Rate of mass of gas released
f, f_s	Frequency in hertz	N	Rotational speed in rpm; number of reaches in pipeline for computation
G	Shear modulus of elasticity	N_R	Rated speed of turbomachine
g	Gravitational acceleration	N_S	Specific speed
gpm	Gallons per minute	N_w	Number of wells
H, H_n	Instantaneous piezometric head; nodal head	$NPSH$	Net positive suction head
\bar{H}	Average or mean pressure head	n	Number of free vibration mode; number of reaches in pipeline
H_a, H_A	Absolute pressure head	n	Exponent of the velocity in the turbulent friction term
H_b, \bar{H}	Barometric head	n	Manning's roughness coefficient; porosity of soil; polytropic exponent
H_p	Piezometric head at unknown computational point in xt plane of characteristics grid	P	Integer in algebraic waterhammer, $P \Delta t = L/a$
H_R	Rated pressure head of turbomachine; reservoir head	P	Solution point in xt plane
H_{sub}	Complex number for instantaneous head at point denoted by subscript	P	Power produced by a turbine; shaft power supplied to pump; wetted perimeter
H_v	Vapor pressure head	\mathbf{P}	Point transfer matrix
H_0	Steady-state or mean pressure head; head drop at a valve	P_G, P_R	Power absorbed by the generator; rated power output of turbine
$H(x)$	Non-time-varying complex number for pressure head	P_k	Packing rate in leak detection
HP	Horsepower	p	Pressure
h	Dimensionless pressure head, H/H_0 or H/H_R ; dimensionless distance	p^*	Choke pressure; absolute pressure
h	Specific enthalpy	\underline{Q}	Instantaneous discharge at a section
h'	Instantaneous oscillatory pressure head	\overline{Q}	Average discharge at a section
h_a	Atmospheric pressure in length units of fluid flowing (abs.)	Q_e	Flow at node in nonpipe element
h_m	Dimensionless maximum pressure head, H_{\max}/H_0	Q_H	Heat added to control volume/unit time
h_v	Vapor pressure in length unit of fluid flowing (abs.)	Q_m, Q_p	Nodal volumetric inflow; pipeline flow at node
I	Polar moment of inertia of rotating parts, WR_g^2/g ; index number	Q_R, Q_B	Rated discharge of turbomachine; flow balance in leak detection
i	Denotes section number along a pipe; $\sqrt{-1}$	Q_{sub}	Complex number for discharge at point denoted by subscript
J	Subscript denoting a particular pipe in a complex system	Q_1	Unit discharge of turbomachine, $Q/(D^2H^{1/2})$
J	Subscript in algebraic waterhammer to refer to time, $t = J \Delta t$		

$Q(x)$	Non-time-varying complex number for discharge	V, V_m	Instantaneous velocity; liquid-gas mix velocity
q	Heat added per unit mass/unit time; $(\mu_y + v_s)/2$ in two-dimensional flow	V_B	Flow balance in leak detection = $Q_B - P_K$
q'	Distributed outflow/unit length; dimensionless flow for turbine stability	V_c	Velocity at point of lowest pressure in pump suction system
R	Instantaneous oscillatory discharge; fluctuations from the average	V_p	Velocity at unknown computational point in xt plane of characteristics solution
R	Hydraulic radius A/P ; parameter in nonlinear soil equation; gas constant	V_T	Velocity entering the penstock at surge tank
R_g	Resistance coefficient; crank radius on reciprocating pump	V_0	Initial fluid velocity; steady state or mean velocity
Re	Radius of gyration	V'	Volume
r	Real part of complex number	V_g'	Volume of gas reduced to standard conditions
r_{sub}	Pipe radius; radial distance	v	Dimensionless velocity, V/V_0 or Q/Q_R ; velocity component in y direction
r_0	Response function	v_i	Phase velocity in soil dynamics
S	Pipe radius corresponding to initial conditions	v_{01}, v_{02}	Initial (final) steady-state dimensionless velocity
S	Connecting rod length; slope of hydraulic grade line	W_a, W_H	Dimensionless turbomachine characteristics
S_K	Solubility coefficient	WR_g^2/g	Polar moment of inertia of rotating parts
SI	Spring constant	w	Velocity component in z direction
s	International metric system	X	Solution of second-order differential equation, function of x only
T	Complex-valued frequency, $s = \sigma + i\omega$; pipeline slope parameter	x, x_1	Distance along pipe from upstream end, from downstream end $x_1 = L - x$
T	Theoretical period of pipe, $4L/a$; tensile force in tube wall; period of surge tank system	x	As a subscript denotes partial differentiation
T	Particular solution (harmonic oscillation) of second-order differential equation	x	Displacement from fully extended position of piston; angular position in pump characteristic curve
T	Instantaneous torque on turbine or pump; absolute temperature	x'	Displacement from fully extended position of piston on discharge stroke
T	Top width of prismatic section	Y	Displacement of main servomotor in turbine governor
T_b	Beat period	y	Difference in elevation between reservoir and surge tank surface
T_d	Dashpot time constant in turbine governor; derivative control time	y	Depth of flow in open channel; dimensionless wicket gate position
T_e	Time constant for nonpipe element	Z_C	Characteristic impedance
T_e, T_f	Torque due to external force; torque due to bearing friction	Z_{sub}	Hydraulic impedance at a point denoted by the subscript
T_f	Period corresponding to the forcing frequency	$Z, Z(x)$	Hydraulic impedance, complex ratio of head fluctuation to discharge fluctuation
T_g	Time of valve closure corresponding to maximum servo velocity	z	Elevation of pipe above datum; depth of soil in vertical direction
T_m	Mechanical starting time of turbine; period of the m th harmonic, $T_m = 2\pi/m\omega$	z	Gas compressibility factor
T_M, T_n	Motor torque; net torque applied to the turbine	α	Void fraction
T_P, T_W	Torque due to hydrodynamic pressure; torque due to weight of rotating disk	α	Angular position of connecting rod in reciprocating pump
T_R	Rated torque of turbomachine; integral control constant	α	Pipe or channel slope; parameter in nonlinear soil equation
T_w, T_P	Hydraulic inertia time; penstock time constant	α	Dimensionless speed ratio, ω/ω_0 or N/N_R
T_a	Promptitude time constant, ratio of change in speed deviation to change in relative servo velocity	α	Inertia multiplier in natural gas flow
t	Time; as a subscript denotes partial differentiation	β	Change of tube diameter per unit length
t'	Dimensionless time, $t/(2L/a)$	β	Dimensionless torque ratio, T/T_0 or T/T_R
t_e, t_w	Time of operation of a valve; pipeline startup time	β	Slope of characteristic line on hv plane, $\tan^{-1}(aV_0/gH_0)$
U	Subscript for upstream end of pipe	$\Gamma(s)$	Complex-valued frequency dependent value of γ_{yx}
U	Overall transfer matrix	γ	Complex number called the propagation constant
u	Soil particle displacement in x direction; velocity component in x direction	γ	Unit weight of fluid; shearing strain, $\partial u / \partial z$
		δ	Amplitude of oscillatory motion of valve

δ	Turbine temporary speed droop
ε	Complex number of representing small change in s ; $\Delta\varepsilon = \Delta\sigma + i\Delta\omega$
ϵ	Unit strain in tube wall
ζ	Inertial factor
η	Turbine or pump efficiency
Θ	Threshold volume in leak detection
θ	Characteristics grid mesh ratio, $\Delta t/\Delta x$
θ	Angular position of crank on suction stroke, or of swing-check valve; pipeline slope
θ_0	Angular displacement when check valve opens in reciprocating pump
λ	Multiplier in characteristics method; wavelength; eigenvalue
μ	Dimensionless gate position for turbine stability
μ	Poisson's ratio; absolute or dynamic viscosity; coefficient of viscosity
ν	Kinematic viscosity
ξ	Unit lateral strain; dimensionless head for turbine stability
ξ_t	Total lateral or circumferential unit strain
ξ_1	Unit longitudinal strain or axial unit strain
ξ_2	Unit lateral strain
ρ	Mass density
ρ_e, ρ_m	Liquid mass density; liquid-gas mix density
σ	Real part of complex valued frequency; dimensionless friction term
σ	Unit stress in tube wall; turbine permanent speed droop
σ_1, σ_2	Axial unit stress; lateral unit stress
τ, τ_m	Shearing stress; maximum shearing stress
τ, τ_i, τ_f	Dimensionless number describing the discharge coefficient times area of opening at a valve, $(C_{DA})/(C_{DA})_0$; initial and final position of valve
τ_0	Dimensionless number describing the valve position corresponding to mean flow conditions; wall shear stress
φ	Dimensionless speed in turbine stability
ϕ	Angular position of crank on discharge stroke; phase angle; dimensionless resistance parameter
ϕ	Speed factor of turbomachine, $DN/(1838H^{1/2})$
ϕ	Exponential attenuation factor
ϕ_0	Angular position of crank at which pumping starts
ϕ_q	Phase angle of the complex impedance
ψ	Dimensionless pressure error; weighing factor in implicit method and in integration
ψ	Factor indicating portion of x momentum leaving laterally; permissible variation in wavespeed; reflection coefficient parameter
ω	Angular or circular frequency; angular velocity
ω'	Angular velocity of crank shaft
ω^*	Dimensionless frequency
ω_f	Angular frequency at which a system is being forced
ω_n	Natural frequency of resonator

Fluid Transient Flow Concepts

There are a number of examples of benefits derived from useful applications of unsteady flow, such as in pulsatile flow in arteries or in the temporary storage of energy in pressurized natural gas systems. However, there are many more examples of the destructive character of the phenomenon. For whatever motivation the subject of unsteady flow of liquids, which began in the middle of the nineteenth century, has expanded to other fluids, and has continued at an accelerated pace particularly after the mid-twentieth century.^{5,41} Well-developed concepts based on fundamental fluid mechanics are available for analysis of transient fluid flow in piping systems. However, since visualization is important, in this chapter we introduce material in a simplified form. Terms are defined and arithmetic expressions that relate flow and pressure pulses are developed. The concept of propagation of pulses at sonic velocity through a single pipeline is presented, including reflections at simple terminations. Causes of transients, the effect of air entrainment, and the conditions leading to column separation are discussed briefly, as well as some of the methods of analysis.

1-1 Classification of Flow: Definitions

In *steady flow* there is no change in conditions at a point with time. In *unsteady flow*, conditions at a point may change with time. Steady flow is a special case of unsteady flow that the unsteady flow equations must satisfy. In *uniform flow* the average velocity at any cross section is the same at any instant; in *nonuniform flow* the velocity varies along the conduit at any given instant. The terms *waterhammer* and *transient flow* are used synonymously to describe unsteady flow of fluids in pipelines, although use of the

former is customarily restricted to water. *Steady-oscillatory*, or *periodic*, or *pulsatile* flow occurs when the flow conditions are repeated identically in every fixed time interval, called the period of the oscillation. The *free vibration* of fluid in a piping system refers to oscillatory flow at one of the natural periods of the system. The term *surge* refers to those unsteady flow situations that can be analyzed by considering the fluid to be incompressible and conduit walls rigid.

Resonance in a piping system is an oscillatory phenomenon in which the amplitude of the unsteady oscillations builds up with time until failure occurs or until a steady-oscillatory flow of unusually large magnitude is reached. Resonance usually occurs at or near one of the natural periods, either the fundamental or a harmonic, of a system.

The term *valve stroking* is restricted in its meaning to the design of boundary conditions such that a transient occurs in a prescribed manner. *Liquid column separation* refers to the situation in a pipeline in which gas and (or) vapor collects at some section.

1-2 Arithmetic Derivation of Transient Flow Equation

The unsteady momentum and continuity equations are first applied to a control volume containing a section of pipe. An overall conservation of mass equation is then developed for the fluid in the pipeline. To better aid in visualization of transient behavior in the pipe, restrictive conditions are imposed; more general derivations are presented in Chapter 2.

The case of instantaneous stoppage of flow at a downstream valve is first described, then the continuity and momentum equations are applied to an incremental change in valve setting. In Fig. 1-1a friction and minor effects are neglected. The instant the valve is closed, the fluid immediately adjacent to it is brought from V_0 to rest by the impulse of the higher pressure developed at the face of the valve. As soon as the first layer is brought to rest, the same action is applied to the next layer of fluid bringing it to rest. In this manner, a pulse wave of high pressure is visualized as traveling upstream at some sonic wavespeed a and at a sufficient pressure to apply just the impulse to the fluid to bring it to rest.

The momentum equation is applied to a control volume, Fig. 1-1b, within which the wavefront is moving to the left with an absolute speed of $a - V_0$ due to a small change in valve setting. The pressure change Δp at the valve is accompanied by a velocity change ΔV . The momentum equation for the x direction states that the resultant x component of force on the control volume is just equal to the time rate of increase of x momentum within the control volume plus the net efflux of x momentum from the control volume. The volume of fluid having its momentum changed is $A(a - V_0)\Delta t$, so the time rate of increase of linear momentum is

$$\frac{A(a - V_0)\Delta t}{\Delta t}[(\rho + \Delta\rho)(V_0 + \Delta V) - \rho V_0]$$

The momentum equation yields

$$-\Delta pA = A(a - V_0)[(\rho + \Delta\rho)(V_0 + \Delta V) - \rho V_0] + (\rho + \Delta\rho)A(V_0 + \Delta V)^2 - \rho AV_0^2$$

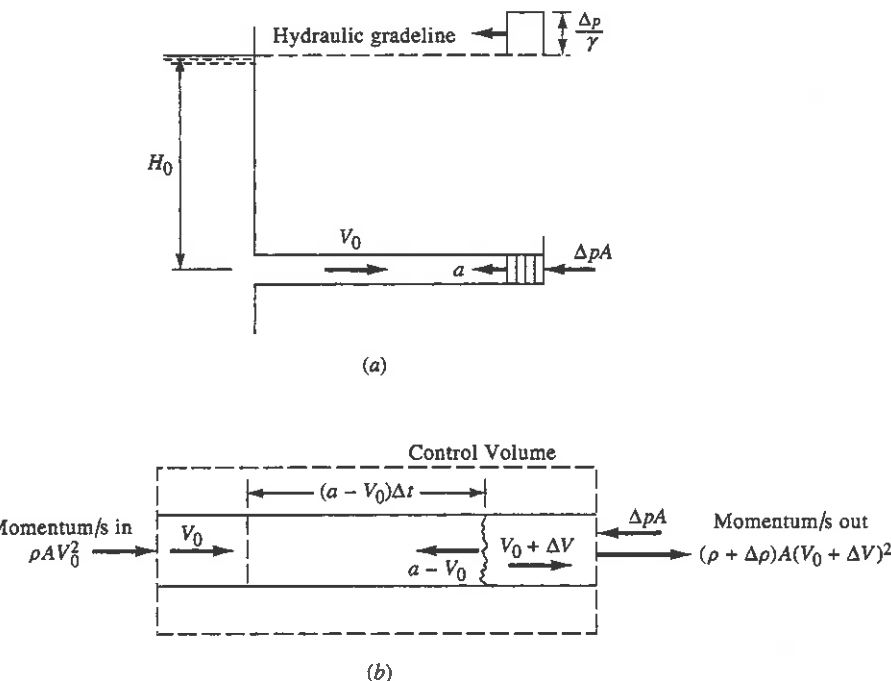


Figure 1-1 (a) Instantaneous stoppage of frictionless liquid in horizontal pipe; (b) momentum equation applied to control volume.

where

- ρ = mass density of fluid
- $\Delta\rho$ = incremental density change
- g = acceleration of gravity
- γ = specific weight of fluid = ρg
- Δp = increment of pressure change
- A = cross-sectional area of pipe
- V_0 = initial velocity
- ΔV = increment of flow velocity
- a = unknown wavespeed

Conservation of mass in the control volume states that at any instant the net mass influx equals the time rate of increase of mass within the control volume. Since the same volume of fluid $A(a - V_0)\Delta t$ is having its density changed, the equation is

$$\rho AV_0 - (\rho + \Delta\rho)A(V_0 + \Delta V) = \frac{A(a - V_0)\Delta t[(\rho + \Delta\rho) - \rho]}{\Delta t}$$

When simplified and combined with the momentum equation, the following basic equation results

$$\Delta p = -\rho a \Delta V \quad (1-1a)$$

Since $\Delta p = \rho g \Delta H$, in which ΔH is the head change,

$$\Delta H = -\frac{a \Delta V}{g} \quad (1-1b)$$

If the flow is stopped completely $\Delta V = -V_0$ and $\Delta H = a V_0 / g$. Equations (1-1) also show that for an increase in velocity at the gate the head there must be reduced. If the valve is on the downstream end of a long pipe and is closed by increments, the equations become

$$\sum \Delta p = -\rho a \sum \Delta V \quad (1-2a)$$

$$\sum \Delta H = -\frac{a}{g} \sum \Delta V \quad (1-2b)$$

which hold for any movements of the valve as long as the pressure pulse wave has not reached the upstream end of the pipe and returned as a reflected wave (i.e., as long as the time is less than $2L/a$, with L the pipe length).

For adjustments in an upstream gate, a similar derivation shows that $\Delta p = \rho a \Delta V$, so

$$\sum \Delta p = \pm \rho a \Delta V \quad (1-3a)$$

$$\sum \Delta H = \pm \frac{a}{g} \sum \Delta V \quad (1-3b)$$

describe the change in flow related to a change in pressure. The minus sign must be used for waves traveling upstream and the plus sign for waves traveling downstream. It is the *basic equation of waterhammer* and always holds in the absence of reflections. Equation (1-3b) is generally attributed to Joukowski,¹⁵ although the literature shows Menabrea²⁰ to have made calculations with the equation.

The magnitude of the wavespeed a has not been determined. Application of the continuity equation yields enough information so that, together with Eq. (1-2), the numerical value of a can be calculated. With reference to Fig. 1-2, if the gate at the downstream end of the pipe is suddenly closed, the pipe may stretch in length Δs , depending on how it is supported. We may assume that the gate moves this distance in L/a seconds,

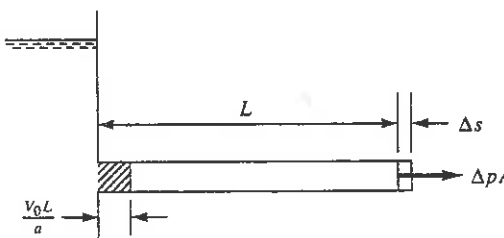


Figure 1-2 Continuity relations in pipe.

or has the velocity $\Delta s a / L$. Hence the velocity of fluid at the gate has been changed by $\Delta V = \Delta s a / L - V_0$. During L/a seconds after gate closure the mass entering the pipe is $\rho A V_0 L / a$, which is accommodated within the pipe by increasing its cross-sectional area, by filling the extra volume due to pipe extension Δs , and by compressing the liquid due to its higher pressure, or

$$\rho A V_0 \frac{L}{a} = \rho L \Delta A + \rho A \Delta s + L A \Delta \rho \quad (1-4)$$

By use of $\Delta V = \Delta s a / L - V_0$ in eliminating V_0 , Eq. (1-4) simplifies to

$$-\frac{\Delta V}{a} = \frac{\Delta A}{A} + \frac{\Delta \rho}{\rho}$$

Now by use of Eq. (1-1a) to eliminate ΔV ,

$$a^2 = \frac{\Delta p / \rho}{\Delta A / A + \Delta \rho / \rho} \quad (1-5)$$

If the pipe is supported so that it cannot extend, then $\Delta s = 0$ and the same Eq. (1-5) is obtained, with or without expansion joints. By bringing in the bulk modulus of elasticity K of the fluid, defined by

$$K = \frac{\Delta p}{\Delta \rho / \rho} = -\frac{\Delta p}{\Delta V / V} \quad (1-6)$$

with $\Delta V / V$ the fractional volume change, Eq. (1-5) may be rearranged to yield

$$a^2 = \frac{K / \rho}{1 + (K / A)(\Delta A / A \Delta p)} \quad (1-7)$$

For very thick-walled pipe $\Delta A / \Delta p$ is very small, and $a \approx \sqrt{K / \rho}$ is the acoustic speed of a small disturbance in an infinite fluid. For very flexible pipe walls, the 1 in the denominator is small and becomes unimportant, so that

$$a \approx \sqrt{\frac{A \Delta p}{\rho \Delta A}} \quad (1-8)$$

The evaluation of the wavespeed in a typical transmission conduit requires knowledge of the fluid bulk modulus and density, and the evaluation of the conduit elasticity as expressed by $\Delta A / \Delta p A$ in Eq.(1-7). A number of different examples are evaluated in Chap. 2. As an illustration a thin-walled pipeline is examined (Fig. 1-3). The change in pipe wall tensile stress, $\Delta \sigma$, is given by

$$\Delta \sigma = \frac{\Delta T_f}{e} = \frac{\Delta p D}{2e} \quad (1-9)$$

in which e is the pipe wall thickness and T_f the circumferential tensile force per unit length of pipe. When Eq. (1-9) is divided by Young's modulus of elasticity for the wall material, E , the change in circumferential unit strain, is obtained. The radial extension is obtained by multiplying by the radius $D/2$, which, when multiplied by

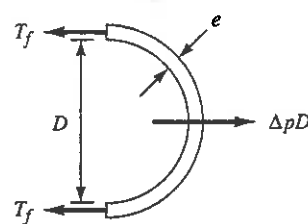


Figure 1-3 Forces on semicylinder of pipe due to waterhammer.

the perimeter πD , yields the change in cross-sectional area as a result of the pressure change: $\Delta A = \Delta p \pi D^3 / (4eE)$. After dividing through by A and Δp , we have

$$\frac{\Delta A}{A \Delta p} = \frac{D}{Ee} \quad (1-10)$$

which, when substituted into Eq. (1-7), yields an equation that may be evaluated for a specific thin-walled pipeline.

$$a = \sqrt{\frac{K/\rho}{1 + (K/E)(D/e)}} \quad (1-11)$$

Small amounts of entrained gas in the liquid, or gas that has come out of solution, greatly modify the acoustic speed in a pipe. After the pressure has been reduced in a pipeline, say by a pump slowdown or stoppage upstream, some gas usually comes out of solution, which reduces the acoustic speed during the transient. The wavespeed does not fully recover its former high value rapidly under higher-pressure conditions. The effect of free air or other gases is discussed in the next section.

For water at ordinary temperatures $\sqrt{K/\rho} = 1440$ m/s. Wavespeeds for large thin-walled steel pipelines may be as low as 1000 m/s, whereas speeds in high-pressure small pipes may be 1200 to 1400 m/s.

With the wavespeed determined by Eq. (1-11), Eqs. (1-3) yield a known relation between change in velocity and change in pressure or head. These equations are of great value in visualizing unsteady flow. For example, with a/g of 100 s, a reduction of 1 m/s velocity creates an immediate head change of 100 m.

The complete cycle, or period, that results from an instantaneous valve closure in a frictionless case is described next.

At the instant of valve closure ($t = 0$) the fluid nearest the valve is compressed, brought to rest, and the pipe wall stretched (Fig. 1-4). As soon as the first layer is compressed, the process is repeated for the next layer. The fluid upstream from the valve continues to move downstream with undiminished speed until successive layers have been compressed back to the source. The high pressure moves upstream as a wave, bringing the fluid to rest as it passes, compressing it, and expanding the pipe. When the wave reaches the upstream end of the pipe ($t = L/a$ seconds), all the fluid is under the extra head H , all the momentum has been lost, and all the kinetic energy has been converted into elastic energy.

There is an unbalanced condition at the upstream (reservoir) end at the instant of arrival of the pressure wave, since the reservoir pressure is unchanged. The fluid

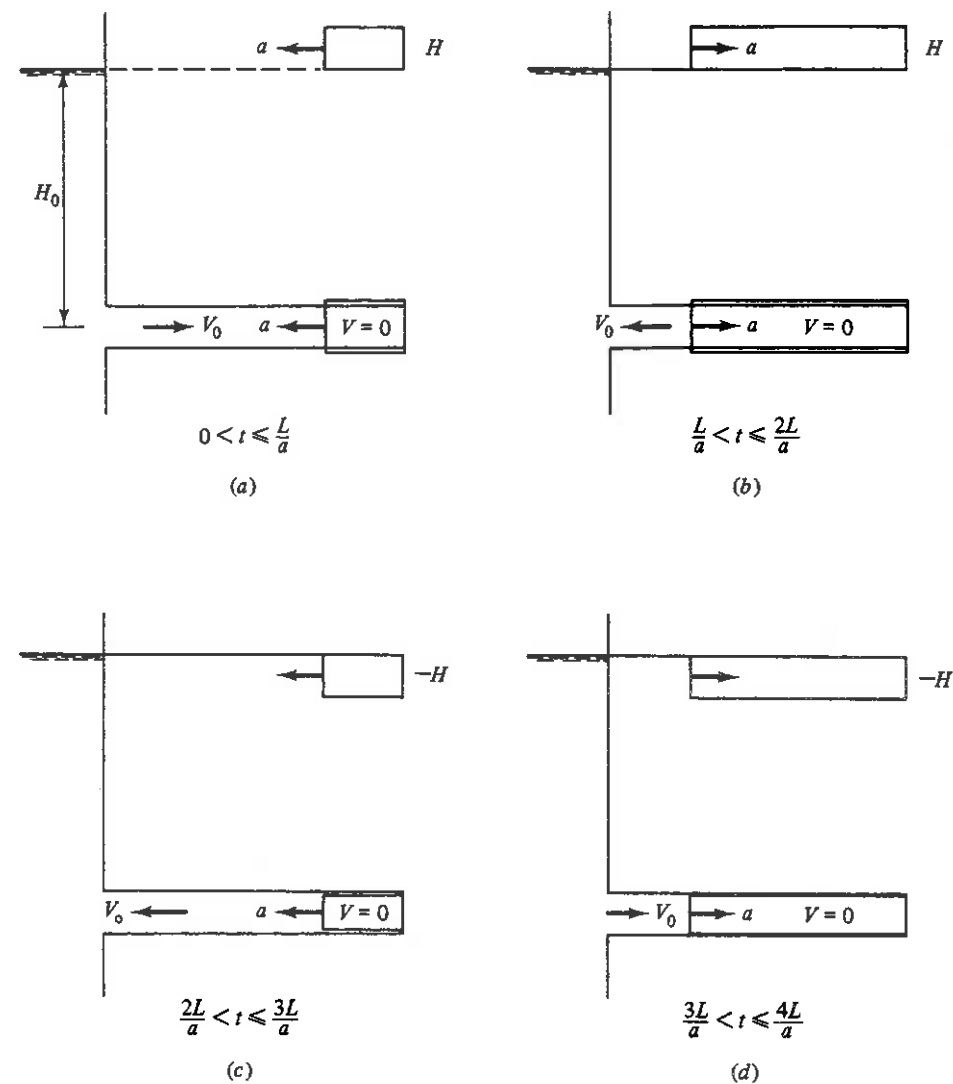


Figure 1-4 Sequence of events for one period after sudden closure of a valve.

starts to flow backward (Fig. 1-4b), beginning at the upstream end. This flow returns the pressure to the value that was normal before closure, the pipe wall returns to normal, and the fluid has a velocity V_0 in the backward sense. This process of conversion travels downstream toward the valve at the speed of sound a in the pipe. At the instant $2L/a$, the wave arrives at the valve, pressures are back to normal along the pipe, and velocity is everywhere V_0 in the backward direction.

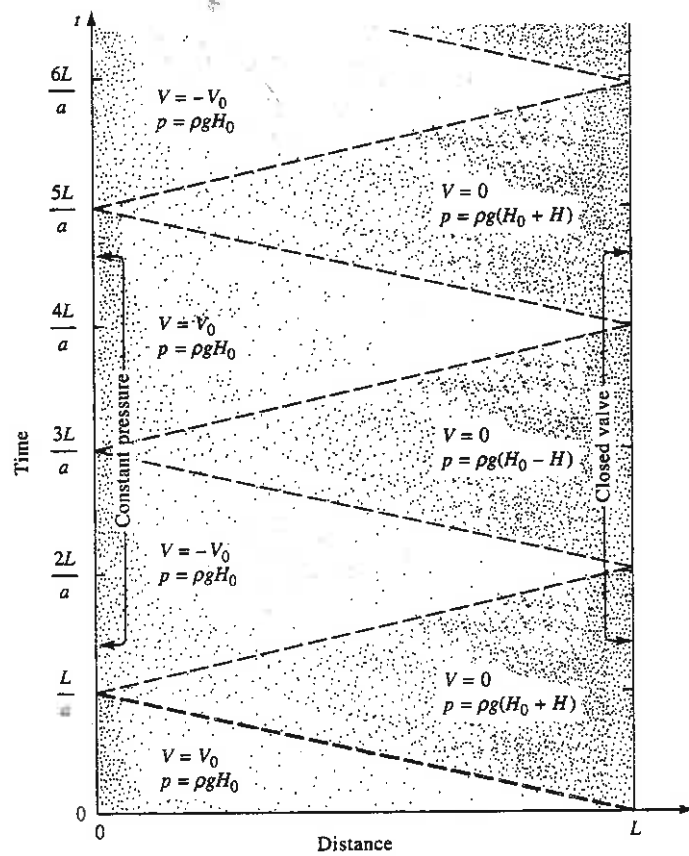


Figure 1-5 Transient in xt plane.

Since the valve is closed, no fluid is available to maintain the flow at the valve and a low pressure $-H$ develops such that the fluid is brought to rest. This low-pressure wave travels upstream at speed a and everywhere brings the fluid to rest, causes it to expand because of the lower pressure, and allows the pipe walls to contract. (If the static pressure in the pipe is not sufficiently high to sustain head $-H$ above vapor pressure, the liquid vaporizes in part and continues to move backward over a longer period of time.)

At the instant the negative-pressure wave arrives at the upstream end of the pipe, $3L/a$ seconds after closure, the fluid is at rest but uniformly at head $-H$ less than before closure. This leaves an unbalanced condition at the reservoir, and fluid flows into the pipe, acquiring a velocity V_0 forward and returning the pipe and fluid to normal conditions as the wave progresses downstream at speed a . At the instant this wave reaches the valve, conditions are exactly the same as at the instant of closure, $4L/a$ seconds earlier. This process is then repeated every $4L/a$ seconds. The action of fluid friction and imperfect elasticity of fluid and pipe wall, neglected heretofore, damps out the vibration and eventually causes the fluid to come to rest permanently.

The transient behavior in a pipeline may be visualized in the xt plane as illustrated in Fig. 1-5. Distance is measured along the pipe from the upstream end and time is

Sec. 1-3 Effects of Air Entrainment

measured from the instant of valve closure. Since it takes L/a seconds for a wave to propagate the length of the pipe, the sloped dashed lines in the xt plane may be visualized as wavefronts traveling either upstream or downstream with increasing time. These lines conveniently divide the xt plane into zones at different pressure levels and with different velocities.

1-3 Effects of Air Entrainment

The propagation velocity of a pressure wave in a pipeline containing a liquid can be greatly reduced if gas bubbles are dispersed throughout the liquid. A straightforward calculation after Kobori et al.¹⁷ and Pearsall²³ demonstrates that this is indeed true, even with a very small amount of air present in the form of bubbles in the liquid. These same authors have laboratory measurements that are in general agreement with their theory.

It is assumed that a pipeline contains a fluid that consists of a liquid with gas bubbles uniformly distributed throughout. Consider a section of pipeline as a control volume. The total volume V of the fluid can be expressed as the sum of the liquid volume V_{liq} and the gas volume V_g . A pressure change brings about a volume change which can be expressed

$$\Delta V = \Delta V_{\text{liq}} + \Delta V_g$$

The gross bulk modulus of elasticity is defined by Eq. (1-6), and the bulk moduli of the individual components can be expressed by

$$K_{\text{liq}} = - \frac{\Delta p}{\Delta V_{\text{liq}}/V_{\text{liq}}}$$

and

$$K_g = - \frac{\Delta p}{\Delta V_g/V_g}$$

Combining these expressions with Eq. (1-6) yields

$$K = \frac{K_{\text{liq}}}{1 + (V_g/V)(K_{\text{liq}}/K_g - 1)} \quad (1-12)$$

By expressing the mixture density in terms of liquid and gas densities,

$$\rho = \rho_g \frac{V_g}{V} + \rho_{\text{liq}} \frac{V_{\text{liq}}}{V} \quad (1-13)$$

and substituting into Eq. (1-11), we can obtain an expression for the wavespeed. If a small amount of gas is present, the effect of the pipe-wall elasticity becomes insignificant and that term is dropped:

$$a = \sqrt{\frac{K}{\rho}} \quad (1-14)$$

where K is defined by Eq. (1-12) and ρ is defined by Eq. (1-13).

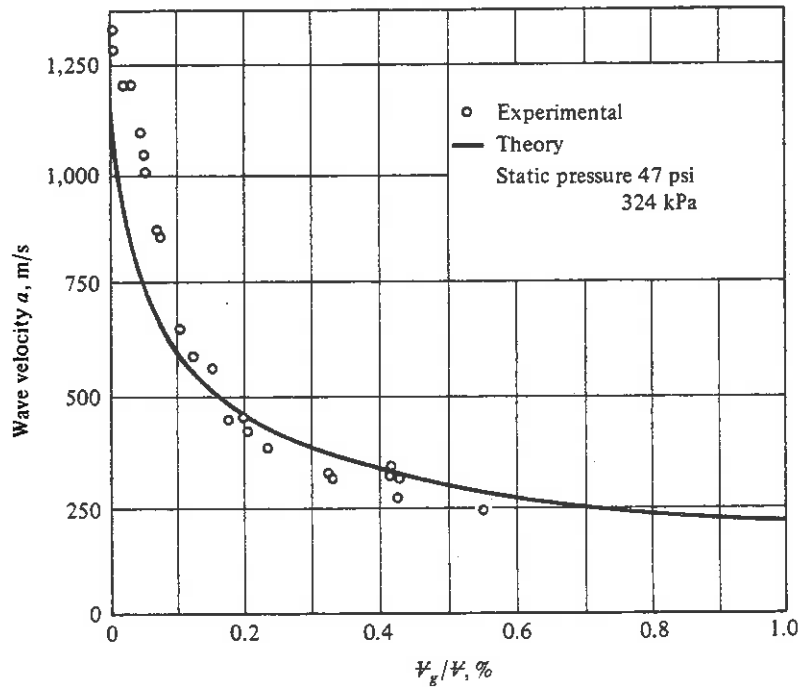


Figure 1-6 Propagation velocity of a pressure wave in pipeline for varying air content (theoretical and experimental results).¹⁷

Figure 1-6 illustrates the effect of air bubbles in a pipeline containing water. The good agreement between experimental results and theory is apparent. It can be noted that a small air content produces a wavespeed less than the speed of sound in air.

It is natural that the gas content in liquids tends to reduce the speed of the pressure pulse. For example, air bubbles in water could be visualized as springs loaded with the water. A pressure pulse compresses the spring, which accelerates the water mass, which, in turn, compresses another spring. Thus the wave would travel through the fluid at a lower velocity than in a homogeneous liquid, in which the wave is transmitted directly from one particle to the next.

Example 1-1

Calculate the wavespeed in a pipeline containing water at atmospheric pressure with 1 percent air content, $K_g = 3000 \text{ lb}/\text{ft}^2$, $K_{\text{liq}} = 4.23(10)^7 \text{ lb}/\text{ft}^2$, $\rho_g = 0.00238 \text{ slug}/\text{ft}^3$, and $\rho_{\text{liq}} = 1.94 \text{ slug}/\text{ft}^3$. From Eq. (1-12), $K = 2.98(10)^5 \text{ lb}/\text{ft}^2$, and from Eq. (1-13), $\rho = 1.92$. Therefore,

$$a = \sqrt{\frac{K}{\rho}} = 396 \text{ ft/s}$$

When free air is present under high-pressure conditions, its volume is greatly reduced and the pipe elasticity becomes important. The equation for wavespeed is then given by Eq. (1-11), with K and ρ defined as in Eq. (1-14). By considering a mass m

of free air present per unit of volume, and that it compresses isothermally, $K_g = p$, the absolute pressure. Then

$$K = \frac{K_{\text{liq}}}{1 + (mRT/p)[(K_{\text{liq}}/p) - 1]}$$

with R the gas constant and T the absolute temperature, or

$$a = \sqrt{\frac{K_{\text{liq}}/\rho}{1 + K_{\text{liq}}D/Ee + (mRT/p)[(K_{\text{liq}}/p) - 1]}} \quad (1-15)$$

Wavespeed for Solid-Liquid Mixture

When fine solid particles are in suspension in a liquid, the bulk modulus of elasticity for the mix is derived in the same manner as Eq. (1-12), yielding

$$K = \frac{K_{\text{liq}}}{1 + (\mathcal{V}_s/\mathcal{V})(K_{\text{liq}}/K_s - 1)} \quad (1-16)$$

in which K_s and \mathcal{V}_s are bulk modulus of elasticity of the solid particles and volume of solid particles, respectively. The mixture density is

$$\rho = \rho_s \frac{\mathcal{V}_s}{\mathcal{V}} + \rho_{\text{liq}} \frac{V_{\text{liq}}}{\mathcal{V}} \quad (1-17)$$

When a waterhammer pressure wave travels through a suspension, there is a motion of the solid particle relative to the liquid for a short time, until the viscous resistance forces between them damps out the motion. The acoustic wavespeed is given by Eq. (1-14) using Eqs. (1-16) and (1-17). The relation between pressure change and velocity change due to a waterhammer wave is given by Eq. (1-2a) neglecting relative motion of solid particles to liquid.

1-4 The Cause of Transients: Role of Valving

A change from steady flow conditions in a piping system occurs when there is a change in operation of elements or facilities in the system. Quite often these are terminals or boundaries of the pipe and may be referred to as boundary conditions. There are many opportunities to introduce transients into fluid systems through active changes in operating conditions. There may also be passive or reactive changes that contribute to the transient behavior. Rather than an exhaustive itemization of the causes of transients only a few different opportunities are listed.

1. Changes in valve settings, accidental or planned
2. Starting or stopping of pumps or compressors
3. Changes in power demand in turbines or governor hunting
4. Action of reciprocating devices
5. Changing level of reservoir or pressure tank

6. Transmission of different oil product through pump
7. Liquid vaporization or vapor condensation
8. Vibration of impellers or guide vanes in turbomachines
9. Vibration of deformable appurtenances such as valves
10. Motion of pipe or other system element
11. Unstable controller or turbomachine characteristic

The study of fluid transients quite often involves analysis of problems having one or more of these conditions.

Traditionally, this study has been one of analysis rather than design or synthesis. A design is made, then the system is analyzed to see if it is satisfactory from a transient viewpoint. If not, alterations in the design are made and it is analyzed again, perhaps with such changes as an increase in the thickness of pipe walls or introduction of surge tanks, accumulators, surge suppressors, and so on.

Routine control of flow in a system is usually effected by adjusting the position of one or more valves. Valves, by introducing losses into a system (except for needle nozzles at the end of a line), control the rate of flow; each adjustment of the valve also sets up pressure pulse waves that traverse the system at the wavespeed for the particular pipe. By making the valve adjustments very slowly, one can keep the transient pressure changes under control. But slow changes may hamper the process under control, so it is desirable to know how to make rapid valve adjustments and still keep the transients within tolerable limits.^{27,30,42} Chapter 9 introduces the theory for a design of valve movements that allows transients to be controlled (i.e., upon completion of a valve adjustment the flow has everywhere in the system substantially assumed its new steady state).

1-5 Column Separation: Gas Release

Vapor Formation

Aside from damaging equipment attached to piping systems, waterhammer may cause the pipe to fail from excessive pressure or to fail by collapse due to pressure less than atmospheric. The phenomenon of column separation may occur within a piping system when boundary conditions are such that the pressure is reduced. A reduction in pressure at the upstream end of a pipe with positive flow causes a negative pulse to be transmitted down the pipe, thereby reducing its velocity; the fluid downstream continues at its steady velocity until the wave arrives. This difference in velocity between portions of the flow tends to put the liquid column into tension, which commercial fluids cannot withstand. When vapor pressure is reached, a vapor cavity forms in the pipe. With a pipeline of varying elevation, column separation usually forms near one of the high points in the profile. This cavity will tend to stay on the downstream side of the high point, with the liquid flowing below the cavity, as in Fig. 1-7. After the cavity is formed it may continue to grow in volume until the flow velocities of the two columns

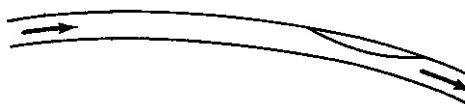


Figure 1-7 Position of vapor cavity in a pipeline.

become equal. Usually, the upstream column will be accelerated and the downstream column decelerated by the boundary conditions, and the upstream column overtakes the downstream column. If the difference in velocity at the instant of collapse of the vapor cavity is ΔV , a pressure increase of $\rho a \Delta V/2$ may be expected. This pressure increase may be of sufficient magnitude to rupture the pipe.

Gas Release

If the liquid in the pipeline contains dissolved air or other gases, a reduction in its pressure below saturation pressure causes gas bubble formation at the many nuclei generally present in commercial liquids. An example could be the reduction of pressure from, say 2 atm to 0.5 atm. These small bubbles greatly decrease the wave speed, as given by the formulas of Sec. 1-3. If the liquid has its pressure reduced to vapor pressure, the bubbles would also contain vapor. If these conditions develop in a system or if the liquid being transported contains free gas, a variable wavespeed exists that is highly pressure dependent.

1-6 Methods of Analysis

All methods of analysis or synthesis of unsteady flow in conduits start with the equations of motion, continuity, or energy, plus equations of state and other physical property relationships. From these basic equations, different methods, employing different restrictive assumptions, have evolved. These methods are discussed briefly in this section under the following classifications:

1. Arithmetic
2. Graphical
3. Characteristics
4. Algebraic
5. Implicit
6. Finite Element
7. Linear analysis

1. Arithmetic waterhammer. This method^{1-3,15} neglects friction and is derived substantially as outlined in Sec. 1-2. Equation (1-3) is integrated and written in the form

$$H \pm \frac{a}{g} V = C \quad (1-18)$$

The plus sign is for a pressure pulse wave traveling from *B* to *A* Fig. (1-8), and takes the form

$$H_A + \frac{a}{g} V_A = H_B + \frac{a}{g} V_B \quad (1-19)$$

Conditions at *A* occur L/a seconds after the conditions at *B*. With H_B , V_B known, one additional piece of information known at *A*, L/a seconds later (a boundary condition), permits H_A and V_A to be determined. For a wave traveling from *A* to *B*,

$$H_A - \frac{a}{g} V_A = H_B - \frac{a}{g} V_B \quad (1-20)$$

in which condition H_A , V_A occur L/a seconds before H_B , V_B . From the application of this pair of equations many times, plus the required boundary conditions (such as a reservoir, a valve, or a dead end), the transient solution is developed and solved. This method was used until the early 1930s, when the graphical methods were developed.

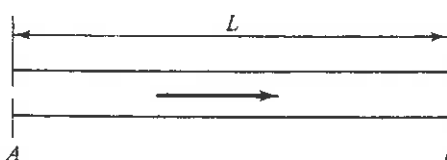


Figure 1-8 Application of arithmetic waterhammer equations to a single pipe.

2. Graphical waterhammer. Graphical waterhammer^{6,7,18,21,40} neglects friction in its theoretical development, but utilizes means to take it into account by a correction. The integrated arithmetic equations (1-18) may be adapted to a graphical solution, as they plot as straight lines on an *HV* diagram (*H* as ordinate and *V* as abscissa). The graphical procedures are outlined in Chapter 5. They were used as the principal way of solving transient problems from the early 1930s to the early 1960s. They have now been generally supplanted by digital computer methods, the subject of this treatment.

3. Method of characteristics. The characteristics method^{10,11,13,31} transforms the partial differential equations of motion and continuity into ordinary differential equations. These are then integrated to obtain a finite difference representation of the variables. The characteristics grid method and, more commonly, the method of specified time intervals provide convenient solution procedures. The characteristics method is favored for most applications in this book, and is developed in detail in Chapters 3 and 4. It has several advantages over other methods that are particularly relevant in waterhammer-type problems. These include a firmly established stability criterion, an explicit solution so that different elements physically removed from one another in systems are handled independently, a procedure that is relatively simple with approximations, if any, readily recognized, an accuracy when executed properly in the characteristics grid method that is unchallenged, and for elementary systems, an implementation that includes a physical interpretation that is simple, yet precise. Its primary disadvantage is the requirement of strict adherence to the time step-distance interval relationship.

4. Algebraic method. The algebraic equations³² are basically the two characteristic equations for sonic pulse waves in the + and - directions in a piping reach. They

are written in such a way that time (an integer) is a subscript. A second subscript is sometimes used to indicate location in a pipeline. One particular advantage is that the equations may be applied over several reaches but use the time increment appropriate to a single reach (a reach of length Δx has a time increment $\Delta t = \Delta x/a$). Another important advantage is the fact that they are easily solved for earlier steps in time, which provides the basis for synthesis of transient flow. These equations are developed and applied to analysis-type situations in Chapter 3.

5. Implicit method. The implicit method is a finite difference procedure that can be used successfully for the solution of a class of unsteady fluid flow problems. Its broadest application is in unsteady free surface flow calculations^{4,19,24}; however, it has been used in other applications. The procedure is particularly applicable in situations where inertia forces are not as important as the storage or capacitance effects. The method is formulated in such a way that the requirement to maintain a certain relationship between the time increment Δt and the length increment Δx is relaxed. In dealing with complex systems, this feature offers the opportunity for a more flexible scheme than that available with other methods; however, it is necessary to use a simultaneous solution for all of the unknowns in the system at each time step. When applied to waterhammer problems it is necessary to adhere to the Courant condition in the time step-distance interval relationship in order to maintain a satisfactory level of accuracy. In these cases the advantages of the method are lost; therefore, other methods are recommended.

6. Finite element method. The finite element method has found wide acceptance in solid and fluid mechanics problems; however, its success in computing pipeline transients is not well established. A hybrid technique is used which usually involves finite elements in the spatial domain and finite difference in time. A satisfactory implementation of a finite element model remains conceptually attractive, however, due to the ease with which variable-size elements of different properties can be represented. Fluid transients in which the flow variables are continuous and not subject to rapid changes may be modeled quite satisfactorily. However, sharp wavefronts associated with rapid transients are dispersed in most formulations, and high-frequency oscillations of the flow variables around sharp changes commonly appear in results. Katopodes¹⁶ has recommended a Petrov-Galerkin method with some success in a variable-wavespeed problem involving free gas in liquid. Rachford²⁵ also has had some success in developing variational methods in liquid transmission systems.

7. Linear analyzing methods. By linearizing the friction term and dropping other nonlinear terms in the equations of motion and continuity, an analytical solution to the equations may be found for sine-wave oscillations.^{22,38} These analyses may be considered in two categories: frequency response analysis and free vibration analysis. The former is effective in treating steady-oscillatory fluctuations set up by some forcing function³² (i.e., by a piston-type positive displacement pump). The impulse response method may also be used to analyze not only periodic flows but also nonperiodic transients, and it is particularly useful to take into account various frequency-dependent factors in systems.^{33,34,35} Free vibration analysis does not inquire into the nature

of the forcing function, but determines the natural frequencies of the system and provides information on the stability of systems and on the rate of attenuation or amplification of the oscillations.^{42,43} The name "impedance methods" has been given to the steady-oscillatory studies. We develop these methods in Chapters 12 and 13.

1-7 Scope and Range of Problems in Unsteady Flow

Unsteady-flow problems arising in the analysis and design of fluid systems may appear quite unrelated (e.g., flow in a large hydro system as compared with the waterhammer effects apparent in an oil-hydraulic lift for a farm tractor, or flow in a diesel fuel injection system). The same methods of analysis apply, however, and it is the purpose of this treatment to present those methods that are of the most value in dealing with a wide variety of applications. Straight analysis of a system, correction of transients in a system, and design to avoid bad transients are all considered. Computer methods are used almost exclusively for analysis and design. Where feasible, experimental evidence of the accuracy of the methods is included.

The subject of waterhammer, with extensions to other fluids, has been the topic of a number of books in recent history. Most notable among these, emphasizing arithmetic and graphical methods, are Rich,²⁶ Parmakian,²¹ Bergeron,⁸ and Jaeger.¹⁴ The expanded use of numerical methods with the ever-increasing use of digital computers has lead to the publication of a number of reference books on unsteady flow. These include, among others, Streeter and Wylie,³² Fox,¹² Wylie and Streeter,⁴² Thorley and Enever,³⁷ Sharp,²⁸ Watters,³⁹ Stephenson,²⁹ Chaudhry,⁹ and Thorley.³⁶ One wonders what will be the primary focus in the next generation.

Problems

- 1-1. Derive Eq. (1-1) for complete stoppage of velocity V_0 by use of the control volume approach.
- 1-2. A valve at the downstream end of a pipe is opened suddenly so that the flow increases from 2 to 2.2 m/s. For $a = 1100$ m/s, what is the pressure change on the upstream side of the valve?
- 1-3. A steel pipe is 4000 ft long and 6 ft in diameter, $e = \frac{3}{4}$ in., $E = 3(10)^7$ psi, and $K = 3(10)^5$ psi. Water is flowing at 3 ft/s. For sudden valve closure in the frictionless pipe, how much flow enters the pipe after closure? How is this volume distributed between pipe cross-sectional area change and liquid compression?
- 1-4. What thickness of a 1-in-ID steel pipe is needed to withstand 100 psi of pressure? Allowable maximum tensile stress is 10,000 psi.
- 1-5. A penstock near the power plant has a head of 350 ft and is 16 ft in diameter. For an overload of 100 percent, which thickness of steel pipe wall is required? The maximum allowable stress is 10,000 psi.
- 1-6. A 2-m-diameter pipe, $e = 20$ mm, has a flow of water at 1 m/s under a head of 100 m. For steel pipe ($E = 207$ GPa) for sudden valve closure, determine (a) the wavespeed

References

- ($K = 2070$ MPa), (b) the pipe circumferential stress before and after closure, and (c) the additional pipe area and its percentage change.
- 1-7. If the wavespeed in a pipe filled with water is 981 m/s, calculate the percentage change in pipe volume for sudden stoppage of a flow velocity of 3 m/s. What is the density change in the water?
 - 1-8. In a simple horizontal frictionless pipe leading from a reservoir to a valve, the valve closes at $t = 0$ s and opens again at $t = 8$ s. $V_0 = 0.98$ m/s, $H_0 = 200$ m, $a = 1200$ m/s, and $L = 1200$ m. Plot (a) H vs. t at the valve for 11 s and (b) V vs. t at the pipe midpoint.
 - 1-9. The initial velocity in the frictionless system in Prob. 1-8 is 0.98 m/s. At $t = 0$ the valve opens to a wider position to create a velocity of 1.96 m/s. For all $t > 0$ s the valve is adjusted instantaneously as needed to maintain the velocity at the valve equal to 1.96 m/s. Plot (a) H vs. t at the valve and (b) V vs. t at the reservoir end of the pipe.
 - 1-10. In Prob. 1-9 calculate the energy flux out of the system during one cycle (power) and the energy flux into the system during one cycle. Neglect kinetic energy.
 - 1-11. A valve is closed in 5 s at the downstream end of a frictionless 9000-ft pipeline that carries water at a velocity of 6 ft/s. If $a = 3000$ ft/s, determine the length of the pipeline subjected to the peak pressure.
 - 1-12. Develop Eq. (1-15) by considering a slice of liquid next to a slice of gas in a pipe segment by use of the momentum equation and the continuity equation. Neglect expansion of the pipe and Poisson ratio effects.
 - 1-13. Find the wavespeed in a pipeline containing water with a 2 percent air content. Assume standard atmospheric conditions at sea level.
 - 1-14. At a pressure of 1 MPa in a pipeline, what air content in water would produce a wavespeed equal to the speed of sound in air alone?

References

1. L. Allievi, "Teoria Generale del Moto Perturbato dell'Acqua Néi Tubi in Pressione," *Annali Della Società Degli Ingegneri ed Architetti Italiani*, Milan, 1903.
2. L. Allievi, "Teoria del Cólpo D'Ariète," *Atti del Collegio Degli Ingegneri ed Architetti Italiani*, Milan, 1913.
3. L. Allievi, *Theory of Water Hammer* (translated by E. E. Halmos), Riccardo Garoni, Rome, 1925.
4. M. Amein, and H. L. Chu, "Implicit Numerical Modeling of Unsteady Flows," *J. Hydraul. Div., ASCE*, Vol. 101, No. HY6, pp. 717-731, June 1975.
5. Alexander Anderson, "Menabrea's Note on Waterhammer: 1858," *J. Hydraul. Div., ASCE*, Vol. 102, No. HY1, pp. 29-39, Jan. 1976.
6. Robert W. Angus, "Simple Graphical Solution for Pressure Rise in Pipes and Pump Discharge Lines," *J. Eng. Inst. Canada*, pp. 72-81, Feb. 1935.
7. L. Bergeron, "Etude des variations de régime dans les conduits d'eau: solution graphique générale," *Rev. Gen. Hydraul.*, Paris, Vol. 1, pp. 12-25, 1935.
8. L. Bergeron, *Water Hammer in Hydraulics and Wave Surges in Electricity* (translated under the sponsorship of the ASME), Wiley, New York, 1961.
9. M. H. Chaudhry, *Applied Hydraulic Transients*, Van Nostrand Reinhold, New York, 1979; 2nd ed., 1987.

10. G. Evangelisti, "Teoria Generale del Cólpo D'Ariète cól Método délle Caratteristiche," *Energ. Electr.*, Milan, Vol XLII, 1965.
11. G. Evangelisti, "Waterhammer Analysis by the Method of Characteristics," *Energ. Electr.*, Milan, Vol. XLVI, Nos. 10, 11, 12, 1969.
12. J. A. Fox, *Hydraulic Analysis of Unsteady Flow in Pipe Networks*, Wiley, New York, 1977.
13. C. A. M. Gray, "The Analysis of the Dissipation of Energy in Water Hammer," *Proc. ASCE*, Vol. 119, pp. 1176-1194, 1953.
14. Charles Jaeger, *Fluid Transients*, Blackie, Glasgow, 1977.
15. N. Joukowsky, "Waterhammer," *Mem. Imp. Acad. Soc. St. Petersburg*, 1898 (translated by O. Simin); *Proc. Am. Waterworks Assoc.*, Vol. 24, pp. 341-424, 1904.
16. N. D. Katopodes, and E. B. Wylie, "Simulation of Two-Dimensional Nonlinear Transients," *Symp. Multi-dimensional Fluid Transients*, ASME, New Orleans, La., pp. 9-16, Dec. 1984.
17. T. Kobori, S. Yokoyama, and H. Miyashiro, "Propagation Velocity of Pressure Wave in Pipe Line," *Hitachi Hyoron*, Vol. 37, No. 10, Oct. 1955.
18. R. Lowy, *Druckschwankungen in Druckrohrleitungen*, Springer, Berlin, 1928.
19. K. Mahmood, and V. Yevjevich (eds.), *Unsteady Flow in Open Channels*, Vols. 1, 2, and 3, Water Resources Publications, Fort Collins, Colo., 1975.
20. L. F. Menabrea, "Note sur les effects de choc de l'eau dans les conduites," *C. R. Acad. Sci.*, Paris, Vol. 47, pp. 221-224, 1858.
21. J. Parmakian, *Water-Hammer Analysis*, Dover New York, 1963.
22. H. M. Paynter, "Studies in Unsteady Flow," *J. Boston Soc. Civil Eng.*, Vol. 39, pp. 120-165, 1952.
23. I. S. Pearsall, "The Velocity of Water Hammer Waves," *Symp. Surges in Pipelines, Proc. Inst. Mech. Eng.*, Vol. 180, Part 3E, 1965-1966.
24. A. Preissman, "Propagation des intumescences dans les canaux et les rivières," *Premier Congrès de l'Association Francaise de Calcul*, Grenoble, France, pp. 433-442, 1960.
25. H. H. Rachford, Jr., and E. L. Ramsey, "Application of Variational Methods to Model Transient Flow in Complex Liquid Transmission Systems," *Paper SPE 5663*, Society of Petroleum Engineers of AIME, Dallas, Sept. 1975.
26. G. R. Rich, *Hydraulic Transients*, Dover, New York, 1963.
27. E. Ruus, "Optimum Rate of Closure of Hydraulic Turbine Gates," *ASME-EIC Fluids Engineering Conf.*, Denver, Apr. 1966.
28. B. B. Sharp, *Water Hammer, Problems and Solutions*, Edward Arnold, London, 1981.
29. D. Stephenson, *Pipeflow Analysis*, Elsevier, Amsterdam, 1984, 204 pp.
30. V. L. Streeter, "Valve Stroking to Control Waterhammer," *J. Hydraul. Div., ASCE*, Vol. 89, No. HY2, *Paper 3452*, pp. 39-66, Mar. 1963.
31. V. L. Streeter, and C. Lai, "Water Hammer Analysis including Fluid Friction," *J. Hydraul. Div., ASCE*, Vol. 88, No. HY3, pp. 79-112, May 1962.
32. V. L. Streeter, and E. B. Wylie, *Hydraulic Transients*, McGraw-Hill, New York, 1967.
33. L. Suo, and E. B. Wylie, "Impulse Response Method for Frequency-Dependent Pipeline Transients," *J. Fluids Eng., ASME*, Vol. 111, No. 4, pp. 478-483, Dec. 1989.
34. L. Suo, and E. B. Wylie, "Hydraulic Transients in Rock-Bored Tunnels," *J. Hydraul. Eng., ASCE*, Vol. 116, No. 2, pp. 194-208, Feb. 1990.

35. L. Suo, and E. B. Wylie, "Complex Wavespeed and Hydraulic Transients in Viscoelastic Pipes," *J. Fluids Eng., ASME*, Vol. 112, pp. 496-500, Dec. 1990.
36. A. R. D. Thorley, *Fluid Transients in Pipeline Systems*, D. & L. George, Herts, England, 1991, 265 pp.
37. A. R. D. Thorley, and K. J. Enever, "Control and Suppression of Pressure Surges in Pipelines and Tunnels," *CIRIA Report 84*, Construction Industry Research and Information Association, London, Sept. 1979, 112 pp.
38. E. J. Waller, "Problems of Pressure Surge Analysis of Positive Displacement Pump Systems," *Publication 107*, Oklahoma State Univ., Stillwater, Okla., Aug. 1959.
39. G. Z. Watters, *Analysis and Control of Unsteady Flow in Pipelines*, 2nd ed., Butterworth, Woburn, Mass., 1984, 344 pp.
40. F. M. Wood, Discussion of "Speed Changes of Hydraulic Turbines for Sudden Changes of Load," by E. B. Stowger and S. L. Kerr, *Trans. ASME*, Vol. 48, 1926.
41. F. M. Wood, "History of Waterhammer," *Report 65*, Dept. of Civil Eng., Queen's Univ. of Kingston, Kingston, Ontario, Canada, Apr. 1970.
42. E. B. Wylie, and V. L. Streeter, *Fluid Transients*, McGraw-Hill, New York, 1978.
43. W. Zielke, and G. Rosl, "Discussion of Resonance in Pressurized Piping Systems," *J. Hydraul. Div., ASCE*, Vol. 97, No. HY7, pp. 1141-1145, July 1971.

Basic Differential Equations for Transient Flow

In this chapter the one-dimensional differential equations of motion and continuity are developed for use in later chapters. These two equations, in general, are simpler than the momentum and continuity equations for developing algebraic finite difference equations to solve transient problems. One special case of a highly deformable continuity equation is also worked out. The general wave equation solutions are given, as well as several special formulas for wavespeeds under various wall conditions. The subscripts x and t denote partial differentiation (i.e., $p_x = \partial p / \partial x$), and a dot over a dependent variable indicates the total derivative with respect to time.

2-1 Equation of Motion

The equation of motion is derived for fluid flow through a conical tube as well as a cylindrical tube or prismatic section. The tube is filled and remains full of fluid of mass density ρ . An average cross-sectional pressure equal to the centerline pressure $p(x, t)$ and an average cross-sectional velocity $V(x, t)$ are assumed in the one-dimensional-equation development. For some applications pressure is converted to the hydraulic grade line $H(x, t)$, sometimes called the *piezometric head*, or in short, the *head*. In most of this treatment the volumetric discharge $Q(x, t)$, the product of the velocity and the pipe area, is used as the preferred dependent variable, along with either p or H . Distance x and time t are the independent variables.

Figure 2-1 shows a free body of fluid of cross-sectional area A at x and thickness δx . The area A is, in general, a function of x , which is the coordinate distance along the axis of the tube from an arbitrary origin. The tube is inclined with the horizontal at

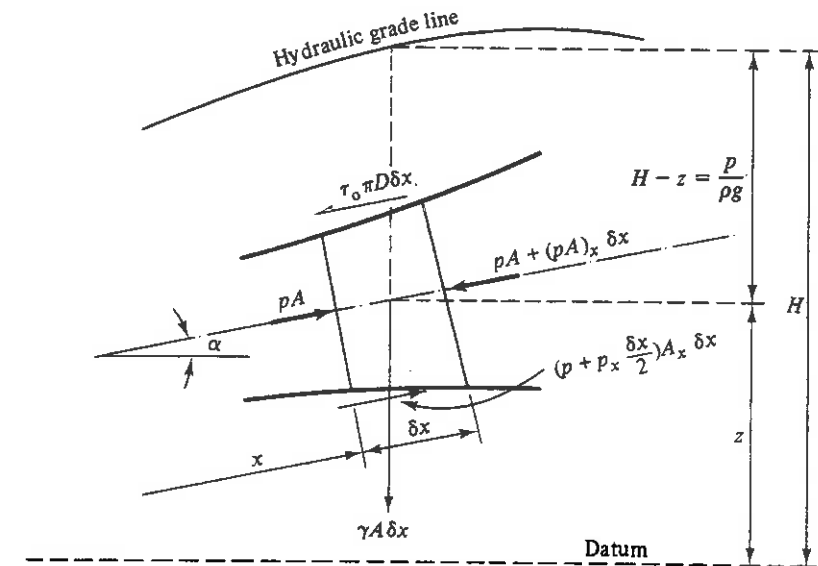


Figure 2-1 Free-body diagram for application of equation of motion.

an angle α , positive when the elevation increases in the $+x$ direction. The forces on the free body in the x direction are the surface contact normal pressures on the transverse faces, and shear and pressure components on the periphery. In addition gravity, the body force, has an x component. The shear stress τ_0 is considered to act in the negative x direction. With reference to the figure, the summation of forces on the slice of fluid is equated to its mass times its acceleration:

$$pA - [pA + (pA)_x \delta x] + \left(p + p_x \frac{\delta x}{2} \right) A_x \delta x - \tau_0 \pi D \delta x - \rho g A \delta x \sin \alpha = \rho A \delta x \dot{V}$$

By dropping out the small quantity containing $(\delta x)^2$ and simplifying, we obtain

$$p_x A + \tau_0 \pi D + \rho g A \sin \alpha + \rho A \dot{V} = 0 \quad (2-1)$$

In transient flow calculations the shear stress τ_0 is considered to be the same as if the velocity were steady, so in terms of the Darcy–Weisbach friction factor f ,⁵

$$\tau_0 = \frac{\rho f V |V|}{8} \quad (2-2)$$

This equation is developed from the Darcy–Weisbach equation,

$$\Delta p = \frac{\rho f L}{D} \frac{V^2}{2} \quad (2-3)$$

with L the length of horizontal pipe, and from a force balance on the pipe in steady flow

$$\Delta p \frac{\pi D^2}{4} = \tau_0 \pi D L \quad (2-4)$$

by eliminating Δp . The absolute value sign on the velocity term in Eq. (2-2) ensures that the shear stress always opposes the direction of the velocity.

The acceleration term \dot{V} in Eq. (2-1) is for a particle of fluid (the slice) having velocity V , hence

$$\dot{V} = VV_x + V_t \quad (2-5)$$

By use of Eqs. (2-2) and (2-5), Eq. (2-1) takes the form

$$\frac{p_x}{\rho} + VV_x + V_t + g \sin \alpha + \frac{fV|V|}{2D} = 0 \quad (2-6)$$

which is valid for converging or diverging pipe flow.

Although V^2 friction was used in deriving the equations, an exponential law may be substituted; for example, if $n = 1.85$ in a power law, then $fV|V|/2D$ may be replaced by

$$\frac{\lambda V|V^{n-1}|}{D^m}$$

λ , n , and m are determined to fit the formula desired.

Equation (2-6) must hold for steady flow, a special case of unsteady flow. Setting $V_t = 0$, it becomes

$$\frac{p_x}{\rho} = -VV_x - g \sin \alpha + \frac{fV|V|}{2D} \quad (2-7)$$

When the common assumption of constant fluid density and pipe area are imposed for steady state (i.e., $V_x = 0$), the equation reduces to

$$\Delta p = -\rho g \Delta x \sin \alpha - \frac{\rho f \Delta x V|V|}{2D} \quad (2-8)$$

which is the equivalent of the Darcy–Weisbach equation for a sloped pipe. Since the term VV_x is not considered in steady state, it is only consistent to exclude the term in unsteady flow. This is a common simplification in Eq. (2-6) for low-Mach-number unsteady flows, reducing Eq. (2-6) to

$$\frac{p_x}{\rho} + V_t + g \sin \alpha + \frac{fV|V|}{2D} = 0 \quad (2-9)$$

The piezometric head H (or elevation of the hydraulic grade line above an arbitrary datum) may replace p . From Fig. 2-1,

$$p = \rho g(H - z)$$

where z is the elevation of centerline of pipe at position x . Then

$$p_x = \rho g(H_x - z_x) = \rho g(H_x - \sin \alpha) \quad (2-10)$$

This partial differentiation considered density to be substantially constant compared with the variations in H or z , which is consistent with the density assumptions made in

connection with steady state. Substitution into Eq. (2-9) yields

$$gH_x + V_t + \frac{fV|V|}{2D} = 0 \quad (2-11)$$

which is the simplified hydraulic-grade-line form of the equation of motion.

Equation (2-6) is valid for any fluid. Equations (2-9) and (2-11) are restricted to less compressible fluids, such as liquids, flowing at low velocities.

2-2 Continuity Equation

In this section a derivation of the one-dimensional continuity equation developed by T. P. Propson (private communication) is presented. It is quite general and has the advantage of portraying the various total derivatives (i.e., derivatives with respect to the motion). Two come directly into the continuity equation: (1) differentiation with respect to the axial motion of the pipe, and (2) differentiation with respect to a particle of fluid mass. The third total derivative is differentiation with respect to the acoustic wave motion, which arises from the characteristics method developed in Chapter 3.

With reference to Fig. 2-2, a moving control volume of length δx at time t may be considered to be fixed relative to the pipe—it moves and stretches only as the inside surface of the pipe moves and stretches. The conservation of mass law may be stated that the rate of mass inflow into this control volume is just equal to the time rate of increase of mass within the control volume, or

$$-[\rho A(V - u)]_x \delta x = \frac{D'}{Dt} (\rho A \delta x) \quad (2-12)$$

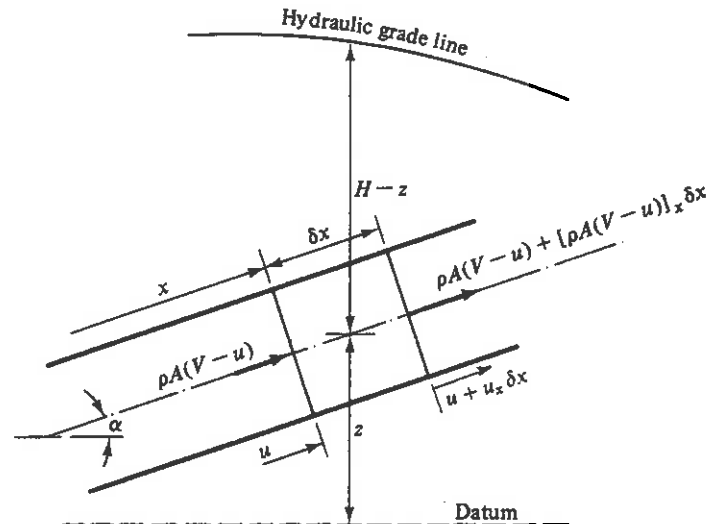


Figure 2-2 Control volume for continuity equation.

Let the upstream face be at x , and u is the velocity of the pipe wall at x . The total derivative with respect to the axial motion of the pipe is given by

$$\frac{D'}{Dt} = u \frac{\partial}{\partial x} + \frac{\partial}{\partial t} \quad (2-13)$$

and the time rate of increase of length δx of the control volume is given by

$$\frac{D'}{Dt} \delta x = u_x \delta x \quad (2-14)$$

By partial expansion of Eq. (2-12) with use of Eq. (2-14),

$$(\rho AV)_x - (\rho Au)_x + \frac{D'}{Dt}(\rho A) + \rho Au_x = 0 \quad (2-15)$$

Additional expansion of Eq. (2-15), using Eq. (2-13), yields

$$(\rho AV)_x - (\rho A)_x u - \rho Au_x + u(\rho A)_x + (\rho A)_t + \rho Au_x = 0$$

or, by simplifying,

$$(\rho AV)_x + (\rho A)_t = 0 \quad (2-16)$$

which may now be written as

$$\rho AV_x + V(\rho A)_x + (\rho A)_t = 0$$

The last two terms represent the derivative of ρA with respect to motion of a mass particle, or

$$\frac{1}{\rho A} \frac{D}{Dt}(\rho A) + V_x = 0 \quad (2-17)$$

in which

$$\frac{D}{Dt} = V \frac{\partial}{\partial x} + \frac{\partial}{\partial t} \quad (2-18)$$

This total derivative is also indicated by a dot over the dependent variable, so

$$\frac{1}{\rho A} (\rho \dot{A} + \dot{\rho} A) + V_x = 0$$

or

$$\frac{\dot{A}}{A} + \frac{\dot{\rho}}{\rho} + V_x = 0 \quad (2-19)$$

This equation holds for converging or diverging tubes as well as for cylindrical pipes on a slope or horizontal. It is also valid for any fluid that fills the section, and for rigid or highly deformable tubes, as no simplifying assumptions have been required. Section 16-1 deals with nonprismatic conduits; the remainder of the present chapter deals with prismatic conduits.

The second term in Eq. (2-19) takes into account the compressibility of the fluid. Pressure is introduced with the definition of bulk modulus of elasticity of a fluid,

Sec. 2-2 Continuity Equation

Eq. (1-6). This substitution excludes thermodynamic effects, thus limiting the resulting equation to slightly compressible fluids only.

$$\frac{\dot{\rho}}{\rho} = \frac{\dot{p}}{K} \quad (2-20)$$

The first term in Eq. (2-19) deals with the elasticity of the pipe wall and its rate of deformation with pressure. For prismatic tubes, area is a function of pressure only

$$\dot{A} = \frac{dA}{dp} \dot{p} \quad (2-21)$$

Substitution of Eqs. (2-20) and (2-21) into Eq. (2-19) yields

$$V_x + \frac{\dot{p}}{K} \left(1 + \frac{K}{A} \frac{dA}{dp} \right) = 0 \quad (2-22)$$

Equation (2-22) may be written

$$\rho a^2 V_x + \dot{p} = 0 \quad (2-23)$$

in which Eq. (1-7) has been introduced

$$a^2 = \frac{K/\rho}{1 + (K/A)(\Delta A/\Delta p)} \quad (1-7)$$

Equation (2-23) is the one-dimensional conservation of mass equation for slightly compressible fluids in a prismatic tube on any slope. When linear elastic fluids and pipe wall materials are considered, the quantity a^2 is taken to be a constant that incorporates the elasticity of the pipe and the fluid it contains.

Equation (2-23) must also describe steady flow as one of the special conditions of unsteady flow. Setting $p_t = 0$ gives us,

$$\rho a^2 V_x + V p_x = 0 \quad (2-24)$$

Since density and tube area variations normally are not considered in steady flow of slightly compressible fluids, $V_x = 0$. Equation (2-24) thus requires that $p_x = 0$, an apparent contradiction for steady flows in sloped tubes with or without friction, or in horizontal tubes with friction. This inconsistency in the continuity equation arises from allowing elastic changes in the unsteady equation through a^2 , but not admitting fluid density or conduit cross-sectional area changes in steady state. The resolution to the inconsistency is found by combining the complete unsteady partial differential equations of unsteady flow, Eqs. (2-6) and (2-23), eliminating V_x by substitution.

$$p_x \left(1 - \left(\frac{V}{a} \right)^2 \right) + \frac{V}{a^2} p_t + \rho V_t + \rho g \sin \alpha + \rho \frac{f V^2}{2D} = 0$$

The Mach number, V/a , appears inside the first parenthesis in the equation due to the presence of $V V_x$ in the equation of motion and $V p_x$ in continuity. If the Mach number is small ($V/a \ll 1$) this combined conservation of mass and momentum equation shows that the term $(V/a)^2$ could be dropped in either steady or unsteady flow without loss in

accuracy. This is precisely what is done in most applications. By dropping the transport term as being small with respect to other terms, Eq. (2-23) becomes

$$\rho a^2 V_x + p_t = 0 \quad (2-25)$$

a simplified continuity equation valid for low-Mach-number unsteady flows.

The head may replace pressure in the same manner as in the equation of motion $p_t = \rho g H_t$, yielding

$$\frac{a^2 V_x}{g} + H_t = 0 \quad (2-26)$$

as a simplified hydraulic grade line form of the unsteady continuity equation.

Equation (2-19) is a general form of the one-dimensional unsteady continuity equation. Equation (2-23) is valid for slightly compressible fluids to which Eq. (2-20) applies. The further limitation to low velocities is imposed on Eqs. (2-25) and (2-26). Chapter 3 deals with the latter forms, and Chapter 4 deals with Eq. (2-23). The more general Eq. (2-19) is addressed in natural gas flow in Chapter 14 and should be used whenever the general energy equation is needed (Chapter 16).

2-3 Wave Propagation Velocities

In Sec. 2-2, a^2 is presented as a collection of parameters involving properties of the fluid and elasticity of the pipe. Although it has not been recognized as the square of the acoustic speed in this chapter, it was in Chapter 1, and it will also become apparent in later chapters. The wavespeed is again examined for a thin-walled pipeline with three different longitudinal support situations, since the pipe may be free to elongate. A few special conduits are then examined to provide equations to determine analytically wave propagation velocities.

If pipe elongation is to be considered, there must be recognition of the relation between material strains in perpendicular directions. This involves the use of Poisson's ratio, μ , defined by

$$\mu = -\frac{\text{lateral unit strain}}{\text{axial unit strain}} = -\frac{\xi}{\xi_1} \quad (2-27)$$

By including Poisson's ratio, dynamic motions in the pipe wall material are possible as well as in the contained fluid.⁶ In this treatment of the interaction between axial and circumferential strains, the dynamic response of the actual pipeline is neglected.

Thin-Walled Elastic Pipeline

Three longitudinal pipe restraint conditions are investigated and the wavespeed formulas developed:

1. Pipe anchored at its upstream end only
2. Pipe anchored throughout against axial movement
3. Pipe anchored with expansion joints throughout

Sec. 2-3 Wave Propagation Velocities

The term $\Delta A/(A \Delta p)$ in Eq. (1-7) must be evaluated for the three cases. The change in area is the result of a total change in lateral or circumferential strain, ξ_T ,

$$\Delta A = \Delta \xi_T \frac{D}{2} \pi D \quad \text{or} \quad \frac{\Delta A}{A} = 2 \Delta \xi_T \quad (2-28)$$

in which

$$\xi_T = \xi_2 + \xi = \xi_2 - \mu \xi_1$$

Stress and strain are related by Young's modulus of elasticity E , thus

$$\xi_2 = \frac{\sigma_2}{E} \quad \xi_1 = \frac{\sigma_1}{E} \quad (2-29)$$

in which σ_1 is the axial or longitudinal unit stress, and σ_2 the lateral or circumferential unit stress resulting from the internal pressure. All three cases have the same relationship for circumferential unit stress in the pipe wall, as defined in Chapter 1.

$$\Delta \sigma_2 = \frac{\Delta T_f}{e} = \frac{D \Delta p}{2e} \quad (2-30)$$

with e the pipe wall thickness and ΔT_f the change in circumferential tensile force per unit length of pipe.

Case 1. The change in axial tensile stress is the force on the pipe cross-sectional area divided by the annular pipe wall area πDe , or

$$\Delta \sigma_1 = \frac{A \Delta p}{\pi De} = \frac{D \Delta p}{4e} \quad (2-31)$$

Then with Eqs. (2-28) to (2-30)

$$\frac{\Delta A}{A \Delta p} = \frac{2 \Delta \xi_T}{\Delta p} = \frac{2}{\Delta p} (\Delta \xi_2 - \mu \Delta \xi_1) = \frac{2}{\Delta p E} (\Delta \sigma_2 - \mu \Delta \sigma_1) = \frac{D}{Ee} \left(1 - \frac{\mu}{2}\right) \quad (2-32)$$

Case 2. For a pipe anchored throughout, $\xi_1 = 0$ and $\Delta \sigma_1 = \mu \Delta \sigma_2$, so

$$\frac{\Delta A}{A \Delta p} = \frac{2}{\Delta p E} (\Delta \sigma_2 - \mu^2 \Delta \sigma_2) = \frac{D}{Ee} (1 - \mu^2) \quad (2-33)$$

Case 3. For expansion joints throughout, $\sigma_1 = 0$ and

$$\frac{\Delta A}{A \Delta p} = \frac{2 \Delta \sigma_2}{\Delta p E} = \frac{D}{Ee} \quad (2-34)$$

By writing the wavespeed as

$$a^2 = \frac{K/\rho}{1 + [(K/E)(D/e)]c_1} \quad (2-35)$$

c_1 takes on the values

1. $c_1 = 1 - \mu/2$
2. $c_1 = 1 - \mu^2$
3. $c_1 = 1$

Thick-Walled Elastic Pipeline

For pipes in which the walls are relatively thick in comparison with the diameter, the stress in the walls is not uniformly distributed throughout the walls. In this condition, as when the ratio D/e is less than approximately 25, the following coefficients³ should be used.

Case 1. The pipeline is anchored at the upstream end only, and

$$c_1 = \frac{2e}{D}(1 + \mu) + \frac{D}{D + e} \left(1 - \frac{\mu}{2}\right) \quad (2-36)$$

Case 2. The pipeline is anchored against longitudinal movement, and

$$c_1 = \frac{2e}{D}(1 + \mu) + \frac{D(1 - \mu^2)}{D + e} \quad (2-37)$$

Case 3. The pipeline has expansion joints throughout its length, and

$$c_1 = \frac{2e}{D}(1 + \mu) + \frac{D}{D + e} \quad (2-38)$$

In the thick-walled pipeline the type of constraint has little effect on the wavespeed. It can be noted that as the thickness e becomes small, each coefficient approaches the corresponding c_1 for the thin-walled pipeline.

Circular Tunnels

By allowing the thickness e in the equation for thick-walled pipes to become larger and larger, c_1 approaches the value $(2e/D)(1 + \mu)$. Substituting the value of c_1 into Eq. (2-35) yields

$$a = \sqrt{\frac{K/\rho}{1 + (2K/E_R)(1 + \mu)}} \quad (2-39)$$

This equation enables the wavespeed in a conduit through solid rock or concrete to be calculated. E_R and μ represent the modulus of rigidity and Poisson's ratio of the tunnel material, respectively.

Lined Circular Tunnels

A steel liner in contact with the tunnel material increases the wavespeed to more than that which would exist in the tunnel alone. If Poisson's ratio effects are neglected in both the steel and tunnel material, a simple expression³ can be presented for the coefficient c_1 in Eq. (2-35):

$$c_1 = \frac{2Ee}{E_R D + 2Ee} \quad (2-40)$$

Equations including Poisson's ratio effect can be developed for lined tunnels³; in most cases, however, additional accuracy for this one factor is not warranted, since other uncertainties are likely to be equally important.

Reinforced Concrete Pipe

The pressure-pulse velocity in reinforced concrete pipe can be estimated by replacing the actual pipe with an "equivalent" steel pipe whose wall thickness is based on the concrete thickness and the reinforcing bars in the pipe. The ratio of the moduli of concrete to steel multiplied by the concrete thickness yields an equivalent steel-pipe thickness. An allowance can be made for the probable cracking of the concrete pipe.

Plastic Pipes

An experimental program by Watters⁹ concluded that the wave velocity as calculated by the traditional equation, Eq. (2-35), is reasonably accurate provided that the appropriate bulk moduli and Poisson's ratio are used. Experiments were conducted in polyvinyl chloride (PVC) pipe and fiber-reinforced plastic pipe. Under buried pipe conditions the constrained pipe formula should be used. Effects of the viscoelastic behavior of plastic pipe, which leads to a frequency-dependent wavespeed, is discussed in Section 12-6.

Rectangular and Other Noncircular Cross Sections

For cross sections other than circular, theoretical wavespeeds may be calculated from Eq. (1-7) if the term $\Delta A/(A \Delta p)$ can be evaluated. Jenkner⁴ has calculated values for both the square and rectangular cases. For the square conduit of sides B and thickness of material e ,

$$\frac{\Delta A}{A \Delta p} = \frac{B}{eE} + \frac{B^2}{15e^3 E} \quad (2-41)$$

The first term on the right side is due to the tension elongation of the sides and the second term is due to bending of the sides. In general, the first term may be neglected.

For the rectangular cross section of width B and depth D , neglecting area increase due to tension,

$$\frac{\Delta A}{A \Delta p} = \frac{B^4 R}{15e^3 E D} \quad (2-42)$$

in which R is a "rectangular factor" given by

$$R = \frac{6 - 5\alpha}{2} + \frac{1}{2} \left(\frac{D}{B}\right)^5 \left[6 - 5\alpha \left(\frac{B}{D}\right)^2\right]$$

with

$$\alpha = \frac{1 + (D/B)^3}{1 + D/B}$$

Thorley and Guymer⁷ have studied thick-walled rectangular conduits, including shear deformation as well as tension and bending. The shear and tension terms comprise 10 to 12 percent of the area change for a width/ thickness ratio of 15. The terms become negligible for large ratios, say 100.

The equations above are arrived at assuming that deformations in the pipe occur within the elastic limits. A number of factors that may influence the wavespeed have not been considered here. These include the nonlinear nature of the bulk modulus of the fluid, particularly in liquids with free gases (see Sec. 1-3 and Chapter 8), and viscoelastic^{1,2} or nonlinear inelastic behavior of some pipe materials.⁸ Some typical elastic material and fluid properties are supplied in Appendix B.

Example 2-1

A 750-mm-diameter pipe is filled with water. $K = 2.2 \text{ GPa}$ and $\rho = 998.2 \text{ kg/m}^3$ for 20°C.

(a) If the pipeline were considered completely rigid, the wavespeed would be

$$a = \sqrt{\frac{K}{\rho}} = \sqrt{\frac{2.2 \times 10^9}{998.2}} = 1484.6 \text{ m/s}$$

(b) Consider the three conditions of restraint on a steel pipeline ($e = 6.35 \text{ mm}$, $\mu = 0.3$, $E = 207 \text{ GPa}$, and $KD/Ee = 1.255$).

Case 1

$$c_1 = 1 - \frac{\mu}{2} = 0.85 \quad a = \frac{1484.6}{\sqrt{1 + 1.255 \times 0.85}} = 1032.7 \text{ m/s}$$

Case 2

$$c_1 = 1 - \mu^2 = 0.91 \quad a = \frac{1484.6}{\sqrt{1 + 1.255 \times 0.91}} = 1014.4 \text{ m/s}$$

Case 3

$$c_1 = 1 \quad a = \frac{1484.6}{\sqrt{1 + 1.255}} = 988.6 \text{ m/s}$$

(c) Consider the three conditions of restraint on a steel thick-walled pipeline of the same internal diameter. $e = 50 \text{ mm}$, $KD/Ee = 0.1594$.

Case 1

$$c_1 = \frac{2 \times 0.05}{0.75} (1 + 0.3) + \frac{0.75}{0.75 + 0.05} \left(1 - \frac{0.3}{2}\right) = 0.970$$

$$a = \frac{1484.6}{\sqrt{1 + 0.1594 \times 0.970}} = 1381.6 \text{ m/s}$$

Case 2

$$c_1 = 0.173 + \frac{0.075}{0.80} \times 0.91 = 1.026 \quad a = \frac{1484.6}{\sqrt{1 + 0.1594 \times 1.026}} = 1376.3 \text{ m/s}$$

Case 3

$$c_1 = 0.173 + \frac{0.075}{0.80} = 1.11 \quad a = \frac{1484.6}{\sqrt{1 + 0.1594 \times 1.11}} = 1368.4 \text{ m/s}$$

(d) Consider a 750-mm tunnel through a concrete dam. $E_R = 20.7 \text{ GPa}$ and $\mu = 0.3$:

$$a = \frac{1484.6}{\sqrt{1 + 2 \times (2.2/20.7)(1 + 0.3)}} = 1314.1 \text{ m/s}$$

(e) Consider a 12.5-mm steel liner inside a concrete tunnel, the inside diameter remaining 750 mm.

$$c_1 = \frac{2 \times 2.07 \times 10^{11} \times 0.0125}{2.07 \times 10^{10} \times 0.75 + 2 \times 2.07 \times 10^{11} \times 0.0125} = 0.25$$

$$\frac{KD}{Ee} = \frac{2.2 \times 10^9 \times 0.75}{2.07 \times 10^{11} \times 0.0125} = 0.638$$

$$a = \frac{1484.6}{\sqrt{1 + 0.638 \times 0.25}} = 1378.7 \text{ m/s}$$

(f) Consider a square steel conduit 100 mm on a side, with thickness 5 mm. From Eq. (2-41),

$$\frac{\Delta A}{A \Delta p} = \frac{0.1}{0.005 \times 2.07 \times 10^{11}} + \left(\frac{0.1}{0.005}\right)^3 \frac{1}{15 \times 2.07 \times 10^{11}} = 2.673 \times 10^{-9}$$

Then from Eq. (1-7),

$$a = \frac{1484.6}{\sqrt{1 + 2.2 \times 10^9 \times 2.673 \times 10^{-9}}} = 566 \text{ m/s}$$

2-4 Forms of the Equations for Special Purposes

Particular solutions of the partial differential equations are obtained for various simplifying assumptions. Only one solution of the equations is discussed in this chapter; this is the solution to obtain the general equations of wave mechanics.

General Wave Equations

The simplified continuity equation, Eq.(2-26),

$$V_x + \frac{g}{a^2} H_t = 0 \quad (2-43)$$

and equation of motion, Eq. (2-11), with the friction term neglected,

$$H_x + \frac{1}{g} V_t = 0 \quad (2-44)$$

yield two linear differential equations that may be solved. By taking the partial derivative of the first equation with respect to t and the second with respect to x , one may eliminate V , which yields

$$H_{tt} = a^2 H_{xx} \quad (2-45)$$

In a similar manner H may be eliminated, giving

$$V_{tt} = a^2 V_{xx} \quad (2-46)$$

The general solution of Eq. (2-45) may be shown to be

$$H - H_0 = F\left(t + \frac{x}{a}\right) + f\left(t - \frac{x}{a}\right) \quad (2-47)$$

by differentiation and substitution into Eq. (2-45). The functions $F(t + x/a)$ and $f(t - x/a)$ are entirely arbitrary and may be selected to satisfy the conditions imposed at the end of the conduit. The function

$$F\left(t + \frac{x}{a}\right)$$

may be interpreted as a wave moving in the $-x$ direction; that is, holding F constant, as t increases, x must decrease at the rate at . This is called an F wave, which one can set up by altering conditions at the downstream end of the pipe. Similarly,

$$f\left(t - \frac{x}{a}\right)$$

may be interpreted as a wave moving in the $+x$ direction. Hence, if an alteration in head is made at the upstream end of the conduit, it is transmitted as an f wave downstream in unchanging form.

Equation (2-46), when integrated, becomes

$$V - V_0 = -\frac{g}{a} \left[F\left(t + \frac{x}{a}\right) - f\left(t - \frac{x}{a}\right) \right] \quad (2-48)$$

The constant g/a and the signs have been introduced to make the solution satisfy the mixed equations in V and H , Eqs. (2-43) and (2-44). Equations (2-47) and (2-48) are sometimes utilized directly in the arithmetic method, although they are not needed for that purpose. They may be used in deriving the graphical waterhammer equations.

Equations Used for the Method of Characteristics

This method permits the nonlinear terms to remain in the differential equations. The equation of motion is written, from Eq. (2-6),

$$L_1 = \frac{p_x}{\rho} + VV_x + V_t + g \sin \alpha + \frac{fV|V|}{2D} = 0 \quad (2-49)$$

The continuity Eq. (2-23) takes the form

$$L_2 = Vp_x + p_t + \rho a^2 V_x = 0 \quad (2-50)$$

Terms L_1 and L_2 are just labels for the equations and are used in Chapter 4 in the development of the numerical method. The simplified Eqs. (2-11) and (2-26) in terms of head and velocity are used in Chapter 3.

Equations Used for the Impedance Method

The impedance method is developed in this treatment for the steady-oscillatory case mainly—the characteristics method is more suitable for the transient case. It is necessary to linearize the friction term, and other small terms are dropped from the equations. It is also convenient to develop these equations with the discharge Q and elevation of hydraulic grade line H as the dependent variables.

Equation (2-11) becomes

$$H_x + \frac{1}{gA} Q_t + \frac{f Q^n}{2g D A^n} = 0 \quad (2-51)$$

where A is the cross-sectional area and the term V^2 has been generalized to $(Q/A)^n$. In this equation the term $V Q_x / g A$ has been dropped.

The simplified continuity equation Eq. (2-26) becomes

$$Q_x + \frac{gA}{a^2} H_t = 0 \quad (2-52)$$

These equations are used in Chapter 12 to derive the impedance equations.

2-5 The Continuity Equation for Highly Deformable Tubes

With highly deformable tubes the effect of density change is unimportant, so the liquid may be considered incompressible. By further making the assumption that the tube is tethered (i.e., held so that its length does not change), one allows only the first and last terms of Eq. (2-19) to enter the equation. Thus

$$\frac{\dot{A}}{A} + V_x = 0 \quad (2-53)$$

Since $A = \pi r^2$, the equation may be written

$$\frac{2\dot{r}}{r} + V_x = 0 \quad (2-54)$$

For highly deformable tubes, there are many ways to define the relation between stress and strain.¹⁰ For this treatment

$$\frac{1}{E} d\left(\frac{pr}{e}\right) = \frac{dr}{r} \quad (2-55)$$

is taken as the strain relationship. For the linear elastic case in which E is constant, this equation can be integrated, which yields

$$\frac{pr}{eE} = \ln \frac{r}{r_0} \quad (2-56)$$

with r_0 the radius of unstressed tube. For rubber and other substances having a Poisson's ratio of about 0.5, the volume of wall material remains constant during deformation, and

the wall continuity relation is

$$e_0 r_0 = e r \quad (2-57)$$

After eliminating e in the last two equations,

$$\frac{pr^2}{e_0 r_0 E} = \ln \frac{r}{r_0} \quad (2-58)$$

This equation can be expressed

$$\frac{p}{2\rho a_0^2} = \left(\frac{r_0}{r}\right)^2 \ln \frac{r}{r_0} \quad (2-59)$$

in which

$$a_0^2 = \frac{E e_0}{2\rho r_0} \quad (2-60)$$

By taking the derivative of Eq. (2-59) with respect to time,

$$\frac{\dot{p}}{2\rho a_0^2} = \frac{\dot{r}}{r} \left(\frac{r_0}{r}\right)^2 \left(1 - 2 \ln \frac{r}{r_0}\right) \quad (2-61)$$

After defining

$$F\left(\frac{r}{r_0}\right) = \left(\frac{r_0}{r}\right)^2 \left(1 - 2 \ln \frac{r}{r_0}\right) \quad (2-62)$$

the continuity equation becomes

$$\frac{\dot{p}}{\rho a_0^2 F} + V_x = 0 \quad (2-63)$$

The equation of motion, Eq. (2-6), is valid for highly deformable tubes.

The basic differential equations derived in this chapter are utilized in the following chapters in developing solutions to the various types of unsteady-flow problems. In the next chapter, the characteristics method of solution is developed.

Problems

- 2-1. Obtain the equation of motion, Eq. (2-6), by writing the unsteady-momentum equation for a control volume of length δx . (Suggestion: Multiply the continuity equation by V and subtract it from the momentum equation.)
- 2-2. A nonprismatic pipeline has a diameter D_0 at $x = 0$ that increases linearly with distance: $D = D_0 + \beta x$. Develop the continuity equation in terms of pressure for this case.
- 2-3. The flow in a copper pipeline is stopped instantaneously with a pressure rise of 100 m of water. If the pipe is anchored at the upstream end only, find the volume stored during L/a seconds due to (a) the pipe area change, (b) the pipe elongation, and (c) the water elasticity. Neglect Poisson's ratio. $D = 13.41$ mm, $e = 1.24$ mm, $L = 102.0$ m, $E = 120$ GPa, and $K = 2.07$ GPa.

References

- 2-4. A 300-m-long 25-mm-diameter pipeline filled with water has a piston in the left end and a closed valve at the right end. The initial pressure is 700 kPa. The piston is moved very slowly, reducing the volume of the system by 160 cm^3 and increasing the pressure by 700 kPa. What is the wave propagation velocity in the system?
Answer: 802.7 m/s
- 2-5. A noncircular closed conduit deforms in such a manner that A increases by 0.5 percent when the pressure increases by 50 psi. For case 3 support, with water the liquid, estimate the wavespeed.
Answer: 847.5 ft/s.
- 2-6. Sketch the manner in which a varies with the ratio D/e for water in steel pipes. $E = 3(10)^7$ psi and $K = 3(10)^5$ psi. Assume that the pipe is anchored at one end only, $\mu = 0.3$.
- 2-7. Show graphically the effect of the modulus of elasticity of the pipe material upon the wavespeed. Assume the fluid to be water and the ratio $D/e = 70$. Include points for each of the wall materials listed in Appendix B.
- 2-8. Calculate the wavespeeds in Example 2-1c, using the equation for thin-walled tubing, and compare the results with those given for the thick-walled condition.
- 2-9. Compare the wavespeed in a water-filled 300-mm-diameter rubber pipeline 6 mm thick with a thick-walled pipeline 70 mm thick. $E = 0.1$ GPa and $\mu = 0.45$. Assume the pipe to be anchored at one end only.
- 2-10. Calculate what the wavespeed would be in the thin-walled pipeline in Problem 2-9 if it were filled with oil. Specific gravity = 0.80; $K = 1.586$ GPa.
- 2-11. Find the wave velocity in a 5-m-diameter tunnel through solid rock. $E_R = 11$ GPa and $\mu = 0.3$.
- 2-12. Calculate the wavespeed in a water-filled copper tube installed without longitudinal restraint. ID = 25 mm; $e = 0.7$ mm; $E = 110$ GPa; $\mu = 0.3$.
- 2-13. A horizontal steel [$E = 3(10)^7$ psi] pipeline 1000 ft long and 1 ft in diameter is filled with water at 10 psi gage. The pipeline is closed at both ends. A volume of water equal to 0.50 ft^3 is slowly injected into the pipeline, raising the pressure to 110 psi. Find the thickness of the pipe wall. Neglect Poisson's ratio.
Answer: 0.1319 in.
- 2-14. By substitution of Eq. (2-48) into Eq. (2-46), prove that it is the solution.
- 2-15. Show that with F and f the same in Eqs. (2-47) and (2-48), the constants in Eq. (2-48) are needed to satisfy Eqs. (2-43) and (2-44).

References

1. P. G. Franke, and F. Seyler, "Computation of Unsteady Pipe Flow with Respect to Visco-elastic Material Properties," *J. Hydraul. Res.*, Vol. 21, No. 5, 1983.
2. M. Gally, M. Guney, and E. Rietord, "An Investigation of Pressure Transients in Viscoelastic Pipes," *J. Fluids Eng., ASME*, Vol. 101, pp. 495-505, 1979.
3. A. R. Halliwell, "Velocity of Waterhammer Wave in an Elastic Pipe," *J. Hydraul. Div., ASCE*, Vol. 89, No. HY4, pp. 1-21, July 1963.

4. W. R. Jenkner, "Über die Druckstoss-Geschwindigkeit in Rohrleitungen mit quadratischen und rechteckigen Querschnitten," *Schweiz. Bauztg.*, Vol. 89 No. 5, pp. 99–103, Feb. 4, 1971.
5. V. L. Streeter, and E. B. Wylie, *Fluid Mechanics*, 8th ed., McGraw-Hill, New York, 1985.
6. S. Stuckenbruck, D. C. Wiggert, and R. S. Otwell, "The Influence of Axial Pipe Motion on Acoustic Wave Propagation," *J. Fluids Eng.*, ASME, Vol. 107, pp. 518–522, 1985.
7. A. R. D. Thorley, and C. Guymer, "Pressure Surge Propagation in Thick-Walled Conduits of Rectangular Cross Section," *Paper 75-WA/FE-15*, ASME, Houston, Nov. 30–Dec. 4, 1975.
8. J. W. R. Twyman, A. R. D. Thorley, and R. Hewavitarne, "Wave Propagation in Plastically Deforming Ducts," *Paper E6, Proc. 3rd Int. Conf. Pressure Surges*, BHRA, Canterbury, England, Mar. 1980.
9. G. Z. Watters, "The Behavior of PVC Pipes under the Action of Water Hammer Pressure Waves," *Project Report PRWG-93*, Submitted to Johns-Manville Corp., Manville, N.J., Mar. 1971.
10. E. B. Wylie, "Flow through Tapered Tubes with Nonlinear Wall Properties," *Symp. Biomechanics*, ASME, New York, 1966.

Solution by Characteristics Method

A numerical solution of the equations that govern unsteady fluid flow in pipelines is developed in this chapter. A general solution to the partial differential equations is not available; however, the partial differential equations may be transformed by the method of characteristics into particular total differential equations. The latter equations may then be integrated to yield finite difference equations, which are conveniently handled numerically.

The equations in their simplest form, not including the smaller terms, are first organized for numerical computations. Various boundary conditions are presented, and simple examples are solved. The equations are presented in forms for direct substitution into a computer compiler language. Basic programs for the solution of unsteady-fluid-flow problems are presented in FORTRAN. Examples of experimental confirmation of the calculations are included. The complete equations are addressed in Chapter 4.

Combinations of system elements are included, such as reservoirs, valves, series and branching pipelines, minor losses, and so on. Special features, such as the effects of high viscous losses in systems, are discussed along with an introduction to vaporization. A so-called algebraic representation of the equations is also presented as an alternative, but similar, method of solution. Additional basic system response information is provided in Chapter 6 where the transmission and reflection of waves at junctions between pipes and other facilities are presented and additional system elements are introduced.

3-1 Characteristics Equations

The momentum and continuity equations (2-11) and (2-26) form a pair of quasilinear hyperbolic partial differential equations in terms of two dependent variables, velocity

and hydraulic-grade-line elevation, and two independent variables, distance along the pipe and time. The equations are transformed into four ordinary differential equations by the characteristics method.^{8,9,11,18,28} In this section the terms of lesser importance are omitted from the equations to provide the simplest possible introduction to the theory in a single pipe.

The simplified equations of motion and continuity are identified as L_1 and L_2 [from Eqs. (2-11) and (2-26):]

$$L_1 = gH_x + V_t + \frac{f}{2D}V|V| = 0 \quad (3-1)$$

$$L_2 = H_t + \frac{a^2}{g}V_x = 0 \quad (3-2)$$

These equations are combined linearly using an unknown multiplier λ :

$$L = L_1 + \lambda L_2 = \lambda \left(H_x \frac{g}{\lambda} + H_t \right) + \left(V_x \lambda \frac{a^2}{g} + V_t \right) + \frac{fV|V|}{2D} = 0 \quad (3-3)$$

Any two real, distinct values of λ will again yield two equations in terms of the two dependent variables H and V that are in every way the equivalent of Eqs. (3-1) and (3-2). Appropriate selection of two particular values of λ leads to simplification of Eq. (3-3). In general, both variables V and H are functions of x and t . If the independent variable x is permitted to be a function of t , then, from calculus,

$$\frac{dH}{dt} = H_x \frac{dx}{dt} + H_t \quad \frac{dV}{dt} = V_x \frac{dx}{dt} + V_t \quad (3-4)$$

Now, by examination of Eq. (3-3) with Eqs. (3-4) in mind, it can be noted that if

$$\frac{dx}{dt} = \frac{g}{\lambda} = \frac{\lambda a^2}{g} \quad (3-5)$$

Eq. (3-3) becomes the ordinary differential equation

$$\lambda \frac{dH}{dt} + \frac{dV}{dt} + \frac{fV|V|}{2D} = 0 \quad (3-6)$$

The solution of Eq. (3-5) yields the two particular values of λ ,

$$\lambda = \pm \frac{g}{a} \quad (3-7)$$

By substituting these values of λ back into Eq. (3-5), the particular manner in which x and t are related is given:

$$\frac{dx}{dt} = \pm a \quad (3-8)$$

This shows the change in position of a wave related to the change in time by the wave propagation velocity a . When the positive value of λ is used in Eq. (3-5), the positive value of λ must be used in Eq. (3-6). A similar parallelism exists for the negative λ . The

substitution of these values of λ into Eq. (3-6) leads to two pairs of equations which are grouped and identified as C^+ and C^- equations.

$$C^+ : \begin{cases} \frac{g}{a} \frac{dH}{dt} + \frac{dV}{dt} + \frac{fV|V|}{2D} = 0 \\ \frac{dx}{dt} = +a \end{cases} \quad (3-9)$$

$$C^- : \begin{cases} -\frac{g}{a} \frac{dH}{dt} + \frac{dV}{dt} + \frac{fV|V|}{2D} = 0 \\ \frac{dx}{dt} = -a \end{cases} \quad (3-10)$$

$$C^- : \begin{cases} -\frac{g}{a} \frac{dH}{dt} + \frac{dV}{dt} + \frac{fV|V|}{2D} = 0 \\ \frac{dx}{dt} = -a \end{cases} \quad (3-11)$$

$$C^- : \begin{cases} -\frac{g}{a} \frac{dH}{dt} + \frac{dV}{dt} + \frac{fV|V|}{2D} = 0 \\ \frac{dx}{dt} = -a \end{cases} \quad (3-12)$$

Thus two real values of λ have been used to convert the original two partial differential equations to two total differential equations, Eqs. (3-9) and (3-11), each with the restriction that it is valid only when the respective Eqs. (3-10) and (3-12) are valid.

It is convenient to visualize the solution as it develops on the independent variable plane (i.e., the xt plane). Inasmuch as a is generally constant for a given pipe, Eq. (3-10) plots as a straight line on the xt plane; and similarly, Eq. (3-12) plots as a different straight line (Fig. 3-1). These lines on the xt plane are the "characteristic" lines along which Eqs. (3-9) and (3-11) are valid. The latter equations are referred to as compatibility equations, each one being valid only on the appropriate characteristic line. No mathematical approximations have been made in this transformation of the original partial differential equations. Thus every solution of this set will be a solution of the original system given by Eqs. (3-1) and (3-2).

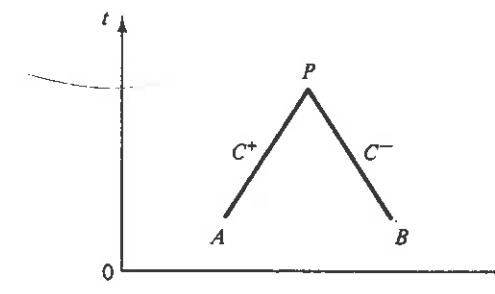
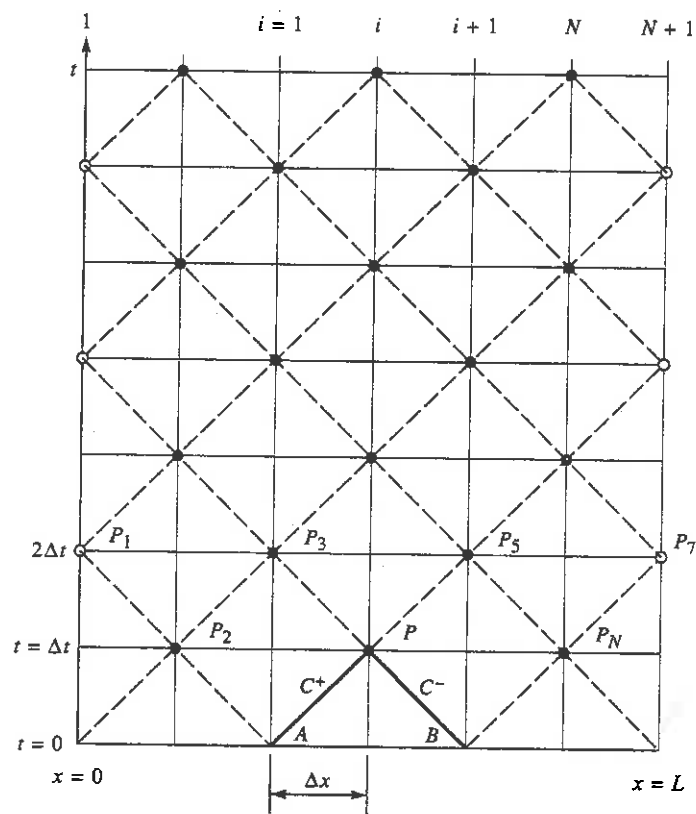


Figure 3-1 Characteristic lines in the xt plane.

3-2 Finite Difference Equations

A pipeline is divided into an even number of reaches, N , each Δx in length,⁸ as shown in Fig. 3-2. A time-step size is computed, $\Delta t = \Delta x/a$, and Eq. (3-10) is satisfied by a positively sloped diagonal of the grid, shown by the line AP . Since N is an even integer the time step is also an even submultiple of the transit time, L/a . If the dependent variables V and H are known at A , then Eq. (3-9), which is valid along the C^+ line, can be integrated between the limits A and P , and thereby be written in terms of unknown

Figure 3-2 xt grid for solving single-pipe problems.

variables V and H at point P . Equation (3-12) is satisfied by a negatively sloped diagonal of the grid, shown by BP . Integration of the C^- compatibility equation along the line BP , with conditions known at B and unknown at P , leads to a second equation in terms of the same two unknown variables at P . A simultaneous solution yields conditions at the particular time and position in the xt plane designated by point P .

By multiplying Eq. (3-9) by $a dt/g = dx/g$, and by introducing the pipeline area to write the equation in terms of discharge in place of velocity, the equation may be placed in a form suitable for integration along the C^+ characteristic (Fig. 3-2).

$$\int_{H_A}^{H_P} dH + \frac{a}{gA} \int_{Q_A}^{Q_P} dQ + \frac{f}{2gDA^2} \int_{x_A}^{x_P} Q|Q| dx = 0 \quad (3-13)$$

The variation of Q with x under the integral in the last term is unknown a priori; thus an approximation must be introduced in this evaluation. A number of options exist. The objective is to maintain a simple form that will provide reasonable accuracy in general unsteady flow and that will hold conditions steady during steady flow. An

integration by parts^{19,36} is used:

$$\begin{aligned} \int_{x_A}^{x_P} Q^2 dx &= Q^2 x \Big|_{x_A}^{x_P} - \int_{x_A}^{x_P} x dQ^2 = Q^2 x \Big|_{x_A}^{x_P} - 2 \int_{x_A}^{x_P} x Q dQ \\ &\approx Q_P^2 x_P - Q_A^2 x_A - 2 \left[\frac{x_P Q_P + x_A Q_A}{2} (Q_P - Q_A) \right] \\ &\approx Q_P |Q_A| (x_P - x_A) \end{aligned} \quad (3-14)$$

The trapezoidal rule was used in this evaluation. It is of second-order accuracy, maintains the linear form of the integrated equations, and is a satisfactory approximation for most problems. The integration of Eq. (3-13), and a similar integration along the C^- characteristic between B and P , yields

$$H_P - H_A + \frac{a}{gA} (Q_P - Q_A) + \frac{f \Delta x}{2gDA^2} Q_P |Q_A| = 0 \quad (3-15)$$

$$H_P - H_B - \frac{a}{gA} (Q_P - Q_B) - \frac{f \Delta x}{2gDA^2} Q_P |Q_B| = 0 \quad (3-16)$$

These two compatibility equations are basic algebraic relations that describe the transient propagation of piezometric head and flow in a pipeline. By solving for H_P , these equations may be written

$$C^+: H_P = H_A - B(Q_P - Q_A) - RQ_P |Q_A| \quad (3-17)$$

$$C^-: H_P = H_B + B(Q_P - Q_B) + RQ_P |Q_B| \quad (3-18)$$

in which B is a function of the physical properties of the fluid and the pipeline, often called the pipeline characteristic impedance:

$$B = \frac{a}{gA} \quad (3-19)$$

and R is the pipeline resistance coefficient:

$$R = \frac{f \Delta x}{2gDA^2} \quad (3-20)$$

The friction factor f may be a constant, or it may be adjusted with the local Reynolds number in accordance with the Moody diagram in each reach at each time step during calculations.

These equations satisfy steady conditions in the pipe since the flows are equal, $Q_A = Q_P = Q_B$, and $RQ_P |Q_A|$ is the steady-state friction head loss over the reach Δx . If an exponential friction formula is preferred, the last term of Eq. (3-17), for example, would become $R' Q_P |Q_A|^{n-1}$, with n the exponent in the friction loss equation and R' the coefficient.

The solution to a problem in liquid transients usually begins with steady-state conditions at time zero, so that H and Q are known initial values at each computing

section (Fig. 3-2), for $t = 0$. The solution consists of finding H and Q for alternate grid points along $t = \Delta t$, then proceeding to $t = 2\Delta t$, and so on, until the desired time duration has been covered. At any interior grid intersection point, point P at section i , the two compatibility equations are solved simultaneously for the unknowns Q_i and H_i . Equations (3-17) and (3-18) may be written in a simple form, namely

$$C^+: H_i = C_P - B_P Q_i \quad (3-21)$$

$$C^-: H_i = C_M + B_M Q_i \quad (3-22)$$

in which the coefficients C_P , B_P , C_M , and B_M are known constants when the equations are applied. Their values in the C^+ and C^- compatibility equations are, respectively:

$$C_P = H_{i-1} + B Q_{i-1} \quad B_P = B + R |Q_{i-1}| \quad (3-23)$$

$$C_M = H_{i+1} - B Q_{i+1} \quad B_M = B + R |Q_{i+1}| \quad (3-24)$$

By first eliminating Q_i in Eqs. (3-21) and (3-22), we have

$$H_i = \frac{C_P B_M + C_M B_P}{B_P + B_M} \quad (3-25)$$

Then Q_i may be found directly from either Eq. (3-21) or (3-22), or from

$$Q_i = \frac{C_P - C_M}{B_P + B_M} \quad (3-26)$$

The subscript notation used in the equations above, which is convenient for computer calculations, is shown in Fig. 3-2. It may be noted that section i refers to any grid intersection point in the x direction. Subscripted values of H and Q at each section are always available for the preceding time step, either as given initial conditions or as the result of a previous stage of the calculations.

Numerical values of H and Q are found at alternate grid intersection points P_2 , P , and P_N (Fig. 3-2) at time $1\Delta t$; then time is incremented by Δt and the procedure is repeated for interior grid intersection points P_3 and P_5 (Fig. 3-2) at time $2\Delta t$. Examination of the grid in Fig. 3-2 shows that the endpoints of the system are introduced every other time step after the initial conditions. Therefore, to complete the solution to any desired time, it is necessary to introduce appropriate end conditions, sometimes called boundary conditions.

3-3 Basic Boundary Conditions

At either end of a single pipe only one of the compatibility equations is available in the two variables. For the upstream end (Fig. 3-3a), Eq. (3-22) holds along the C^- characteristic, and for the downstream boundary (Fig. 3-3b), Eq. (3-21) is valid along the C^+ characteristic. These are linear equations in Q_i and H_i ; each conveys to its respective boundary the complete behavior and response of the fluid in the pipeline during the transient. An auxiliary equation is needed in each case that specifies Q_P , H_P ,

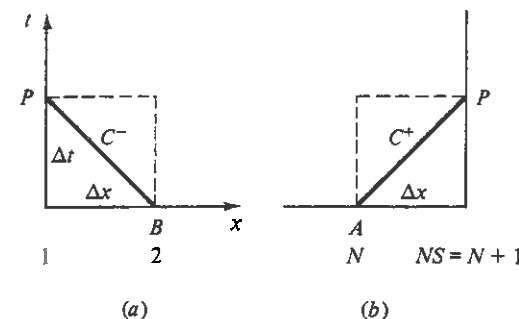


Figure 3-3 Characteristics at boundaries.

or some relation between them. That is, the auxiliary equation must convey information on the behavior of the boundary to the pipeline. This may be just the end condition of the pipeline, or it may be a different element or facility attached to the end of the pipe. Each boundary condition is solved independently of the other boundary, and independently of the interior point calculations. A few boundary conditions are now considered.

Reservoir at Upstream End with Elevation Specified

At a large upstream reservoir the elevation of the hydraulic grade line normally can be assumed constant during a short-duration transient. This boundary condition is described, $H_1 = H_R$, in which H_R is the elevation of the reservoir surface above the reference datum. If the reservoir level changes in a known manner, say as a sine wave, the boundary condition is

$$H_1 = H_R + \Delta H \sin \omega t \quad (3-27)$$

in which ω is the circular frequency and ΔH is the amplitude of the wave. At each time step in either of the cases above, H_1 is known, and Q_1 is determined by a direct solution of Eq. (3-22):

$$Q_1 = \frac{H_1 - C_M}{B_M} \quad (3-28)$$

The subscript 1 refers to the upstream section, at point P , Fig. 3-3a; C_M and B_M are variables in the computational procedure but are dependent only on known values from the previous time step, in this case point B , section 2.

Discharge as a Specified Function of Time at Upstream End

The flow delivered from a positive displacement pump may be expressed as an explicit function of time, for example,

$$Q_1 = Q_0 + \Delta Q |\sin \omega t| \quad (3-29)$$

With Q_1 known at any instant, Eq. (3-18) or (3-22) is applied directly to find H_1 at each time step.

Each of the foregoing end conditions to the pipeline defines one of the variables at any instant of time. The dead end described below is similar. Some pipeline terminations involve elements in which the interaction of the variables is important, then a relationship between H and Q must be written to describe the physical behavior of the end element or facility. The operating centrifugal pump, valve, and orifice are examples of such elements.

Centrifugal Pump at the Upstream End with the Head-Discharge Curve Known

The response of a centrifugal pump operating at a constant speed may be included in an analysis by defining the pump characteristic curve. In a computer program this may be accomplished by storing tabular data to describe the curve, or by using an equation to relate the variables. If the pump is applying flow from a suction reservoir, whose surface elevation is used as the reference datum for the hydraulic grade line, the energy equation would state that the energy added by the pump would be just equal to the energy in the discharge pipe, section 1. Therefore, if the kinetic energy is neglected,

$$H_1 = H_S + Q_1(a_1 + a_2 Q_1) \quad (3-30)$$

in which H_S is the shutoff head, and a_1 and a_2 are constants, normally negative, to describe the pump characteristic curve. Equation (3-30) provides an analytical relationship between the two variables that must be solved simultaneously with Eq. (3-22). The solution to the resulting quadratic equation is

$$Q_1 = \frac{1}{2a_2} \left[B_M - a_1 - \sqrt{(B_M - a_1)^2 + 4a_2(C_M - H_S)} \right] \quad (3-31)$$

in which, since a_2 is negative, the negative root is selected to yield a positive flow. With Q_1 known, H_1 can be obtained from either Eq. (3-22) or (3-30).

Dead End at the Downstream End of Pipe

The downstream end of a pipeline that is divided into N reaches is at section $NS = N+1$ (Fig. 3-3b). If the pipeline contains a closed end, then $Q_{NS} = 0$, and H_{NS} is obtained directly from either Eq. (3-17) or (3-21).

Valve at the Downstream End of Pipe

If the datum for elevation of hydraulic grade line is taken at the elevation of the valve, the energy equation at the valve, relating the energy in the pipeline at section NS to the energy on the downstream side of the valve, is $H_{NS} = \Delta H +$ elevation zero. Kinetic energy has been neglected, and ΔH is the instantaneous drop in hydraulic grade line

across the valve. The energy drop across the valve may be expressed in terms of a loss coefficient, which is a function of time if the valve position changes.

$$\Delta H = K \frac{V^2}{2g} = \frac{K}{A^2} \frac{Q_{NS}^2}{2g} \quad (3-32)$$

Alternatively, an orifice equation may be used:

$$Q_{NS} = C_d A_G \sqrt{2g \Delta H} \quad (3-33)$$

in which $C_d A_G$ is the area of valve opening times the discharge coefficient. For steady-state flow the parallel equations are

$$H_0 = K_0 \frac{V_0^2}{2g} = \frac{K_0}{A^2} \frac{Q_0^2}{2g} \quad (3-34)$$

and

$$Q_0 = (C_d A_G)_0 \sqrt{2g H_0} \quad (3-35)$$

in which the subscript zero refers to steady conditions for each variable. A dimensionless valve opening is useful in specifying valve motions as a function of time and is defined

$$\tau = \frac{C_d A_G}{(C_d A_G)_0} = \sqrt{\frac{K_0}{K}} \quad (3-36)$$

For the steady flow of Q_0 and the corresponding energy loss of H_0 , $\tau = 1$, and for no flow with the valve closed, $\tau = 0$. The value of tau may be larger than unity if the valve is opened from the steady-state initial position. By dividing the unsteady Eq. (3-32), or Eq. (3-33), by the respective steady flow Eq. (3-34), or (3-35),

$$Q_{NS} = \frac{Q_0}{\sqrt{H_0}} \tau \sqrt{H_{NS}} \quad (3-37)$$

since $\Delta H = H_{NS}$ when the valve elevation is taken as the reference datum and the flow discharges to the atmosphere.

The solution to Eq. (3-21), applied at section NS , and Eq. (3-37) is

$$Q_{NS} = -B_P C_v + \sqrt{(B_P C_v)^2 + 2C_v C_P} \quad (3-38)$$

in which $C_v = (Q_0 \tau)^2 / 2H_0$. The corresponding value of H_{NS} can be determined from either Eq. (3-21) or (3-37).

The hydraulic characteristics of valves differ greatly depending primarily on the configuration of the flow path through the valve opening. The steady-state loss coefficients, as a function of valve position, for a few different valve types, are provided in Appendix C.^{3,32}

Orifice at Downstream End of Pipe

The same equations are used for the fixed orifice as for the valve with the simplification that $\tau = 1$.

3-4 Single-pipeline Applications

The procedure to solve a transient fluid flow problem numerically involves a number of repetitious calculations. A computer program to solve a problem involving a single pipe leading from a reservoir to a valve (Fig. 3-4) has the following elements:

1. Read in values of data that describe the system and the character of the particular transient.
2. Calculate constants and initial steady-state conditions, and store initial values of Q_i and H_i for $t = 0$.
3. Print out values of Q_i and H_i at each section, plus printout time and valve opening.
4. Increment time by $2\Delta t$, and at intermediate time Δt calculate interior points at even-numbered sections Q_2, H_2 to Q_N, H_N .
5. Calculate interior points at odd-numbered sections Q_3, H_3 to Q_{N-1}, H_{N-1} , and then calculate the boundary values Q_1, H_1, Q_{NS} , and H_{NS} .
6. Transfer back to the print statement (No. 3), or to increment time (No. 4), and check to see if T_{max} , the duration of the transient, has been exceeded. If not, continue with the calculations.

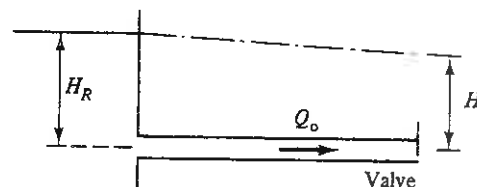


Figure 3-4 Single pipeline.

Example 3-1

The valve closure relationship for the pipeline shown in Fig. 3-4 is given by the equation

$$\tau = \tau_i - (\tau_i - \tau_f) \left(\frac{t}{t_c} \right)^{\frac{E_m}{E_m}}$$

in which t_c is the time of operation, τ_i the initial value of valve opening, and τ_f the final value. The steady-state open position of the valve is defined by a value of $(C_d A_G)_0$ in Eq. (3-35). The initial valve opening may be zero or any positive number, in this case $\tau_i = 1$. The input data for the problem are: $L = 600$ m, $a = 1200$ m/s, $D = 0.5$ m, $f = 0.018$, $H_R = 150$ m, $t_c = 2.1$ s, $\tau_i = 1$, $\tau_f = 0$, $T_{max} = 4.3$ s, $E_m = 0.75$, $(C_d A_G)_0 = 0.009$, $g = 9.806$ m/s², and $N = 10$.

Figure D-1 in Appendix D presents a FORTRAN listing of a program for use with MS-DOS on a PC to solve for the pressure head and flow response as a result of a specified valve motion. The input data are listed at the end of the program and are read from a separate file named SINGLE.DAT. In addition to all input data listed above, two new parameters are included. These are IPR, a control parameter that controls the number of time increments, $\Delta T = 2\Delta t$, between each printout of calculated results, and IGRAF, a section number at which pressure head data are stored for later graphing if desired.

Steady-state discharge, Q_0 , is calculated in the program to balance the pipe friction and valve losses corresponding to $(C_d A_G)_0$ with the energy available in the reservoir. The initial flow, Q_i , for the specific problem is calculated for the given initial valve opening, τ_i .

The computer output is shown in Fig. D-1b, and a graphical display of head at the valve, discharge at the reservoir, and valve opening as a function of time are shown in Fig. 3-5.

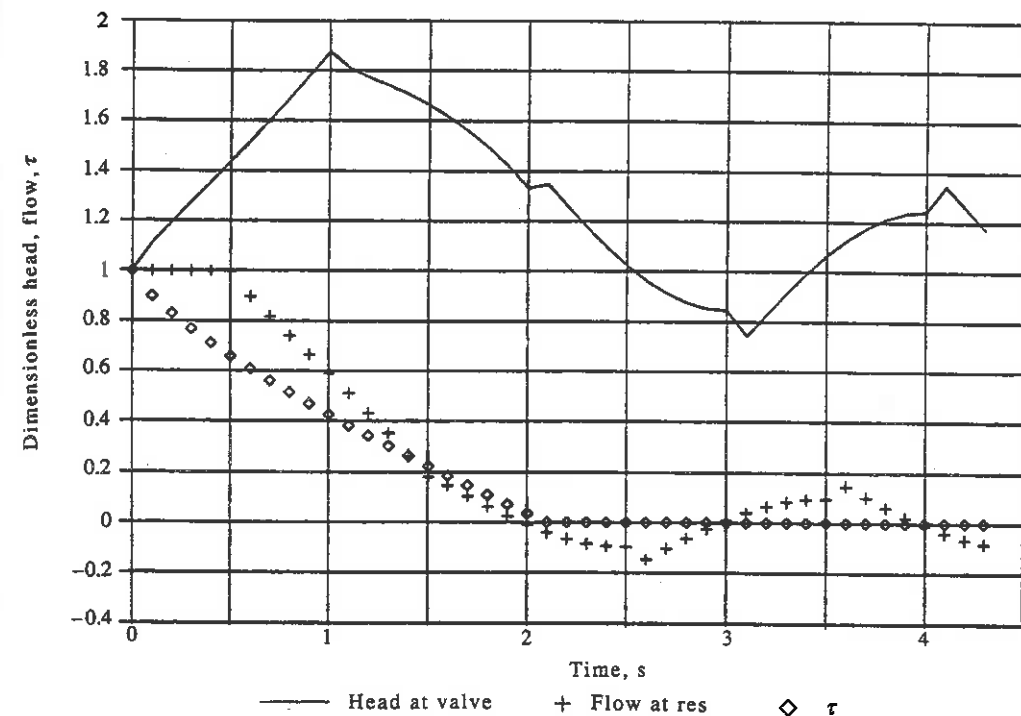


Figure 3-5 Response in single pipeline due to valve closure.

Included in the FORTRAN program is a collection of variables to store transient information to graph if desired. These data are stored in the file attached to device 8. They include the initial pipe profile and hydraulic grade line, transient head profiles along the pipeline at each successive pair of time steps, and a time history of pressure head at section IGRAF. A separate program written in BASIC for the IBM-PC is provided in Fig. D-2, Appendix D, to read and graph these data with IBM GRAPHICS. It is a fairly primitive and simple graphics package and is provided only as a useful tool to examine transient results, not as an exposition of recommended graphic displays. The same program, called GRAF, will be available for use by other programs in this book.

Example 3-2

Consider a single horizontal pipeline as shown in Fig. 3-4 with the valve closed at the downstream end. Assume that a series of sinusoidal waves passes over the reservoir

surface at the pipe inlet, so that $H_1 = H_R + 10 \sin \pi t$. Write the complete equations for both boundary conditions so that they are ready to be programmed for computer solutions.

Upstream boundary:

$$B = \frac{a}{gA} \quad R = f \Delta \frac{x}{2gDA^2}$$

$$C_M = H_2 - BQ_2 \quad B_M = B + R|Q_2|$$

$$H_1 = H_R + 10 \sin \pi t$$

$$Q_1 = \frac{H_1 - C_M}{B_M}$$

Downstream boundary:

$$C_P = H_N + BQ_N \quad B_P = B + R|Q_N|$$

$$Q_{NS} = 0$$

$$H_{NS} = C_P - B_P Q_{NS} = C_P$$

Example 3-3

A centrifugal pump is delivering $0.1 \text{ m}^3/\text{s}$ water to a 250-mm-diameter pipeline at a pressure head of 50 m. The pump shutoff is 70 m. In this operating zone the head-discharge curve can be described by an equation of the form of Eq. (3-30), in which $a_1 = 0$. At the downstream end of the 400-m horizontal line, the valve setting suddenly changes from $\tau = 1$ to $\tau = 0.5$ at time t_c . The valve is discharging into the atmosphere. With values of f and a known, write the necessary equations to handle the boundary conditions in a computer program.

For the pump boundary condition at the upstream end, the constants in Eq. (3-30) for the characteristic curve of the pump must be evaluated first. Then use Eqs. (3-31) and (3-30).

$$H_s = 70$$

$$a_2 = \frac{50 - 70}{(0.1)^2} = -2000$$

$$B = \frac{a}{gA} \quad R = \frac{f \Delta x}{2gDA^2}$$

$$C_M = H_2 - BQ_2 \quad B_M = B + R|Q_2|$$

$$Q_1 = \frac{B_M - \sqrt{B_M^2 + 4a_2(C_M - H_s)}}{2a_2}$$

$$H_1 = H_s + a_2 Q_1^2$$

For the valve boundary condition, the initial steady-state head drop at the valve must be evaluated.

$$H_0 = 50 - \frac{fL}{D} \frac{Q_0^2}{2gA^2}$$

When $t \leq t_c$,

$$H_{NS} = H_0 \quad Q_{NS} = Q_0$$

When $t > t_c$

$$C_P = H_N + BQ_N \quad B_P = B + R|Q_N|$$

$$C_v = \frac{(0.5Q_0)^2}{2H_0}$$

$$Q_{NS} = -B_P C_v + \sqrt{(B_P C_v)^2 + 2C_v C_P}$$

$$H_{NS} = C_P - B_P Q_{NS}$$

Experimental results compared with the solution by the method of characteristics have appeared in the literature and the validity of the solution is well established.^{7,23,24,28} One example is presented in Fig. 3-6. The test pipeline is a 3-in.-diameter horizontal pipeline, 56 ft in length, connected to the suction flange of a reciprocating pump. The triplex pump operating at a speed of 95.9 rpm, was modeled by a specified flow-time relationship in the characteristics method analysis. The upstream boundary condition was a reservoir. Calculated and measured pressures at the suction flange are illustrated in Fig. 3-6. The computed points are from a characteristics method program; the solid line is the pressure trace from a Dynisco transducer.

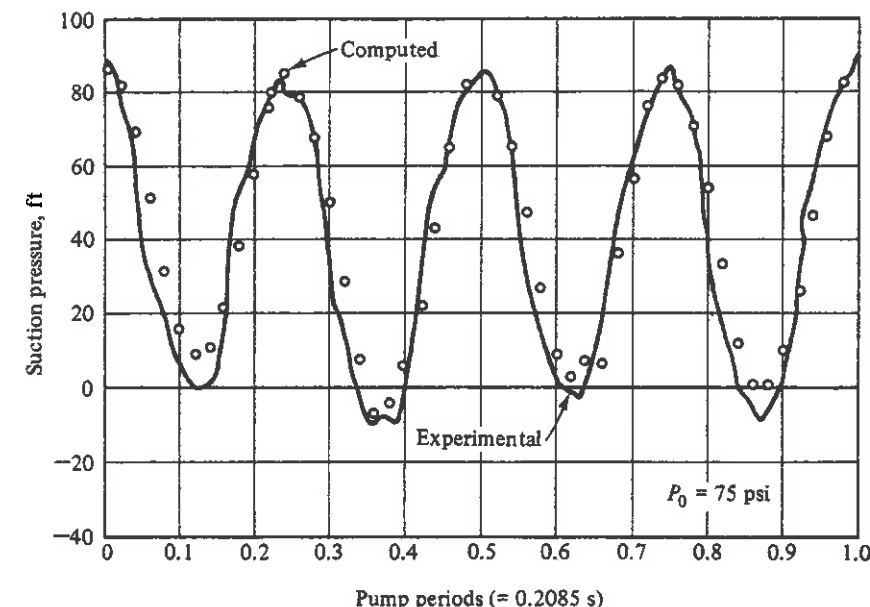


Figure 3-6 Comparison of experimental and calculated results on a single pipe connected to a reciprocating pump.²⁹

Experimental data from 36 m (118.1 ft) of 19.05-mm (0.75-in.)-ID copper tubing in the G.G. Brown Fluids Engineering Laboratory of the University of Michigan²⁵ have also been compared with calculated results using the method of characteristics. A fast-closing $\frac{1}{2}$ -in., one-quarter-turn ball valve was used at the downstream end and a constant-pressure tank at the upstream end. Steady-state friction-drop measurements were taken and, for this initial velocity of 0.239 m/s (0.784 ft/s), the friction factor was 0.0325. The measured wavespeed in the copper tubing was 1280 m/s (4200 ft/s). The experimental and computer results are shown in Fig. 3-7, where it can be observed that the valve closure time was about 15 ms. The agreement is seen to be quite acceptable over the displayed time, representing approximately the first $5L/a$ seconds.

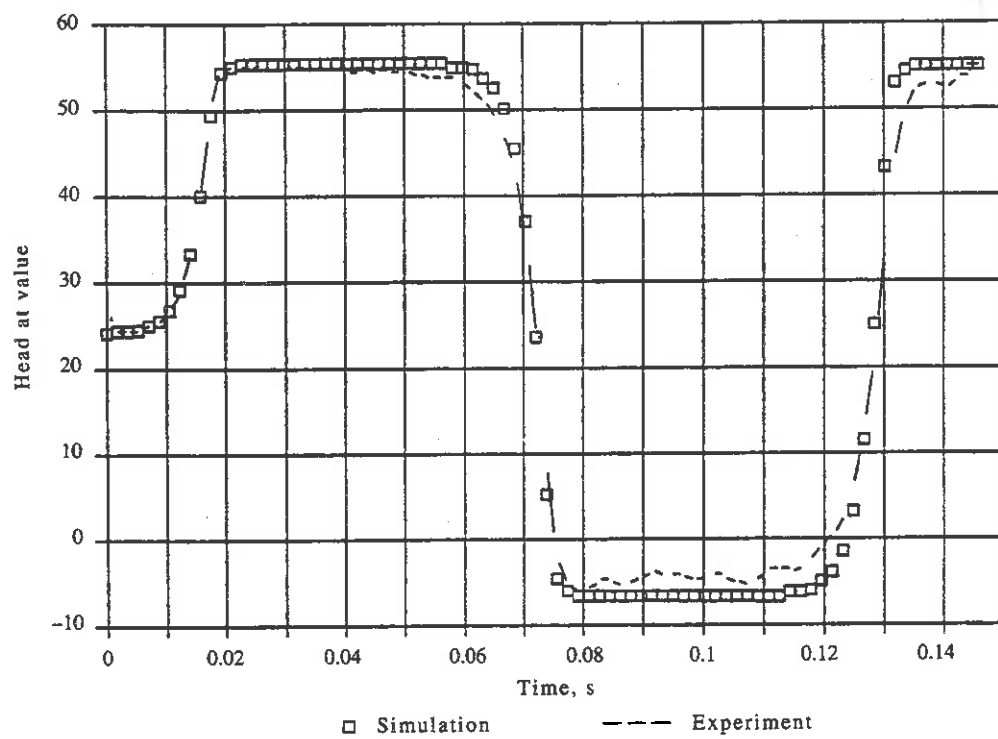


Figure 3-7 Measured and calculated head-time curve.

3-5 Series, Branches, and Other System Facilities

The basic waterhammer program for a single pipeline provides the fundamental elements that are necessary for the treatment of more complex piping systems. Different types of boundary conditions may be introduced by changing only the part of the program that deals with the particular end condition. When the system contains more than one pipeline, the interior sections of each pipeline are treated independently of other

parts of the system at each instant of time. The end conditions for each pipeline must interface with adjoining pipelines or with other boundary elements. Again each boundary condition is treated independently of other parts of the system. The explicit nature of the solution procedure is one of its strongest attributes. Additional boundary conditions and multipipe systems are treated in this section.

At a connection of pipelines of different properties, the continuity equation must be satisfied at each instant of time, that is, there is no storage capacity at the junction. Also, a common hydraulic-grade-line elevation is normally assumed at the junction at each instant of time. The latter assumption is the same as saying that there are no minor losses at the connection and that the velocity head terms may be neglected. This is not necessary, as will be demonstrated later, but it is an acceptable procedure in most cases.

When a large number of pipelines are included in a system it is necessary either to use double-subscript notation, or to use continuous sectioning in the entire system. In the double-subscript scheme, the first subscript refers to the pipe number and the second refers to the pipe section number, as in the single pipe.

Series Connection

This type of junction, although shown in Fig. 3-8 as a diameter change, applies equally well to a single-diameter pipe with a change in roughness, thickness, or constraint condition, or any combination of these possible variables. At the junction (Fig. 3-8),

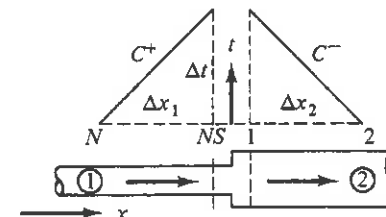


Figure 3-8 Series junction.

Eq. (3-21) is available for pipe 1, and Eq. (3-22) is available for pipe 2. The continuity expression and the condition of a common hydraulic-grade-line elevation provide two equations, as follows, when written in double-subscript notation.

$$Q_{1,NS} = Q_{2,1} \quad H_{1,NS} = H_{2,1} \quad (3-39)$$

By solving these equations simultaneously with Eqs. (3-21) and (3-22), we obtain

$$Q_{2,1} = \frac{C_{P_1} - C_{M_2}}{B_{P_1} + B_{M_2}} \quad (3-40)$$

The other unknowns can be determined directly from the appropriate equation.

General Junction

A junction is visualized as a point connection of elements in a system, at which there are two variables: a nodal flow, Q_n , which may be zero, inflow being positive, and a

nodal pressure or hydraulic-grade-line elevation. The elements connected at the junction may be any system facilities, such as valves, pumps, or pipelines.^{14,37} In this section only a junction of pipelines is considered, with a potential nodal flow, Q_n . There are two types of junctions or nodes:

1. A constant or a prescribed pressure (i.e., a known value as a function of time, in which case the nodal flow must be a free variable)
2. A constant or a forced flow, in which case the junction pressure must be a free variable.

Figure 3-9 shows a schematic of a branching connection with a nodal flow and four pipelines. A continuity equation is written at the junction summing the inflow, which must add to zero at any instant.

$$\sum Q_{in} = \sum Q_p + Q_n = 0 \quad (3-41)$$

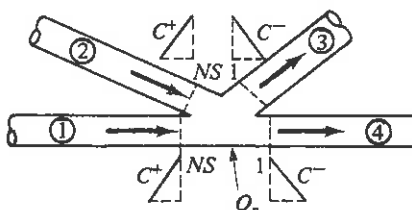


Figure 3-9 Pipeline junction.

In Eq. (3-41), $\sum Q_p$ is the summation of all instantaneous pipeline flows. When minor effects are neglected the energy equation requires a common pressure head in each element at the junction:

$$H = H_{1,NS} = H_{2,NS} = H_{3,1} = H_{4,1} \quad (3-42)$$

The compatibility equations are also available in each pipe: Eq. (3-21) for pipes 1 and 2, and Eq. (3-22) for pipes 3 and 4.

For a junction with known pressure head, and therefore unknown nodal flow, such as at a reservoir or pressure tank, the pipeline flows are determined directly from appropriate use of Eqs. (3-21) and (3-22), and the nodal flow is then determined directly from Eq. (3-41).

At a junction with known Q_n (may be zero), and therefore an unknown pressure head, the compatibility equations are written in the following form:

$$Q_{1,NS} = \frac{C_{P_1}}{B_{P_1}} - \frac{H}{B_{P_1}}$$

$$Q_{2,NS} = \frac{C_{P_2}}{B_{P_2}} - \frac{H}{B_{P_2}}$$

$$-Q_{3,1} = \frac{C_{M_3}}{B_{M_3}} - \frac{H}{B_{M_3}}$$

$$-Q_{4,1} = \frac{C_{M_4}}{B_{M_4}} - \frac{H}{B_{M_4}}$$

The summation of these equations gives

$$\sum Q_p = S_C - S_B H \quad (3-43)$$

in which $S_C = \sum C_P/B_P + \sum C_M/B_M$ and $S_B = \sum (1/B_P) + \sum (1/B_M)$ and includes all the pipelines connected to the junction. Substitution into Eq. (3-41) yields an equation form similar to the compatibility equations to compute the pressure head:

$$H = C_n + B_n Q_n \quad (3-44)$$

in which $C_n = S_C/S_B$ and $B_n = 1/S_B$. The compatibility equations then yield the flow in each pipe. This method may be applied to any number of pipes, including the series connection. This concept of a general junction is extended to include nonpipe elements in the next section and in Chapter 6.

Parallel Pipelines and Networks

Since networks and looped pipes consist of series and branching connections (i.e., no general junctions), no new boundary conditions are needed to develop a solution procedure to handle complicated network configurations.

Sectioning for Piping Systems

In dealing with complex piping systems of two or more pipes, it is necessary that the time increment be taken equal for all pipes. This involves a certain amount of care in the selection of Δt and the number of reaches N_J in each of J pipes. In each pipe it is required that

$$\Delta t = \frac{L_J}{a_J N_J} \quad (3-45)$$

in which N_J is an even integer. It is quickly realized that this relation probably cannot be exactly fulfilled in most systems. A few practical options exist to help with this constraint in the selection of an acceptable time-step size. In addition to the requirements of Eq. (3-45) other factors also influence the selection of time-step size. These include the degree of detail being sought in the transient response. It is not cost-effective to utilize a time step of 0.01 s if detail at 0.1 s is adequate for evaluation and if it describes the behavior adequately. The time-step size must be small enough to represent adequately the response of other facilities in the system. This is particularly important when dealing with dynamic elements, as discussed in Chapter 6. The limits on distance-interval lengths, thus time-step size, in connection with accurate friction modeling is presented in Sec. 3-7.

Some of the options for the treatment of multipipe systems in which it is difficult to satisfy Eq. (3-45) are listed. Prudent engineering judgment is needed in deciding which option is preferred for a given application since, except for item 1, each introduces an approximation.

1. Use the algebraic concepts presented in Sec. 3-9 to use small time steps appropriate to short pipes without computing interior points in longer pipes in the system.

That is, allow the characteristics to extend more than one Δx in longer pipes by reaching back further in time than one Δt .

2. Inasmuch as the wavespeed is probably not known with great accuracy, it may be permissible to adjust a_1, a_2, \dots , slightly, so that even integers N_1, N_2, \dots , may be found. In equation form this may be expressed

$$\Delta t = \frac{L_j}{a_j(1 \pm \psi_j)N_j} \quad (3-46)$$

in which ψ_j is a permissible variation in the wavespeed, always less than some maximum limit of, say, 0.15. By starting with a short pipe, one can generally satisfy Eq. (3-46). In general, a slight modification in wavespeed is more preferable than discarding or adding pipe lengths to satisfy the requirement.

3. In the simulation model, relocate junctions, delivery points, physical location of high or low elevation points, and so on, modest distances along a line to better accommodate the requirements of Eq. (3-45). The timing of reflected and transmitted waves is influenced by these relocations, so caution and judgment are needed. Again it is not recommended that pipe lengths be added or discarded.
4. A disproportionately short pipe in a system may be particularly troublesome inasmuch as the use of Δt determined by its length in Eq. (3-46) would give an uneconomically small Δt from a computing standpoint. It may be possible to treat such a short pipe as if the fluid were incompressible (i.e., as a lumped element). This option is discussed in Chapter 6.
5. The interpolation scheme, discussed in Chapter 4, is also an alternative to ease the constraint of Eq. (3-45). However, the numerical solution quickly loses accuracy for large linear interpolations.

Approximation to Variable-Property Series System

A system with numerous minor changes in properties may be approximated by use of an "equivalent" uniform reach length that spans minor discontinuities. If the changes in pipeline properties, such as pipe-wall thickness, diameter, and so on, are minor, the transient flow response predicted by use of this approximation is likely to be quite satisfactory for engineering purposes. The procedure involves the use of variable reach lengths along the system, with mean properties used in each reach such that the numerical requirement of a common time step is maintained.⁹ The wave travel time of the physical system is maintained by using the actual total system length ($\sum \Delta x_i = \sum L_j$) and an equivalent wave propagation velocity a_{e_i} given by

$$\frac{\Delta x_i}{a_{e_i}} = \sum \frac{L_j}{a_j} \quad (3-47)$$

In this equation Δx_i and a_{e_i} refer to the i th reach length and equivalent wavespeed, respectively, and L_j and a_j refer to the actual pipeline characteristics for the portions of the system included in reach i . The momentum flux weighed over the entire system

$\rho Q V_i \Delta x_i = \rho Q^2 \Delta x_i / A_{e_i}$ also is maintained in the two systems.²² Inasmuch as the actual system length is maintained in the approximate model, the cross-sectional area is determined by

$$\frac{\Delta x_i}{A_{e_i}} = \sum \frac{L_j}{A_j} \quad (3-48)$$

in which A_{e_i} is the equivalent area, sized so that the mass of fluid in length Δx_i has the same momentum as the fluid in the corresponding portion of the actual system. In Eqs. (3-17) to (3-22) the equivalent characteristic impedance B of the reach is defined by use of Eqs. (3-47) and (3-48),

$$B_{e_i} = \frac{a_{e_i}}{g A_{e_i}} = \frac{1}{g} \frac{\sum (L_j / A_j)}{\sum (L_j / a_j)} \quad (3-49)$$

The same head loss in steady flow is maintained in the two systems. An equivalent resistance coefficient for the i th reach is defined as

$$R_{e_i} = \frac{f_{e_i} \Delta x_i}{2g D_{e_i} A_{e_i}^2} = \sum \frac{f_j L_j}{2g D_j A_j^2} \quad (3-50)$$

The "equivalent" system does not allow for partial reflections at the physical discontinuities in the actual system, or does it maintain the correct distribution of inertial or frictional forces, or elastic effects. However, when used with full knowledge and understanding of the assumptions, it is often a satisfactory approximation in systems with minor discontinuities.

Use of Staggered Grid

The characteristics grid in Fig. 3-2, utilized in the development of the numerical method in this chapter, is based on the use of a diamond-shaped staggered grid. This is differentiated from the double grid of characteristics that is popularly used. Clearly, both approaches use the same time step-distance interval rectangular grid. Some of the considerations in choosing between the methods are presented.

The double grid of characteristics carries along two totally independent calculations as time progresses during a transient. This is the case in a single pipeline with any number of reaches or in a series system with even or odd numbers of reaches in each pipe. This can be verified by studying the results of an analysis of an instantaneous transient in a system. The results when studied at any computing section will show pairs of identical data in time, even in the presence of large viscous losses. This property has to be interpreted as a duplication in computing effort to obtain a specified degree of accuracy.

The staggered grid avoids this duplication and as such should be more cost-effective for the same accuracy. However, it has the requirement of an even number of reaches in each pipeline, a condition that may be a penalty in computing effort in some situations. The penalty is most noticeable in examples in which only one reach is used in the double grid, a case that would require two reaches in the staggered grid. Since in

most studies pipes have more than one reach, the reduced computing effort for the same accuracy in the staggered grid is viewed as a significant benefit.

If $\Delta t = L/Na$ for each method, the number of section-time step computations to reach a given duration of a transient, T , measures the computing effort. For the same accuracy the effort is $(N + 1)T/\Delta t$ for the double grid vs. $(N + 1)T/(2\Delta t)$ for the staggered grid, that is, half the effort in the latter. For the same detail at the boundaries (i.e., Δt for each method), the effort is $(N + 1)T/\Delta t$ for the double grid vs. $(2N + 1)T/\Delta t$ for the staggered grid, that is, almost double the effort for the latter. For the same computing effort in the two methods the staggered grid would use approximately $\sqrt{2}$ times the number of reaches used in the rectangular grid and would produce a more accurate modeling of the energy loss term in the compatibility equations.

3-6 General Systems

When valves, pumps, surge devices, and so on, are introduced into the piping network to form a more general system it is helpful to visualize the total system to consist of (1) junctions or nodes, and (2) system facilities or elements consisting of pipeline elements and nonpipe elements. The physical system is then schematized for numerical study into a network of nodes and elements. Several benefits are derived generalizing complex systems in this manner. A few nondynamic nonpipe elements are discussed in this section.

General Junction

The general junction equations in Section 3-5 are expanded to include nonpipe elements.^{14,37} Figure 3-10 shows a general junction with the nodal inflow and a number of different elements, including pipelines and nonpipe elements. The continuity equation Eq. (3-41) is written to include the summation of all instantaneous nonpipe flows, $\sum Q_e$:

$$\sum Q_{in} = \sum Q_p + \sum Q_e + Q_n = 0 \quad (3-51)$$

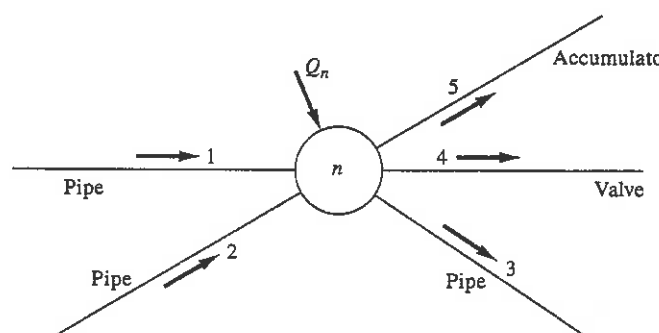


Figure 3-10 General junction.

Sec. 3-6 General Systems

With the assumption of common pressure head at the junction at any instant, Eq. (3-44) is modified to include the element flows:

$$H = C_n + B_n Q_n + B_n \sum Q_e \quad (3-52)$$

This equation contains three variables, $\sum Q_e$, H , and Q_n , with either H or Q_n having to be specified at each junction. Coefficients C_n and B_n incorporate the combined behavior of all the pipelines at the node. The form of the equation is most useful in general networks, as will be noted in later chapters.

Valve or Orifice

Valves or orifices may be located within a given pipeline, between two different lines, at reservoirs, at pipeline terminations, or in any number of other positions in systems. Additionally, the opportunity for flow reversal should be available. A more complete treatment of a valve or orifice than in Sec. 3-3 is needed. Figure 3-11a shows a valve between two pipelines, and Fig. 3-11b shows a schematic representation of the valve with nodes a and b as the interconnecting junctions on both sides of the valve. Use of the steady-state orifice equation neglects any inertia effects in accelerating or decelerating flow through the valve opening and also implies that there is no opportunity for a change in the volume of fluid stored in the valve body. For positive flow, Fig. 3-11b, with $H_{1,NS} = H_a$ and $H_{2,1} = H_b$, the orifice equation is

$$Q_{1,NS} = Q_{2,1} = Q_v = \frac{Q_0 \tau}{\sqrt{H_0}} \sqrt{H_a - H_b} \quad (3-53)$$

in which H_0 is the steady-state drop in hydraulic grade line across the valve with a flow of Q_0 when $\tau = 1$. With $Q_{1,NS} = Q_v$, Eq. (3-52) reduces to Eq. (3-21) in pipe 1, and with $Q_{2,1} = Q_v$ it reduces to Eq. (3-22) in pipe 2, since only one pipeline exists on each side of the valve and $Q_n = 0$ at both nodes. When combined with Eq. (3-53), a quadratic equation results which may be solved to yield

$$Q_v = -C_v(B_{P_1} + B_{M_2}) + \sqrt{C_v^2(B_{P_1} + B_{M_2})^2 + 2C_v(C_{P_1} - C_{M_2})} \quad (3-54)$$

in which $C_v = Q_0^2 \tau^2 / 2H_0$. For flow in the negative direction the orifice equation is

$$Q_{1,NS} = Q_{2,1} = Q_v = -\frac{Q_0 \tau}{\sqrt{H_0}} \sqrt{H_b - H_a} \quad (3-55)$$

and when combined with Eqs. (3-21) and (3-22), the solution is

$$Q_v = C_v(B_{P_1} + B_{M_2}) - \sqrt{C_v^2(B_{P_1} + B_{M_2})^2 - 2C_v(C_{P_1} - C_{M_2})} \quad (3-56)$$

An examination of the equations shows that a negative flow is possible only if $C_{P_1} - C_{M_2} < 0$. Thus Eq. (3-54) is used if $C_{P_1} - C_{M_2} \geq 0$, and Eq. (3-56) is used if $C_{P_1} - C_{M_2} < 0$. Once the flow is known, Eqs. (3-21) and (3-22) are used to find the hydraulic grade line.

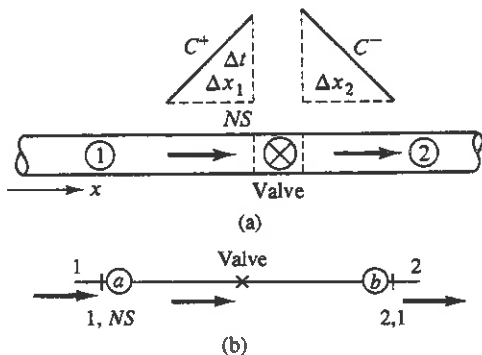


Figure 3-11 Valve-in-line.

If the valve is discharging to a reservoir rather than into pipe 2, node b becomes a fixed pressure node with $H_b = \text{constant}$ and with nodal flow $Q_b = -Q_v$. Equations (3-54) and (3-56) may be written

$$Q_v = -SC_v B_{P_1} + S\sqrt{(C_v B_{P_1})^2 + 2SC_v(C_{P_1} - H_b)} \quad (3-57)$$

with S being $+1$ or -1 , depending on the sign of $C_{P_1} - H_b$.

Valves with low-loss coefficients (large $C_D A$) may have significant flow with very little pressure drop during a transient event. The second term under the radical in Eqs. (3-54) and (3-56) may become very small with respect to the first term. When this happens numerical computations may yield erratic results, even if double precision is used. In Sec. 8-2 a linearization is employed to avoid this potential problem. Simpson and Bergant²⁶ have addressed this issue as well.

Kinetic Energy and Minor Loss

If the kinetic energy is a significant part of the total energy, or if a minor loss is important at a boundary in a system, it is necessary to use the energy equation. The pipe entrance condition at a reservoir is used as an example. The energy and hydraulic grade lines are shown in Fig. 3-12a and b for flow in either direction at the reservoir, and the schematic representation is shown in Fig. 3-12c. If the pipe entrance loss coefficient is K , and with $H_a = H_R$, $H_b = H_1$ and $Q_a = Q_1$, the energy equation is

$$H_R = H_1 + (1 + K)\frac{Q_1^2}{2gA^2} \quad (3-58)$$

When this equation is combined with Eq. (3-22), a quadratic equation results that yields the positive flow into the pipe. For reverse flow (Fig. 3-12b) all kinetic energy is lost and the boundary equation is

$$H_1 = H_R = H_a = H_b \quad (3-59)$$

A direct solution for Q_1 is possible by use of Eq. (3-22).

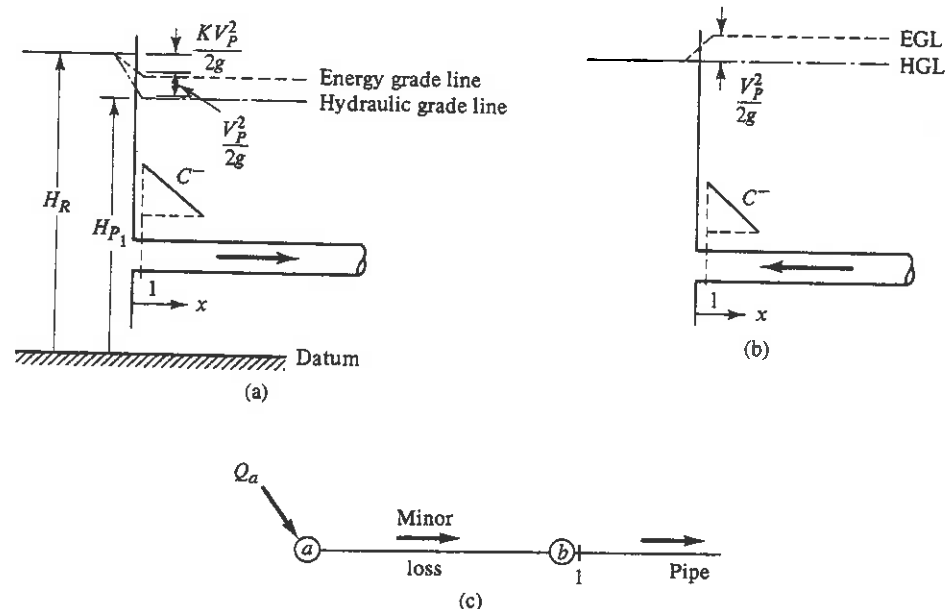


Figure 3-12 Minor loss and kinetic energy.

Centrifugal Pump Startup

During pump startup, if the pump and motor come up to speed in a known manner, the influence of the speed change can easily be included in a boundary relationship by using homologous conditions. The homologous conditions for a turbomachine of fixed size are

$$\frac{H}{\alpha^2} = \text{const} \quad \frac{Q}{\alpha} = \text{const}$$

in which H is the head rise across the pump and α is the speed ratio, normalized by use of the rated speed. For pump startup α often may be assumed to vary from 0 to 1 linearly. In homologous form the curve for the pump in Fig. 3-13 takes the form

$$H_{2,1} - H_{1,NS} = \alpha^2 H_S + a_1 \alpha Q_{1,NS} + a_2 Q_{1,NS}^2 \quad (3-60)$$

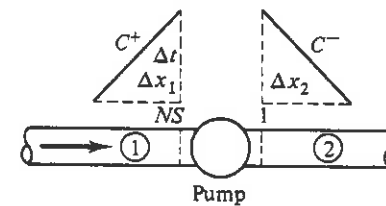


Figure 3-13 Centrifugal pump.

Eq. (3-60) is similar in form to the parabolic relation in Eq. (3-30). If the speed were constant at rated condition ($\alpha = 1$), Eq. (3-60) reduces to Eq. (3-30). When Eq. (3-60) is combined with Eqs. (3-21) and (3-22) the discharge may be determined as

$$Q_{1,NS} = \frac{B_{P_1} + B_{M_2} - a_1\alpha}{2a_2} \left\{ 1 - \left[1 - \frac{4a_2(\alpha^2 H_S + C_{P_1} - C_{M_2})}{(B_{P_1} + B_{M_2} - a_1\alpha)^2} \right]^{1/2} \right\} \quad (3-61)$$

If the pump is operating directly from a suction reservoir, the equation may be simplified by the elimination of the C^+ compatibility equation in the suction pipe.

Example 3-4

Prepare the equations to handle the pump boundary condition shown in Fig. 3-14. The pump is to be started with a linear speed rise to rated speed in t_s seconds. The undamped check valve permits flow in the positive direction only. When partially or fully open it is

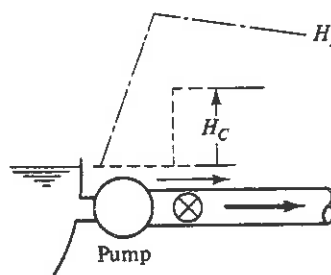


Figure 3-14 Pump and check valve.

assumed to have negligible head loss. Assume that the check valve opens instantaneously when the pump has developed enough head to exceed H_C , the initial static head on the downstream side of the valve (Fig. 3-14).

The equations for the boundary condition are

$$B = \frac{a}{gA}$$

$$C_M = H_2 - BQ_2 \quad B_M = B + R|Q_2|$$

$$\alpha = \begin{cases} \frac{t}{t_s} & \text{if } t \leq t_s \\ 1 & \text{if } t > t_s \end{cases}$$

If $\alpha^2 H_S \leq H_C$,

$$Q_1 = 0 \quad \text{and} \quad H_1 = C_M$$

If $\alpha^2 H_S > H_C$,

$$Q_1 = \frac{B_M - a_1\alpha}{2a_2} \left\{ 1 - \left[1 - \frac{4a_2(\alpha^2 H_S - C_M)}{(B_M - a_1\alpha)^2} \right]^{1/2} \right\}$$

$$H_1 = C_M + B_M Q_1$$

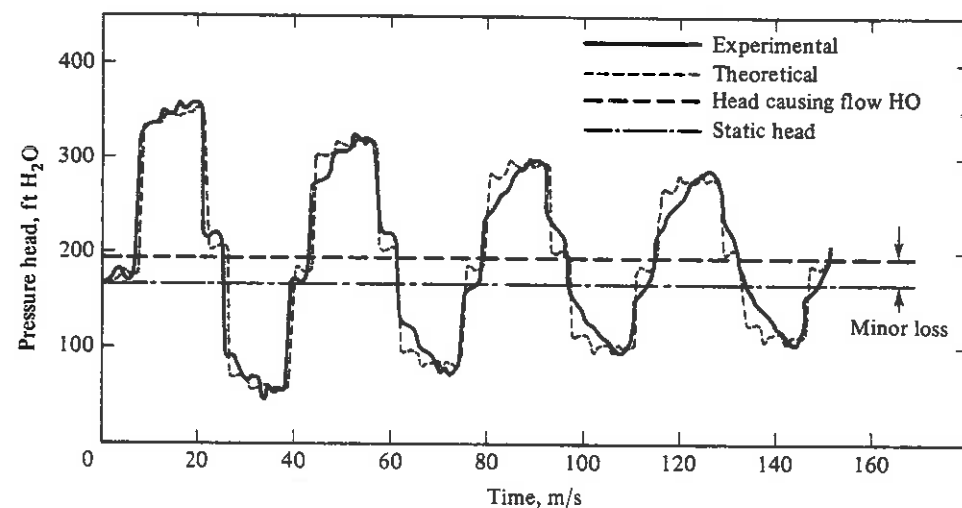


Figure 3-15 Experimental versus theoretical results in minor loss experiment.⁷

An experimental result from a system containing a concentrated minor loss is compared with results calculated using the method of characteristics in Fig. 3-15. Experiments were conducted in 40 ft of copper tubing, 0.5 in. ID, with three orifices concentrated at the midpoint between the reservoir and valve. A solenoid valve was used to initiate the pressure pulse. The pressure transducer was located 10 ft from the valve. Additional comparisons between experimental and computed results appear elsewhere in the book: for example, in Chapters 8, 9, 12, and 13. Other boundary conditions, most of them more complicated, are treated in Chapters 6, 7, and 10.

3-7 High Friction, Attenuation, and Frequency Dependence

In unsteady-flow cases in which energy losses due to viscous effects are very important, the approximation introduced in the integration of the friction term in the compatibility equations may be cause for concern. Examples may include long oil pipelines, cases of very high flow velocities, or small-diameter highly viscous flows. The consequence of inaccurate modeling of the friction term is likely to be an incorrect result, which may or may not be readily apparent.

Among other models the most commonly applied approximation assumes the flow constant, and equal to Q_A ,^{6,10,30,35,38} along the C^+ characteristic line (Fig. 3-2).

$$\int_{x_A}^{x_P} \frac{f Q^2}{2gDA^2} dx = R|Q_A|Q_A \quad (3-62)$$

This produces equations that are linear in the dependent variables, so it offers computational appeal. It is, however, of first-order accuracy and in extreme cases may produce an unstable solution. A stability study,³⁸ based on a linearized form of the equations, shows a necessary limit in discretization in order to have a stable solution utilizing Eq. (3-62)

$$\frac{f \Delta x \bar{Q}}{2 D A a} \leq 1 \quad (3-63)$$

in which \bar{Q} is an average flow. This criterion describes a fairly extreme example, and even with it satisfied, inaccurate results may be generated unless the left-hand side is considerably less than unity.

Other more accurate integration procedures that lead to compatibility equations that are nonlinear in Q have been suggested.³⁸ The error introduced by a particular approximation depends on the magnitude of each of the parameters in Eq. (3-63) and on the manner in which the flow rate changes along the characteristic line. As an example of the magnitude of the error, a linear variation of Q may be assumed along the characteristic line AP , $Q = Q_0 + bx$. When the integration of Eq. (3-62) is compared to the exact integration, an error of $Q_0 b \Delta x^2 + b^2 \Delta x^3/3$ is produced. A similar comparison utilizing the integration in Sec. 3-3 yields an error of $b^2 \Delta x^3/3$, whereas the nonlinear evaluations show a smaller error of $b^2 \Delta x^3/6$ or less, depending on the form of the evaluation.^{36,38}

A stability study similar to that used to produce Eq. (3-63) applied to the integration in Sec. 3-3, or to the nonlinear evaluations, shows these approximations to be stable for any magnitude of the friction term. However, each integration still represents an approximation to the differential equations, so the correct solution is not guaranteed. The accuracy of the solution generated by each of the models can always be improved by reducing the distance interval, Δx . However, there is a Δx_{\min} beyond which the benefit gained by a smaller distance interval is not noticeable in improved numerical results. In systems with major computational effort the objective is to use distance intervals larger than Δx_{\min} but shorter than a Δx_{\max} that produce an unacceptable error. A firm criterion for Δx_{\max} to produce an accurate solution based on the left side of Eq. (3-62) is not possible since any error is heavily dependent on the amplitude and frequency of the disturbance. As a guide, values of the left side of Eq. (3-63) below 0.15 should produce sufficiently accurate results for most applications when the integration in Sec. 3-3 is used.

Attenuation and Line Pack

The initial upsurge following flow stoppage, aV_0/g , is often referred to as the *potential surge*. In short pipelines with low friction a sudden closure of a valve causes the upstream flow to be brought to rest as the compression wave moves at acoustic speed through the line. In long pipelines, and in shorter high-friction cases, the total drop in hydraulic grade line over the pipeline length for the initial flow may be much more than the potential surge. In this case the passage of the compression wave does not bring the

flow to rest. The magnitude of the potential surge is lessened as it travels upstream. This reduction is called *attenuation*.²⁰ Inasmuch as the flow is stopped only partially with the passage of the compression wave, yet is stopped totally at the valve, an increase occurs in the mass stored, which is called *line packing*. The pressure continues to rise, the pipe wall expands, and the liquid is compressed.

This total process can be visualized by referring to Fig. 3-16. If it is first imagined that the initial head rise at the valve merely rises up the original hydraulic grade line as shown, it can be seen that the same slope of the hydraulic grade line exists following the passage of the wave. Thus the flow has been stopped completely at the valve, but it cannot remain stationary upstream from the valve because of the identical, but elevated, hydraulic grade line. Since the change in velocity at the wavefront is less than V_0 , the head rise is less (i.e., the potential surge is attenuated).

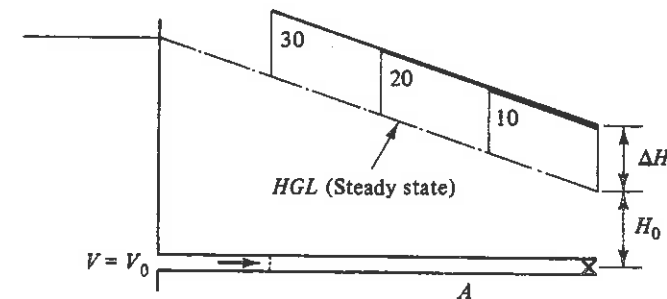


Figure 3-16 Incorrect hydraulic grade line for long pipeline.

Figure 3-16 is actually incorrect; attenuation of the wave front and rise in pressure behind the wave front are displayed more correctly in Fig. 3-17. The potential surge resulting from an abrupt flow stoppage is quite often a small percentage of the final maximum head rise. The locus of the head rise at the wave front is shown as a dashed line in Fig. 3-17 and is seen to approach the original hydraulic grade line asymptotically in the infinitely long line.

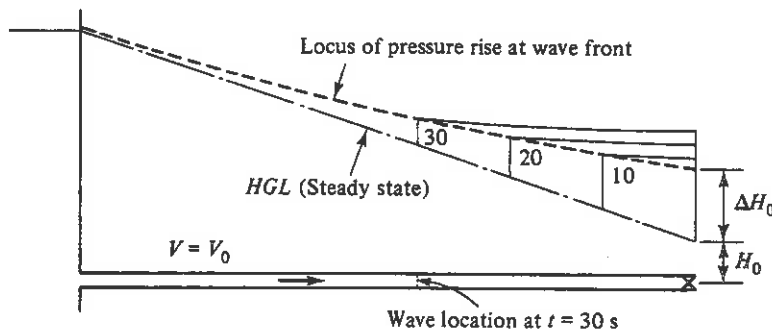


Figure 3-17 Attenuation in long pipeline.

The characteristics method with proper treatment of the friction term incorporates all the properties of the potential surge, attenuation, and line packing. Figure 3-18 shows the computer results of a sudden valve closure in a 125-mile-long, 30-in.-diameter pipeline. The initial steady-state velocity was 4.25 ft/s and the wavespeed was 3300 ft/s. At 200 s after valve closure, the attenuated wave reaches the upstream boundary and is reflected. The dashed lines indicate the extent of the pipeline influenced by the reflected wave as the grade line continues to rise. At 9 min after the valve closure, the hydraulic grade line has reached its maximum level and the forward velocity has been reduced to zero. The adverse grade line produces flow in the opposite direction. The surging condition continues until friction losses in the system cause the flow to come to rest.

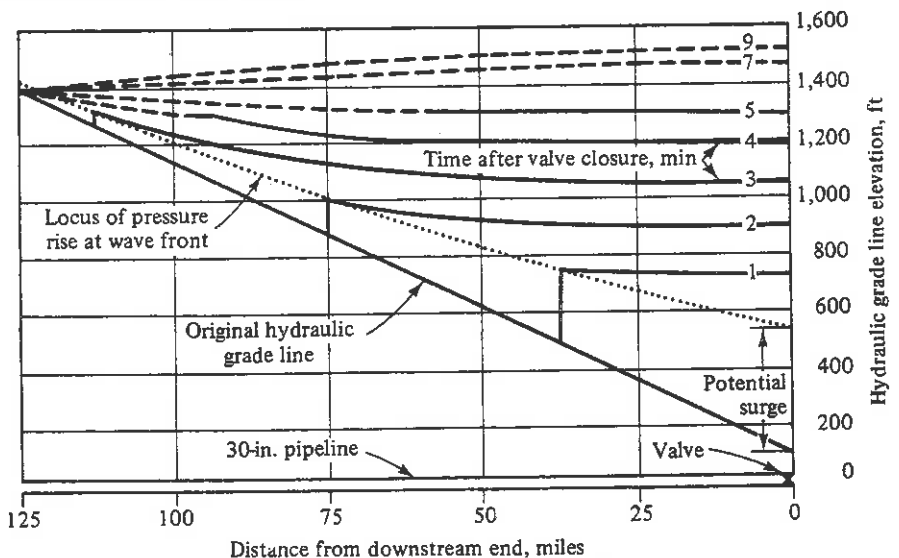


Figure 3-18 Results of computer solution of valve closure in long pipeline.¹³

Frequency-Dependent Friction

A graph of the pressure history at an abrupt valve closure in a reservoir-pipeline-valve system with large losses is shown in Fig. 3-19. The data for the dashed line labeled "steady-state friction" were obtained from a program such as SINGLE, modified for laminar flow viscous losses. Reasonable agreement between these data and the experimental record exists for the first $2L/a$ seconds; then the physical results show a more rapid decay, with increased rounding of the sharp corners as time progresses. Ultimately, the physical record takes on the appearance of a decaying sine wave. This lack of agreement after early time in the record suggests that the numerical model is not providing a proper description of the transient behavior of the physical system. Some of the factors that have not been included in the model and that may be influencing the physical wave decay include: nonlinear inelastic behavior of the pipe wall, nonlinear inelastic behavior of the fluid, free gas in the liquid or release of dissolved gases during the low-pressure side of the cycle, frequency-dependent wall properties, or

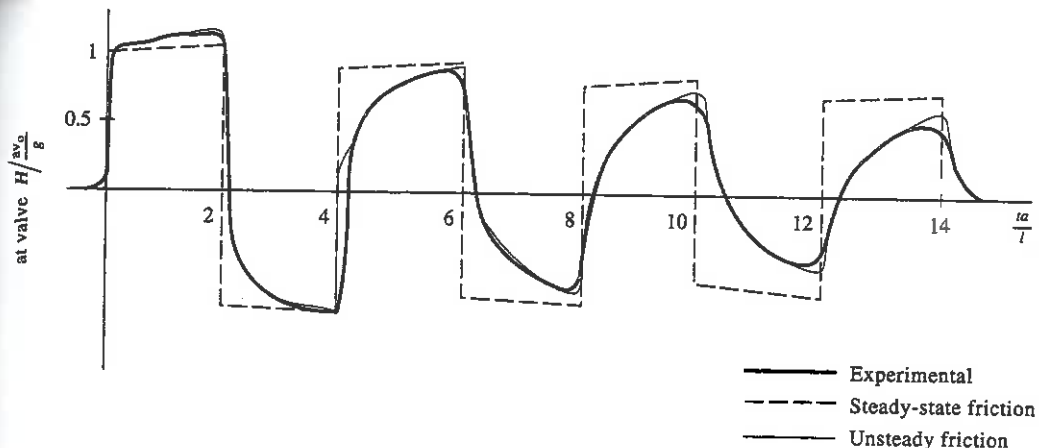


Figure 3-19 Pressure history at valve after instantaneous valve closure.^{12,39}

frequency-dependent frictional losses in the fluid. At least in oscillating laminar flow the latter mechanism has been demonstrated as a major reason for additional losses and for dispersion of sharp wave patterns. A brief discussion³⁹ of frequency dependence follows. Some of the other reasons are addressed in other sections of this book.

In laminar flow the shear stress at the pipe wall is given by $\mu \partial u / \partial r$, with μ the viscosity and $\partial u / \partial r$ the velocity gradient at the wall. In unsteady flow the pressure gradient affects the fluid in the boundary layer and that in the central portion of the pipe differently. The velocity near the wall responds in phase with the pressure gradient since inertial forces are small and friction dominates, whereas in the central portion of the pipe the pressure gradient is in phase with the fluid acceleration since inertial forces dominate. As a result, the velocity gradient at the wall, and therefore the shear stress, will change before the mean velocity. This means that a friction term based on V^2 will not adequately model unsteady losses. For sine-wave pulsations in laminar flow a solution is available³³ for this behavior which provides a frictional loss that is frequency dependent. Zielke⁴⁰ used a weighting function applied to the time history of the unsteady flow at a section to achieve a time-domain solution with the method of characteristics. Trikha³¹ developed an approximate weighting function which offers the advantage of not requiring storage of the entire flow history. Various high- and low-frequency approximations have also been made.^{1,21}

The extension of this work to turbulent flow modeling has not been rapid, although extensive efforts have been placed in periodic flows. For periodic flow with zero mean velocity, Kongeter¹⁵ shows that the influence of frequency decreases with increasing Reynolds number and the influence of the unsteadiness of flow increases with the dimensionless frequency, $D\sqrt{w\rho/\mu}$. A series of papers by Ohmi et al.²¹ provide additional information on periodic flows. Brekke,⁵ in a study of surge tank stability and turbine governing stability, utilized a frictional damping force consisting of both steady and dynamic terms. The dynamic term was a function of the steady flow friction loss coefficient, the cross-sectional area, the frequency, and the amplitude of the oscillations. This frequency-domain analysis was verified in full-scale tests in six hydro power plants that included rough, blasted tunnels, and penstocks and tunnels with steel linings. The cross-sectional areas ranged from 3 to 50 m² and the frequency ranged from 0.006 to 8.0 rad/s. Vardy and Hwang³⁴ successfully demonstrated the use of a quasi two-dimensional

model of transient flows in pipes using the one-dimensional method of characteristics in concentric cylindrical annuli. The method relates well to Zielke's model⁴⁰ even in certain regions of turbulent flow. Arlt² produced a reasonable correlation in transient turbulent pressure pulse transmission through a stagnant fluid in a pipe by utilizing an empirical weighting factor.

Until such time as a more complete time-domain turbulent flow model is developed, the quasi-steady modeling proposed in Sec. 3-3 is the only feasible solution for general transients. Fortunately, the model is normally sufficiently accurate during early time in a transient. The frequency-dependent influence is most pronounced at high frequencies and in highly viscous flows, and is less significant at high Reynolds numbers.

3-8 Localized Column Separation

During transient liquid flows in pipelines, when the pressure drops to vapor pressure vaporization occurs. Vapor bubbles may be physically dispersed homogeneously, or collected into single or multiple void spaces, or a combination of the two. The result is referred to as liquid column separation and its occurrence may have a significant impact on subsequent transient response in the system. The presentation in this section deals with cases which are dominated by inertial forces, that is, cases in which the flow dynamics would cause the pressure to drop below vapor pressure if it were not for the pressure constraint at vaporization. Vaporization also occurs at elevated temperatures without significant pressure change in a process that is largely thermodynamically controlled. Many flow situations also have free gases entrained with the liquids, or dissolved gases that evolve when the pressure drops below saturation pressure. This leads to a two-component flow of gas and liquid that is not considered in this section but is addressed in Chapter 8.

The consequences of vaporization are a reduction in the effective wave propagation speed in the vaporized region of the pipeline and a constraint on the low-level pressures. The most common concerns in analyzing this type of liquid vaporization are prediction of the extent of the column separation and prediction of the magnitude of the pressure rise when the vapor bubbles collapse. In cases of localized vaporization such as at pipeline terminations or at physical high points in the pipeline, a simple analysis procedure provides a reasonable simulation of the behavior. This is called a discrete-vapor-cavity model and is characterized by vapor cavities forming at computing sections along the pipe, with the method of characteristics applied in pure liquid between the computing sections.^{16,27,38} It assumes the pipe reach between computing sections to remain filled with liquid during the event. Although the method is easily implemented, and reproduces faithfully many of the essential features of a physical event, it has a deficiency. Numerical oscillations are generated during the existence of multicavities in the pipeline. Once developed they tend to persist in a simulation and may result in unrealistic high-frequency pressure excursions that discredit the overall value of the results. Continuity and momentum principles are satisfied in the system, however, and the general wave pattern is maintained. The source of the semirandom fluctuations is wave reflections off multicavities in the system, the latter effectively becoming

fixed pressure boundary conditions. With the constant pure liquid wavespeed in the reaches, sharp wavefronts may be generated that are not always physical. In systems with clearly defined isolated cavity positions, acceptable results are normally produced. Alternatives to this model are provided in Chapter 8, but due to the simplicity of the discrete-vapor-cavity model and its ability to handle many problems adequately, it is presented in this section.

Discrete-Vapor-Cavity Model

The premise for this computational scheme is that whenever a section has a pressure at or below vapor pressure, the section may be treated as a fixed pressure location. The pressure is held at vapor pressure, inflow and outflow are computed, and a cavity is permitted to grow and collapse in accordance with conservation of mass principles at the section. The assumption of vaporous cavities concentrated at computing sections is reasonable if the system has elevated regions where vapor pockets are able to coalesce, or if only a portion of the system is subject to vapor pressure. The size of a vapor cavity must be considerably less than the volume within a distance interval so that liquid occupies the reach over which the characteristic line extends at full liquid wavespeed.

During the existence of the cavity, if Q_U is the average inflow to the section, and Q the average outflow during the time Δt , the cavity volume is given by $\sum(Q - Q_U)\Delta t$, where the summation is over the time from inception of vapor pressure. At the time the cavity vanishes, the head rise, due to contact of the two liquid columns, is given by

$$\Delta H = \frac{a}{2gA}(Q_U - Q) \quad (3-64)$$

From this point on, as long as the hydraulic grade line remains above vapor pressure the liquid remains continuous and a standard liquid transient solution may be used. The process may repeat itself over several cycles and at several sections.

The procedure is readily handled within the framework of the staggered grid method of characteristics. By referring to Fig. 3-20, an internal boundary condition is established at section i , as follows:

1. Set $H_i = Z_i - \bar{H} + H_v$.
2. Calculate Q_{Ui} and Q_i (Fig. 3-20).
3. Calculate V_{cav} , the size of the cavity.

As long as the cavity size is positive, vapor pressure persists. As soon as the cavity size becomes zero or negative:

1. Set $V_{cav} = 0$.
2. Calculate $H_i = (C_P B_M + C_M B_P)/(B_P + B_M)$.
3. Proceed as usual with an internal section.

During the existence of the cavity its size is calculated at each computational step from the average flow of liquid out of and into the section. Z_i is the elevation of the top of the pipe at the section, based on the same datum as the hydraulic grade line. H_v is

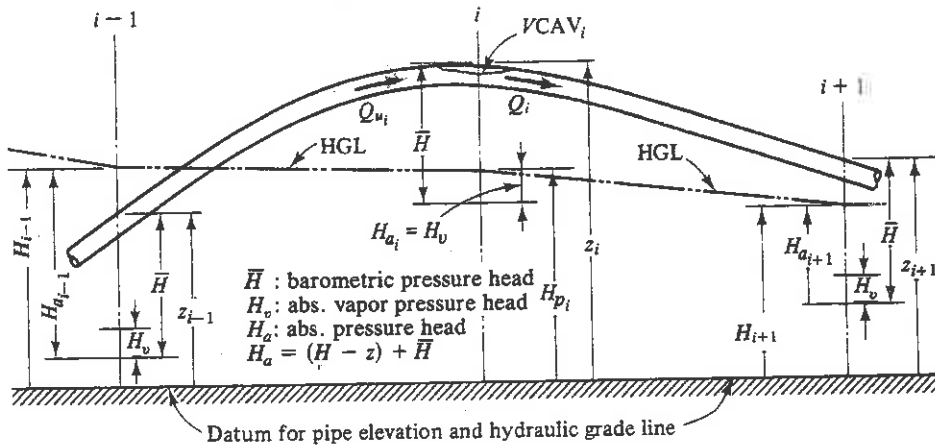


Figure 3-20 Definition sketch for column separation and absolute heads.

the absolute vapor pressure head, a positive number. \bar{H} is the barometric pressure head. The absolute pressure head is also defined in Fig. 3-20, $H_a = \bar{H} - Z + H$. Figure 3-21

```

DO 110 I1=2,3
DO 100 I=I1,N,2
    QUO=QU(I)
    QO=Q(I) ?
    CP=H(I-1)+QU(I-1)*B
    CM=H(I+1)-QU(I+1)*B
    BP=B+R*ABS(Q(I-1))
    BM=B+R*ABS(QU(I+1))
    IF (VCAV(I).GT.0.) GOTO 80
    H(I)=(CP*BM+CM*BP)/(BP+BM)
    IF (H(I).LT.Z(I)-HB+HV) GOTO 70
    GOTO 90
 70   H(I)=Z(I)-HB+HV
 80   QU(I)=(CP-H(I))/BP
    Q(I)=(H(I)-CM)/BM
    VCAV(I)=VCAV(I)+DT*(Q(I)+QO-QU(I)-QUO)
    IF (VCAV(I).GT.0.) GOTO 100
    VCAV(I)=0.
    H(I)=(CP*BM+CM*BP)/(BP+BM)
 90   QU(I)=(CP-H(I))/BP
    Q(I)=QU(I)
100  CONTINUE
    IF (N.EQ.2) GOTO 120
110  CONTINUE
120  CONTINUE

```

Figure 3-21 Internal section calculation with column separation.

Sec. 3-9 Algebraic Method

lists the FORTRAN code for an internal section calculation. End conditions are handled similarly.

An experimental record¹⁷ of an isolated cavity formation at the downstream side of a valve is shown in Fig. 3-22. These data were taken in a 2-in. plastic pipe with 31.3 ft of length downstream of the valve. The wavespeed was measured to be 2070 ft/s, and the initial fluid velocity in this case was 4.58 ft/s. The duration of existence

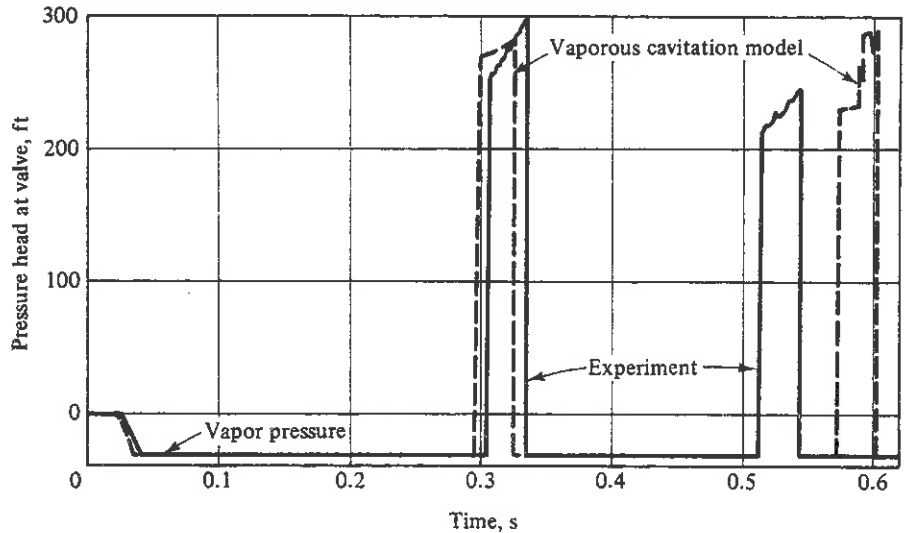


Figure 3-22 Column separation downstream from valve.

of the first cavity at the valve may be seen to be about $17L/a$ seconds. The vaporous cavitation model described above was used to model this experiment, and the results are presented in Fig. 3-22. It may be seen that the timing and magnitude of the pressure rise upon collapse of the first cavity are in reasonable agreement. The calculated maximum size of the cavity was about 0.0058 ft^3 . However, the growth and collapse of the second cavity in experiment and numerical model are clearly not in agreement. The physical measurements indicate considerably more dissipation than the analytical study, and a short-duration pulse appears in the numerical results that is not present in the experimental record.

3-9 Algebraic Method

In many low-friction systems, and in systems with sensitive dynamic boundary conditions that require extremely small time steps, an algebraic representation of the compatibility equations offers appeal. In this procedure the characteristic lines extend more than one reach, generally the full pipe length, but time steps are utilized that are related by integers to L/a seconds. The algebraic equations are also an integral part of the valve stroking developments in Chapter 9.

The algebraic form of the equations have the following properties²⁹:

1. They are compatibility equations applied over one or more reaches of a pipe.
2. Time is indicated by an integer subscript.
3. The time increment is $\Delta t = L/(Na)$, with N an integer.
4. The section numbers along the system may also be subscripted or, on simple systems, the location of head and discharge may be identified by a change in variable name (e.g., H_A, Q_A).

Advantages of these equations over the usual method are:

1. They are normally applied over several reaches, with no need to calculate the transient at the intervening sections.
2. They are computationally efficient for solution of multipipe systems such as networks, as interior point calculations are avoided.
3. They use a small $\Delta t = L/(Na)$, so boundary condition detail is preserved.
4. They may be solved in the spatial direction backward in time, a necessary step in valve stroking.
5. They are applicable with N being either an even or an odd integer in each pipe. If the staggered grid is adopted, an even number is required. If the rectangular grid is adopted, N may be even or odd. For the same end condition time-step detail the computational effort is the same with either method. The rectangular grid is adopted here so that N may be either even or odd.
6. They are useful for hand calculations, pocket calculators, and microcomputers.
7. Information needs to be preserved at only a small number of sections.

Disadvantages in the use of the equations are:

1. Since the characteristic lines are generally extended over more than one reach, the friction term may not be as accurate in high-friction systems (see Sec. 3-7).
2. Information must be retained from time steps extending backward in time more than one time step, a condition that could result in more computer storage.

Equations with Time as Subscript; Continuous Storage

Several organizational concepts are helpful for numerical studies, although not absolutely necessary. The schematic diagram of a series system is shown in Fig. 3-23 with nodes at pipe ends, continuous sectioning, and an integer number of normal reaches for each pipe, $N = L/(a \Delta t)$. It is noted that each pipe needs only two computational sections, one at each end. With the data shown, the equations extending the full pipe length become:

$$C^+ : H_{2,K} = H_{1,K-N_1} - B_1(Q_{2,K} - Q_{1,K-N_1}) - R_1|Q_{1,K-N_1}|Q_{2,K} \quad (3-65)$$

$$C^- : H_{3,K} = H_{4,K-N_2} + B_2(Q_{3,K} - Q_{4,K-N_2}) + R_2|Q_{4,K-N_2}|Q_{3,K} \quad (3-66)$$

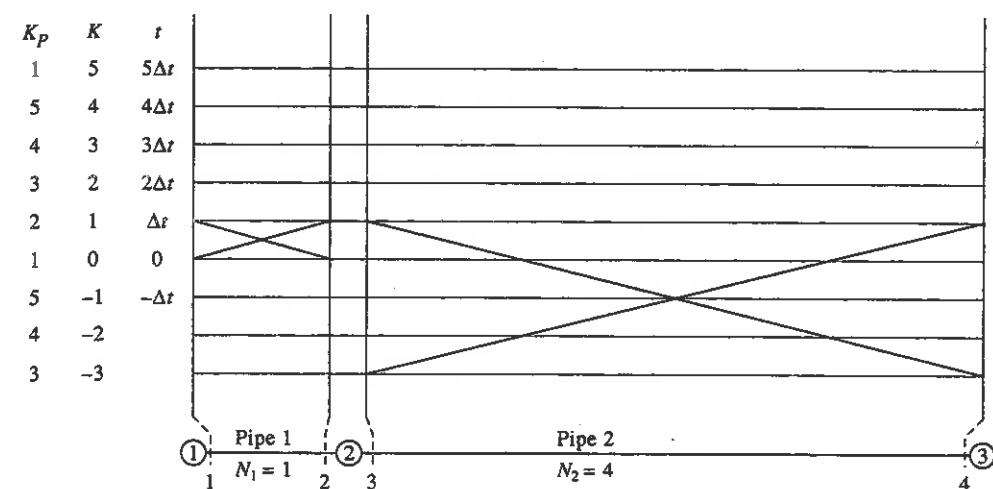


Figure 3-23 *xt* diagram for algebraic equations in series system.

in which the first subscript indicates section number and the second indicates the time counter $K = t/\Delta t$. The resistance coefficient applies to the total pipe length, $R = fL/(2gDA^2)$.

In this example information must be retained in pipe 2 for $N_2+1 = 5$ computational steps. Since, for this system, pipe 2 characteristic lines extend back the farthest, $K_M = 5$. By utilizing a pointer K_P to identify the location of the current time step in the vectors H and Q , a rotational use of storage can be utilized effectively, without requiring assignment statements. This continuous use of storage is illustrated in Fig. 3-24 with reference to Fig. 3-23. Each of the variables H and Q is dimensioned to the size of the maximum value K_M in the entire system, $K_M = L/(a \Delta t) + 1$. The integer K is used as a counter for each time step, and K_P is used as a pointer to identify the position in the vector H or Q at which current values of the variables are stored. At each iteration when K is incremented, so is K_P , the value of the pointer. When K_P exceeds K_M , the value is set back to unity, so it points to the first position in the vector. In this manner, values of H and Q at each section are stored as subscripted variables in the positions indicated by values of K_P in Fig. 3-24, which refers to the system in Fig. 3-23. The value of K_P points to the values of the variables at the current time step. A few lines of code are shown in Fig. 3-24 to accomplish these steps. A pointer is also needed to identify subscripts of earlier values of H and Q at the remote ends of the characteristic lines. This is illustrated in the lower portion of the code. Integer K_B points back to identify the position in the vectors in each pipe. By starting the *xt* diagram $K_M - 1$ computational increments before the transient starts (Fig. 3-23), and storing the steady-state values, the equations may be solved at each pipe end, with the incorporation of boundaries and nodal conditions.

```
*****
K=K+1
T=DT*K
KP=KP+1
IF (KP.GT.KM) KP=1
*****
KB=KP-N(J)
IF (KB.LT.1) KB=KM+KB
*****
```

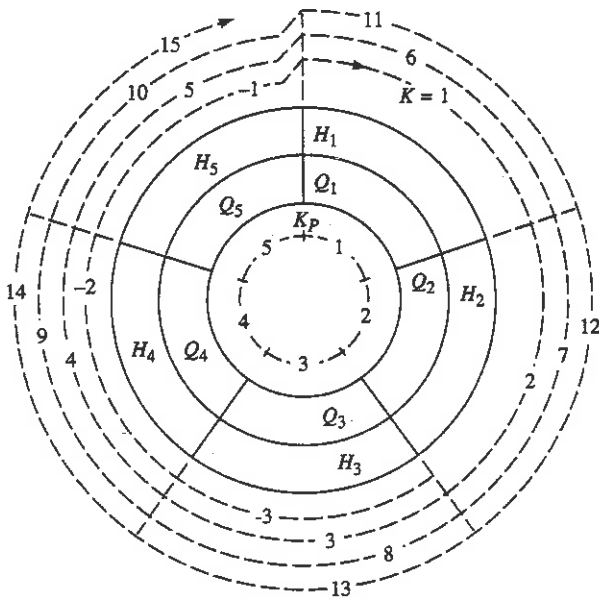


Figure 3-24 Continuous storage.

Indexing

Before introducing an example of the use of the algebraic form of the equations in multipipe systems, and to build upon the general systems concept introduced in Sec. 3-6, a discussion of data handling is helpful. An index vector is provided which offers one form of bookkeeping to describe the system topology. It is oriented around the nodes of the system and, for each node, the following information is summarized: the node number, the number of elements attached to the node, and for each element attached, the element number with a sign to indicate whether it is the upstream or downstream end of the element, and the number of the element section adjacent to the node. In this vector a minus sign is appended to the element number to designate that the upstream end of the element is attached to the node. This is consistent with a convention that states inflow to a node positive and outflow from a node negative. The form of the vector is: node number, number of elements, \pm element number, element section number adjacent to the node, \pm element number, element section number adjacent to the node, and so on. The specific vector for Fig. 3-23 follows:

$$1, 1, -1, 1, 2, 2, 1, 2, -2, 3, 3, 1, 2, 4$$

The first four numbers refer to node 1, which has 1 element attached; the element is number 1 shown as -1 since it is the upstream end; and the upstream section is number 1. The next six numbers describe node 2, which has two pipes attached. Each node in the system is repeated in the same pattern.

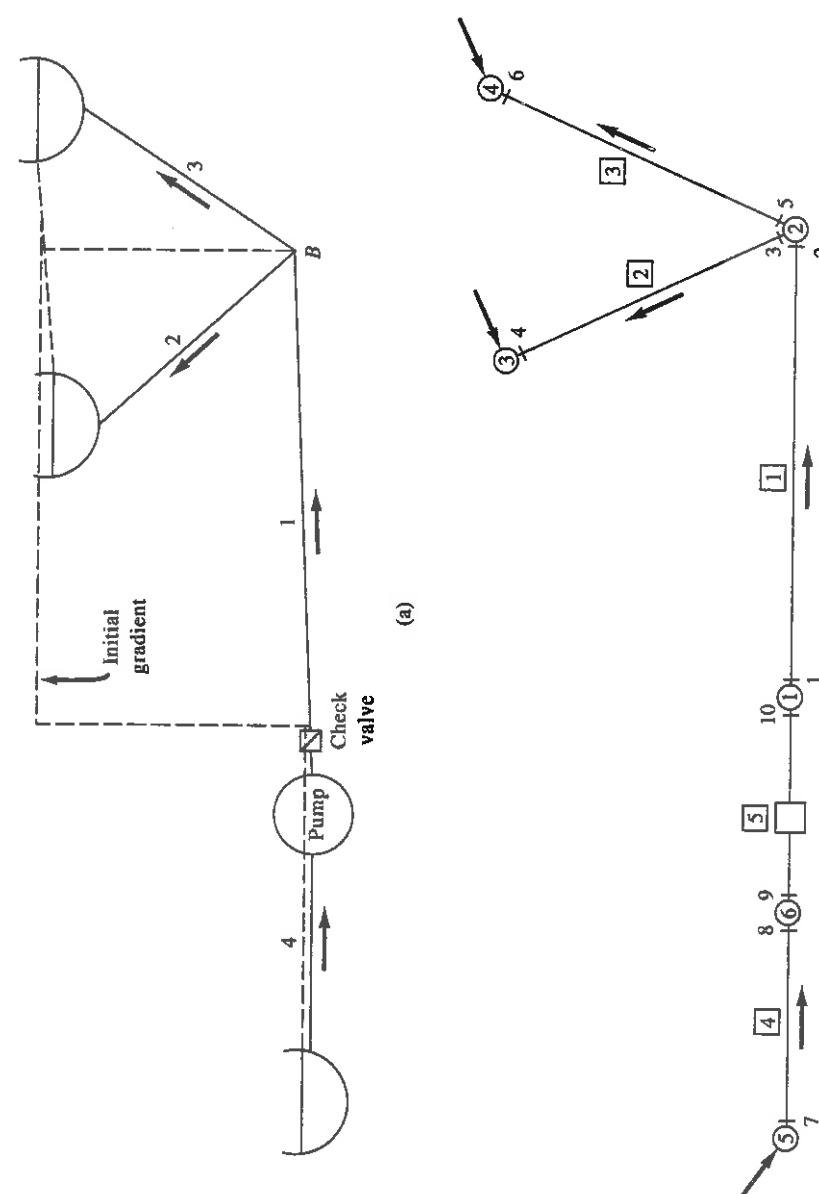


Figure 3-25 Branching system with pump and check valve. Pump startup by algebraic method.

The index vector does not include all of the information that is needed for the transient analysis, but it does provide the necessary data to enable calculations at junctions and boundaries. The physical parameters that describe each element are needed, as well as nodal information such as the nodal flow, pressure, elevation, and node type: fixed pressure (type 3) and fixed nodal flow (type 1). With systematic introduction of element and junction data an algorithm may be written to form the index vector in the program. In the example that follows the index vector is prepared externally and added to the input data.

Branching System with Pump Startup

The system shown in Fig. 3-25(a), in which initially the pump is shut off and steady flow occurs out of the upper reservoir, is used as an example. The pump is started and comes up to rated speed in T_s seconds (i.e., $\alpha = t/T_s$ for $t < T_s$, and $\alpha = 1$ for $t > T_s$). A lossless check valve at the pump opens when the pump produces enough head to exceed the initial head in pipe 1. Eventually, steady flow is established into the two upper reservoirs. Equation (3-60) is used to represent the head rise across the pump as a function of pump speed and flow.

A schematic diagram is shown in Fig. 3-25(b), with nodes and elements numbered. The elements are described as running from one node to another in the assumed positive flow direction. A FORTRAN program for this case is provided in the disk included in the back inside cover of this book. The pipeline lengths, wavespeeds, and number of sections are preselected to provide a common Δt , which is calculated in the program. Nodal hydraulic grade lines are also provided, from which initial flows are established. Results from the program with the data given are also provided in the disk.

The characteristics method is used almost exclusively throughout this treatise, with the exception of part of Chapter 5 and Chapters 12 and 13. In Chapter 4 the complete equations are treated in the method of characteristics.

Problems

- 3-1. The results from a characteristics method solution should check the original partial differential equations of continuity and motion. Place Eqs. (3-1) and (3-2) into finite difference form directly, find the numerical value of each term, and see if each equation adds to zero. Numerical data in Fig. D-1b may be used, but output with a larger number of significant digits would be better. A centered finite difference approximation could be used (e.g., $H_x = (H_{P_1} + H_{S_1} - H_{P_2} - H_{S_2})/2/2\Delta x$).
- 3-2. Check the size of the terms that were dropped from Eqs. (3-1) and (3-2) to see if this action is justified. Numerical values from Fig. D-1b may be used in a manner similar to Problem 3-1.
- 3-3. A 0.3-m-diameter pipe connects two reservoirs as shown in Fig. 3-26. A steady-state velocity of 1.5 m/s exists in the pipeline. $L = 1000$ m, $f = 0.03$. Write the portion of the computer program that will establish initial conditions at six sections along the pipe.

Problems

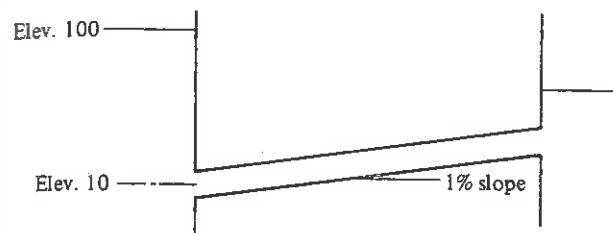


Figure 3-26

- 3-4. A valve discharges a steady flow of $0.5 \text{ m}^3/\text{s}$ water to a reservoir whose surface elevation is 15 m. The steady-state pressure on the upstream side of the valve (elevation 10 m) is 588 kN/m^2 .

(a) Find the value of $(C_D A_G)_0$.

(b) If the discharge is $0.2 \text{ m}^3/\text{s}$ during a transient condition in the system when the hydraulic-grade-line elevation upstream from the valve is 80 m, what is the value of τ ?

(c) If the discharge is $-0.1 \text{ m}^3/\text{s}$ when the hydraulic-grade-line elevation upstream from the valve is 12 m, what is the value of τ ?

Answers: (a) 0.0152; (b) 0.368; (c) 0.856.

- 3-5. Utilize the program SINGLE.FOR to:

(a) Initiate flow from rest in the system in Example 3-1 by opening the valve in 0.05 s.

(b) Compare the results with the theoretical value computed by assuming an incompressible fluid in a rigid pipe.

$$t = \frac{L Q_0}{2g H_R A} \ln \frac{1 + Q/Q_0}{1 - Q/Q_0} = \frac{L Q_0}{2g H_R A} \ln \frac{1 + (\Delta H/H_0)^{1/2}}{1 - (\Delta H/H_0)^{1/2}}$$

In this equation ΔH is the head drop across the valve when the flow is Q . Graphs of either flow or head at the valve are particularly revealing.

(c) Repeat parts (a) and (b) with $C_D A_0 = 0.015$.

(d) Repeat parts (a) and (b) with $C_D A_0 = 0.005$.

(e) In each of the cases above, calculate the valve impedance $2H_0/Q_0$ and relate it to the pipeline impedance $a/(gA)$.

- 3-6. Introduce pipe elevations into the program SINGLE.FOR and calculate gage pressures.
 3-7. Place a reservoir on the downstream side of the valve in the program SINGLE.FOR and change the valve boundary condition to permit negative flow.
 3-8. Introduce a Reynolds number-dependent friction factor into the program SINGLE.FOR. Base the selection of f on known velocities in the reach of pipe.
 3-9. A pump failure occurs on a long pipeline (Fig. 3-27). Assume that a bypass exists at the pump so that, following a failure, the flow is free to move in either direction. The head produced by the pump is 60 ft at a discharge of $45.5 \text{ ft}^3/\text{s}$. $D = 3 \text{ ft}$, $L = 10,000 \text{ ft}$,

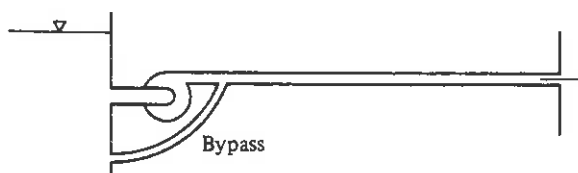


Figure 3-27

$a = 3000 \text{ ft/s}$, $f = 0.028$. Neglect minor losses. Follow the transient condition until vapor pressure occurs at some point in the pipeline.

- 3-10. In 1950, through a series of operating errors and mechanical failures, a butterfly valve closed in about 0.3 s, causing a major penstock failure at Oigawa Power Station, Japan.⁴ Valve closure created a high pressure which ruptured the pipe near the valve. This was followed by the collapse of an extended section of upstream pipe. The accident may be simulated by using the program SINGLE.FOR with some minor modifications.

The high pressure can be created by closing the valve, and the pipe break can be simulated by opening the valve τ to a position that would produce a small loss coefficient of one or two velocity heads at the pipe end. A statement to cause this to happen can be introduced in the downstream boundary condition when the hydraulic grade line exceeds some design level. It is only necessary to follow the transient to observe the low pressure that caused the upstream pipe collapse to occur. A more realistic response will be observed with GRAF if pipeline elevations are introduced.

The following data apply: $A = 3280 \text{ ft}^2$, $XL = 800 \text{ ft}$, $D = 9.0 \text{ ft}$, $F = 0.018$, $HR = 400 \text{ ft}$, $TMAX = 0.65 \text{ s}$, $CDAO = 4.25$, $TI = 1$, $TF = 0$, $TC = 0.3 \text{ s}$. With the reference datum through the valve the profile is described in the following table.

$x :$	0	240	400	800
$z :$	345	345	225	0

- 3-11. A horizontal pipe has a dead end downstream and a reservoir upstream with waves given by $DH \sin(2\pi t/T)$. The system is at rest at $t = 0$. $a = 3000 \text{ ft/s}$, $L = 4000 \text{ ft}$, $D = 1.5 \text{ ft}$, $f = 0.25$, $N = 4$, $DH = 2 \text{ ft}$, and $HR = 60 \text{ ft}$. Modify the program SINGLE.FOR to study potential resonance in the system with each of the following periods of excitation:
(a) $T = 4L/a$; (b) $T = 2L/a$; (c) $T = 4L/3a$.

- 3-12. A centrifugal pump takes water from a suction reservoir at elevation zero and delivers it through 5000 m of 1.0-m-diameter pipe to a reservoir at elevation 84 m. $f = 0.02$, and $a = 1000 \text{ m/s}$. The pump equation is

$$H(1) = 100\alpha^2 - Q(1)^2$$

with α the dimensionless speed, which reduces to zero with time

$$\alpha = 1 - 0.125t$$

A check valve at the pump does not permit backflow. Modify the program SINGLE.FOR to study the transient for 20 s.

- 3-13. A valve controller at the downstream end of a pipe has a discharge-HGL relationship given by

$$Q(NS) = 0.2 - 0.001H(NS)$$

The valve does not permit negative flows. Modify the program SINGLE.FOR to include the evaluation of steady state and the transient generated by changing the upstream reservoir by 1 m after the first time step. $L = 1000 \text{ m}$, $a = 1000 \text{ m/s}$, $f = 0.02$, $D = 0.5 \text{ m}$, $N = 4$, $HR = 100 \text{ m}$, $TMAX = 25 \text{ s}$.

- 3-14. A series system consists of three pipes of lengths 60, 80, and 74 ft, and wavespeeds of 2500, 2000, and 1000 ft/s, respectively. Find the number of sections needed in each pipe and the time-step size.

- 3-15. For a series pipe system $L_1 = 2500 \text{ m}$, $L_2 = 3415 \text{ m}$, $L_3 = 1600 \text{ m}$, $a_1 = 1000 \text{ m/s}$, $a_2 = 1075 \text{ m/s}$, and $a_3 = 940 \text{ m/s}$, determine N_1 , N_2 , N_3 , and the adjusted wavespeeds that permit use of a time step of approximately 0.35 s.

- 3-16. Show the necessary steps to arrive at Eqs. (3-54) and (3-56) for a valve located between two pipelines.
- 3-17. Obtain the solution for Q_1 in a pipeline leading from a reservoir, including minor losses and the velocity head as shown in Eq. (3-58). Show the range of validity of the equation and write the equation to handle the balance of the flow domain.
- 3-18. Carry out the algebra to obtain Eq. (3-61). Simplify the relationship to handle the case of no suction pipeline.
- 3-19. Write the energy equation to handle a minor loss and the kinetic energy at a pipeline series connection. Solve the equation with the appropriate compatibility equations.
- 3-20. A 20-mile pipeline, $D = 1.128 \text{ ft}$, $f = 0.018$, has a velocity variation of 4 ft/s at the upstream end to zero at the downstream end along a C^+ characteristic line. $H_0 = 500 \text{ ft}$.
(a) Find the exact friction drop along the C^+ characteristic line for the length of the pipe.
(b) Find the error in friction drop using the integration presented in Sec. 3-2 ($N = 2$).
(c) Find the error in friction drop using a first-order integration (i.e., by evaluating with the velocity at the upstream end of the characteristic line in each reach).
(d) Repeat parts (b) and (c) with $N = 6$.

- 3-21. A 80-km pipeline carries a flow of $0.376 \text{ m}^3/\text{s}$ water. $D = 0.7 \text{ m}$, $a = 1000 \text{ m/s}$, $f = 0.02$, and $HR = 200 \text{ m}$. Use the program SINGLE.FOR to study the transient with a valve closure in 80 s. Study five different cases with $N = 20, 10, 6, 4$, and 2. For each case evaluate the coefficient given by Eq. (3-63). Draw some conclusions on accuracy and on an acceptable value of the coefficient for satisfactory results for this example.

- 3-22. The second-order integration of the friction term in the compatibility equations may be accomplished by²³

$$\int_{x_A}^{x_P} V^2 dx \approx \frac{V_P^2 + V_A^2}{2}(x_P - x_A)$$

or

$$\int_{x_A}^{x_P} V^2 dx \approx \left(\frac{V_P + V_A}{2}\right)^2(x_P - x_A)$$

For a linear variation of velocity with position x in the pipeline, make a comparison with the exact evaluation and show the second integration is preferred.

- 3-23. A pipeline slopes downward 1.8 ft along its length of 31.1 ft, where it dumps into a reservoir whose surface is at the top of the pipe. The flow is controlled in the following manner as it drops from $0.1 \text{ ft}^3/\text{s}$ to zero: $Q = 0.1 - 9.09t$, where t is in seconds. $D = 0.1667 \text{ ft}$, $a = 2074 \text{ ft/s}$, $f = 0.022$, $H_v = 0.6 \text{ ft}$, and barometric head is 33.9 ft. Modify the program SINGLE.FOR to solve this problem, including liquid column separation.

- 3-24. When an interior section vapor cavity disappears during a simulation, Eq. (3-25) is used to find the new hydraulic-grade-line elevation. Reduce this equation to a frictionless flow case and simplify the result so that it shows the relationship between the flow change and the head rise. Explain the result. Is the same result obtained if a cavity collapses at a closed valve or a dead end?

- 3-25. Remove pipe 3 and node 4 from the system in Fig. 3-25. Prepare the index vector IND to describe the new system topology.

- 3-26. In program ALGEBRA.FOR, allow the pump to come up to a dimensionless speed of $\alpha = 1.1$ in T_s seconds, and compare the results with those given in the disk.

References

1. J. L. Achard, and G. M. Lepinard, "Structure of the Transient Wall-Friction Law in One-Dimensional Models of Laminar Pipe Flows," *J. Fluid Mech.*, Vol. 113, pp. 283-298, 1981.
2. H. Arlt, "Experimentelle Untersuchungen über das instationäre turbulente Reibungsverhalten bei aufgeprägten Druckimpulsen in einer Rohrleitung mit Kreisquerschnitt," *Mitteilungsheft 102*, Inst. Wasserbau und Wasserwirtschaft, Technical Univ. of Berlin, 1983.
3. J. W. Ball, and J. P. Tullis, "Cavitation in Butterfly Valves," *J. Hydraul. Div., ASCE*, Vol. 99, No. HY9, pp. 1303-1318, Sept. 1973.
4. C. C. Bonin, "Water-Hammer Damage to Oigawa Power Station," *J. Eng. Power, ASME*, pp. 111-119, Apr. 1960.
5. H. Brekke, "Surge Tank Stability and Turbine Governing Stability Analyzed with an Approved Approach to the Frictional Damping of Oscillatory Flow in Rough Tunnels and Penstocks," *Proc. 2nd Meeting of the IAHR Working Group on the Behavior of Hydraulic Machinery under Steady Oscillatory Conditions*, Mexico City, Sept. 1985.
6. M. H. Chaudhry, *Applied Hydraulic Transients*, 2nd ed., Van Nostrand Reinhold, New York, 1987.
7. D. N. Contractor, "The Reflection of Waterhammer Pressure Waves from Minor Losses," *Trans. ASME, Ser. D*, Vol. 87, June 1965.
8. G. Evangelisti, "Teoria Generale Cólpo D'Ariète cól Método délle Caratteristiche," *Energ. Electr.*, Milan, Vol. XLII, 1965.
9. G. Evangelisti, "Waterhammer Analysis by the Method of Characteristics," *Energ. Electr.*, Milan, Vol. XLVI, Nos. 10, 11, 12, 1969.
10. J. A. Fox, *Hydraulic Analysis of Unsteady Flow in Pipe Networks*, Wiley, New York, 1977.
11. C. A. M. Gray, "The Analysis of the Dissipation of Energy in Water Hammer," *Proc. ASCE*, Vol. 119, Paper 274, pp. 1176-1194, 1953.
12. E. L. Holmboe, "Viscous Distortion in Wave Propagation as Applied to Waterhammer and Short Pulses," Doctoral thesis, Carnegie Institute of Technology, Pittsburgh, Pa., 1964.
13. M. Kaplan, V. L. Streeter, and E. B. Wylie, "Computation of Oil Pipeline Transients," *J. Pipeline Div., ASCE*, Vol. 93, No. PL3, pp. 59-72, Nov. 1967.
14. B. W. Karney, "Analysis of Fluid Transients in Large Distribution Networks," Ph.D. thesis, Univ. of British Columbia, Vancouver, Sept. 1984.
15. J. Kongeter, "Rohreibungslusten einer Oszillierenden, turbulenter Strömung in einem Kreisrohr konstanten Querschnitts," *Mitteilungsheft 95*, Inst. Wasserbau und Wasserwirtschaft, Technical Univ. of Berlin, 1980.
16. C. A. Kot, and C. K. Youngdahl, "The Analysis of Fluid Transients in Piping Systems, Including the Effects of Cavitation," *Conf. Fluid Transients and Acoustics*, ASME, San Francisco, pp. 45-52, 1978.
17. Wen-H. Li, and J. P. Walsh, "Pressure Generated by Cavitation in a Pipe," *J. Eng. Mech. Div., ASCE*, Vol. 90, No. EM6, pp. 113-133, Dec. 1964.
18. M. Lister, "The Numerical Solutions of Hyperbolic Partial Differential Equations by the Method of Characteristics," in Antony Ralston and H. S. Wilf (eds.), *Numerical Methods for Digital Computers*, Wiley, New York, 1960.

References

19. Qizhao Liu, Private Communication, East China Technical University of Water Resources, Nanjing, China, 1982.
20. Milton Ludwig, and S. P. Johnson, "Prediction of Surge Pressures in Long Oil Transmission Lines," *Proc. API, Div. Transp.*, Vol. 30, No. 5, pp. 62-70, 1950.
21. M. Ohmi, and M. Iguchi, "Flow Pattern and Frictional Losses in Pulsating Pipe Flow," *Bull. JSME*, Vol. 24, No. 196, pp. 1756-1771, 1981.
22. J. Parmakian, *Water-Hammer Analysis*, Dover New York, 1963.
23. T. P. Propson, Discussion of "Unsteady Flow Calculations by Numerical Methods," by V. L. Streeter, *J. Basic Eng., ASME*, pp. 465-466, June 1972.
24. T. J. Sheer, R. J. Baasch, and M. S. Gibbs, "Computer Analysis of Waterhammer in Pumping Systems," *S. Afr. Mech. Eng.*, Vol. 23, No. 7, pp. 130-157, July 1973.
25. A. R. Simpson, "Large Water Hammer Pressures Due to Column Separation in Sloping Pipes," Ph.D. dissertation, Univ. of Michigan, Ann Arbor, Mich., 1986.
26. A. R. Simpson, and A. Bergant, "Quadratic Equation Instabilities for Water Hammer Boundary Conditions," *J. Hydraul. Div., ASCE, Tech. Brief*, Vol. 117, Nov. 1991.
27. V. L. Streeter, "Unsteady Flow Calculations by Numerical Methods," *J. Basic Eng., ASME*, pp. 457-466, June 1972.
28. V. L. Streeter, and C. Lai, "Water Hammer Analysis Including Fluid Friction," *J. Hydraul. Div., ASCE*, Vol. 88, No. HY3, pp. 79-112, May 1962.
29. V. L. Streeter, and E. B. Wylie, *Hydraulic Transients*, McGraw-Hill, New York, 1967.
30. A. R. D. Thorley, and K. J. Enever, "Control and Suppression of Pressure Surges in Pipelines and Tunnels," *CIRIA Report 84*, Construction Industry Research and Information Association, London, Sept. 1979.
31. A. K. Trikha, "An Efficient Method for Simulating Frequency-Dependent Friction in Transient Liquid Flow," *J. Fluids Eng., ASME*, Vol. 97 pp. 97-105, Mar. 1975.
32. J. P. Tullis, (ed.), *Control of Flow in Closed Conduits*, Colorado State Univ., Fort Collins, Colo., p. 399, 1971.
33. S. Uchida, "The Pulsating Viscous Flow Superimposed on the Steady Laminar Motion of Incompressible Fluid in a Circular Pipe," *ZAMP Vol. VII*, pp. 403-422, 1956.
34. A. E. Vardy, and K. L. Hwang, "A Characteristics Model of Transient Friction in Pipes," *J. Hydraulic Research, IAHR*, Vol. 29, No. 5, pp. 669-684, 1991.
35. G. Z. Watters, *Analysis and Control of Unsteady Flow in Pipelines*, 2nd ed., Butterworth, Woburn, Mass., 1984, 349 pp.
36. E. B. Wylie, "Advances in Use of MOC in Unsteady Pipeline Flow," *4th Int. Conf. Pressure Surges*, BHRA, Bath, England, 1983.
37. E. B. Wylie, "Liquid Transient Flow in Piping Systems," in *Advances in Aerodynamics, Fluid Mechanics, and Hydraulics*, ASCE, Minneapolis, Minn., pp. 50-57, 1986.
38. E. B. Wylie, and V. L. Streeter, *Fluid Transients*, McGraw-Hill, New York, 1978.
39. W. Zielke, "A Short Review of Resistance Laws for Unsteady Flow through Pipes and Orifices," *First Meeting of the IAHR Working Group on the Behavior of Hydraulic Machinery under Steady Oscillatory Conditions*, Milan, pp. K1-K15, Sept. 1983.
40. W. Zielke, "Frequency-Dependent Friction in Transient Pipe Flow," *J. Basic Eng., ASME, Ser. D*, Vol. 90, No. 1, pp. 109-115, Mar., 1968.

The Complete Equations

A simplified set of the equations of motion and continuity for one-dimensional pipe flow formed the basis for the numerical method in Chapter 3. In the present chapter the complete set of equations, as developed in Chapter 2, are used in the numerical procedure. A number of complexities arise in the treatment, so prudent judgment should be exercised before embarking on their use in favor of the form presented earlier. However, there are applications when the transport terms in both equations and the slope term in the continuity equation may be important. These are likely to be cases of higher-Mach-number flows, of more compliant fluids such as liquids with a free gas content, of systems with more flexible pipe wall materials, or of transmission systems in which the vertical runs are a significant part of the total length. The method of characteristics is used, including the method of specified time intervals in the numerical procedure. Interpolations are necessary in the implementation. As an alternative, the characteristics grid is presented for special applications.

This chapter contains material of a highly specialized nature that is likely to be of interest to only the few industries in which the topic might be important. Basic understanding of one-dimensional transients in slightly compressible closed systems can be achieved without a detailed study of this chapter. The book is written so that this chapter may be skipped without loss of continuity.

4-1 Nonsimplified Equations

The continuity equation for one-dimensional unsteady flows in fluid-filled sloping pipes is given by Eq. (2-19):

$$\frac{\dot{A}}{A} + \frac{\dot{\rho}}{\rho} + V_x = 0 \quad (4-1)$$

Introduction of the fluid bulk modulus, Eq. (1-6),

$$\frac{\dot{\rho}}{\rho} = \frac{\dot{p}}{K} \quad (4-2)$$

and the wavespeed definition, Eq. (1-7),

$$a^2 = \frac{K/\rho}{1 + (K/A)(\dot{A}/\dot{\rho})} \quad (4-3)$$

enables the continuity equation to be written in terms of the dependent variables p and V :

$$V p_x + p_t + \rho a^2 V_x = 0 \quad (4-4)$$

Equation (4-4) is limited to prismatic pipelines.

The equation of motion describing one-dimensional unsteady flows in fluid-filled sloping pipes is given by Eq. (2-6).

$$\frac{p_x}{\rho} + V V_x + V_t + g \sin \alpha + \frac{f V |V|}{2D} = 0 \quad (4-5)$$

The Darcy–Weisbach equation has been used in defining frictional losses.

4-2 The Method of Characteristics

When Eqs. (4-4) and (4-5) are transformed by the method of characteristics as in Sec. 3-1, the following equations, which are more general than those in Chapter 3, result.

$$\lambda \left[p_x \left(V + \frac{1}{\lambda \rho} \right) + p_t \right] + \left[V_x \left(V + \lambda \rho a^2 \right) + V_t \right] + g \sin \alpha + \frac{f V |V|}{2D} = 0 \quad (4-6)$$

$$\frac{dx}{dt} = V + \frac{1}{\lambda \rho} = V + \lambda \rho a^2 \quad (4-7)$$

The equality in Eq. (4-7) leads to

$$\lambda = \pm \frac{1}{\rho a} \quad (4-8)$$

which, when substituted back into Eq. (4-7), yields

$$\frac{dx}{dt} = V \pm a \quad (4-9)$$

If x is limited to the particular function of time specified in Eq. (4-9), use of the appropriate positive and negative values of lambda permits writing of the following sets of ordinary differential equations:

$$C^+ \left\{ \begin{array}{l} \frac{dV}{dt} + \frac{1}{\rho a} \frac{dp}{dt} + g \sin \alpha + \frac{f V |V|}{2D} = 0 \\ \frac{dx}{dt} = V + a \end{array} \right. \quad (4-10)$$

$$C^- \left\{ \begin{array}{l} \frac{dV}{dt} + \frac{1}{\rho a} \frac{dp}{dt} + g \sin \alpha + \frac{f V |V|}{2D} = 0 \\ \frac{dx}{dt} = V - a \end{array} \right. \quad (4-11)$$

$$C^- \left\{ \begin{array}{l} \frac{dV}{dt} - \frac{1}{\rho a} \frac{dp}{dt} + g \sin \alpha + \frac{fV|V|}{2D} = 0 \\ \frac{dx}{dt} = V - a \end{array} \right. \quad (4-12)$$

(4-13)

The C^+ and C^- characteristics described by Eqs. (4-11) and (4-13) now appear in general as curved lines on the xt plane, inasmuch as $V = V(x, t)$ and a may or may not be constant.

An assumption of constant density and pipe area (i.e., $dV = 0$ in steady state) is no longer reasonable in the application of these equations.⁸ To demonstrate, Eq. (4-11) is combined with Eq. (4-10) to yield an equation that is valid along a C^+ characteristic line.

$$adV + \frac{dp}{\rho} + \left(g \sin \alpha + \frac{fV|V|}{2D} \right) \frac{dx}{(V/a) + 1} = 0 \quad (4-14)$$

This equation must be valid for the limiting case of steady state as well as unsteady flow. For any slope with $V = 0$, Eq. (4-14) yields the correct result of $dp = -\rho g dz$. However, if there is a velocity, then, as examples, if the pipeline is horizontal,

$$dp = -\rho a dV - \rho \frac{fV|V|}{2D} \frac{dx}{(V/a) + 1} \quad (4-15)$$

or if the line is vertical and frictionless,

$$dp = -\rho a dV - \rho g \frac{dx}{(V/a) + 1} \quad (4-16)$$

By visualizing a high velocity it may be noted that these equations make sense only if dV has a numerical value. This implies that either density or pipe area, or both, vary with distance. With the inclusion of variations of density and pipe area, the pressure variation becomes a nonlinear function of distance along the pipeline. The use of piezometric head is of little value now since one of its attractive features, spatial linearity in steady state, is lost.

The finite difference representation of Eqs. (4-10) to (4-13) is necessary for the numerical procedure. In addition to the independent variables of x and t , the quantities p , ρ , V , a , K , and D or A remain as variables in the four differential equations, and Eqs. (4-2) and (4-3) are available to relate the dependent variables. The pipe slope is assumed constant in a given reach, and f is either a constant or a known function of velocity. A number of options exist to proceed. In this treatment the wavespeed, a , and the bulk modulus of elasticity, K , are considered constant. When Eq. (4-2) is introduced into Eq. (4-10) to eliminate pressure in favor of density as one of the dependent variables, integration of the positive compatibility and characteristic equations (Fig. 4-1), leads to

$$a(V_P - V_R) - K \left(\frac{1}{\rho_P} - \frac{1}{\rho_R} \right) + ag \sin \alpha (t_P - t_R) + \frac{afV_P|V_P|}{2D} (t_P - t_R) = 0 \quad (4-17)$$

$$x_P - x_R = (V_R + a)(t_P - t_R) \quad (4-18)$$

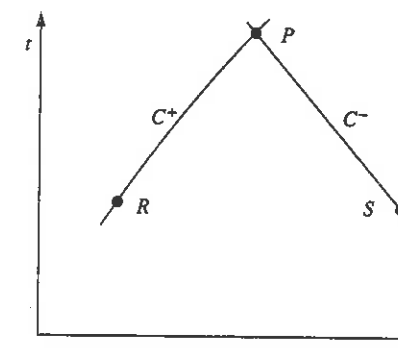


Figure 4-1 Characteristic lines.

The only approximation in Eq. (4-17) is in the integration of the friction term, in which diameter is held constant and an approximate integration by parts is used in evaluating $V^2 dt$. A first-order integration is used in Eq. (4-18). A similar integration of the C^- equations (Fig. 4-1), provides a set of equations that can be solved numerically:

$$a(V_P - V_S) - K \left(\frac{1}{\rho_P} - \frac{1}{\rho_S} \right) + ag \sin \alpha (t_P - t_S) + \frac{afV_P|V_S|}{2D} (t_P - t_S) = 0 \quad (4-19)$$

$$x_P - x_S = (V_S - a)(t_P - t_S) \quad (4-20)$$

Integration of Eq. (4-2) permits the calculation of pressure once density is known.

$$p_P = p_0 + K \ln \frac{\rho_P}{\rho_0} \quad (4-21)$$

The area variation is found by combining Eqs. (4-2) and (4-3) and eliminating pressure:

$$\frac{dA}{A} = \frac{K}{a^2} \frac{dp}{\rho^2} - \frac{dp}{\rho} \quad (4-22)$$

Integration of Eq. (4-22) yields the new area in terms of density:

$$A_P = A_0 \frac{\rho_0}{\rho_P} \exp \left[\frac{K}{a^2} \left(\frac{1}{\rho_0} - \frac{1}{\rho_P} \right) \right] \quad (4-23)$$

If the mass flow rate, $\rho A V$, were computed at a section, the actual area, density, and velocity at that section should be used. However, the assumption of a constant diameter in the friction term in Eqs. (4-17) and (4-19) is not considered a serious approximation since its variation would not have a significant influence on the friction loss.

In this treatment the wavespeed and liquid bulk modulus have been considered constants in a pipeline that is nominally prismatic. Other formulations would be required for variable bulk modulus, variable wavespeed, nonprismatic tubes, nonlinear wall properties, and so on.

Before proceeding with implementation of the numerical method, it is desirable to discuss steady state, since that is the normal initial condition prior to the initiation of a transient.

4-3 Steady-State Solution

By differentiating the mass flow rate, $\rho A V$, which is constant for steady flow,

$$\frac{dV}{V} + \frac{dp}{\rho} + \frac{dA}{A} = 0 \quad (4-24)$$

The combination of Eqs. (4-22) and (4-24) yields

$$\frac{dp}{\rho^2} = -\frac{a^2 dV}{K V} \quad (4-25)$$

Substitution of Eqs. (4-3) and (4-25) into Eq. (4-14) to eliminate pressure and density yields an equation in terms of velocity, which is valid in the downstream direction.

$$\frac{dV^2}{dx} = 2 \frac{V^2}{a^2} \frac{g \sin \alpha + f V^2 / 2D}{1 - (V/a)^2} \quad (4-26)$$

Although an exact integration of Eq. (4-26) is possible,³ it is more useful to use the same integration in the steady-state solution as will be used in the unsteady compatibility equations. By considering $(V/a)^2 \ll 1$, holding D constant, and defining

$$s = \frac{2g \sin \alpha}{a^2} \quad (4-27)$$

integration from $V = V_R$ at $x = 0$ to $V = V_P$ at $x = \Delta x$ yields

$$V_P = \frac{V_R}{\exp(-s \Delta x / 2) - f V_R |V_R| \Delta x / (2D a^2)} \quad (4-28)$$

Substitution of Eq. (4-25) into Eq. (4-26) and utilizing the same approximations yields

$$K \frac{dp}{\rho^2} = -\left(g \sin \alpha + \frac{f V^2}{2D}\right) dx \quad (4-29)$$

With V_P known at $x = \Delta x$, integration yields the density ρ_P at $x = \Delta x$.

$$\frac{1}{\rho_P} = \frac{1}{\rho_R} + \left(g \sin \alpha + \frac{f V_P |V_R|}{2D}\right) \frac{\Delta x}{K} \quad (4-30)$$

With the density known, Eqs. (4-21) and (4-23) are available to determine the pressure and area, respectively. Equations (4-28) and (4-30) are not the exact solutions to the steady-state equations, but they are accurate for low Mach numbers with practical reach lengths. They also accomplish the objective of providing agreement with the integrated compatibility equations.

4-4 The Numerical Method: Interpolations

The four integrated equations for unsteady flow, Eqs. (4-17) to (4-20), are written in terms of four variables, x_P , t_P , ρ_P , and V_P . Two approaches are possible to obtain a

numerical solution: use of grid of characteristics and use of specified time intervals. The latter method, as used in Sec. 3-2, offers several advantages in most fluid transient problems, since x_P and t_P are assigned definite values throughout the computation, permitting a very orderly solution to be carried forward in time in a system. The characteristics grid method is discussed in the next section.

Interpolations

In the method of specified time intervals, and utilizing the staggered grid, an interpolation procedure is necessary to find the positions of points R and S in Fig. 4-2, and to find the values of ρ and V at each point. A linear time-line interpolation is used in this treatment. From Fig. 4-2

$$\frac{V_A - V_R}{V_A - V_D} = \frac{t_P - t_R - \Delta t}{2\Delta t} \quad (4-31)$$

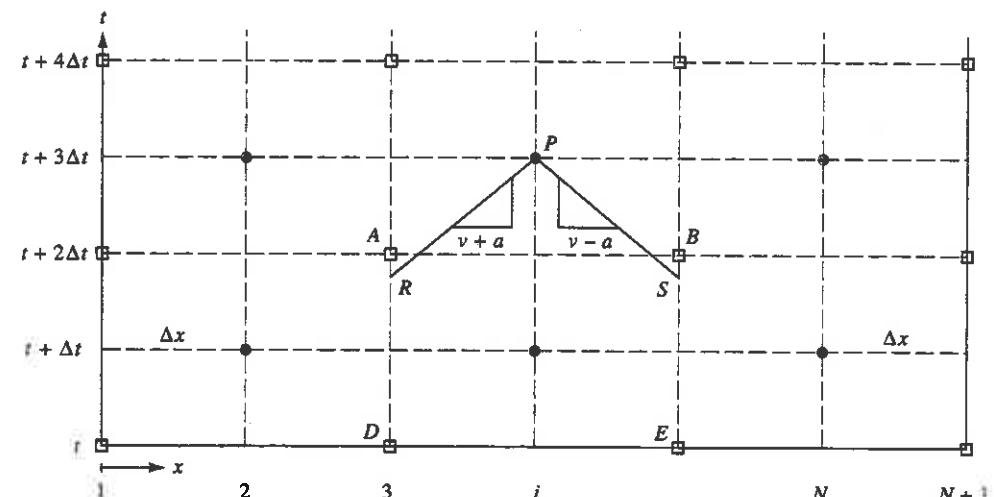


Figure 4-2 Interpolations in method of specified time intervals.

By use of Eq. (4-18), recognizing that $x_P - x_R = \Delta x$, we obtain

$$(V_A - V_R)(V_R + a) = \left(\theta - \frac{V_R + a}{2}\right)(V_A - V_D) \quad (4-32)$$

The grid-mesh ratio is defined by 2θ .

$$\theta = \frac{\Delta x}{2\Delta t} \quad (4-33)$$

The solution for V_R in Eq. (4-32) is

$$V_R = V_X + \sqrt{V_X^2 - [(V_A - V_D)(\theta - a/2) - aV_A]} \quad (4-34)$$

in which $V_X = 3V_A/4 - V_D/4 - a/2$. The reciprocal of ρ_R to be used in Eq. (4-17) is then obtained by a similar linear interpolation:

$$\frac{1}{\rho_R} = \frac{1}{\rho_A} - \left(\frac{\theta}{V_R + a} - \frac{1}{2} \right) \left(\frac{1}{\rho_A} - \frac{1}{\rho_D} \right) \quad (4-35)$$

Interpolated values for V_S and the reciprocal of ρ_S are obtained similarly, with $V_Y = 3V_B/4 - V_E/4 + a/2$.

$$V_S = V_Y + \sqrt{V_Y^2 - [(V_B - V_E)(\theta - a/2) - aV_B]} \quad (4-36)$$

$$\frac{1}{\rho_S} = \frac{1}{\rho_B} + \left(\frac{\theta}{V_S - a} + \frac{1}{2} \right) \left(\frac{1}{\rho_B} - \frac{1}{\rho_E} \right) \quad (4-37)$$

The Numerical Method

In using the defined grid with interpolations it is necessary to solve six equations in turn to find V_P and ρ_P for any interior section in a pipeline. They are Eqs. (4-34) to (4-37) and Eqs. (4-17) and (4-19). The latter two equations may be written in a form similar to Eqs. (3-21) and (3-22), with new definitions for C_P , B_P , C_M , and B_M .

$$C_P = \frac{1}{\rho_R} - BV_R + \frac{Bg \Delta x \sin \alpha}{V_R + a} \quad (4-38)$$

$$B_P = B + \frac{R|V_R|}{V_R + a} \quad (4-39)$$

$$C_M = \frac{1}{\rho_S} + BV_S + \frac{Bg \Delta x \sin \alpha}{V_S - a} \quad (4-40)$$

$$B_M = B - \frac{R|V_S|}{V_S - a} \quad (4-41)$$

In these equations $B = a/K$ and $R = af \Delta x / (2DK)$. Equations (4-17) and (4-19) become

$$\frac{1}{\rho_P} = C_P + B_P V_P \quad (4-42)$$

$$\frac{1}{\rho_P} = C_M - B_M V_P \quad (4-43)$$

The simultaneous solution at an interior point P , Fig. 4-2, yields

$$V_P = \frac{C_M - C_P}{B_M + B_P} \quad (4-44)$$

$$\rho_P = \frac{B_P + B_M}{C_P B_M + C_M B_P} \quad (4-45)$$

With reference to Fig. 4-2, initial conditions are defined at time t . Time is incremented to $t + \Delta t$ and variables are calculated at sections 2, 4, ..., N . Time is incremented to $t + 2\Delta t$ and variables are calculated at sections 3, 5, ..., $N - 1$. End conditions are then introduced at sections 1 and $N + 1$.

Boundary Conditions

At the upstream end, equations associated with the C^- characteristic are used, namely Eqs. (4-36), (4-37), (4-40), (4-41), and (4-43). Equations (4-21) and (4-23) are generally needed as well to incorporate all of the variables: pressure, density, velocity, and area. As in Chap. 3, at least one condition is needed to describe the boundary condition. For example, if a closed pipe condition existed at section 1 of Fig. 4-2, Eq. (4-43) would be used to evaluate the density ρ_P , with $V_P = 0$. Then Eq. (4-21) could be used to calculate the pressure. If needed, the area could be found from Eq. (4-23). Alternatively, if the mass flow rate, m_P , were specified, a simultaneous solution of $m_P = \rho_P A_P V_P$ together with Eqs. (4-23) and (4-43) would be necessary.

At the downstream end, section $N + 1$ (Fig. 4-2), equations associated with the C^+ characteristic must be solved simultaneously with equations describing the attached facility. For example, if a valve discharges to an external pressure, p_c , the valve equation may be written

$$V_P = \frac{C_d A_G}{A_P} \sqrt{\frac{2(p_P - p_c)}{\rho_P}} \quad (4-46)$$

in which the subscript P refers to the downstream section at the current time and $C_d A_G$ is the product of the valve discharge coefficient and area of opening at the instant. If the dimensionless valve position, τ , is introduced [Eq. (3-36)], Eq. (4-46) may be written

$$V_P = \frac{V_0 A_0}{A_P} \tau \sqrt{\frac{\rho_{00}}{\Delta \rho_{00}}} \sqrt{\frac{p_P - p_c}{\rho_P}} \quad (4-47)$$

in which $\tau = C_d A_G / (C_d A_G)_0$, and the subscripts 00 and 0 refer to the reference values at section $N + 1$. The combination of Eqs. (4-47) and (4-2), integrated over two time steps at section $N + 1$,

$$p_P = p + K \ln \frac{\rho_P}{\rho} \quad (4-48)$$

yields

$$V_P^2 = C_V \left[\frac{p + K \ln(\rho_P/\rho) - p_c}{\rho_P} \right] \quad (4-49)$$

in which $C_V = (V_0 A_0 \tau)^2 \rho_{00} / (\Delta \rho_{00} A_P^2)$ and the nonsubscripted values of p and ρ refer to section $N + 1$ two time steps earlier. When Eqs. (4-49) and (4-42) are combined, we obtain

$$F = V_P^2 - C_V \left\{ p - p_c - K \ln \left[\rho (C_P + B_P V_P) \right] \right\} (C_P + B_P V_P) = 0 \quad (4-50)$$

Newton's method may be used to solve Eq. (4-50) for the unknown V_P . Equation (4-42) may be used to find ρ_P , Eq. (4-48) to find p_P , and Eq. (4-23) to find A_P if needed. Equation (4-50) is valid for positive flow only.

Stability

Characteristic lines appear as curved lines in the xt plane as a consequence of including the convective transport terms VV_x and Vp_x in the partial differential equations, even with a constant wave propagation velocity. This fact brought about interpolations since characteristic lines could no longer extend between fixed grid intersection points in the method of specified time intervals. With interpolations the theory of the method of characteristics is no longer followed precisely, so the question of stability of the numerical method arises. That is, there is not complete freedom to interpolate randomly in the xt plane and still maintain a numerically stable solution. The Courant^{1,2} condition provides a necessary guide in the selection of the grid-mesh ratio:

$$\Delta t(|V| + a) \leq \Delta x \quad (4-51)$$

Figure 4-3 provides an interpretation of the condition. Characteristic lines QAP' and UBP' together with noncharacteristic line QU enclose a domain of dependence. Conditions at point P can be determined by utilizing information inside this domain. It is seen that the interpolation procedure above, which uses points A and D to determine point R and points B and E to determine point S , satisfies the requirement, and Eq. (4-51) is satisfied with the indicated grid-mesh ratio. Clearly, other points on this grid could be used in interpolating to satisfy the requirement, and other grids could be utilized that would satisfy the requirement and would offer different interpolation procedures.⁴⁻⁶

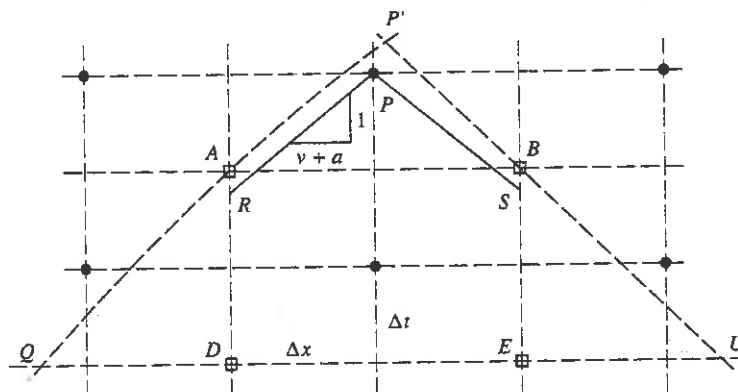


Figure 4-3 Stability in MOC.

Interpolation Errors

An interpolation procedure is necessary in the method of specified time intervals when the small terms are kept in the basic equations. Interpolations are also necessary if there is a variable wavespeed due to variable fluid properties, a pressure-dependent wavespeed, variable wall materials, and so on. Additionally, interpolations may be helpful to maintain a common time step in a multipipe system. However, there is a major disadvantage in the use of interpolations since artificial numerical damping is introduced in the results. It is most critical in damping high-frequency components in transients,⁷ which includes most cases in which rapid changes occur during a single time step.

The manner in which damping enters the solution can be visualized by an examination of a single frictionless pipeline leading from a constant-pressure source. If a sharp transient is introduced at point B in the xt plane (Fig. 4-4), its effect should be felt at the other end of the pipeline at point D . However, if two reaches are used in the pipe and an extreme interpolation of 50 percent is used in the numerical solution (i.e., $\Delta t = \Delta x/2a$), it can be seen that 50 percent of the change will be transferred to point S and therefore be transmitted to point U one Δt after point B . Furthermore, 50 percent of this change will be transferred to point W , and therefore will be transmitted to the point Y . Thus 25 percent of the original disturbance will arrive at the other end of the pipeline ahead of the proper time. Also, it will be reflected at the pressure tank

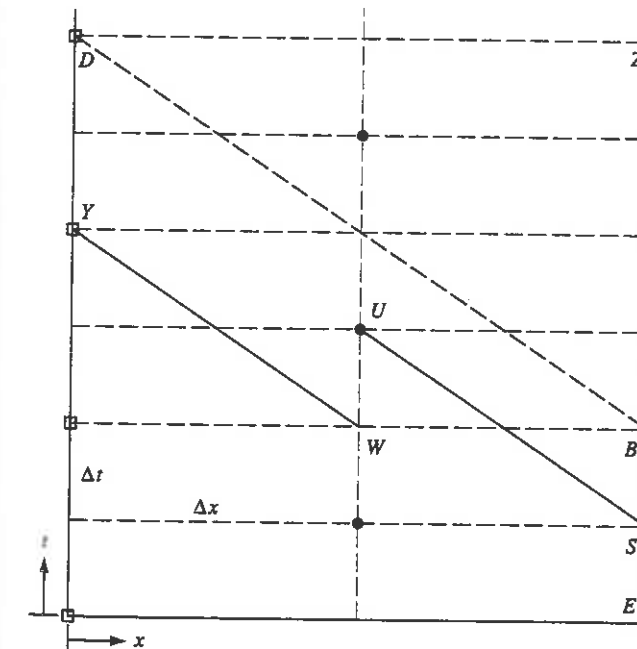


Figure 4-4 Interpolation error, xt plane.

back to the source in advance of the physical wave, thereby dampening the transient. In this case a negative wave one-sixteenth the size of the original positive wave would arrive at the source, point *Z*, just when the physical wave reaches the pressure tank.

This situation can be greatly improved by using a larger number of reaches (i.e., finer discretization). A smaller interpolation is equally effective in reducing the numerical error, that is, use a grid mesh ratio that keeps point *S* near point *B*. The best advice is to avoid interpolations whenever possible. If it is not possible, a large number of reaches should be used and the degree of interpolation should be kept to a minimum.

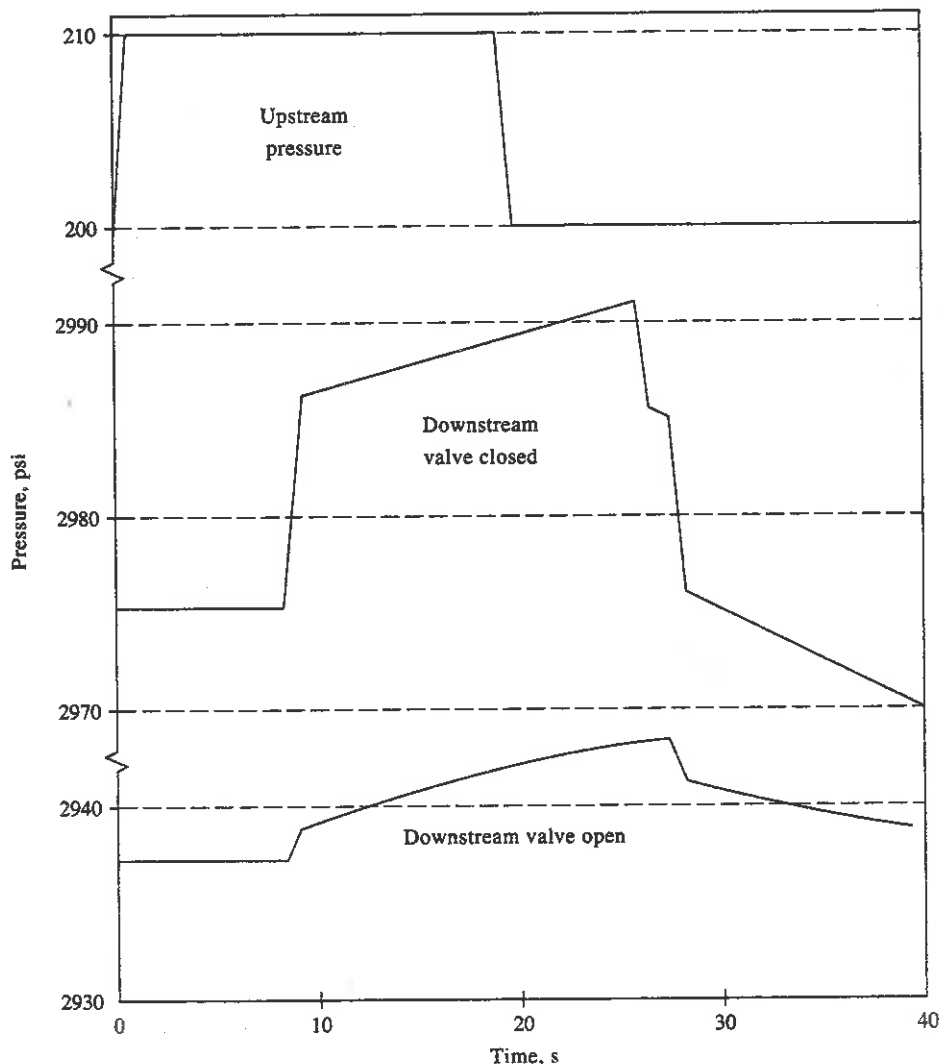


Figure 4-5 Example 4-1, pressure history at downstream end for closed valve and open valve.

Example 4-1

A small-diameter armored flexible hose is used to transmit a pressure pulse to initiate motion of an operator downhole in an offshore oil well. The 9000-ft line has an inside diameter of 1 in., $a = 1000 \text{ ft/s}$, $f = 0.035$, and it slopes down at approximately 45 degrees. It is supplied at the surface from a 200-psi source. The valve, $C_d A_0 = 0.00005$, at the downstream delivery point may initially be open or closed. The receiving tank pressure at the downstream end is $P_c = 2760 \text{ psi}$.

The program called GENEQUA.FOR, included in the disk in the back of this book, calculates the initial flow in the system for either an open or a closed valve. This program accommodates positive or negative initial flow, depending on the pipe slope and the initial terminal pressures. Double precision is used in the calculations. The influence of the area variation with pressure at the downstream valve is not included. A data set for the closed valve is appended, along with the initial output for the case of an open valve with an excitation of a 10-psi pulse introduced at the upstream end for 20 s. Figure 4-5 shows the pressure history at the downstream end for both cases. The influence of the viscous loss is clearly evident; however, the influence of the change in density and pipe area is not so obvious. For the no-flow case there is a pressure difference of 17.5 psi at the downstream end, depending initially on whether these effects are included or not (see Prob. 4-5).

4-5 The Characteristic Grid

In Chapter 3 and earlier sections of this chapter we used the method of specified time intervals to set up an orderly numerical process. As stated, the interpolation procedure may lead to appreciable error in highly variable wavespeed examples, or in cases with low wavespeed in which the fluid particle velocity may be of the same order of magnitude as the wave propagation velocity.

The characteristic-grid method avoids the possibility of this interpolation error by using a direct solution of Eqs. (4-17) to (4-20) for the four variables, V_P , ρ_P , x_P , and t_P . A free-floating grid develops in the xt plane, as shown in Fig. 4-6, since the position of intersection of characteristic lines is no longer fixed. The programming details involved in the characteristic-grid solution are similar to those of the rectangular grid. A subscripted notion is desirable to keep track of the location of each point. Normally, one begins with equal reach lengths, as shown in Fig. 4-6. Conditions are considered known along the pipe at the initial time; then, through the use of Eqs. (4-17) to (4-20), one can find conditions at points *a*, *b*, and *c* (Fig. 4-6). With values of *x*, *t*, *V*, and ρ known at each of these locations, the grid can be continued to points *d* and *e*.

Simultaneous solution of Eqs. (4-18) and (4-20) gives the solution for *x* and *t* at the interior points.

$$t_P = \frac{x_R - x_S - (V + a)_R t_R + (V - a)_S t_S}{(V - a)_S - (V + a)_R} \quad (4-52)$$

$$x_P = x_R + (V + a)_R (t_P - t_R) \quad (4-53)$$

With *t* known, Eqs. (4-17) and (4-19) can be solved simultaneously for V_P and $1/\rho_P$. If the convective acceleration terms are deemed unimportant in a particular problem,

simplifications are realized by replacing $(V \pm a)$ with $\pm a$ in Eqs. (4-18) and (4-20). Also, a higher-order integration could be used to give improved accuracy in critical cases.

A solution may be obtained at interior points along a pipeline as described above. The influence of the boundary conditions on the solution is apparent in Fig. 4-6. At the boundaries the position of x_P is generally known, so that t_P may be solved directly from the appropriate characteristic equation. The solution of the boundary condition equation with the appropriate compatibility equation proceeds as in the rectangular grid method.

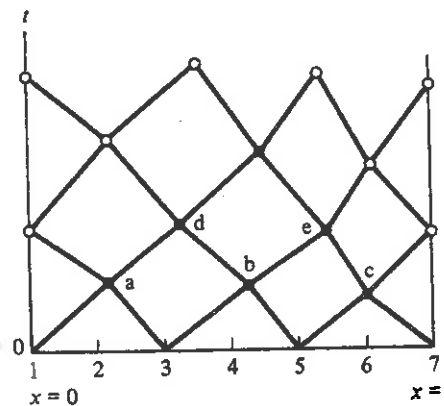


Figure 4-6 Characteristics grid.

An itemized comparison between the characteristics grid (CG) and the rectangular grid (RG) methods follows. It is presumed that the RG method would always be used when there is no need for interpolations.

1. Accurate results at grid intersection points are provided in the CG method. However, results are not directly available at a particular instant along the pipe nor at a particular section as a function of time. Some interpolation scheme must be used to obtain this information if it is needed. The RG method is capable of providing results where needed; however, it suffers from inaccuracies introduced by interpolations at each time step, and the greater the interpolation, the larger the error.

2. A control cannot be maintained on the position of grid intersection points in the xt plane in the CG method. Intersection points may move outside the region of the pipeline and thus lose physical significance. To overcome the problem of distortion of the grid under extreme conditions in the CG method a procedure has been used to straighten the grid by an adjustment of the grid after a certain number of time steps.^{5,9} It involves a double interpolation scheme in the region of the xt plane in which data are already computed. Once regular spacing is reestablished, the CG method can be continued over another time span. The number of times this type of interpolation

Problems

is needed is dependent on the severity of the variation in wavespeed. The numerical damping introduced with this interpolation is not nearly as significant as that introduced in the rectangular grid.

3. The Courant condition for stability is always satisfied in the CG method, whereas in the RG method, the user must be sure that the grid complies with the requirements.

4. In the CG method, the user has no direct control on the time of input variables at boundaries, whereas boundary conditions may be introduced at predefined times in the RG approach. This point renders the former approach almost useless in complex systems. On the other hand, this is probably the strongest point in favor of the latter method.

5. Equal-length reaches may be selected and maintained along the pipeline in the RG method.

The characteristics method in one form or another is used almost exclusively throughout this book. In Chapter 5 we provide a brief introduction to some other methods. In Chapters 12 and 13 we use a sine-wave analysis in the frequency domain.

Problems

- 4-1. Perform the integration of Eq. (4-26) to yield Eq. (4-28).
- 4-2. Develop the interpolation equations, Eqs. (4-36) and (4-37), using the C^- characteristic line.
- 4-3. Develop linear interpolation equations for the case in which the convective terms may be dropped, that is, when $(V \pm a)$ may be replaced with $\pm a$.
- 4-4. Complete all of the steps to arrive at Eq. (4-50). Repeat the steps for negative flow at the valve.
- 4-5. In Example 4-1, find the pressure and steady-state flow at the downstream end neglecting the change in density and in the pipe wall size for (a) the closed end and (b) the open valve with $C_d A_0 = 0.00005$. By referring to the results in the example, what is the pressure difference in the two calculation procedures?
- 4-6. In Example 4-1, the half-interval method is used to find the initial steady flow in the system with an open valve at the downstream end. Explain the details of the procedure. Could another method, such as Newton's method, be used?
- 4-7. A vertical pipe, $\alpha = 90^\circ$, of length 1000 m, $D = 0.15$ m, $a = 1000$ m/s, $f = 0.02$, has water flowing at $V_0 = 3$ m/s at the upstream end. $\rho_0 = 1000$ kg/m³, $K = 2.07$ GPa. Calculate and graph V/V_0 , ρ/ρ_0 , and A/A_0 vs. distance x along the pipe for steady flow.
- 4-8. A series system consisting of three pipes has lengths and wavespeeds of 60, 80, and 18 ft and 2500, 2000, and 1000 ft/s, respectively. If no interpolations are to be used, and the transport terms are to be neglected, what is the number of reaches in each pipe?

References

1. G. Evangelisti, "Waterhammer Analysis by the Method of Characteristics," *Energ. Electr.*, Milan, Vol. XLVI, Nos. 10, 11, 12, 1969.
2. M. Lister, "The Numerical Solutions of Hyperbolic Partial Differential Equations by the Method of Characteristics," in Antony Ralston and H. S. Wilf (eds.), *Numerical Methods for Digital Computers*, Wiley, New York, 1960.
3. S. Stuckenbruck, and D. C. Wiggert, Discussion of "Fundamental Equations of Waterhammer," by E. B. Wylie, *J. Hydraul. Div.*, ASCE, Vol. 111, No. 8, pp. 1195–1196, Aug. 1985.
4. A. K. Trikha, "Variable Time Steps for Simulating Transient Liquid Flow by Method of Characteristics," *J. Fluids Eng.*, ASME, Vol. 99, pp. 259–261, Mar. 1977.
5. J. P. Tullis, V. L. Streeter, and E. B. Wylie, "Waterhammer Analysis with Air Release," *Proc. 2nd Int. Conf. Pressure Surges*, BHRA, Bedford, England, Sept. 1976.
6. A. E. Vardy, "On the Use of the Method of Characteristics for the Solution of Unsteady Flows in Networks," *Proc. 2nd Int. Conf. Pressure Surges*, BHRA, Bedford, England, Sept. 1976.
7. D. C. Wiggert, and M. J. Sundquist, "Fixed-Grid Characteristics for Pipeline Transients," *J. Hydraul. Div.*, ASCE, Vol. 103, pp. 1403–1413, 1977.
8. E. B. Wylie, "Fundamental Equations of Waterhammer," *J. Hydraul. Div.*, ASCE, Vol. 110, No. 4, pp. 539–542, Apr. 1984; "Discussions and Closure," Vol. 111, No. 8, pp. 1185–1200, Aug. 1985.
9. E. B. Wylie, and V. L. Streeter, "One-Dimensional Soil Transients by Characteristics," *Proc. 2nd Int. Conf. Numerical Methods in Geomechanics*, VPI, Blacksburg, Va., June 1976.

Other Methods of Solution

For rapid transients in liquid pipeline systems the method of characteristics is generally considered to be the numerical method by which others may be judged for accuracy and efficiency. Other methods are available and in certain situations there are valid reasons to consider their use. In this chapter we introduce some of the alternatives without providing an in-depth exposition.

5-1 Rigid Water Column Theory

In a number of unsteady flow examples, changes in pressures and flows are relatively slow with respect to L/a seconds. In many of these cases the change in mass storage in the pipeline is unimportant and the fluid may be considered incompressible and the pipe walls completely rigid. This leads to the incompressible or rigid liquid column theory, in which the mass density remains constant and the pipe undeformable regardless of pressure. This effectively implies an infinite wave propagation velocity and a common fluid particle velocity along the pipe at any instant.

The linear momentum equation applied to the control volume (Fig. 5-1), states that at any instant the summation of forces applied to the fluid in the control volume equals the time rate of increase of linear momentum within the control volume plus the net efflux of linear momentum from the control volume. With a common velocity at any instant in the x direction the last term is zero, and the equation becomes

$$-\frac{\partial p}{\partial x} \delta x A - \rho g A \delta x \sin \alpha - \tau_0 \pi D \delta x = \rho A \delta x \frac{\partial V}{\partial t} \quad (5-1)$$

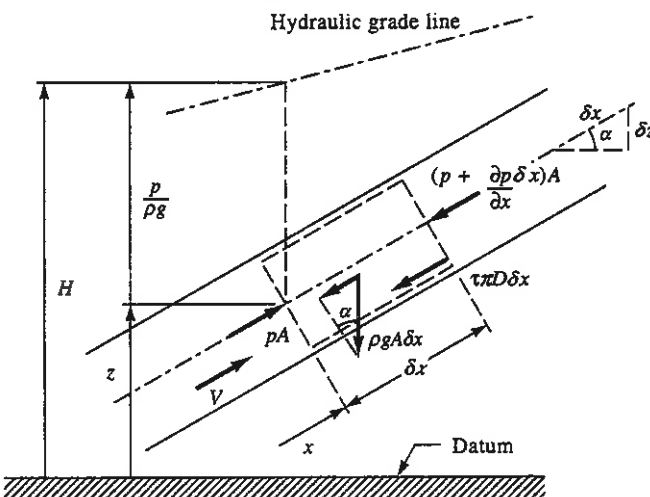


Figure 5-1 Control volume for lumped analysis.

Inasmuch as $V = V(t)$, the last term may be written as a total derivative. Introduction of the Darcy-Weisbach equation to describe the viscous loss leads to the final form:

$$\frac{\partial p}{\partial x} + \rho g \sin \alpha + \frac{\rho f V |V|}{2D} + \rho \frac{dV}{dt} = 0 \quad (5-2)$$

Introduction of the piezometric head [Fig. 5-1 and Eq. (2-10)], leads to

$$\frac{\partial H}{\partial x} + \frac{f V |V|}{2gD} + \frac{1}{g} \frac{dV}{dt} = 0 \quad (5-3)$$

Since $V = Q/A$, this may be written

$$\frac{\partial H}{\partial x} + \frac{f Q |Q|}{2gDA^2} + \frac{1}{gA} \frac{dQ}{dt} = 0 \quad (5-4)$$

Since V , or equivalently Q , is a function of time only, the change of p (or H) with x is also a function of time only. That is, the piezometric head, or hydraulic grade line, is a straight line at any instant between H_U and H_D (Fig. 5-2), and $\partial H/\partial x = (H_D - H_U)/L$. Equation (5-3) can be written in terms of the pipeline velocity and the upstream and downstream end pressures, at any instant, as

$$H_D - H_U + \frac{f LV |V|}{2gD} + \frac{L}{g} \frac{dV}{dt} = 0 \quad (5-5)$$

It is noted that the pipeline elevation does not appear in Eq. (5-5), nor does it matter how the elevation varies between the endpoints as long as the pressure is above vapor pressure throughout. If written in terms of pressure rather than hydraulic grade line, the terminal pipeline elevations would be present.

In Eq. (5-5) the upstream and downstream pressures may vary with time along with the velocity, in which case a numerical integration is probably necessary. A closed-form

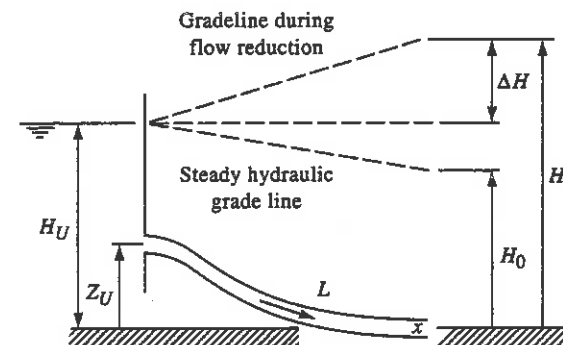


Figure 5-2 Pipeline for lumped analysis.

integration is possible if $H_D - H_U = \Delta H$ is a constant. With initial conditions of $V = V_0$ at $t = 0$, and defining

$$C_1 = \frac{g \Delta H}{L} \quad C_2 = \frac{f}{2D}$$

integration yields the variation of velocity with time:

$$V = \sqrt{C_1/C_2} \tan \left[\tan^{-1}(V_0/\sqrt{C_1/C_2}) - \sqrt{C_1 C_2} t \right] \quad (5-6)$$

Among other examples, the time to stop the flow with a fixed positive ΔH can be found by equating the bracketed quantity to zero.

A time constant, referred to as the startup time, may be calculated by integrating Eq. (5-5) with $f = 0$. This is the time required to start the liquid mass in a pipe from zero to Q when acted upon by a constant pressure difference. The integration leads to

$$t_w = - \frac{LQ}{g \Delta HA} \quad (5-7)$$

The time for flow to become established in a pipeline, including friction when a valve is suddenly opened, may also be determined by introducing the valve equation into Eq. (5-5) and integrating. The steady energy equation, together with the valve relation Eq. (3-33), provides the steady velocity in the pipe, V_0 , with the corresponding head drop across the valve, H_0 .

$$H_U = H_0 + \frac{f LV_0^2}{2gD} \quad (5-8)$$

For a fixed open valve the head drop across the valve H_D is related to the flow in the pipe V during unsteady flow by

$$\left(\frac{V}{V_0} \right)^2 = \frac{H_D}{H_0} \quad (5-9)$$

Combination of Eqs. (5-5) and (5-9) yields

$$\left(H_0 + \frac{f LV_0^2}{2gD} \right) \frac{V^2}{V_0^2} - H_U + \frac{L}{g} \frac{dV}{dt} = 0$$

When Eq. (5-8) is substituted, direct integration from the initial no-flow condition to the velocity at any time yields

$$\int_0^t dt = \frac{LV_0^2}{gH_U} \int_0^V \frac{dV}{V_0^2 - V^2}$$

$$t = \frac{LV_0^2}{gH_U} \ln \frac{V_0 + V}{V_0 - V} \quad (5-10)$$

It is noted that the velocity approaches steady state asymptotically in this lumped solution. The value of the head in the pipe upstream from the valve for this solution may be found by combining Eqs. (5-9) and (5-10) to eliminate V .

Example 5-1

By use of the rigid water column theory, find the time for the flow to reach 2.5 m/s following an instantaneous opening of the downstream valve in a system in which $L = 100$ m, $D = 0.1$ m, $f = 0.032$, $H_U = 20$ m, and $C_d A_G = 0.0024$. At that instant find the piezometric head upstream of the valve.

The combination of Eqs. (3-33) and (5-8) provides the solution for the final steady-state values of V_0 and H_0 .

$$H_U = H_0 \left[1 + \frac{fL}{D} \frac{(C_d A_G)^2}{A^2} \right]$$

$$H_0 = 5.015 \text{ m} \quad V_0 = 3.031 \text{ m/s}$$

Substituting $V/V_0 = 2.5/3.031$ into Eq. (5-10) yields $t = 1.933$ s. From Eq. (5-9) the head at the valve at that instant is

$$H_D = H_0 \left(\frac{V}{V_0} \right)^2 = 3.412 \text{ m}$$

5-2 Graphical Method

The inclusion of a brief treatment of the graphical method could be justified on the basis of historical reasons only. However, as will be seen, visualization of a number of transient situations may be greatly enhanced by utilizing the dependent variable plane. This is true for resonance studies, valve stroking, and for visualizing system response with some types of boundary conditions. For a full treatment of the topic, either Bergeron¹ or Parmakian⁷ should be consulted.

The graphical method and the pictorial representation of the characteristics method have much in common. In the latter, the characteristics appear on the independent variable x, t plane upon which the solution for the dependent variables H and V is followed. The graphical representation is on the dependent-variable pressure-flow plane, where the characteristic lines relate pressure and flow at one location and time to the same variables at another point in the pipe (distance Δx from the first point) at time $\Delta x/a$ later.

In Sec. 2-4 the general solution of the simplified, frictionless waterhammer equations was provided in Eqs. (2-47) and (2-48) in terms of general functions $F(t + x/a)$ and $f(t - x/a)$. The interpretation of the function $F(t + x/a)$ is that it represents an F wave moving undiminished in the upstream ($-x$) direction through the pipe. Similarly, the function $f(t - x/a)$ represents an unchanging wave moving in the downstream ($+x$) direction. In any given pipeline of constant geometric properties, each of these plane pressure waves moves with constant speed a . When they meet within the pipeline, they continue in their respective directions without mutual interference.

The same functions can be developed from the integrated compatibility equations that are valid along characteristic lines from Chapter 3. Equation (3-16) may be written

$$H_{x,t} - H_{x_1,t_1} = \frac{a}{g} (V_{x,t} - V_{x_1,t_1}) \quad (5-11)$$

by dropping the friction term. This equation is valid along the C^- characteristic line, which states that the parameters x and t must obey the relationship $x = x_1 - a(t - t_1)$. Thus Eq. (5-11) may be interpreted as representing an F function and may be visualized in the hv plane (Fig. 5-3), as an F wave traveling upstream in the $-x$ direction.

Quite often, as in Fig. 5-3, a dimensionless representation is used by defining

$$h = \frac{H}{H_0} \quad v = \frac{V}{V_0}$$

Then Eq. (5-11) can be written, with $B = aV_0/gH_0$, as

$$\Delta h = B \Delta v \quad (5-12)$$

By beginning with Eq. (3-15), which is valid along the C^+ characteristic line, $x = x_1 + a(t - t_1)$, the following equation is related to the f function and may be interpreted as an f wave traveling in the downstream direction in the hv plane (Fig. 5-3):

$$H_{x,t} - H_{x_1,t_1} = -\frac{a}{g} (V_{x,t} - V_{x_1,t_1}) \quad (5-13)$$

On the dimensionless hv diagram, Fig. 5-3, Eq. (5-13) may be written

$$\Delta h = -B \Delta v \quad (5-14)$$

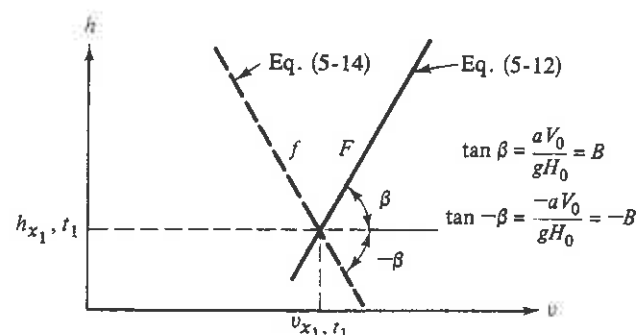


Figure 5-3 Dependent-variable diagram for graphical method.

It is only a matter of preference whether the dimensional variables H and V (or Q) or the dimensionless variables h and v are used.

Everything presented is valid only in a single frictionless pipeline in which the acoustic speed a is constant over the length. To continue with the solution the pipe end conditions must be considered and introduced on the dependent variable plane. Examples involving transients in a single pipeline follow.

Graphical Analysis

The single horizontal pipeline shown in Fig. 5-4 is used for the examples that follow, the first with a sudden valve closure at time $t = 1$. Using the given values yields

$$B = \frac{aV_0}{gH_0} = \frac{1200 \times 0.98}{9.8 \times 120} = 1$$

Steady-state flow is portrayed in the graphical solution (Fig. 5-5) at $v = 1$, $h = 1$ for all points within the pipe. Since the valve closes at $t = 1$, and $L/a = 1$, the solution starts at B_0 (the subscript refers to the time and the letter to the location). This is an f wave

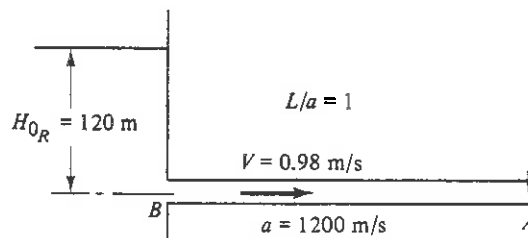


Figure 5-4 Single-pipeline system.

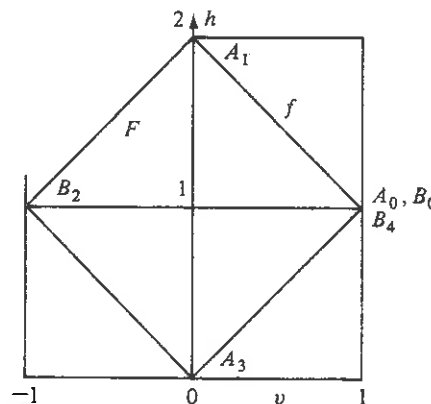


Figure 5-5 Graphical solution for sudden valve closure.

beginning at the known condition B_0 ($h = 1$, $v = 1$) with slope $-B$. The conditions at A_1 must fall on this line. Since the valve is closed at $t = 1$, A_1 must also fall on the ordinate axis where $v = 0$; thus it occurs as shown. Now proceeding from A_1 to B_2 , the B_2 condition must lie on the F wave through A_1 . At the reservoir the head is $h = 1$; hence the intersection of $h = 1$ and the F wave through A_1 yields the location of B_2 . Continuing this procedure, we locate A_3 and B_4 . Then A_5 , B_6 , A_7 , and B_8 are a repetition of the first cycle, and so on for succeeding cycles.

For gradual valve closure the gate equation in dimensionless form must be used, $v = \tau\sqrt{h}$. Taking a valve closure as given by Fig. 5-6, in place of the smooth closure we assume that the valve closes each L/a seconds by a sudden increment. The value of τ for each L/a increment is read from the τ -time curve. On the hv diagram, the valve equation becomes a particular parabola for each τ value (Fig. 5-7). At each time shown

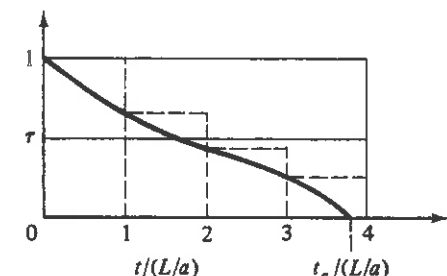


Figure 5-6 τ -time curve for valve closure.

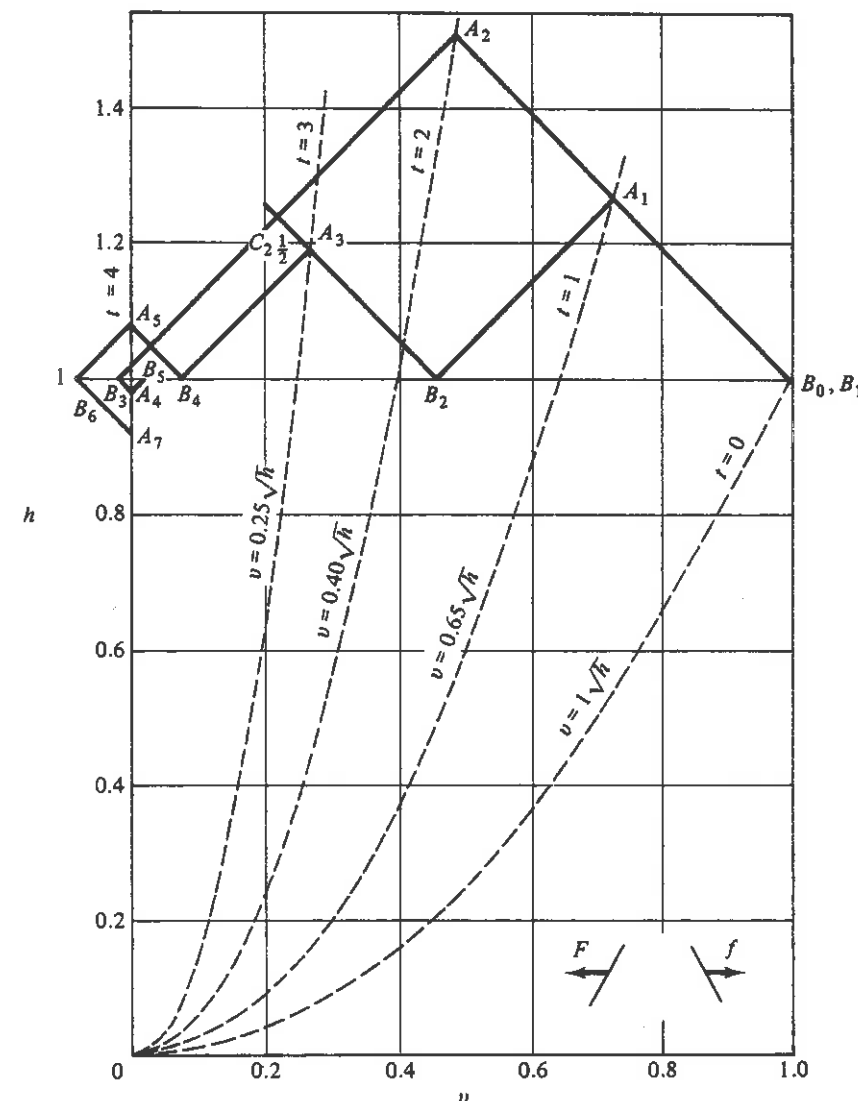


Figure 5-7 Gradual valve-closure solution.

on the parabola, the h and v value at the valve must occur (i.e., A_1 must be on the $t = 1$ parabola, etc.). At the other end of the pipe (Fig. 5-4), $h = 1$ because of the reservoir. To start the solution, begin at the steady condition B_0 and construct the f line through B_0 . On this line, A_1 must be found, which is also on the parabola $t = 1$. By proceeding on the F line from A_1 to B_2 , the intersection of the F line with $h = 1$ yields B_2 . Then construct an f line from B_2 to A_3 on parabola $t = 3$, and an F line from A_3 to B_4 . At all times after $t = 4$ the gate is closed, so A is on the ordinate axis $v = 0$ and B is on $h = 1$. To provide extra detail, start with B_1 (undisturbed because the first valve movement is at $t = 1$), proceed on an f line to the $t = 2$ parabola A_2 , then proceed to B_3, A_4, A_5 , and so on, as shown.

The graphical method is the most visual of all methods. Reflections at the end conditions are taken care of automatically by proper representation of the boundary conditions on the graph. A considerable amount of detail is available on the transients in the pipeline from the diagram. For example, the velocity at the reservoir at 1-s intervals is apparent. To find the value of h and v at the pipe midpoint C , we note that a wave leaving A_2 on an F line would arrive at $C_{1/2}$, and similarly, a wave leaving B_2 on an f line would arrive at $C_{1/2}$.

Note that the time interval selected in these examples was L/a . This permitted the determination of detail at the pipe midpoint. By taking more detail in the τ -time curve, say for each $L/2a$, intersections of the f and F lines can be interpreted to yield values of v and h at the quarter points.

Example 5-2

Consider a linear valve opening in time $4L/a$ on the system shown in Fig. 5-4. Determine the pressure variation at the valve.

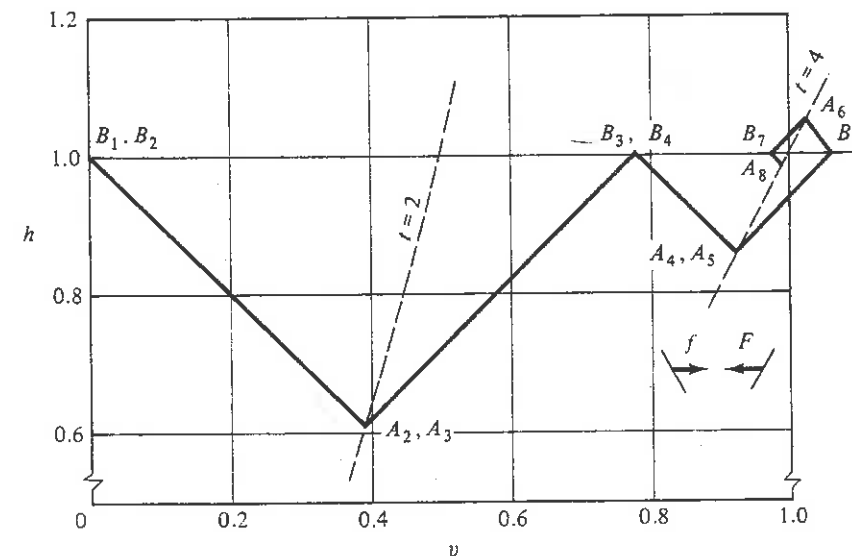


Figure 5-8 Valve opening.

Since there is no velocity for steady state, any V_0 may be assumed in computing B , say $V_0 = 0.98 \text{ m/s}$. Then $B = 1$. The time increment can be taken as large as $2L/a$, so assume that the valve opens in two steps: at $2L/a$ and at $4L/a$. Start the solution at B_1 ($v = 0, h = 1$) and move along an f line to A_2 on the parabola $t = 2$ (Fig. 5-8). An F line can then be drawn to point B_3 along the line $h = 1$ for conditions at the reservoir. The solution continues as shown. More detail can be obtained by starting B_2 ($v = 0, h = 1$).

Effects of Fluid Friction

Although head losses due to frictional effects are actually distributed along the length of the pipeline, a system that artificially includes losses is relied upon in the graphical technique. This amounts to lumping the total losses at selected points along the system.^{1,7} The simplest assumption is that the entire head loss is concentrated at the inlet end of the pipeline. Then the boundary condition at the upstream end is not represented by a horizontal straight line, $h = 1$, but by a head-loss curve. The entrance loss, velocity head, and pipe friction can be lumped together. Thus

$$h_f = \left(1 + K + \frac{fL}{D}\right) \frac{V_0^2 v^2}{2g H_0} \quad (5-15)$$

Then the parabola represented by the equation $h = H_{0R}/H_0 - h_f$ forms the boundary condition for the upstream end.

Example 5-3

Say that the pipeline diameter in Fig. 5-9 is 150 mm and the friction factor is 0.02. Solve the problem graphically including friction for the slow valve closure given in Fig. 5-6. Neglect the velocity head and entrance loss.

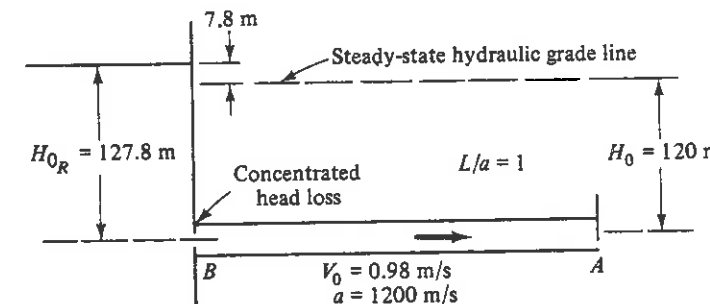


Figure 5-9 Single pipeline, including friction.

Equation 5-15 becomes

$$h_f = \frac{0.02(1200)}{0.15} \frac{0.98^2 v^2}{2(9.8)(120)} = 0.065 v^2$$

The initial pressure gradient is shown in Fig. 5-9. Point B is now assumed to be on the pipe side of the artificial loss mechanism. The graphical solution begins at B_0 ($h = 1, v = 1$) (Fig. 5-10), and proceeds as before, using the head-loss parabola as the upstream boundary condition.

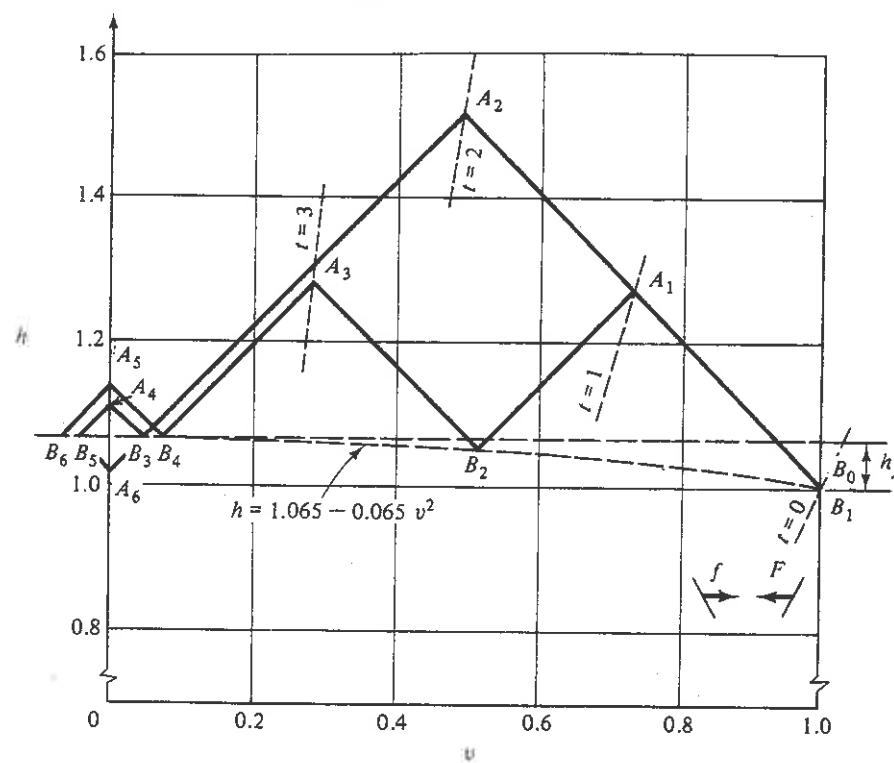


Figure 5-10 Valve closure with lumped friction.

Utilization of the hv plane for visualization of unsteady behavior in a system can be helpful. Figure 5-11 shows four examples, focusing attention only on the immediate region of the hv plane around coordinates (1, 1). In each case it is visualized that a disturbance has been created at some location upstream in the system, point B_1 . The objective is to observe the response provided by the downstream boundary as the waves reflect in the simple system.

In the first three cases an open valve, which appears with a slope $dh/dv = 2$ on the dimensionless hv plane, is indicated. It is easily visualized that the presence of such a device has a stabilizing influence on any transient introduced into the system. However, it is also noted that the magnitude of the pipeline impedance, as represented in the parameter B , relative to the valve impedance, which has a dimensionless value of 2, affects the type of response. In case (a) of Fig. 5-11, $B < 2$, it is seen that the decay involves oscillation around the final steady condition. In case (b), $B = 2$, the oscillation is damped without reflection. This is the case of a matched impedance. In case (c), $B > 2$, the oscillation approaches the final value from one direction only. The number of oscillations depends on the ratio of the pipeline to valve impedances. In case (d) a device that provides a negative characteristic is attached at the downstream end. This could be a perfect governor that operates a gate to provide constant power. The unstable nature of the response is apparent with the magnifying oscillations.

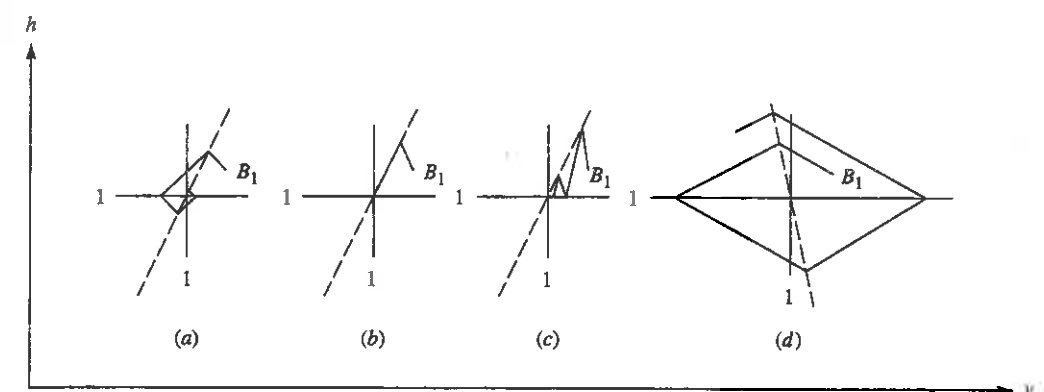


Figure 5-11 Graphical display of response in systems.

The visualization of the response of other devices attached to either end of a single pipeline is helpful on these graphical sketches. Oscillating valves, reciprocating pumps, operating centrifugal pumps are a few of the examples. Analysis of more complicated series and branching pipeline systems, although possible, is better accomplished by other methods.

5-3 Implicit Method

In the implicit finite difference method, pipelines are divided into reaches and the equations are solved simultaneously for the entire system at each time step. The main advantage in the method is that the time step is not limited to the Courant condition for stability of the solution procedure. However, to achieve reasonable accuracy in most transient pipeline problems the time step-distance interval relationship specified by the Courant condition is, in fact, a requirement.

The simplified equations of motion and continuity, Eqs. (2-11) and (2-26), may be written

$$H_x + \frac{Q_t}{gA} + \frac{f Q^2}{2gDA^2} = 0 \quad (5-16)$$

$$H_t + \frac{a^2}{gA} Q_x = 0 \quad (5-17)$$

If a centered implicit scheme is used (Fig. 5-12), the partial derivatives are approximated and the equations are placed in a finite difference form as follows:

$$\frac{H'_B + H_B - H'_A - H_A}{2\Delta x} + \frac{Q'_A + Q'_B - Q_A - Q_B}{2gA\Delta t} + \frac{f(Q_A + Q_B)^2}{8gDA^2} = 0$$

$$\frac{H'_A + H'_B - H_A - H_B}{2\Delta t} + \frac{a^2}{gA} \frac{Q'_B + Q_B - Q'_A - Q_A}{2\Delta x} = 0$$

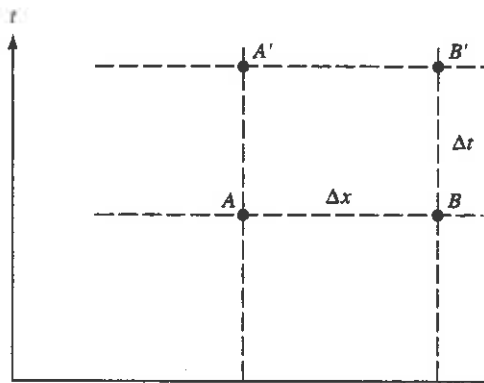


Figure 5-12 xt plane for implicit method.

Rearranging, the equations become

$$H'_B - H'_A + \frac{B}{C_r}(Q'_A + Q'_B) = C_1 \quad (5-18)$$

$$H'_B + H'_A + C_r B(Q'_B - Q'_A) = C_2 \quad (5-19)$$

in which $B = a/gA$, the characteristic impedance, and the Courant number⁶ is defined

$$C_r = \frac{a \Delta t}{\Delta x} \quad (5-20)$$

and

$$C_1 = -\frac{f \Delta x (Q_A + Q_B)^2}{4gDA^2} - (H_B - H_A) + \frac{B}{C_r}(Q_A + Q_B)$$

$$C_2 = H_A + H_B + C_r B(Q_A - Q_B)$$

It is assumed that conditions are known at an earlier time, points A and B in Fig. 5-12, and computations are to evaluate the quantities at a later time. The loss term has been approximated utilizing the known values in the cell for simplicity, although a higher-order evaluation would be preferred in high-friction cases.

There are four unknowns in Eqs. (5-18) and (5-19). When a pipe is divided into n reaches with $n + 1$ sections, there are $2n + 2$ variables at each time step. Two equations are available in each reach, which together with one at each end condition, enables a unique solution. In a single pipeline or serial system a banded matrix results which is convenient for the simultaneous solution. An example is used to illustrate the application of the method in a simple problem.

Example 5-4

A pipeline with a closed end downstream is filled with water at zero pressure and no flow. $L = 1000$ m, $a = 1000$ m/s, $A = 0.102$ m 2 , and $f = 0$. At $t > 0$ the upstream pressure is raised instantaneously to 10 m and held at that level. Find the pressure history at the downstream end and the flow history at the upstream end using one reach in the pipeline for time steps of (a) 1 s, the Courant condition, (b) 2 s, and (c) 0.5 s. Compare

the results to the analytic solution.

- (a) For each case $B = 1000$ s/m 2 . For $\Delta t = 1$ s, $C_r = 1$, and Eqs. (5-18) and (5-19) may be written, with $Q'_B = 0$ and $H'_A = 10$ m for $t > 0$,

$$H'_B - 10 + 1000Q'_A = H_A - H_B + 1000Q_A$$

$$H'_B + 10 - 1000Q'_A = H_A + H_B + 1000Q_A$$

At $t = 1$ s the simultaneous solution of these equations yields $Q'_A = 0.01$ m 3 /s and $H'_B = 0$ m. As time is incremented sequentially by 1 s, the equations may be used to compute the following values.

t	H_A	Q_A	H_B
0	0	0	0
1	10	0.01	0
2	10	0.01	20
3	10	-0.01	20
4	10	-0.01	0
5	10	0.01	0
6	10	0.01	20

- (b) For $\Delta t = 2$ s, $C_r = 2$. Substitution into Eqs. (5-18) and (5-19) and solving simultaneously yields the following table of values:

t	H_A	Q_A	H_B
0	0	0	0
2	10	0.0080	6.0
4	10	-0.0016	18.8
6	10	-0.0061	3.44
8	10	0.0089	9.07
10	10	-0.0046	17.67

- (c) For $\Delta t = 0.5$ s, $C_r = 0.5$, and the following results are generated.

t	H_A	Q_A	H_B
0	0	0	0
0.5	10	0.0080	-6.0
1.0	10	0.0180	6.8
1.5	10	0.0131	22.16
2.0	10	-0.0019	27.79
2.5	10	-0.0153	19.19
3.0	10	-0.0166	3.23
3.5	10	-0.0045	-7.31
4.0	10	0.0111	-4.00

Calculations have been completed to 10 s and graphed in Fig. 5-13.

The results in Fig. 5-13 clearly show the need for adhering to the Courant condition to model rapid transients. Slower transients in systems with larger effective storage, either through low wave speeds or additional storage elements in the system, and highly viscous systems are more amenable to use of this method. These are situations in which

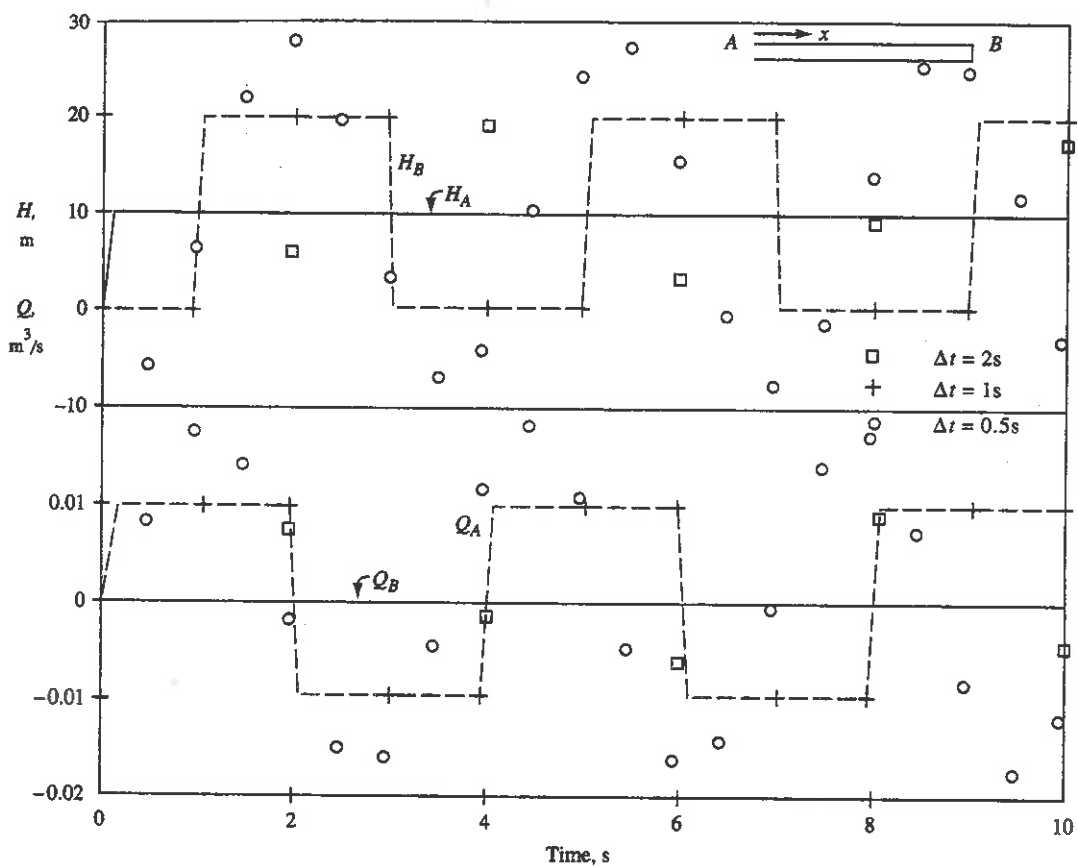


Figure 5-13 Example 5-4, implicit solution results.

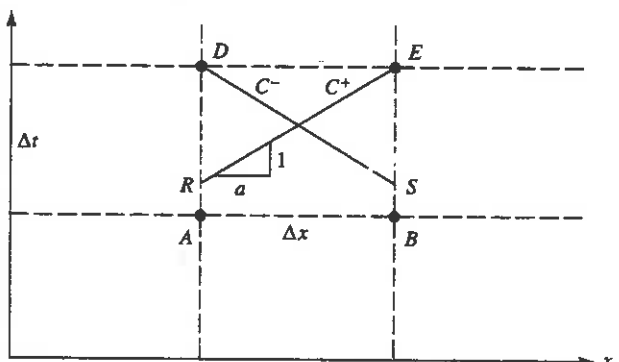


Figure 5-14 Implicit method of characteristics.

the benefits of Courant numbers greater than unity may be realized. Free surface flows and long-period natural gas transients are examples where the method may be attractive.

It is also possible to develop an implicit method of characteristics.³ By referring to Fig. 5-14, the compatibility equations, Eqs. (3-15) and (3-16), may be written

$$H_E - H_R + B(Q_E - Q_R) + RQ^2 = 0$$

$$H_D - H_S - B(Q_D - Q_S) - RQ^2 = 0$$

With a suitable evaluation of the variables at points *R* and *S*, which includes use of the unknowns at points *D* and *E*, and a suitable representation of the friction term, a simultaneous solution similar to the previously described implicit method may be developed. When the characteristics are viewed as shown in Fig. 5-14, it is clear why the Courant condition must be satisfied to handle rapid pipeline transients satisfactorily.

5-4 Finite Element Method

Although there is no attempt to develop and utilize the finite element method in this treatment, a few comments on the method as it relates to and differs from other methods seem appropriate. The finite element method has found wide acceptance in a variety of flow problems, but its success in computing liquid pipeline transients has been limited.^{5,8-10} There is considerable motivation to utilize the method, however, since in applications where it can be used it provides great flexibility in handling variable-size elements of different properties.

A method of weighted residuals is most commonly used. A trial function (shape function) substituted into the differential equation generally does not equal the exact solution, the difference being the residual. This residual, multiplied by a weighting function, yields a weighted residual. The finite element method attempts to force the weighted residuals to zero in an average sense. The particular choice of the weighting function provides a different weighted residual. One of these choices, the Galerkin method, requires the weighting function to be equal to the trial function. The limited success of the classical Galerkin principle is due to the fact that optimum approximations resulting from application of this method to elliptic and parabolic problems do not generalize to the hyperbolic problems associated with wave propagation.² Two problems arise: (1) the difference equations are dispersive which results in individual wave components propagating at different speeds depending on the frequency, and (2) the approximate difference equations are nondissipative, which results in the generation of spurious oscillations in the vicinity of sharp changes of the flow variables.

Alternative formulations may bring about improvements. One such formulation has met with some success in modeling rapid changes in open-channel problems.⁴ Based on a variance of the Galerkin principle that utilizes unequal trial and weighting function, it is referred to as the Petrov-Galerkin method. An example of the application of the procedure in a variable wavespeed pipeline problem has also been presented.⁵

All the methods introduced in this chapter, along with the method of characteristics, solve unsteady flow equations in the time domain. These methods may be applied to

analyze steady oscillatory or periodic flows. However, to deal with such a specific type of unsteady flow, more efficient methods are available, which proceed mainly in the frequency domain and provide solutions in the time domain ultimately. Discussions of the methods in this category—for example, the frequency response, the Fourier transform method, and the impulse response method—are left for Chapters 12 and 13. Throughout the remainder of this book the method of characteristics is the method of choice for time-domain modeling of pipeline transients. To extend the application of the method, in Chapter 6 we introduce other elements that interface with pipelines so that more complex systems may be analyzed and so that control devices and control operations may be designed.

Problems

- 5-1. For negative flow the friction term in Eq. (5-5) changes sign. Develop the equation relating V to time to initiate flow from rest in the negative direction with a positive ΔH .
- 5-2. Draw sketches of velocity vs. time and H_D vs. time up to a velocity of $0.99V_0$ in Example 5-1.
- 5-3. Consider the valve closure of Fig. 5-6. At $t/(L/a) = 2$, however, the valve closure stops and remains in that position. Determine the head variation at A (Fig. 5-4), until $t/(L/a) = 10$, and compare it with the head variation at A from Fig. 5-7.
- 5-4. A valve on a simple pipeline is closed in the manner shown. For the data given, find the pressure variation at the valve and midpoint. $L = 600$ m, $a = 1200$ m/s, $V_0 = 1.3$ m/s, and $H_0 = 60$ m.

$t:$	0.0	0.5	1.0	1.5	2.0	2.5
$\tau:$	1.0	0.9	0.75	0.55	0.30	0.0
- 5-5. Assume (Problem 5-4) that the pipe is 200 mm in diameter and that $f = 0.018$. Find the pressure-head variation at the valve.
- 5-6. A valve at the end of a simple pipeline opens and closes in a cyclic manner every $4L/a$ seconds. Sketch the graphical diagram to show the resulting transients (assume that the valve is initially closed). Sketch the pressure-head and velocity variations at the valve in dimensionless terms. Assume a value for B .
- 5-7. In a simple frictionless reservoir-pipeline-valve system with $B = 2$ and $L/a = 1$ s, a linear valve (linear τ) motion is used to close the valve in t_c seconds. At $t = 1$ s the velocity at the valve is 7.65 ft/s. Steady-state velocity in the pipeline is 9.0 ft/s. Find the time of closure and the maximum pressure head.
- 5-8. A valve at the downstream end of a pipe has a discharge in m^3/s given by $Q = 0.22 - 0.001H$, in which H is the head drop across the valve. $L = 1000$ m, $a = 1000$ m/s, $D = 0.7$ m, $H_R = 120$ m. At $t > 0.0$ set the reservoir level to 119 m. Assume a frictionless pipeline and solve the problem graphically.
- 5-9. A single frictionless pipeline from a reservoir upstream to a valve downstream operates with a flow of 1 m/s when the valve is wide open. Initially, the valve is closed and the system is at rest. $a/g = 100$ s, $H_0 = 100$ m.
 - (a) A sine wave of amplitude 5 m with a period of $4L/a$ seconds begins to pulse the system at the upstream end. Graphically find the oscillations that develop.

References

- (b) After three complete periods the valve is opened to the wide-open position. Show the oscillating pattern from the initial pattern to the final oscillatory condition.
- 5-10. Consider the pipeline shown in Fig. 5-15 with the valve at the upstream end. In the graphical method use two steps to describe the linear valve closure in 4 s. $L = 3000$ ft, $V_0 = 10.73$ ft/s, $a = 3000$ ft/s, and $D = 10$ ft. Find the maximum head in the pipeline for this closure.

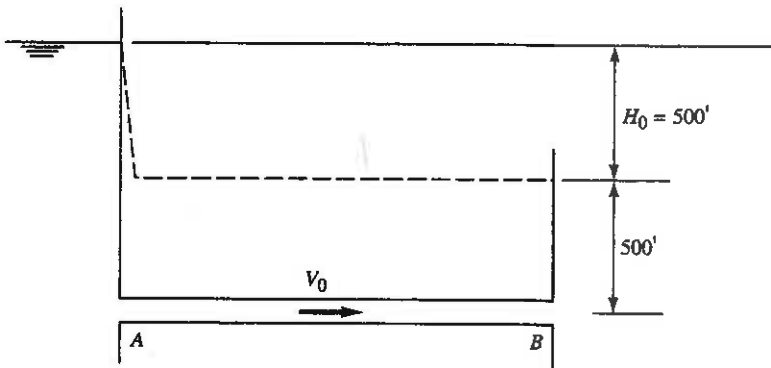


Figure 5-15 Problem 5-10.

- 5-11. A single pipeline leads from a reservoir at elevation H_1 to a downstream reservoir at elevation H_3 . A valve is located at each end of the pipeline. With a steady flow of $1.0 \text{ m}^3/\text{s}$, the loss at the upstream valve is 25 m and at the downstream valve 50 m. $a = 980$ m/s, $D = 1.25$ m. The upstream valve is moved instantaneously to a new position in such a manner that there is no reflection in the system. Find the value of τ for the upstream valve required for this to happen.

- 5-12. Complete the calculation to 10 s in Example 5-4 for each of cases (a), (b), and (c).

References

1. L. Bergeron, *Water Hammer in Hydraulics and Wave Surges in Electricity* (translated under the sponsorship of the ASME), Wiley, New York, 1961.
2. J. E. Dendy, "Two Methods of Galerkin-Type Achieving Optimum L^2 Rates of Convergence for First-Order Hyperbolics," *SIAM J. Numer. Anal.*, Vol. 11, pp. 637–653, 1974.
3. D. E. Goldberg, and E. B. Wylie, "Characteristic Method Using Time-Line Interpolations," *J. Hydraul. Div., ASCE*, Vol. 109, No. HY1, Jan. 1983.
4. N. D. Katopodes, "A Dissipative Galerkin Scheme for Open-Channel Flow," *J. Hydraul. Div., ASCE*, Vol. 110, No. 4, pp. 450–466, Apr. 1984.
5. N. D. Katopodes, and E. B. Wylie, "Simulation of Two-Dimensional Nonlinear Transients," *Symp. Multi-dimensional Fluid Transients*, ASME, New Orleans, La., pp. 9–16, Dec. 1984.
6. Chintu Lai, "Numerical Modeling of Unsteady Open-Channel Flow," Chap. 3 in V. T. Chow and B. C. Yen (eds.), *Advances in Hydroscience*, Vol. 14, Academic Press, New York, pp. 161–333, 1986.

7. J. Parmakian, *Water-Hammer Analysis*, Dover, New York, 1963.
8. H. H. Rachford, Jr., and Todd Dupont, "Some Applications of Transient Flow Simulation to Promote Understanding the Performance of Gas Pipeline Systems," *Soc. Pet. Eng. AIME*, pp. 179-186, Apr. 1974.
9. H. H. Rachford, Jr., and E. L. Ramsey, "Application of Variational Methods to Model Transient Flow in Complex Liquid Transmission Systems," *Paper SPE 5663, 50th Annual Fall Meeting*, Society of Petroleum Engineers of AIME, Dallas, Sept. 28-Oct. 1, 1975.
10. C. S. Watt, A. P. Boldy, and J. M. Hobbs, "Combination of Finite Difference and Finite Element Techniques in Hydraulic Transient Problems," *Proc. 3rd Int. Conf. Pressure Surges*, BHRA, Canterbury, England, pp. 43-62, Mar. 1980.

6

Complex Systems with Multipipe and Nonpipe Elements

In Chapter 3 a number of basic boundary conditions were introduced which provided relationships between the variables at pipeline terminals. The boundaries were all of the nondynamic type: one variable was specified, or an algebraic relationship between two variables was provided, or an algebraic relationship between flow, pressure, and other additional variables was used. In this chapter additional nondynamic pipeline terminations are discussed, behavioral characteristics of complex systems are presented, and a few dynamic system elements, which require the use of differential equations to describe their behavior, are introduced. As in the algebraic relationships at boundaries, the differential equation may describe the time variation of flow and pressure; or a combination of algebraic and differential equations may relate flow, pressure, and additional variables. Special computational procedures are presented to deal with contiguous nonpipe elements.

6-1 Wave Transmission and Reflection

Unsteady liquid flows in pipeline systems offer a challenge in visualization, particularly when there is interaction among different system facilities. Changes in pipeline cross section, valves, orifices, accumulators, and other elements commonly encountered in systems may provide unique unsteady behavioral characteristics. The influences of discontinuities in pipelines⁷ and of orifices¹ on wave propagation and transmission are used herein as examples to improve unsteady flow visualization.¹⁴

Series Connection

Figure 6-1 shows a frictionless series pipeline with a change in pipeline area, or wavespeed, or both. An incident wave of magnitude H_W is approaching the connection from downstream. Three compatibility equations may be written along the characteristic lines shown in Fig. 6-1, and solved for the three variables, Q_W , H_j , and Q_j , in terms of the characteristic impedances of the adjoining pipes. First, Eq. (3-15) in pipe 2, with the friction term dropped, yields

$$Q_W = Q_0 - \frac{H_W - H_0}{B_2} \quad (6-1)$$

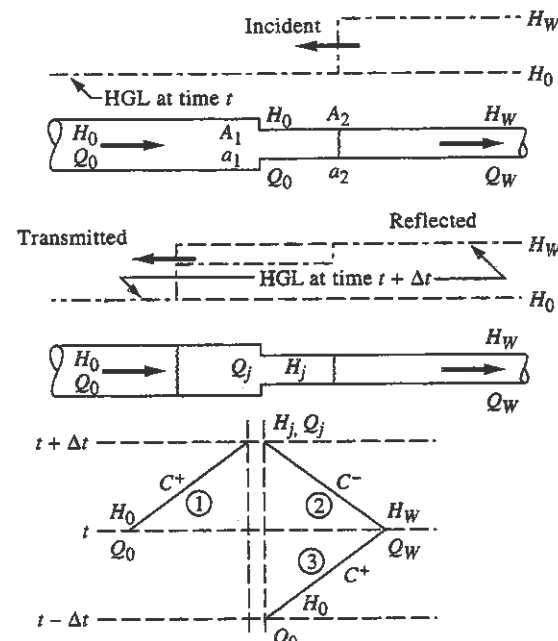


Figure 6-1 Series pipeline reflections.

The combination of Eq. (3-15) in pipe 1 and Eq. (3-16) in pipe 2, together with Eq. (6-1), provides the reflected and transmitted flow and pressure after the initial wave has interacted at the junction,^{6,7} in terms of the characteristics of the pipelines only.

$$\frac{H_j - H_0}{H_W - H_0} = \frac{2}{1 + B_2/B_1} = \frac{2}{1 + a_2 A_1 / a_1 A_2} \quad (6-2)$$

$$\frac{Q_j - Q_0}{Q_W - Q_0} = \frac{2}{1 + B_1/B_2} \quad (6-3)$$

In Eq. (6-2) if $A_2 = A_1$ and $a_2 = a_1$, the junction has no influence on the incident wave. With a constant wave propagation velocity, if $A_1 < A_2$, Eq. (6-2) shows the magnitude of the incident wave to be magnified at the junction. In the limit as A_1 approaches zero (dead end) the incident pressure wave doubles in magnitude. Similarly, if $A_1 > A_2$,

Eq. (6-2) shows attenuation of the incident wave and, in the limit, as A_1 becomes very large the junction pressure is not influenced by the incident wave.

By similar reasoning the response at the junction of a stiff pipe with a soft pipe may be visualized. Two configurations are shown in Fig. 6-2 to illustrate. In Fig. 6-2a the wave propagating in the steel pipe is transmitted and reflected with a much smaller magnitude at the junction with the rubber tube. The influence of air, which is very compressible, trapped in a pressure-sensing device is illustrated in Fig. 6-2b. Only a small portion of a sharp incident wave would be sensed by the transducer.

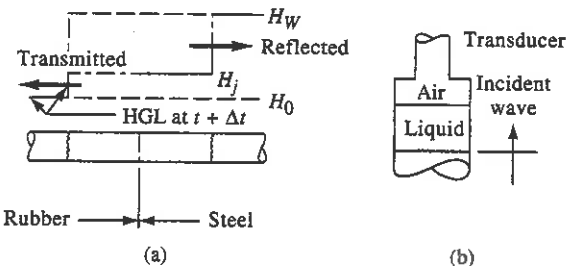


Figure 6-2 Pipelines with different wavespeeds in series.

Multiple serial area, or wavespeed, changes can be analyzed by repeated applications of Eqs. (6-2) and (6-3). It is easily demonstrated that the incident pulse will have a magnitude, at the n th step change, of

$$\frac{H_n - H_0}{H_W - H_0} = 2^n \prod_{j=1}^n \frac{1}{1 + B_{j+1}/B_j} \quad (6-4)$$

A graph of Eq. (6-4), in which an equal ratio of characteristic impedances at each junction is considered, is shown in Fig. 6-3. The line designated $n = 1$ illustrates Eq. (6-2).

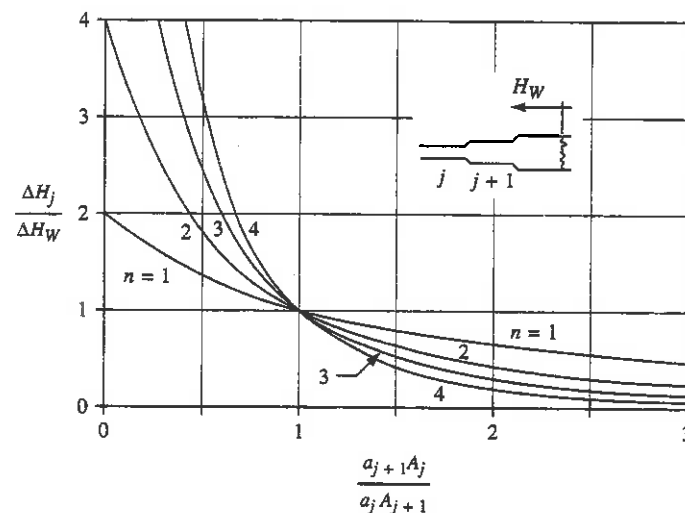


Figure 6-3 Incident wave in series system.

As an example, the interesting condition that develops if a constant-wavespeed pipeline is reduced in diameter by a factor of 4 (area reduction of 16) is visualized. Table 6-1 shows the consequences of making the reduction in a single step or in a larger number of equal steps. The first passage of the incident pulse increases the magnitude to 1.88 the original value if only a single step is used, while it increases to 3.16 the original value if four step changes are used, each reducing the area 50 percent to provide the same total area reduction. This example shows that the manner in which an area reduction in a pipeline is achieved can have a significant influence on the ultimate magnitude of a rapid pressure pulse during a transient. Waves can be focused, thereby achieving a magnitude greater than double that of the original incident wave.

TABLE 6-1 MAGNIFICATION OF INCIDENT PULSE

n	$\frac{A_{j+1}}{A_j}$	$\frac{H_n - H_0}{H_w - H_0}$
1	16.00	1.88
2	4.00	2.56
3	2.52	2.94
4	2.00	3.16

Orifice-in-Line

The degree to which high-loss elements in a pipeline modify waves propagating in the system is of considerable interest. An in-line orifice provides a vehicle for the study. The response at other elements, such as elbows, expansion pipes, constrictors, and so on, may be inferred from these results.

A pipeline with constant characteristic impedance carries a steady frictionless flow, with energy loss only at the in-line orifice. With flow of Q_0 , the steady head loss across the orifice is H_0 . If the loss coefficient for the orifice expresses the number of velocity heads lost, then, for steady flow,

$$H_0 = H_U - H_D = K \frac{Q_0^2}{2gA^2} \quad (6-5)$$

and for conditions after the passage of the wave,

$$H_R - H_T = K \frac{Q^2}{2gA^2} \quad (6-6)$$

Equation (6-6) is valid for unsteady flow if there is no fluid storage in the orifice and if inertial effects are neglected. Figure 6-4 displays the conditions at the orifice. Also shown in Fig. 6-4 are three characteristic lines along which compatibility equations may be written to be used with Eq. (6-6) to find the unknowns of H_R , H_T , Q , and Q_W . It is convenient to relate the size of the transmitted wave to the original downstream pressure, $\Delta H_T = H_T - H_D$, and the reflected wave to the original upstream pressure,

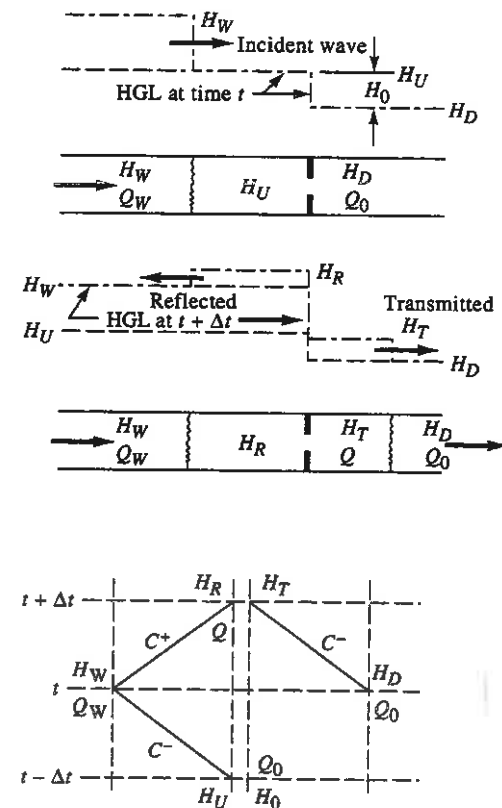


Figure 6-4 Conditions at in-line orifice.

$\Delta H_R = H_R - H_U$. After algebraic combinations of the four equations the following expressions provide the transmitted and reflected waves in terms of dimensionless parameters H_0/BQ_0 , and $\Delta H_w Kg/2a^2$, in which $\Delta H_w = H_w - H_U$.

$$\frac{\Delta H_T}{\Delta H_w} = \frac{-(1 + H_0/BQ_0) + \sqrt{(1 + H_0/BQ_0)^2 + 2(Kg/2a^2) \Delta H_w}}{(Kg/2a^2) \Delta H_w} \quad (6-7)$$

$$\frac{\Delta H_R}{\Delta H_w} = 2 - \frac{\Delta H_T}{\Delta H_w} \quad (6-8)$$

If there is no initial flow, the parameter H_0/BQ_0 is set to zero in these equations. With zero initial flow, Fig. 6-5 shows the dimensionless magnitude of the transmitted wave to vary from zero for the high-loss element, to full transmission of the wave at an element with a small loss ($K \approx 0$). The reflected wave varies in magnitude from zero for the low-loss element to double the incident wave for the high-loss element ($K \gg 0$). With an initial flow ($H_0/BQ_0 > 0$) there is always some reflection at the orifice and a corresponding transmission of a reduced wave.

It may be noted in Fig. 6-5 that with no initial flow, a value of $Kg \Delta H_w/2a^2$ greater than approximately 4 transmits 50 percent or less of an incident wave (reflects 50 percent or more). This corresponds to a loss coefficient greater than 10^4 if an

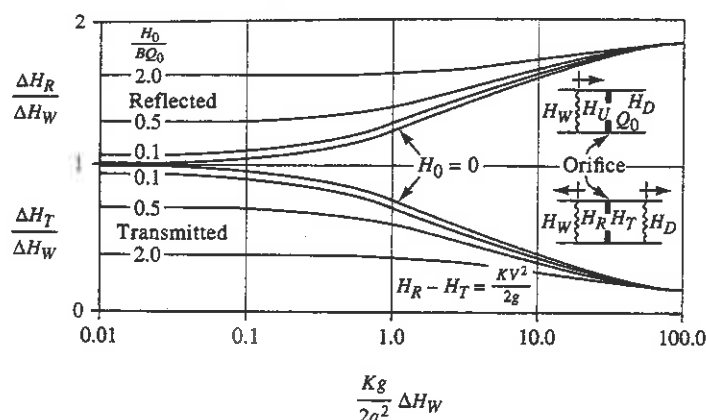


Figure 6-5 Orifice reflection and transmission.

incident wave amplitude of 80 m is assumed in a pipe with a wavespeed of 1000 m/s. With the same orifice in the same pipe but with an initial flow $H_0/BQ_0 > 0$, there is a larger reflection and smaller transmission. Another feature to note in Fig. 6-5 is that larger-amplitude waves have a larger portion of their magnitude reflected than do smaller-amplitude waves through the same opening. These generalized observations are of value in assessing the influence of elbows, tees, and so on, on the magnitude of one-dimensional waves in a piping system. For example, a fixed elbow, which is a low-loss element, would have little influence on the magnitude and shape of a pressure wave.

Orifice at Pipe End

The orifice located at the termination of a pipeline, with constant receiving pressure, produces a markedly different effect than that of the in-line orifice. Figure 6-6 shows conditions at the orifice before and after wave reflection. Again the combination of Eq. (6-6), setting $H_T = H_D$, with the upstream compatibility equations yields the magnitude of the reflected pressure wave and flow.

$$\frac{\Delta H_R}{\Delta H_W} = 2 - \frac{\psi}{(Kg/2a^2) \Delta H_W} \quad (6-9)$$

$$\frac{Q - Q_0}{aA} = \frac{2}{K} \psi \quad (6-10)$$

In these equations

$$\psi = -\left(\frac{1}{2} + \frac{H_0}{BQ_0}\right) + \sqrt{\left(\frac{1}{2} + \frac{H_0}{BQ_0}\right)^2 + \frac{2Kg \Delta H_W}{2a^2}}$$

For zero initial flow the parameter H_0/BQ_0 is zero.

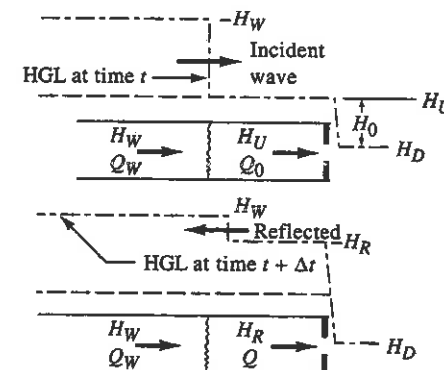


Figure 6-6 Reflection at pipe-end orifice.

Figure 6-7 shows the variation in magnitude of the reflected wave with the parameter $\Delta H_W Kg/2a^2$ for various values of H_0/BQ_0 . For the case of zero initial flow, reflections of zero at the open end ($K = 0$) and double at the closed end ($K \approx \infty$) are apparent. Also, with values or the ordinate $\Delta H_W Kg/2a^2 > 1$, a positive reflection of the incident wave occurs, while if the abscissa equals 1, the reflected wave is exactly equal to the incident wave, a condition that produces no reflection and is known as a matched-impedance orifice. The latter concept is sometimes useful in a design to avoid undesirable residual reflected waves.

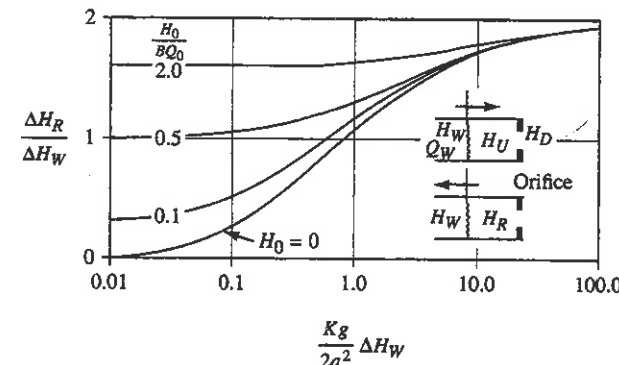


Figure 6-7 Orifice reflections at pipe end.

Example 6-1

Use a pipe-to-orifice diameter ratio of (a) 10 and (b) 2 for a no-initial-flow case and for $H_0/BQ_0 = 0.5$. Find the relative magnitude of the reflected wave for a sharp incident wave of 50 m in a pipe in which $a = 1000$ m/s. Use the approximation $K = (D/D_0)^4/C_d^2$, with $C_d = 0.6$.

For (a), $D/D_0 = 10$:

$$K = 27,780 \quad \frac{Kg}{2a^2} \Delta H_W = 6.806$$

For (b), $D/D_0 = 2$:

$$K = 44.44 \quad \frac{Kg}{2a^2} \Delta H_W = 0.0109$$

By use of Eq. (6-9) for the end-of-pipe orifice and Eqs. (6-7) and (6-8) for the in-line orifice, the following table of values is prepared:

D/D_0	End-of-pipe orifice		In-line orifice	
	$H_0 = Q_0 = 0$	$H_0/BQ_0 = 0.5$	$H_0 = Q_0 = 0$	$H_0/BQ_0 = 0.5$
10	1.53	1.58	1.58	1.63
2	0.04	1.00	1.01	1.34

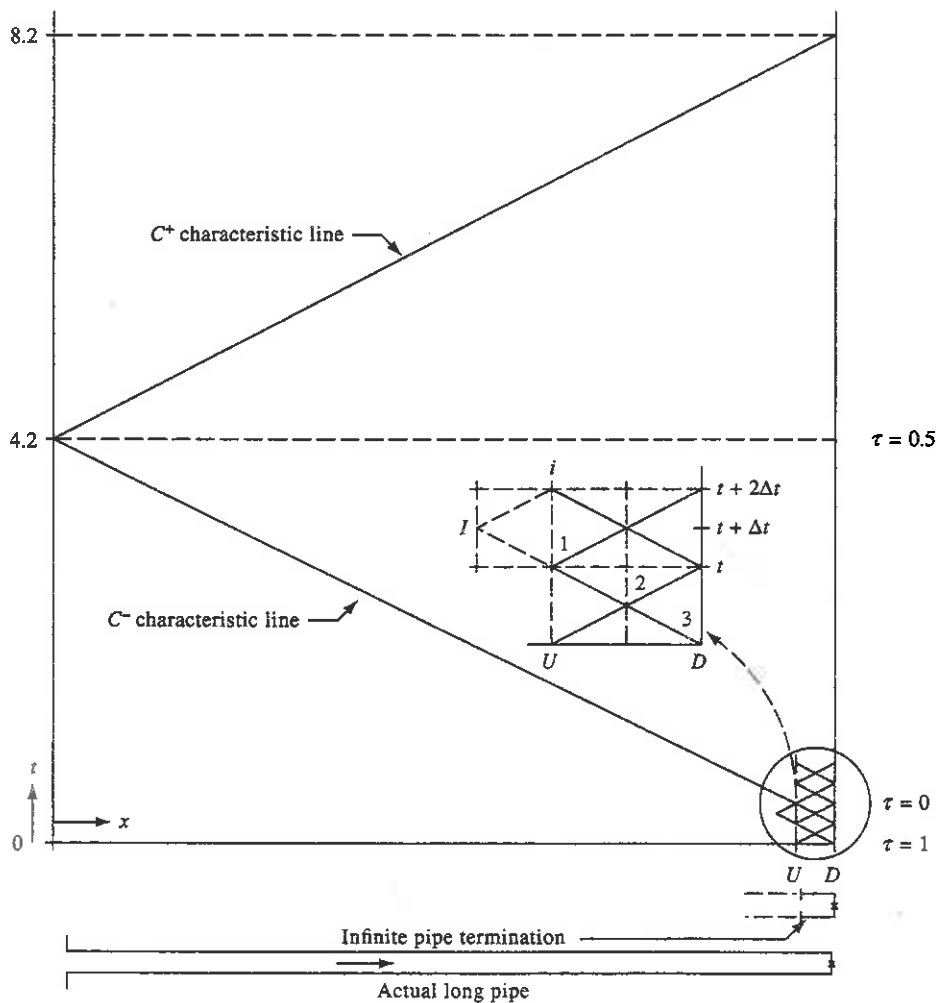


Figure 6-8 Long pipeline with infinite pipe termination.

6-2 Infinite Pipeline

In a long pipeline system the analyst may be interested in the transient details locally and not in the long-term behavior of the extended system. Under these conditions it is helpful to use an alternative model,¹⁶ but one that will respond similarly to the long pipe. This substitute element, which is to respond like the long pipe, is useful only up until a reflection would return from the other extremity of the long pipe (i.e., until $2L/a$ seconds), where L and a refer to the actual long line.

Conceptually, the characteristic impedance of the pipeline should provide the desired termination. However, the impedance B in the relationship $\Delta H = \pm B\Delta Q$ is valid only for frictionless systems. Figure 6-8 provides a sketch in which the desired termination would be located at point U, two distance intervals upstream from the exciter in the system. For illustration purposes a valve has been used for the exciter in this high-friction system, although it could be a pump or any other dynamic element.

Inasmuch as the only reflections in the system are from the friction gradient, any disturbances created at the exciter, point D, pass upstream only. Therefore, values of the variables at point I (Fig. 6-8), are extrapolated along a characteristic line beyond the modeled pipe termination one Δx . Although a linear extrapolation produces reasonable results, second order is better and is recommended:

$$H_I = 3H_1 - 3H_2 + H_3 \quad Q_I = 3Q_1 - 3Q_2 + Q_3 \quad (6-11)$$

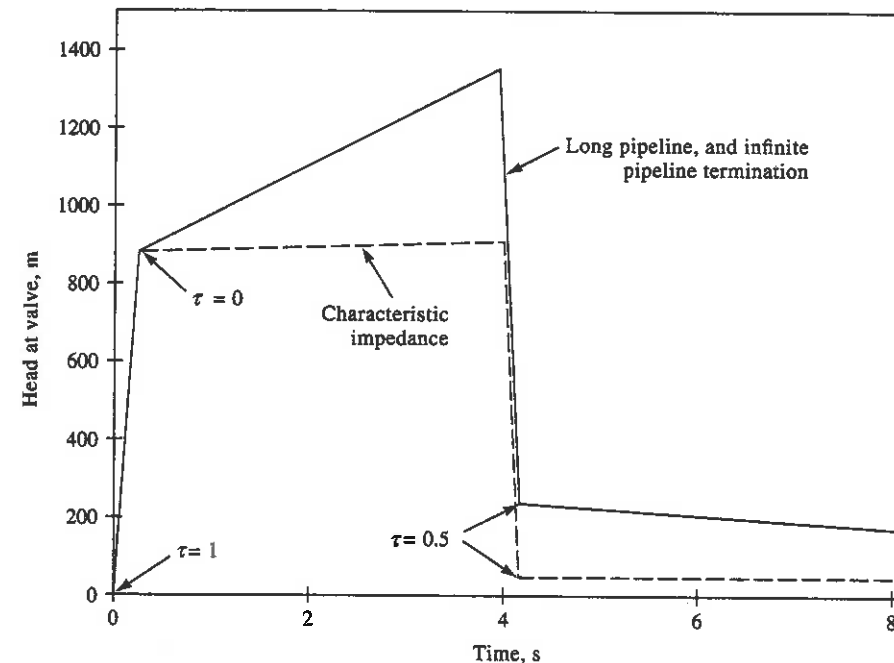


Figure 6-9 Infinite pipe termination response.

With values of the variables at point I available, a standard C^+ compatibility equation can be used, and a typical interior point calculation can be performed at section i .

Figure 6-9 shows results from an example with a rapid valve closure at $t = 0.2$ s and rapid opening to $\tau = 0.5$ at $t = 4.2$ s in the pipe in Fig. 6-8. The data are $L = 4800$ m, $D = 0.2$ m, $f = 0.018$, $a = 1200$ m/s, $Q_0 = 0.210$ m³/s, $H_0 = 27.88$ m, $N = 40$. Three different results at the valve are shown in Fig. 6-9: the actual values from the long pipe simulation, the values with the infinite pipe model as described above, and the values from use of the characteristic impedance termination. The latter two terminations were located at point U , 240 m upstream from the valve.

This represents a high-friction system, $f \Delta x Q_0 / 2 D A a = 0.03$, and it is seen that the results from the infinite pipe termination are indistinguishable in the sketch. The largest discrepancy, of approximately 2.9 m, occurred at the end of the simulation. For slower transients or lower-friction cases the results would be considerably better. Use of the pipeline impedance, although perfect in the frictionless case, is seen to be unacceptable in this high-friction rapid transient.

6-3 Lumped Elements

All one-dimensional fluid piping systems should be represented by distributed parameters since they are continuous systems. This is exactly how the important fluid parameters in pipelines are handled by the method of characteristics: the frictional losses, the fluid inertia, and the capacitance are all distributed along the pipeline. There are, however, situations when it is quite permissible to use a lumped-parameter analysis of portions of the continuous system. Simplifications may be achieved or economies in the analysis may be realized. In these cases the lumped elements must interact with the appropriate compatibility equations in the adjoining pipelines.

In a general pipeline system, short pipes and highly deformable elements are likely candidates for lumping the inertia and capacitance (elasticity or compressibility) parameters, respectively. High-loss elements in which neither inertia nor capacitance is important may be lumped by use of an equivalent orifice. It is recognized that even if lumped behavior of certain elements in the physical system exists, the method of characteristics is still valid since the physical behavior is incorporated in the equations, as long as the assumption of one-dimensional flow is realistic. The motivation to use a lumped model for an element is most often one of expediency.

Lumped Inertia

Short connectors between a main pipeline and an accumulator or surge device, standpipes, and short pipelines in longer systems may often be considered to be inelastic and to contain an incompressible fluid. If this assumption is made, it is inferred that the elasticity of this part of the system is not nearly as important as its inertia in determining the transient response. The liquid mass is then treated as a solid and the equation of motion with all forces acting, including friction, is written to describe its unsteady behavior (see Sec. 5-1).

The decision to use lumped inertia may be made by relating frequency, period, or wavelength of the excitation to the element length and wavespeed. Frequency and period are related:

$$T = \frac{2\pi}{\omega} = \frac{1}{f} \quad (6-12)$$

in which f is the frequency in cycles per second (hertz), ω the circular frequency, and T the period of the forcing action. The nature of a disturbance in a system is also characterized by its amplitude and waveform. If a wave is sinusoidal in form, the frequency is easily identified, but in the more general transient it is more difficult to quantify. An abrupt valve closure contains very high frequency components, whereas the oscillation of a sizable surge tank is a low-frequency phenomenon. The wavelength, λ , and wavespeed, a , are related to the parameters in Eq. (6-12):

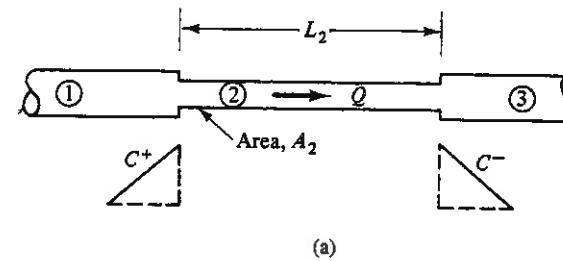
$$\lambda = Ta = \frac{2\pi a}{\omega} = \frac{a}{f} \quad (6-13)$$

A conservative criterion, although empirical, requires that the element length be less than about 4 percent of the wavelength in order to consider the use of a lumped inertia element. By Eq. (6-13) this may be expressed

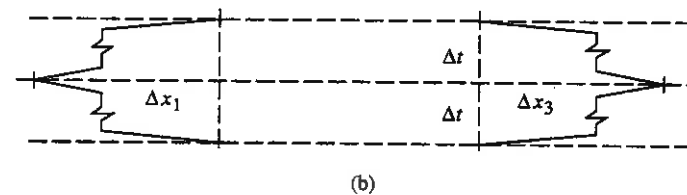
$$L < 0.04\lambda = 0.04Ta = 0.04 \frac{2\pi a}{\omega} = \frac{0.04a}{f} \quad (6-14)$$

The equation of motion applied to the short segment in Fig. 6-10a is

$$F_1 - F_3 - F_f = \frac{\gamma A_2 L_2}{g} \frac{dV}{dt} \quad (6-15)$$



(a)



(b)

Figure 6-10 Lumped inertia element.

in which F_1 and F_3 are the pressure forces on the upstream and downstream ends and F_f is the frictional force on the fluid. Integrating over two time steps in the staggered grid (Fig. 6-10b) and placing the equation in terms of volumetric flow rate yields

$$\gamma A_2 \left(\frac{H'_1 + H_1}{2} - \frac{H'_3 + H_3}{2} - \frac{f_2 L_2}{2g D_2 A_2^2} Q'_2 |Q_2| \right) = \frac{\gamma A_2 L_2 (Q'_2 - Q_2)}{g A_2 2\Delta t} \quad (6-16)$$

The primed quantities refer to the current variables, and the unprimed quantities refer to the variables two time steps earlier. A second-order approximation is used in evaluating the friction term and the trapezoidal rule has been used on the head terms. The equation may be written

$$H'_1 - H'_3 = C_1 + C_2 Q'_2 \quad (6-17)$$

in which

$$\begin{aligned} C_1 &= H_3 - H_1 - \frac{L_2 Q_2}{g A_2 \Delta t} \\ C_2 &= \frac{L_2}{g A_2} \left(\frac{f_2}{D_2 A_2} |Q_2| + \frac{1}{\Delta t} \right) \end{aligned} \quad (6-18)$$

Equation (6-17) is a linear relationship in the three variables that can be solved simultaneously with the compatibility Eqs. (3-21) and (3-22).

Lumped Capacitance

The elastic behavior of a small volume can be effectively lumped (Fig. 6-11). The entire region within the dashed line is assumed to be at the same pressure head at any instant, frictional effects are considered small and neglected, and inertial effects are much less important than capacitance or elastic effects. An effective bulk modulus of elasticity, K' , is used to describe the elastic effects of the fluid and the container:

$$K' = \frac{\Delta p}{\Delta V/V} \quad (6-19)$$

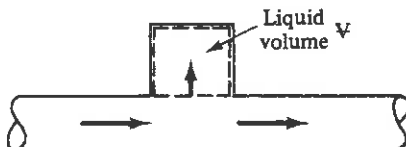


Figure 6-11 Lumped capacitance.

The volume of the container is given by V . If the flow is positive into the container, integration of the continuity condition, $dV/dt = \text{inflow}$ over two time steps in the staggered grid, yields ΔV , the volume of fluid entering the container in $2\Delta t$. In finite difference form, the relationship is

$$\Delta V = (Q' + Q) \Delta t \quad (6-20)$$

Equations (6-19) and (6-20), when combined, become

$$H' = H + \frac{K' \Delta t}{\gamma V} (Q + Q') \quad (6-21)$$

This equation provides a linear relationship between the variables H' and Q' which is easily solved with the compatibility equations. If there is a significant fractional change in the volume of the container, V should be updated at each time step.

The lumped capacitance model is useful in treating a short dead-end pipeline, a liquid accumulator, a liquid volume such as a cooling-water condenser water box, a short soft tube in a system, and so on.

6-4 Air Chamber or Accumulator

In the analysis of the single accumulator shown in Fig. 6-12 the pressure at any instant is assumed the same throughout the volume. The compressibility of the liquid in the vessel is considered negligible compared with air compressibility. Inertia and friction are neglected. The gas is assumed to follow the reversible polytropic relation

$$H_A V^n = C_A \quad (6-22)$$

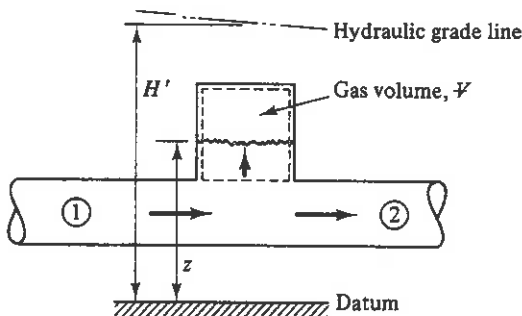


Figure 6-12 Simple accumulator.

in which H_A is the absolute head equal to the gage plus barometric pressure heads, $H_A = H' - z + \bar{H}$, V the gas volume, n the polytropic exponent, and C_A a constant. The exponent n depends on the thermodynamic process followed by the gas in the vessel. If a perfect gas is assumed, at one extreme the process may be isothermal, $n = 1$, or at the other limit it may be isentropic (reversible, adiabatic), in which case $n = 1.4$ for air. The particular situation dictates the type of process, the latter being more conservative since it predicts larger pressure changes for the same volume change. For small chambers with fast response times the process may be taken as isentropic. In larger systems with a large water volume and small air mass the transformation may approach an isothermal process. Often an average value of 1.2 is used in design calculations. It has been pointed out that the value of n should be allowed to vary for inflow to and outflow from the air chamber.^{3,4}

Since Eq. (6-22) applies at any instant it is written at the end of the time increment by introducing the integrated continuity equation, $dV/dt = -Q$. The minus sign is necessary since the air volume reduces with positive inflow.

$$(H' + \bar{H} - z)[V - \Delta t(Q' + Q)]^n = C_A \quad (6-23)$$

In this equation V is the air volume two time steps earlier. A junction continuity equation, the two compatibility equations, and Eq. (6-23) are solved simultaneously for the variables.

Example 6-2

Suppose that a pocket of air is trapped in a system (Fig. 6-13). The upstream end of the pipe is subjected to a large pressure by opening a valve or starting a pump. Write the downstream condition to handle the behavior of the air pocket at the end of the pipe. Assume the air volume to be small compared with the liquid volume in a computing reach.

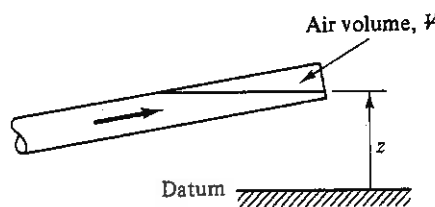


Figure 6-13 Example 6-2, trapped air volume.

Newton's method is used to solve Eqs. (3-21) and (6-23) simultaneously. When combined these two equations may be written

$$F_1 = (C_P - B_P Q' - z + \bar{H}) [V - \Delta t (Q' + Q)]^n - C_A = 0$$

which is a nonlinear equation in the variable Q' . Newton's method finds a correction to an estimated value of Q' by use of the expression

$$F_1 + \frac{dF_1}{dQ'} \Delta Q = 0$$

in which, after simplification

$$\frac{dF_1}{dQ'} = -\frac{n \Delta t C_A}{V - (Q' + Q) \Delta t} - B_P [V - (Q' + Q) \Delta t]^n$$

The FORTRAN code for this condition may take the following form, beginning with an estimated value of Q' at the new time step.

```

CP = H(N) + B*Q(N)
BP = B + R*ABS(Q(N))
DO 10 I = 1,KIT
VP = V - DT*(QP(NS) + Q(NS))
IF(VP.LT.VSMALL) VP = VSMALL
F1 = (CP - BP*QP(NS) - Z(NS) + HBAR)*VP**EN - CA
DFDQ = -EN*DT*CA/VP - BP*VP**EN
DQ = -F1/DFDQ
10 QP(NS) = QP(NS) + DQ
V = V - DT*(QP(NS) + Q(NS))
IF (V.LT.0.) V = 0.
HP(NS) = CP - BP*QP(NS)

```

The constant CA is defined by Eq. (6-23) using the initial static volume and pressure head. Other variable definitions include barometric pressure head = $HBAR$, air volume = V , polytropic exponent = EN , $dF_1/dQ' = DFDQ$, number of iterations in Newton's method = KIT , and a minimum-size air volume $VSMALL$, to avoid division by zero.

6-5 Other Surge Devices

Surge-arresting devices take on many configurations, depending on the manufacturer. Most are relatively easy to model in an analysis program by using the lumped elements described in Secs. 6-3 and 6-4, together with a lumped friction-loss element such as an orifice. Two examples are included.

Accumulator with Inertia and Dissipation

The air vessel in Fig. 6-14 is connected to the main pipeline by a short pipeline. In this analysis the lumped inertia model, including friction, is used in the connector. Equation (6-17) is applied to the connector, pipe 3,

$$H' - H'_4 = C_1 + C_2 Q'_3$$

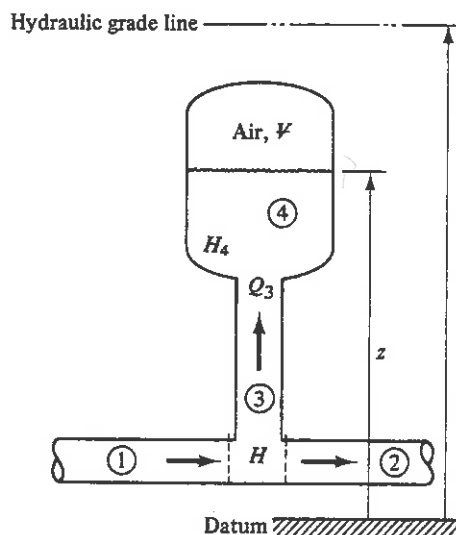


Figure 6-14 Air vessel with inertia and friction.

in which C_1 and C_2 for connector 3 are defined in Eq. (6-18). Equation (6-23) is applied to the accumulator,

$$(H'_4 + \bar{H} - z)[V - (Q'_3 + Q_3) \Delta t]^n = C_A$$

The continuity equation is used at the junction,

$$Q'_1 = Q'_3 + Q'_2 \quad (6-24)$$

and the compatibility Eqs. (3-21) and (3-22) are used in the attached pipelines. These five equations permit a simultaneous solution for the five unknowns Q'_1 , Q'_2 , Q'_3 , H' , and H'_3 . After each solution the air volume, V , must be computed before proceeding to the next time step.

Throttled Surge Tank

Figure 6-15 shows a surge tank with an asymmetric restriction at the entrance. The discharge coefficient, C_{DA} , is a function of flow direction. For positive flow into the tank

$$Q'_3 = C_{DA_P} \sqrt{2g(H' - H'_3)} \quad (6-25)$$

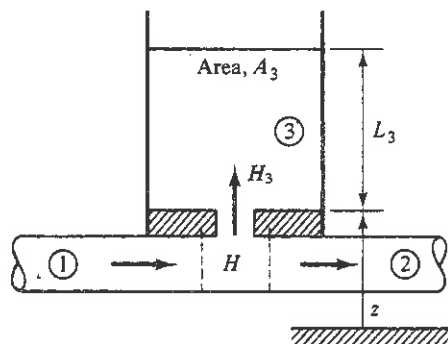


Figure 6-15 Throttled surge tank.

and for reverse flow

$$Q'_3 = -C_{DA_R} \sqrt{2g(H'_3 - H')} \quad (6-26)$$

The continuity condition in the tank relates the surge rise in the chamber to the inflow:

$$\frac{dL_3}{dt} = \frac{Q_3}{A_3} \quad (6-27)$$

or, after integration over two time steps in the staggered grid,

$$L'_3 - L_3 = \frac{Q'_3 + Q_3}{A_3} \Delta t \quad (6-28)$$

The compatibility equations in the main pipeline, Eqs. (3-21) and (3-22), and continuity at the branch connection are used to solve for the variables Q'_1 , Q'_2 , Q'_3 , H' , H'_3 , and L'_3 . An additional strategy must be decided upon to relate L'_3 to H'_3 . The surge chamber may be treated as a simple storage reservoir if it has a large cross-sectional area and therefore low velocities. In this case inertial forces and frictional losses in the tank are neglected and a hydrostatic pressure variation is assumed.

$$H'_3 = L'_3 + z \quad (6-29)$$

Alternatively, for a smaller surge shaft in which vertical velocity changes may be significant, the lumped inertia model should be used:

$$H'_3 + H_3 - 2z - (L'_3 + L_3) - \frac{f_3 L_3}{g D_3 A_3^2} Q'_3 |Q_3| = \frac{L_3}{g A_3 \Delta t} (Q'_3 - Q_3) \quad (6-30)$$

Thus, either Eq. (6-29) or (6-30) is used with Eqs. (3-21), (3-22), (6-24), (6-28), and depending upon flow direction, either Eq. (6-25) or (6-26).

6-6 Cooling-Water Condenser

The condenser contains a number of small-diameter tubes with a water box at each end (Fig. 6-16). The identical multiparallel pipes may be treated correctly as one element by using a flow cross-sectional area equal to the sum of the areas of the individual pipes and a resistance factor that is appropriate to the small-diameter pipe. The factor R in the compatibility equations, Eqs. (3-21) to (3-24), when the Moody diagram friction factor is used, becomes

$$R_c = \frac{f_s \Delta x}{2g D_s A_T^2} \quad (6-31)$$

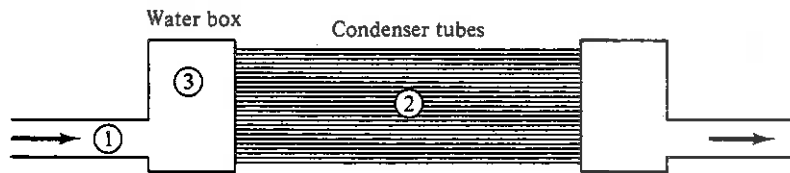


Figure 6-16 Schematic cooling-water condenser.

in which f_s and D_s refer to the smaller-diameter tubes while A_T refers to the total flow area. The wave propagation velocity must be appropriate to the smaller-diameter tubes and $B = a_s/g A_T$. Since this special element is treated as a pipeline in the method of characteristics, it is subject to the Courant condition, $a_s \Delta t = \Delta x$. The full flow, Q , passes through the element. If the tubes are identical in every respect, the transient wave propagation in each pipe will be the same and this special element will portray the physical behavior of this portion of the condenser. For purposes of water column separation, different pipe clusters at different average elevations could be treated as parallel elements.

The condenser water boxes (Fig. 6-16), are treated as lumped capacitance elements, and Eq. (6-21) provides the relationships among the important parameters. The effective bulk modulus, K' , must be estimated to provide a combined effect of the water compressibility and water box elasticity. The solution of variables in the two water boxes at each time step is independent due to the characteristics method link in the condenser tubes. The upstream water box is handled by a combined solution of Eq. (3-21) in pipe 1, the modified Eq. (3-22) in element 2, Eq. (6-21) in the water box, and continuity Eq. (6-24). An air-inlet valve can be incorporated in the water box as discussed in the next section.

6-7 Air-Inlet Valve

To protect a pipeline from vacuum conditions (or low absolute pressures) air-inlet (and outlet) valves may be positioned at high points along the line. When the line pressure at an air valve drops below atmospheric pressure, the air valve opens to admit air. When pressure in the pipeline increases to above atmospheric pressure, air is allowed to escape to the atmosphere. The boundary condition for these valves is rather complex but may be handled within the usual framework of the characteristics method. The analytics of the boundary condition are given in this section.

The following assumptions are made:

1. Air enters and leaves the pipe through the valve under isentropic flow conditions.
2. The air mass within the pipe follows the isothermal law in that the mass is generally small and large areas of pipe and liquid surface provide heat capacity to hold the temperature close to the liquid temperature.
3. The air admitted to the pipe stays near the valve, where it can be expelled.
4. The elevation of the liquid surface remains substantially constant, and the volume of air is small compared with the liquid volume of a pipeline reach.

The mass rate of flow of air through the valve depends on the values of atmospheric absolute pressure p_0 and absolute temperature T_0 outside the pipe, as well as the absolute temperature T and pressure p within the pipe. Four cases must be provided for:

1. Subsonic air flow in

$$\dot{m} = C_{in} A_{in} \sqrt{7 p_0 \rho_0 \left[\left(\frac{p}{p_0} \right)^{1.4286} - \left(\frac{p}{p_0} \right)^{1.714} \right]} \quad p_0 > p > 0.53 p_0 \quad (6-32)$$

in which

- \dot{m} = mass rate of inflow of air
- C_{in} = valve discharge coefficient
- A_{in} = area of valve opening
- ρ_0 = mass density of atmospheric air = p_0/RT_0
- R = gas constant
- p = pressure inside pipe

2. Critical flow in

$$\dot{m} = C_{in} A_{in} \frac{0.686}{\sqrt{RT_0}} p_0 \quad p < 0.53 p_0 \quad (6-33)$$

3. Subsonic air flow out

$$\dot{m} = -C_{out} A_{out} p \sqrt{\frac{7}{RT} \left[\left(\frac{p_0}{p} \right)^{1.4286} - \left(\frac{p_0}{p} \right)^{1.714} \right]} \quad \frac{p_0}{0.53} > p > p_0 \quad (6-34)$$

A_{out} is the area of valve opening, and C_{out} is its discharge coefficient.

4. Critical flow out

$$\dot{m} = -C_{out} A_{out} \frac{0.686 p}{\sqrt{RT}} \quad p > \frac{p_0}{0.53} \quad (6-35)$$

The boundary condition at a junction of two reaches is treated like the usual internal section when no air is present in the pipe and the head is greater than atmospheric. When the head drops below pipe elevation, the air valve opens, flow enters, and the general gas law for constant internal temperature

$$pV = mRT \quad (6-36)$$

is to be satisfied at the end of each time increment of the calculation until the air is expelled. From Fig. 6-17,

$$p[V_i + \Delta t(Q_i - Q'_{U_i} - Q'_{U_i} + Q'_i)] = [m_0 + \Delta t(m_0 + \dot{m})]RT \quad (6-37)$$

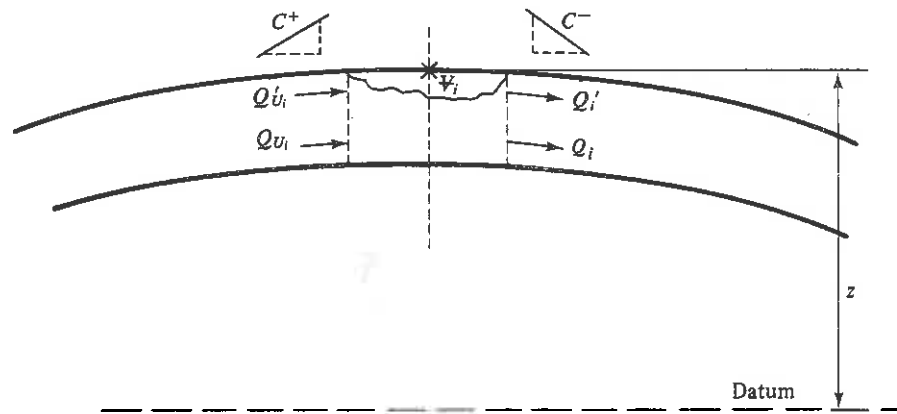


Figure 6-17 Air-inlet valve flow notation.

in which

- V_i = volume of cavity $2\Delta t$ earlier
- Q_i = initial outflow from cavity $2\Delta t$ earlier
- Q'_i = final outflow from cavity (at current time)
- Q_{U_i} = initial inflow to cavity
- Q'_{U_i} = final inflow in cavity
- m_0 = initial mass of air in cavity
- \dot{m}_0 = initial rate of air mass flow into or out of cavity
- \dot{m} = final rate of air mass flow into or out of cavity
- RT = product of gas constant R and absolute temperature

The C^+ and C^- equations, in short form, are

$$C^+: H'_i = C_P - B_P Q'_{U_i} \quad C^-: H'_i = C_M + B_M Q'_i \quad (6-38)$$

and the relation between H' and p is

$$\gamma(H' - z + \bar{H}) = p \quad (6-39)$$

with \bar{H} is the barometric head, γ the specific weight of liquid, and z the elevation of the air valve above datum for H' . Equations (6-37) to (6-39), and one of Eqs. (6-32) to (6-35), depending on the type of flow, provide the relations to solve for the variables H'_i , p , \dot{m} , Q'_{U_i} , and Q'_i .

Other more complex cases may be studied, such as a bandwidth of head reduction before opening of the air valve, dropping of the liquid surface within the pipe, the trapping of an air volume, a surge suppressor type of closure after the air is ejected to allow liquid escape, and a predetermined air valve opening and closing as a function of time.

6-8 Spring-Mass Systems

There are various situations in fluid systems in which the transient pressure waves may act on elastic structural members or spring-loaded masses. The resulting physical movement of the structural mass may significantly influence the fluid behavior. Spring-loaded relief valves and safety valves, and suspended and nonanchored piping systems, are examples. A spring-loaded mass with viscous damping and Coulomb friction is analyzed herein.

Figure 6-18 shows a piston at the end of a pipeline that is free to move horizontally, the motion being resisted by a spring force, viscous damping in a dashpot, and Coulomb friction. The variables associated with this boundary are H' , x , Q' , and V' . If the hydraulic-grade-line datum is at the centerline of the pipe, the equation of motion is

$$\gamma AH - F \frac{|V|}{V} - S_K x - \mu V = M \frac{dV}{dt} \quad (6-40)$$

in which F is the Coulomb frictional force, S_K the spring constant, μ the viscous damping factor of the dashpot, M the mass of the piston, and V the piston velocity. The position of the piston is related to the velocity and discharge:

$$\frac{dx}{dt} = V = \frac{Q}{A} \quad (6-41)$$

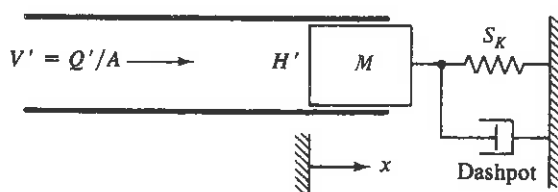


Figure 6-18 Spring-mass system.

Sec. 6-9 Dynamic Check Valve

A second-order approximation in integrating Eqs. (6-40) and (6-41) yields

$$\gamma A(H' + H) - F \frac{|Q'| + Q|}{Q' + Q} - S_K(x' + x) - \frac{\mu}{A}(Q' + Q) = \frac{M}{A \Delta t}(Q' - Q) \quad (6-42)$$

$$x' - x = \frac{Q' + Q}{A} \Delta t \quad (6-43)$$

to be solved simultaneously with Eq. (3-21).

If the response time of the spring-mass system is rapid, it may be necessary to use a higher-order integration scheme in handling Eqs. (6-40) and (6-41). Third- or fourth-order Runge-Kutta has been used successfully.¹³ An interpolation scheme is needed in the characteristics method to provide information at intermediate time increments at the boundary for the higher-order Runge-Kutta methods.

6-9 Dynamic Check Valve

Check valves, or nonreturn valves, are placed in pipelines to prevent back flow, usually at pumping stations, but may also be used at other locations in systems. Ideally, when the flow reverses at the location of the check valve, it closes, preventing back flow. More realistically, since the valve position is controlled by the flow and valve dynamics, closure occurs after some level of back flow is established. This causes an instantaneous stoppage of the reverse flow with the corresponding pressure rise. Figure 6-19 shows a possible velocity time history at the valve with several possible options for valve closure following removal of the driving force in the system. A study to determine the reverse

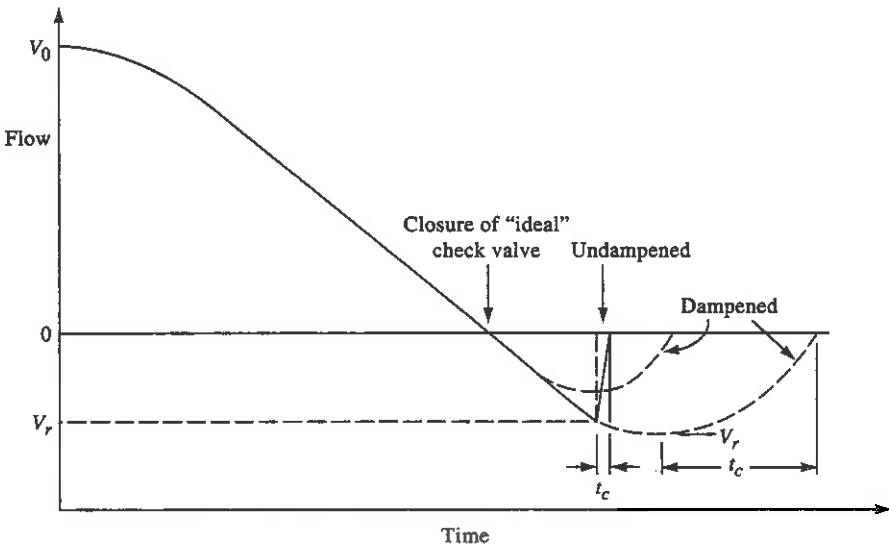


Figure 6-19 Flow at check valve.

velocity, V_r , and the time of closure, t_c , requires a dynamic analysis of the particular valve in the actual system. In most cases experiments are necessary to determine some of the valve coefficients.

These valves typically contain a relatively freely moving part such as a disk, plug, or ball, whose motion is dictated by the movement of the fluid, by its weight, by external forces such as a spring or weight, by friction, and possibly by a damping device. There are two general categories of nonreturn valves: a swing or rotational type and a translation type. Either a dynamic torque or force equation is needed in the analysis together with an energy equation to describe the losses across the valve.

Swing-Check Valve

Figure 6-20 provides a schematic in which θ is the angle of the valve door, and with clockwise moments about the pivot point considered positive.^{2,9,11} The torque equation yields

$$T_w + T_e + T_f + T_p = I \frac{d^2\theta}{dt^2} \quad (6-42)$$

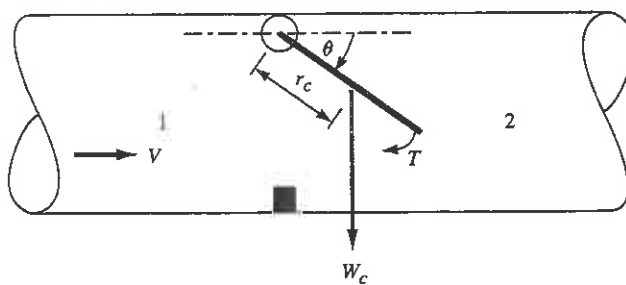


Figure 6-20 Schematic of swing-check valve.

I is the moment of inertia about the hinge of the valve disk together with an added mass for the fluid that is moved. The torque due to the weight of the rotating disk is given by T_w . The buoyancy torque can be included by using the submerged weight of the disk. Any external torque resulting from a ballast weight or spring is included in T_e . Bearing friction is included in T_f and would be negative during closure. The torque due to the hydrodynamic pressures, depending on the flow, the valve position, and angular velocity, is given by T_p , and may be positive or negative.

If the submerged weight of the disk is W_c , and the distance from the disk pivot point to the center of gravity of the door is r_c (Fig. 6-20),

$$T_w = W_c r_c \cos \theta \quad (6-43)$$

If a spring with a torsional spring stiffness of s is acting, and θ_s is the initial angle of the spring with the disk in the closed position,

$$T_e = s(\theta_s - \theta) \quad (6-44)$$

The frictional torque may be a constant related to a frictional coefficient,⁸ the pivot pin radius, and the submerged weight of the gate, but is also more likely to depend on at

least the angular velocity¹²

$$T_f = k_1 + k_2 \left(\frac{d\theta}{dt} \right)^n \quad (6-45)$$

The coefficients are viewed as constants.

The torque due to hydrodynamic pressures on the disk is given by

$$T_p = - \int_A \Delta p r dA \quad (6-46)$$

in which r measures the distance to an elemental disk area where the pressure difference across the disk is Δp . The pressure difference is a function of the flow, the angular position, the angular speed of the valve disk, and it is impossible to determine in sufficient detail to integrate Eq. (6-46). As an approximation a valve equation relating flow to pressure drop may be used:

$$Q = \pm C_d A_0 \sqrt{2g \Delta H} \quad (6-47)$$

in which ΔH represents the average pressure head change across the valve, C_d a function of the shape of the flow passage and Reynolds number, and A_0 represents the open area through which the flow passes. If the Reynolds effects are neglected, only a valve opening as a function of θ is needed, an expression that depends on the configuration of the valve. Equation (6-46) is now written

$$T_p = \gamma \Delta H \bar{r} A_v \quad (6-48)$$

in which \bar{r} is the distance from the pivot point to the point of application of the average pressure change across the valve, a position that is likely to change with valve opening, and A_v is the disk area over which ΔH acts.

Substitution into Eq. (6-42) yields

$$F_1 = W_c r_c \cos \theta + s(\theta_s - \theta) + k_1 + k_2 \left(\frac{d\theta}{dt} \right)^n + \frac{\gamma \bar{r} A_v Q |Q|}{2g(C_d A_0)^2} - I \frac{D^2\theta}{dt^2} = 0 \quad (6-49)$$

an equation that is a function of Q , θ , and various coefficients that are difficult to quantify and which are likely to be functions of θ . When combined with Eq. (6-47), written

$$F_2 = H_1 - H_2 - \frac{Q |Q|}{2g(C_d A_0)^2} = 0 \quad (6-50)$$

and with the compatibility equations in the adjoining pipelines, a solution is possible for θ , Q , H_1 , and H_2 .

Check Valve with Translating Disk or Plug

Newton's law for linear motion replaces Eq. (6-42) for this type of valve:

$$F_w + F_e + F_f + F_p = M \frac{d^2 V_d}{dt^2} \quad (6-51)$$

The forces, which parallel the torques in the rotational type valve, are gravitational, including buoyancy, external forces such as spring forces or ballast, friction, and hydrodynamic. The mass of the translational disk and associated parts along with an added mass for the fluid that is moved are included on the right-hand side, with V_d being the velocity of the disk. If a damper were involved, an additional force would be necessary. Figure 6-21 provides a schematic. Once again the hydrodynamic force is the most difficult with which to cope, even when experimental measurements have been acquired. Further discussions of check valves appear in Chapter 10, where check valve design and selection parameters are considered.

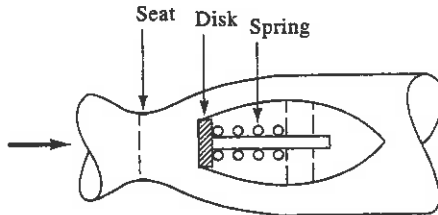


Figure 6-21 Schematic of translating-check valve.

6-10 Controllers

Dynamic controllers are frequently used to maintain a desired operating condition in a system or process. In the context of unsteady pipeline flow the variable to be controlled may be pump speed, turbine speed, turbine power output, pump torque, pump station discharge pressure, liquid level in tanks, pressure drop across a valve, element flow, and so on. The normal input to the controller is an error signal, which is the deviation in the variable to be controlled away from a reference value or set point. The controller output signal, which provides operating information for a control variable in the system, is a function of the dynamic response of the controller, with its particular settings, to the magnitude and rate of variation of the input signal.

If a valve in a system were to be controlled to hold the discharge pressure at a particular set value, then the deviation in the discharge pressure away from the set point would be the input signal to the controller, and the valve position the output signal (Fig. 6-22). The following variables are identified in the figure as general

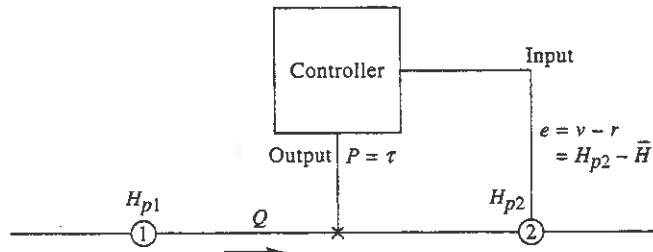


Figure 6-22 Dynamic controller to operate an in-line valve.

quantities, and as specific variables for the valve example: r is the reference value or set point, v the control variable, $e = v - r$, the error signal, P the output variable. A proportional-integral-differential (PID) controller is used as an example of a control device herein. It is described by the equation

$$P = K_p \left(e + \frac{1}{T_R} \int e dt + T_d \frac{de}{dt} \right) \quad (6-52)$$

in which K_p is the proportional control constant (gain), T_R is integral control constant (reset time), and T_d the derivative time. By setting $T_d = 0$, the equation describes a proportional-integral device. The equation is also used in the derivative form,

$$\frac{dP}{dt} = K_p \left(\frac{de}{dt} + \frac{e}{T_R} + T_d \frac{d^2 e}{dt^2} \right) \quad (6-53)$$

A first-order integration of Eq. (6-53) for the valve example in Fig. 6-22 yields

$$\tau_P - \tau = K_p \left[H_{P_2} - H_2 + \frac{(H_{P_2} - \bar{H})2\Delta t}{T_R} + T_d \frac{H_{P_2} - 2H_2 + H_{O_2}}{2\Delta t} \right] \quad (6-54)$$

in which the variable subscripts P_2 , 2 , and O_2 refer to the current value of the control variable, the value two time steps earlier, and the value four time steps earlier, respectively. The set point is \bar{H} , and the dimensionless valve positions at the current time step and two time steps earlier are τ_P and τ . Equation (6-54) can be solved with the two compatibility equations and the valve equation for the four variables: H_{P_1} , H_{P_2} , τ_P , and valve flow. With appropriate control parameters the controller should simulate the dynamic valve behavior with the unsteady flow and pressure response, and produce an acceptable error signal for the downstream pressure during a transient event in the system.

6-11 Adjacent Nonpipe Elements in Systems

In handling multiple nonpipe elements in a system, the standard approach, and the simplest, is to be sure that a reach of pipe exists between each nonpipe element. This is done during the schematization of the physical system for the simulation. By following this concept, in the method of characteristics, it keeps the solution procedure explicit at each computing section. Adherence to this plan sometimes requires approximations, or may be constraining. The concept of the general junction in Secs. 3-5 and 3-6 provides the opportunity for simultaneous solution of equations at interconnecting points of nonpipe elements, with or without pipeline elements.^{5,10,15} Individual groupings of nonpipe elements in a general system are treated independently at each time step, with the explicit characteristic equations in adjoining pipelines isolating the groupings, one from the other.

A general junction is a point connection of elements, Sec. 3-5, at which there are two variables: a nodal flow and a nodal pressure. Systems consist of elements and

junctions (or nodes), the latter being one of two types: a known nodal flow or a known nodal pressure. Equation (3-51), which is repeated here,

$$\sum Q_{in} = \sum Q_p + \sum Q_e + Q_n = 0 \quad (6-55)$$

sums up the inflow contributions to the node, which must add to zero at any instant. In Eq. (6-55) $\sum Q_p$ refers to the summation of all instantaneous pipeline flows, $\sum Q_e$ refers to the summation of all nonpipe element flows at the instant, and Q_n is the nodal inflow.

For a junction with unknown nodal flow (known pressure) the pipeline flows may be determined explicitly from the compatibility equations, Eqs. (3-17) and (3-18). Element flows are determined as discussed below, and the nodal flow is determined directly from Eq. (6-55). At a junction with unknown nodal pressure (known Q_n), the pipeline inflows are summed as in Eq. (3-43):

$$\sum Q_p = S_C - S_B H_n \quad (6-56)$$

in which $S_C = \sum (C_P/B_P) + \sum (C_M/B_M)$ and $S_B = \sum (1/B_P) + \sum (1/B_M)$. When Eq. (6-56) is substituted into Eq. (6-55), a function F_n is defined that is a function of variables H_n and the nonpipe element flows.

$$F_n = H_n - C_n - B_n Q_n - B_n \sum Q_e = 0 \quad (6-57)$$

Coefficients $C_n = S_C/S_B$ and $B_n = 1/S_B$ incorporate the combined behavior of all pipelines at the node. An equation must be available to describe the flow in each element. By writing an equation similar to Eq. (6-57) for each node in an isolated portion of the system that contains interconnected nonpipe elements, a set of simultaneous equations is available for solution. Other regions of the system may also contain nonpipe elements, but as long as the regions are isolated by pipelines, each region is treated independently at each time step.

For illustration purposes Fig. 6-23 shows a schematic diagram of a portion of a system that contains three common elements without intermediate pipelines. The pump is subjected to a speed change and the valve is adjusted to generate a transient. The air accumulator provides a capacitance in the system without loss or inertia.

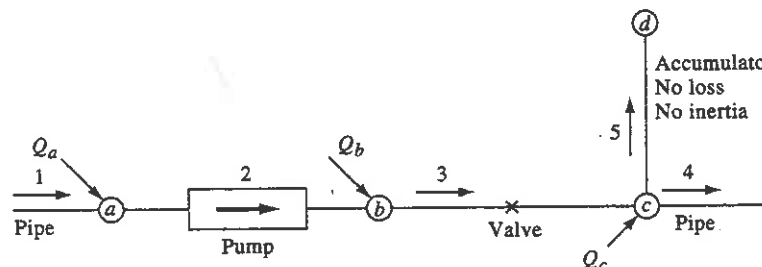


Figure 6-23 Contiguous nonpipe elements in system.

The nodal equations are first written. Node d does not need an equation since there is no nodal flow and $H_d = H_c$.

$$F_a = H_a - C_a - B_a Q_a - B_a (-Q'_2) = 0 \quad (6-58)$$

$$F_b = Q_b + Q'_2 - Q'_3 = 0 \quad (6-59)$$

$$F_c = H_c - C_c - B_c Q_c - B_c (Q'_3 - Q'_5) = 0 \quad (6-60)$$

Next the element equations are presented beginning with the pump described by Eq. (3-60) in which the pump speed α is known at any instant.

$$F_2 = H_a - H_b + \alpha^2 H_s + a_1 \alpha Q'_2 + a_2 Q'_2^2 \quad (6-61)$$

The coefficients H_s , a_1 , and a_2 describe the pump head discharge curve. Equation (3-53) is used to describe the in-line valve

$$F_3 = H_b - H_c - \frac{Q'_3 |Q'_3|}{2C_v} = 0 \quad (6-62)$$

in which C_v is defined in Sec. 3-3. Equation (6-23) is used to describe the air accumulator:

$$F_5 = (H_c + \bar{H} - z)V_p^n - C_A = 0 \quad (6-63)$$

in which $V_p = V - (Q'_5 + Q_5)\Delta t$ is the air volume at the current instant and is calculated from the previous volume plus the average inflow over the two time steps in the staggered grid.

There are numerous alternatives to solve the six equations for the variables H_a , H_b , H_c , Q'_2 , Q'_3 , and Q'_5 . Since the last three equations are nonlinear in flow, Newton-Raphson could be used. The six equations for this example may also be written in the following matrix form:

$$\begin{bmatrix} 1 & 0 & 0 & B_a & 0 & 0 \\ 0 & 0 & 0 & 1 & -1 & 0 \\ 0 & 0 & 1 & 0 & -B_c & +B_c \\ 1 & -1 & 0 & a_1\alpha + 2a_2 Q'_2 & 0 & 0 \\ 0 & 1 & -1 & 0 & -\frac{|Q'_3|}{C_v} & 0 \\ 0 & 0 & 1 & 0 & 0 & -\frac{n \Delta t C_A}{V_p^{n+1}} \end{bmatrix} \begin{Bmatrix} \Delta H_a \\ \Delta H_b \\ \Delta H_c \\ \Delta Q_2 \\ \Delta Q_3 \\ \Delta Q_5 \end{Bmatrix} = \begin{Bmatrix} -F_a \\ -F_b \\ -F_c \\ -F_2 \\ -F_3 \\ -F_5 \end{Bmatrix} \quad (6-64)$$

Clearly, further simplifications are possible, but the matrix is left in this form since it represents a more generalized presentation that has implications in other combinations of nonpipe elements. An iterative solution to this matrix and correction of the variables is necessary.

Additional nonpipe elements in systems are covered in later chapters. In particular, turbomachines are treated in some detail in Chapter 7.

Problems

- 6-1. Write the three compatibility equations to determine wave transmission and reflection at a series connection. Verify Eqs. (6-2) and (6-3).
- 6-2. Show that Eq. (6-4) is valid for a set of serially connected pipelines.
- 6-3. Check the values shown in Table 6-1 for the ratio of the final wave amplitude to the initial incident wave.
- 6-4. Perform the algebraic combination of equations to yield Eq. (6-7) for the in-line orifice.
- 6-5. Combine Eq. (6-6) and the compatibility equations at the pipe end to generate Eq. (6-9) for the reflected wave magnitude at the end-of-pipe orifice.
- 6-6. In Example 6-1, if $\Delta H_w = 50$ ft and $a = 3000$ ft/s, find the size of the reflected wave for each case.
- 6-7. Modify the program SINGLE.FOR in Appendix D to include the infinite pipeline termination in place of the upstream reservoir. Use the same data as in Example 3-1 to study the response. Increase the length of the pipe while using the same reach length to study the accuracy of the infinite pipe termination.
- 6-8. Show that Eq. (6-16) is valid for a vertical lumped inertia element.
- 6-9. Consider a lumped mass analysis of a frictionless simple system. If a constant pressure head, $\Delta H = CaV_0/g$, is applied to stop the flow, find the value of C in terms of the variables in the problem, including t_c , the time to stop the flow.
- 6-10. In Fig. 6-24 the system is shut down by closing the valve slowly, then shutting the pump off. The pump is started with the control valve closed. Calculate the pressure rise in the system during pump startup from an initial static condition. Assume that the pump starts

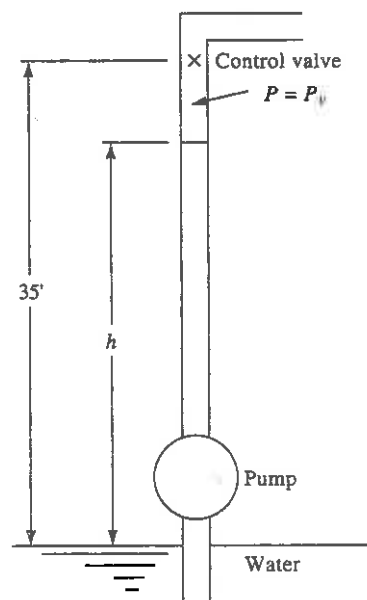


Figure 6-24 Problem 6-10.

Problems

instantaneously and develops a constant head of 60 ft. Neglect friction and assume a fixed mass of liquid to be accelerated. $D = 2$ ft, $a = 3220$ ft/s, vapor pressure = -33 ft.

- 6-11. A 1-m-diameter pipeline has 1 m³ of air trapped at the pipe end. The initial hydraulic grade line in the system is 100 m, and $Q = 0$. The elevation of the pipe end is 20 m. If the polytropic exponent is assumed to be 1.2, calculate the constant in the equation.
- 6-12. In Example 6-2 the air volume is 1 ft³, the fluid is water, and the static pressure is 10 psi gage. If the pressure changes to 100 psig, what is the air volume? The polytropic exponent is 1.2.
- 6-13. A pipeline has a length of 1 m of air trapped at the downstream end as shown in Fig. 6-13. $D = 0.3$ m, $f = 0$, $a = 970$ m/s, $L = 485$ m, $\bar{H} = 10.3$ m, and $z = 7$ m. The initial conditions in the system are $H = 30$ m, and $Q_0 = 0$. If the valve opens instantaneously and the pump at the upstream end produces a hydraulic-grade-line elevation of 70 m at time zero, find the flow, the HGL at the air pocket, and the volume of air at (a) $t = L/a$ s and (b) $t = 2L/a$ seconds.
- 6-14. A one-way surge tank is often used to avoid column separation downstream from pumping stations. The surge tank has sufficient capacity to fill a void that could develop during column separation. It does not need to extend up to the steady-state hydraulic grade line since the design includes a one-way check valve. Write the equations to handle this boundary condition as shown in Fig. 6-25.

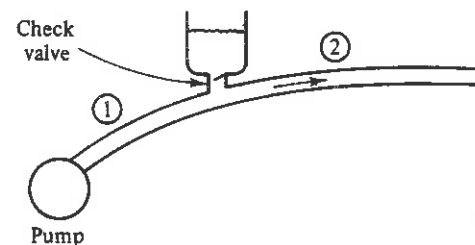


Figure 6-25 Problem 6-14, one-way surge tank.

- 6-15. (a) Simplify Eq. (6-40) so that it applies to an unforced spring-mass system only. Combine with Eq. (6-41) and find the solution for x . What is the natural frequency?
- (b) The Helmholtz resonator (Fig. 6-26) can be visualized as a spring-mass system. By combining Eq. (6-16), using simplifications as applied in part (a), with Eqs. (6-19) and (6-20), find the solution for the change in volume. What is the natural frequency of the fluid system?

Answer: (a) $\omega_n = \sqrt{S_K/M}$; (b) $\omega_n = \sqrt{K'A/\rho V L}$.

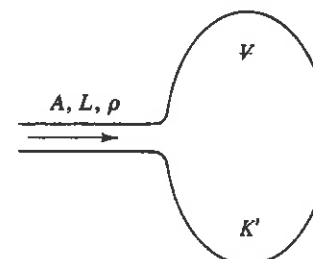


Figure 6-26 Problem 6-15, Helmholtz resonator.

Methods for Controlling Transients

Ideally, the design process for fluid pipeline systems includes an adequate investigation and specification of equipment and operational procedures to avoid undesirable transients. Unfortunately, this is not always the case, and remedial measures are required to keep transient conditions from seriously disturbing proper functioning of an existing system. Unexpected sources of unsteady flow also appear in some newly constructed systems. In previous chapters, emphasis has been placed on analysis, with some discussion of methods for reducing transients. Chapter 6 deals with the simple surge tank, accumulator, check valve, and air-inlet valve, in Chapter 7 we discuss the effect of increasing moment of inertia of rotating parts of turbomachines in reducing transients, and Chapter 9 deals with valve stroking as a design method for controlling transients.

In this chapter examinations of many of the methods for controlling transients are made from an analysis viewpoint rather than for complete system design. The concept of optimum system design, including operating methods to control transients, has an unlimited future potential when one visualizes the combination of design calculations as presented in Chapter 9 with the control capabilities of microcomputers. Selection of the appropriate surge control device for a given installation must include not only a study of its effectiveness and dependability, but also an evaluation of relative initial costs and of the character and frequency of maintenance requirements over an extended period.

When one considers the relationship between head rise, wavespeed, and flow change ($\Delta H = -a \Delta Q/gA$), and also recognizes the benefits generally received as a result of wave reflections, the types of control may be somewhat categorized. Slower valve action or reductions in the rate of change of flow allow time for the potential benefits of reflections. Wavespeed reduction can provide a direct improvement, pressure-limiting devices provide direct relief, and system geometrical design changes can alter the response pattern of a system to yield improved operation.

10-1 Wavespeed Reduction Methods

Since the head change for a given flow change is directly proportional to the wave propagation velocity, the reduction of wavespeed is likely to be beneficial in the control of transients. Wavespeeds depend on (1) elastic wall properties and geometry, (2) liquid compressibility, and (3) free-gas content in the pipeline. The response frequencies of complete systems may be altered by the wavespeed change in component parts of the system, thereby eliminating resonance as a result of a particular forced oscillation.

Bleeding in Air

Entrainig air into the liquid flow in a system is widely used to eliminate unwanted transients. Usually, a section in the system is selected in which the pressure is less than atmospheric, such as the entrance to a draft tube. Here, the air is beneficial in reducing the severity of cavitation and also in reducing transient oscillations related to wavespeeds in the draft tubes. In Sec. 6-7 air-inlet valves for low-pressure points on pipelines are discussed.

Rather than bleed in air, one may hold the air along the length of the pipe within a small flexible hose in the pipe that is sealed in at closely spaced sections so that the air is trapped. Thus the effective bulk modulus of elasticity of the system is reduced. This device was developed by Remenieras¹⁴ and was patented in France in 1951.

Noncircular Conduit

When subject to internal pressure, a noncircular cylinder is generally deformed into a shape more nearly approaching a circular cylinder; this increases the cross-sectional area per unit pressure change more rapidly than it would if it were circular. The wavespeed can be greatly reduced in this manner. Depending on the pipe supports, large pipes tend to deform into noncircular cross sections, which decrease the wavespeed.

Flexible Hose

In small systems flexible hose is frequently employed as a means of reducing the severity of transients. Many plastic hoses also provide this feature. Similarly, additional viscoelastic pipes may be utilized as pressure surge suppressors in piping systems.⁴

10-2 Air Chamber or Accumulator

The accumulator, air bottle, air vessel, or air chamber, as discussed in Sec. 6-4, may be designed to keep the pressure from exceeding a predetermined value or to prevent low pressures and column separation. When properly designed it can protect against rapid transients as well as against longer-period surges in a system. It is basically a closed container partially filled with the system liquid topped with air or gas. The gas may be

in contact with the liquid, in which case an air compressor, or gas supply, is used to maintain the proper mass of air or gas, or the gas may be separated from the liquid by a flexible membrane or a piston. In an analysis of this device the resistance and inertance built into it by orifices, nozzles, or by a connecting pipe should be considered. Similarly, the mass and resistance to motion of a piston or a diaphragm should be taken into account.

The accumulator generally operates at the local system pressure. In Fig. 10-1a, if the valve is closed abruptly the flow enters the air chamber, the air is compressed, and the flow in the main pipeline is gradually reduced as the pressure builds up. The peak pressure can be reduced considerably in this situation. A similar small-volume air chamber can be very effective in smoothing out short transients generated by reciprocating pumps or other positive displacement devices.

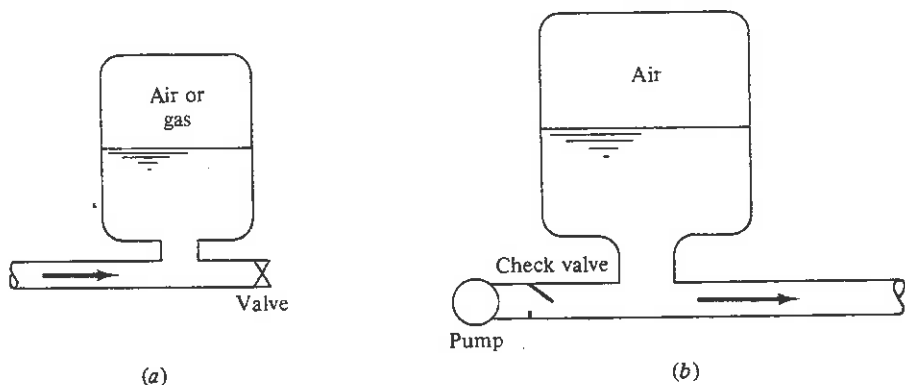


Figure 10-1 Accumulator.

Figure 10-1b shows a large air chamber installed at the discharge side of a centrifugal pumping station to protect against low pressures and column separation during stoppage of the pumps. Generally, a check valve is used as shown to prevent backflow. Care must be taken to design the connectors between accumulator and pipeline so that there is a little delay in the action of the air chamber. The size of the air volume, to control the maximum pressure, and the size of liquid volume to avoid emptying the tank during the low-pressure cycle may be determined by a lumped-parameter analysis as discussed in Chapter 6. Losses in asymmetric designs may be accounted for properly in the study. Some designs call for a check valve with a smaller-diameter bypass line in the throat to the air chamber. This allows for an easy supply of the liquid during the low-pressure cycle and constricted flow during the high-pressure period. The duration of long-period surging is generally reduced by this design. Design charts are very helpful for preliminary sizing of air chambers and for selection of throttling elements.^{5,17}

10-3 Surge Tanks

Surge tanks are open tanks connected to the piping system. They take several forms, depending on their number, arrangement, and the nature of restrictions between the surge tanks and the piping system. A *simple* surge tank has very little resistance to flow of liquid into or out of it (Fig. 10-2) and is generally sized so that it will not be drained

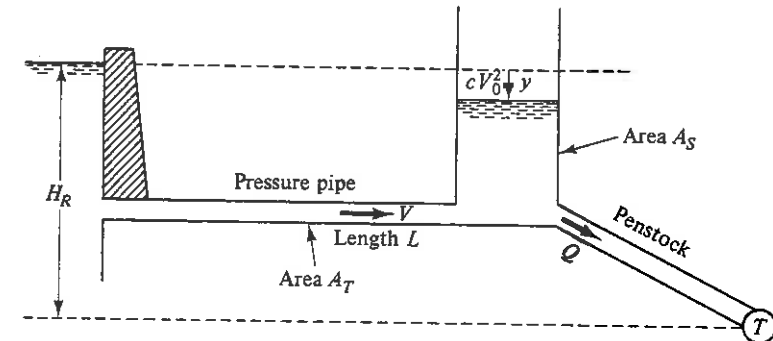


Figure 10-2 Simple surge tank.

by maximum flow demand and will not be overtapped by downstream reduction of flow. Sometimes spillways are provided so that the tank may be overtapped. Simple surge tanks, chimneys, or standpipes, as they are sometimes called, serve as partial reflection points for pressure waves, thereby protecting longer tunnels from excessive short-period pressure oscillations. An *orifice* surge tank (Fig. 10-3) has a restricted connection between tank and piping system, frequently with a lower discharge coefficient for flow into the tank. A *differential* surge tank is, in effect, two surge tanks, a simple surge tank and an orifice surge tank. They may be combined, as in Fig. 10-4a, or separated, as in Fig. 10-4b. A *one-way* surge tank, usually designed to avoid column separation, does not need to extend up to the hydraulic grade line, and needs only sufficient capacity to

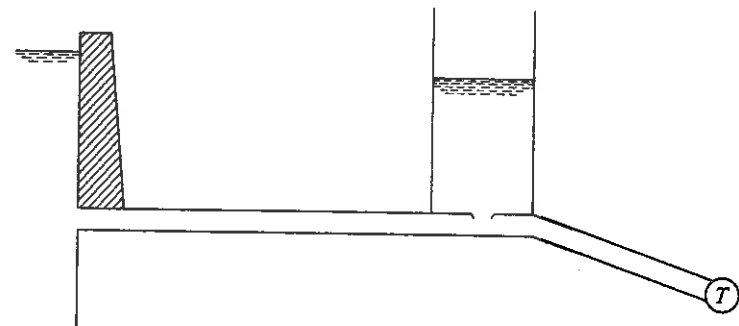


Figure 10-3 Orifice surge tank.

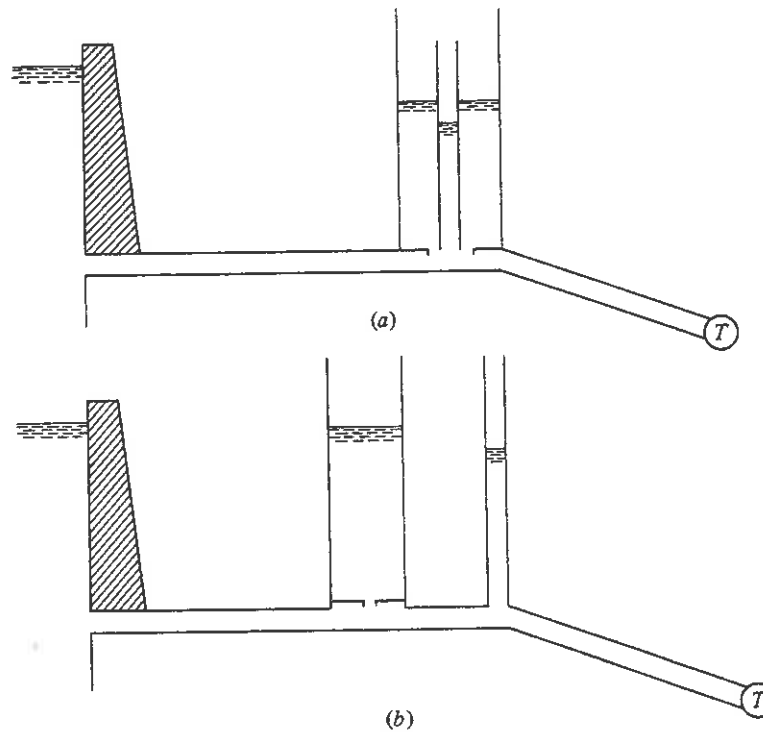


Figure 10-4 Differential surge tank arrangements.

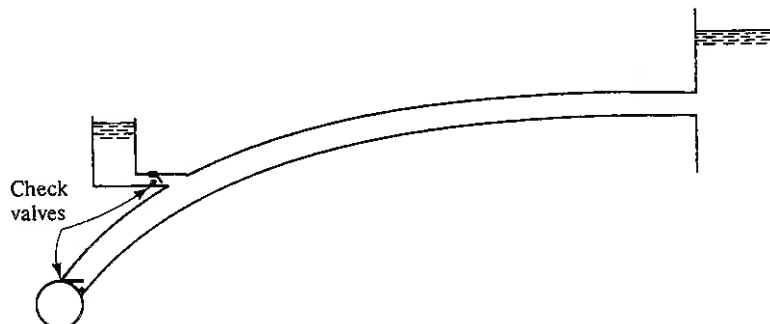


Figure 10-5 One-way surge tank in pumping system.

fill the void caused by a column separation. One-way surge tanks are used primarily in connection with pumping plants (Fig. 10-5).

Sizing of Surge Tanks

The sizing of surge tanks in hydropower systems to guarantee stability is not treated in any detail herein. Jaeger^{6,7} and Chaudhry¹ review the problem of stability and provide an

extensive bibliography on the subject. The period of oscillation of a system (Fig. 10-2), neglecting friction, is given by

$$T = 2\pi \sqrt{\frac{LA_s}{gA_T}} \quad (10-1)$$

Waterhammer effects in the penstock are generally of much shorter period than surge-tank fluctuations; hence the two problems of surge oscillation and waterhammer are generally treated separately. A waterhammer analysis of the surge tank–penstock–turbine system should be investigated over the range of surge-tank oscillations. The complete action of the governor, as discussed in Chapter 7, must be included.

For surge oscillations the governor is able to adjust the gates of the turbine to hold approximately constant power. Since the penstock is usually short, the surge analysis of the pressure tunnel and surge tank usually assumes that the constant power relation exists at the upstream end of the penstock. By assuming small-amplitude oscillations, and writing the surge equation for the tunnel, continuity at the surge tank, and constant power to the penstock, the Thoma criteria^{1,6,7} for required minimum surge tank area for stability may be determined.

$$A_{TH} = \frac{LA_T}{cV_0^2(H_R - cV_0^2)} \frac{V_0^2}{2g} \quad (10-2)$$

A computer analysis of the complete equations is possible without the limiting assumptions imposed to obtain the analytical solution given in Eq. (10-2). For the simple surge-tank system the equation of motion for the pressure pipe is (Fig. 10-2)

$$\gamma A_T \left[y - \left(1 + k + \frac{fL}{D_T} \right) \frac{V|V|}{2g} \right] = \frac{\gamma A_T L}{g} \frac{dV}{dt}$$

or

$$\frac{dQ_T}{dt} = \frac{gA_T}{L} \left(y - \frac{cQ_T|Q_T|}{A_T^2} \right) \quad (10-3)$$

in which

$$c = \frac{1 + k + fL/D_T}{2g}$$

is the coefficient and k is the entrance loss coefficient. The continuity equation is (Fig. 10-2)

$$Q_T + A_S \frac{dy}{dt} = Q \quad (10-4)$$

in which A_S is the area of the surge tank, Q the penstock discharge, and Q_T the pressure pipe discharge. The power relation may take the form

$$Q(H_R - y) = F_1(t) \quad (10-5)$$

in which $F_1(t)$ is any arbitrarily imposed function of time. For constant power output, neglecting penstock losses,

$$Q(H_R - y)\eta = \text{const} \quad (10-6)$$

in which η is the turbine efficiency and must be obtained from the turbine characteristics for the appropriate head and discharge. For the case of assumed constant η , Eq. (10-6) combined with Eq. (10-4) yields

$$\frac{dy}{dt} = \frac{[\text{const}/(H_R - y)\eta] - Q_T}{A_S} \quad (10-7)$$

Runge-Kutta methods can be used to solve Eqs. (10-3) and (10-7). Differential surge tank systems may be treated similarly. It may be noted that this is a lumped inertia analysis in which the liquid has been assumed incompressible. A standard waterhammer analysis of this problem should provide the same response as the surge analysis. It would, however, require excessive computer time to cover the full duration of the surge oscillations.

10-4 Check Valves

Check valves are frequently installed at the discharge flange of a pump to prohibit reversal of flow through the unit when power is shut down. They are also used in industrial applications that require quick shutoff of flow in case of a major system component failure. The purpose in check valve use is multiobjective: prevention of the loss of liquid during reverse flow, prevention of reverse runaway of the pump if one is present, and provision for a controlled shutdown of the system within acceptable pressure constraints. The ideal check valve may be one that closes the instant the flow velocity at the valve reaches zero. This is likely to control valve slam but may not yield pressures at acceptable levels. The decision as to the best type of valve in a particular installation depends on the characteristics of the pipeline system.

In 1980, Provoost¹² introduced the concept of the dynamic characteristic of the undamped nonreturn or check valve, defined as the relationship between the reversed liquid velocity at closure and the deceleration of the liquid passing the valve. He recommended¹³ further that the dynamic characteristic should be provided by the valve manufacturer since it depends on valve type, dimensions, presence of springs, counter weights, and so on, and is somewhat less dependent on the system in which it is tested. Collier and Hoerner² suggested a similar parameter, emphasizing the importance of liquid deceleration. A number of investigators^{3,11,15-17} have followed this lead in defining and using the dynamic characteristic of the check valve. Koetzier et al.⁸ introduce scale laws and provide a dimensionless dynamic characteristic as well as examples to use the data, when available, in valve selection for a particular installation. The material that follows is based largely on the latter paper. The variability of the dynamic characteristic of different valve types is seen in Fig. 10-6. In this diagram the horizontal axis represents the mean deceleration, $|dV/dt|$, of the fluid column during valve closure. The vertical axis is the maximum velocity of the backward flow, $|V_r|$, which occurs generally just before final valve closure. Ideally, the maximum reverse velocity would be zero under all conditions of fluid velocity reduction.

If the check valve dynamic characteristic is available, the pressure transients in a particular system may be determined. The deceleration flow rate is the most important

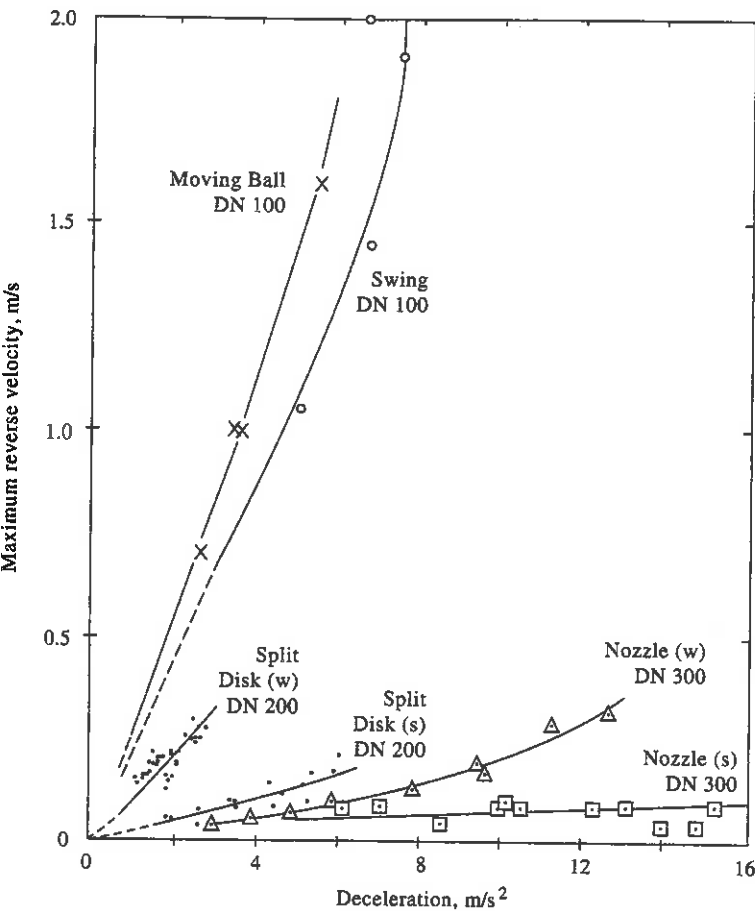


Figure 10-6 Dynamic characteristic of different valve types. (s) and (w) refer to data for valves fitted with strong and weak springs, respectively (Thorley, 1983,¹⁵ by permission of BHRA, Cranfield, Bedford, U.K.).

parameter and it can be determined by analyzing the system without the check valve. When the fluid deceleration rate has been determined at the check valve site, the maximum backflow velocity V_r can be determined from the dynamic characteristic of the check valve. At the instant the fluid velocity in the computer simulation is equal to V_r , valve closure is assumed and the resulting pressure transient may be observed. Clearly, valve losses have not been included, and a linear deceleration of the fluid is presumed. This analysis is considerably simpler than that presented in Sec. 6-9, but it is predicated on the availability of the particular check valve dynamic characteristic.

A dimensionless dynamic characteristic for a nozzle-type translating check valve has been proposed and substantiated by experimental data.⁸ It is based on conditions of dynamic similitude utilizing a check valve of inlet diameter D_i in a pipeline of the same diameter. The check valve is spring loaded such that the closing force is exerted

by a spring, whose force can be characterized by a critical velocity V_0 . This is the fluid velocity at the inlet section when the valve is just fully open. Ratios of spring forces in both the fully open and closed positions are assumed equal for every spring. The valve is assumed to be initially fully open, $V > V_0$ (Fig. 10-7). Dimensional analysis of the variables, including ρ_m , the density of the material of the moving elements in the valve, leads to the functional relationship

$$\frac{V_r}{V_0} = f\left(\frac{dV/dt}{V_0^2} D_i, \frac{\rho_m}{\rho}\right) \quad (10-8)$$

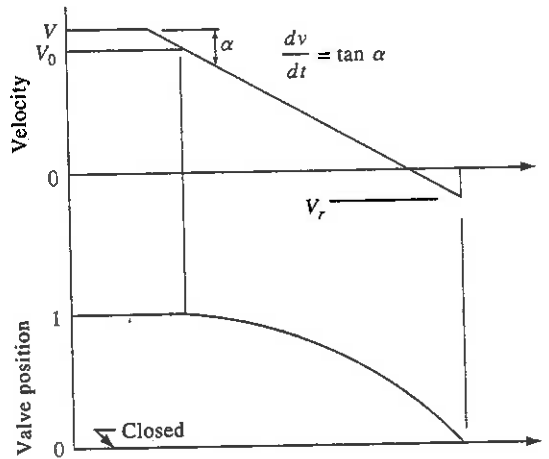


Figure 10-7 Dynamic behavior of check valve.

The function f must be determined from test results or from calculated results if sufficient valve data are available.

Figure 10-8 provides results of dynamic tests of a heavily damped 300-mm (12-in.) valve. Two different spring loadings were used to provide the two critical velocities of 1.28 and 2.60 m/s. If a valve in this series were to be used in a setting in which the valve is fully open at 80 percent of the design velocity V in the pipe and the backflow velocity is restricted to 20 percent of V , then

$$V_0 = 0.8V \quad |V_r| < 0.2V$$

and

$$\frac{|V_r|}{V_0} < 0.25$$

From Fig. 10-8

$$\frac{|dV/dt|D_i}{V_0^2} < 0.33$$

With $V_0 = 0.8V$,

$$\left|\frac{dV}{dt}\right| D_i < 0.211 V^2$$

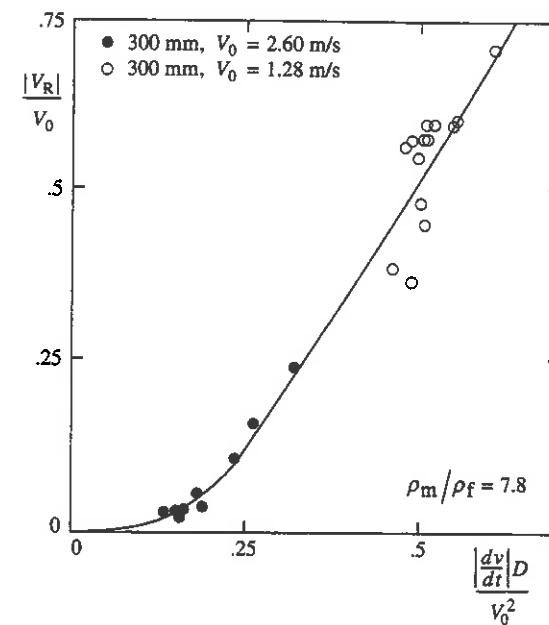


Figure 10-8 Measured dimensionless characteristics, heavily damped⁸ (Thorley, 1989,¹⁶ by permission of ASME, New York).

The maximum allowable fluid deceleration for any valve diameter and design velocity may be found using the last equation. Clearly, more data are needed on different valve types, but the procedure presented provides a guide based on current technology to assist in check valve selection.

10-5 Flow-Control Methods and Valving

Air chambers and surge tanks are probably the safest and most maintenance-free solutions to transient problems. A reduced rate of flow change, through slower valve action or increased moment of inertia in turbomachines, is an effective solution to many problems. If a regular maintenance program is practiced, auxiliary valving and flow-control valves may provide a more economical and satisfactory solution. A careful initial design is generally required as well as a continuous service program to ensure operation in accordance with the design.

The *relief valve* is one of the common devices to control excess pressures. It may be loaded by a spring (Fig. 10-9), or by weights; the valve opens when the set pressure is exceeded. It may close immediately when the pressure drops below the setting, or it may have a damped closure to allow for a much longer closure time. It is important for a relief valve to have a low inertia so that it can open before the set pressure is greatly exceeded. A *rupture disk* is an alternative safety measure if not activated too frequently. It consists of an opening in the pipe covered by a diaphragm that ruptures and relieves pressure beyond a certain limit. The rupture disk protects equipment from excessive pressure but is troublesome to replace.

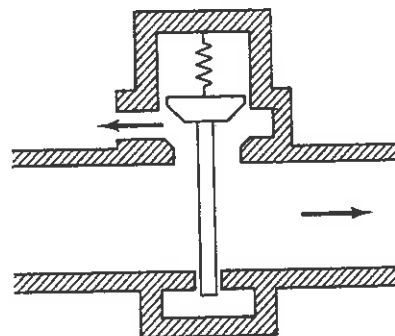


Figure 10-9 Relief valve.

Check valves at the discharge flange of a pump prohibit reversal of flow through the unit when power is shut off and avoid the danger of high head buildup due to the running away of the pump backwards. The effectiveness of a check valve in controlling transients depends on its dynamic characteristic, as discussed in Section 10-4. Flow-control valves designed for optimum closure in accordance with the principles presented in Chapter 9 can be very effective in pump discharge lines. The design can call for a valve closure schedule with two or more closure rates that will permit maximum head buildup to any arbitrary value above the downstream reservoir. At the same time the reverse rotation of the pump may be controlled.

Various forms of *surge suppressors*,⁹ and bypass valving, are also possible. Two alternatives of the latter are shown in Fig. 10-10 for protection of a pumping station. To

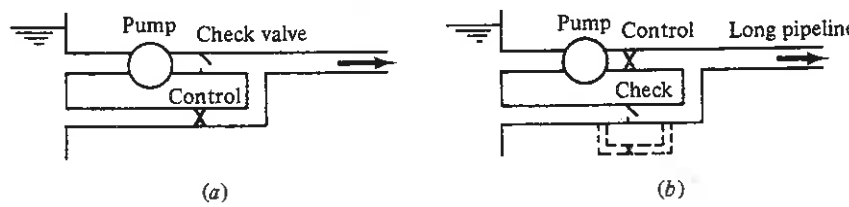


Figure 10-10 Pumping station with bypass pipeline.

prevent back-flow through the pump a check valve is installed in Fig. 10-10a, with a control valve in a smaller bypass line. The control valve is opened after pump failure and then is allowed to close slowly. Care must be exercised to be sure the control valve is not opened too soon. In some installations this could increase the danger of column separation. In long pipelines where there is little concern for excessive backflow the pump can be isolated from the pipeline transient by a pump discharge-control valve as shown in Fig. 10-10b. A check valve in a bypass line allows free flow to the pipeline to prevent low pressures and column separation. In long lines with a small gravity load, long-duration surges may exist in such a system. Although these are not particularly dangerous, they persist for some time since the losses are generally low. A small-diameter bypass of the check valve shown schematically with dashed lines in Fig. 10-10b may help alleviate this condition.

In reaction turbine installations a flow diverter or relief valve is often provided to divert the flow during load rejection. An energy dissipater must be provided to absorb the excess power in the penstock. The diverter closes gradually to reduce the penstock flow in a controlled manner.

For protection against low-pressure, air-inlet valves (Sec. 6-7), are provided at critical points in a piping system. They must be located at the correct position to provide the necessary protection, and they must be sized to allow sufficient air into the line. Once the air has been admitted it must also be expelled slowly during startup or excessively high pressures can be generated (see Chapter 8). Air can also travel along the pipe with the flow and may be troublesome to remove.

It is clear that various valving-piping combinations can be designed to protect most situations. In each case regular servicing is an essential feature to be assured that the hardware will operate as designed when needed.

10-6 System Geometrical Design Changes

The transient performance of a piping system may be improved, in general, by increasing piping diameter. Since head change is directly proportional to velocity change, doubling of the diameter reduces pressure fluctuations by a factor of about 4. This design change may be particularly effective in suction lines, since it greatly decreases the possibility of cavitation.

A surge tank or air chamber should be added to a system if the resulting reduction of waterhammer makes the entire system more economical. Surge tanks and air chambers should be located as close to turbines and pumps as possible to prevent exposure of long pressure pipes to severe transients. This also improves the hydraulic stability of surge tanks during power regulation.

For steady-oscillatory excitation of a piping system, a small change in length may greatly improve system performance by increasing the time difference between the natural period of the system and the period of one of the harmonics of the excitation. An example, based on a computer study, showed a reduction of transients in the suction line of a quintuplex pump from ± 100 ft to ± 30 ft, effected by decreasing the suction-line length from 7 ft to 6.4 ft.

The *tuned stub* may be very effective in eliminating a significant oscillation at a given frequency. It is a dead-end branch originating at a chosen point along the system and of such a length that its response nullifies oncoming waves. Two or more stubs of appropriate length and location may control transients over a range of frequencies. The concepts of oscillatory flow and free vibrations presented in Chapters 12 and 13 are useful in such designs.

Changes in wavespeed may accomplish the same effect. A section of rubber or other flexible hose in a metal piping system generally increases the natural periods of the system. Also, since head fluctuations are proportional to wavespeeds, their magnitudes are reduced within the flexible hose reaches, as discussed in Sec. 10-1.

In certain existing systems with unsatisfactory transients of a steady-oscillatory nature, the solution may be one of decreasing the harmful effects¹⁰ of the resonance by stiffening and bracing the system at the loop points of the pressure fluctuations.

In summary, by proper design of components such as valve controls, pipeline sizes, pump flywheels, and so on, and by informed operational procedures, transient effects in fluid systems generally may be controlled within satisfactory limits. The provision of an air chamber or surge tank is an excellent design option, followed in a priority ranking by other pressure- or flow-limiting devices, such as relief valves, check valves, air valves, bypasses with valving, and so on. Combinations of these components, and others, may also be desirable in some situations. The same concepts apply to both large- and small-scale hydraulic systems. Occasionally, the source of the disturbance cannot be identified or, once located, the oscillations are impossible to eliminate. In this case stiffening and bracing of the piping system may be the only solution so that the system can be used without risk of failure.

References

12. G. A. Provoost, "Dynamic Behavior of a Swing Check Valve," *3rd Int. Conf. Pressure Surges*, BHRA, Canterbury, pp. 415-428, Mar. 1980.
 13. G. A. Provoost, "A Critical Analysis to Determine Dynamic Characteristics of Non-return Valves," *Paper F4, 4th Int. Conf. Pressure Surges*, BHRA, Bath, England, pp. 275-286, Sept. 1983.
 14. G. Remenieras, "Dispositif simple pour réduire la Célérité des ondes élastiques dans les conduits en charge," *Houille Blanche*, Special A, pp. 172-196, 1952.
 15. A. R. D. Thorley, "Dynamic Response of Check Valves," *4th Int. Conf. Pressure Surges*, BHRA, Bath, England, Sept. 1983.
 16. A. R. D. Thorley, "Check Valve Behavior under Transient Flow Conditions," *J. Fluids Eng., ASME*, Vol. 111, pp. 178-183, June 1989.
 17. A. R. D. Thorley, *Fluid Transients in Pipeline Systems*, D.&L. George, Herts, England, 1991, 265 pp.
-
- ## References
1. M. H. Chaudhry, *Applied Hydraulic Transients*, 2nd ed., Van Nostrand Reinhold, New York, 1987.
 2. S. L. Collier, and C. C. Hoerner, "A Facility and Approach to Performance Test of Check Valves," paper presented at *Energy Sources Conf. and Exhibition*, ASME, Petroleum Division, New Orleans, La., Mar. 1982.
 3. J. Ellis, and W. Mualla, "Selection of Check Valves," *Paper H1, 5th Int. Conf. Pressure Surges*, BHRA, Hannover, Germany, Sept. 1986.
 4. P. Ghilardi, and A. Paoletti, "Additional Viscoelastic Pipes as Pressure Surge Suppressors," *Paper E2, 5th Int. Conf. Pressure Surges*, BHRA, Hannover, Germany, Sept. 1986.
 5. H. R. Graze, and H. B. Horlacher, "Design Charts for Throttled (By-Pass) Air Chambers," *Tech. Note 7, 5th Int. Conf. Pressure Surges*, BHRA, Hannover, Germany, pp. 309-322, 1986.
 6. C. Jaeger, "Contribution to the Stability Theory of Systems of Surge Tanks," *Trans. ASME*, Vol. 80, pp. 1574-1584, 1958.
 7. C. Jaeger, "A Review of Surge-Tank Stability Theory Criteria," *J. Basic Eng., ASME*, pp. 765-783, Dec. 1960.
 8. H. Koetzier, A. C. H. Kruisbrink, and C. S. W. Lavooij, "Dynamic Behavior of Large Nonreturn Valves," *Paper H4, 5th Int. Conf. Pressure Surges*, BHRA, Hannover, Germany, Sept. 1986.
 9. C. W. Lundgren, "Charts for Determining Size of Surge Suppressors for Pump-Discharge Lines," *J. Eng. Power, ASME*, Jan. 1961.
 10. S. Malamet, "Operation of Pumped Storage Schemes," *Proc. Int. Symp. Waterhammer in Pumped Storage Projects*, ASME, Chicago, Nov. 1965.
 11. H. D. Perko, "Check Valve Dynamics in Pressure Transient Analysis," *Paper H3, 5th Int. Conf. Pressure Surges*, BHRA, Hannover, Germany, Sept. 1986.

Open-Channel Transient Flow

The preceding portions of this book have dealt primarily with unsteady flow in close conduits. Piping systems are frequently connected to open channels, and it is important to know how the transient is transmitted through the open channel. Practical examples of this are the forebay channel that leads to a hydroelectric installation, as well as systems where water is pumped into and out of channels or rivers. Included in the general problem is flood routing in rivers or canals.

In this chapter the differential equations for free-surface unsteady flow, including friction, are developed and then solved numerically. This treatment is restricted to flow through prismatic sections, although the methods are easily adapted to irregular channels such as rivers. Two methods of solution are discussed: the specified-time-interval method of characteristics, and the implicit method. The chapter concludes with a brief discussion on the adjustment of control devices in canals to provide optimum operation in changing the flow from one steady regime to another.

15-1 Differential Equations for Unsteady Open-Channel Flow

The basic equations for one-dimensional flow are presented for a prismatic channel of irregular cross section. Friction losses are included by use of either the Chezy or Manning equations. A lateral inflow (outflow) along the channel is included such as might be encountered in the distributed inflow (outflow) to channels from groundwater, outflows to irrigation systems, inflows from rainfall, outflows at overflow weirs, and so on. The assumption is made that the channel slope α is small enough that $\cos \alpha \approx 1$. This condition is met in all but the steepest of channels, which are not common in free surface flows. Hydrostatic conditions are assumed to prevail along any vertical line in the fluid (i.e., vertical accelerations are not considered).

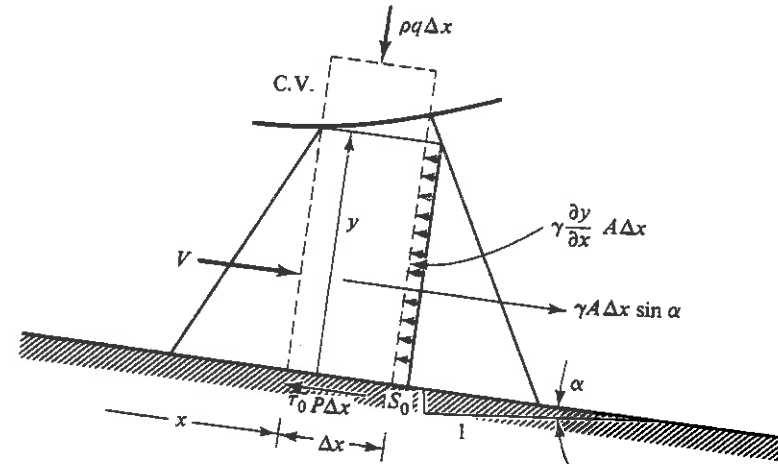


Figure 15-1 Control volume for application of the unsteady-momentum equation.

Figure 15-1 shows a control volume enclosing an elemental strip of liquid; the x direction is taken parallel to the channel bottom, and the depth y is measured normal to the bottom. In application of the unsteady-momentum equations, the net hydrostatic force on the two faces is $-\gamma y_x \Delta x A$ (for $\cos \alpha \approx 1$), the shear force on the wetted area is given by $-\tau_0 P \Delta x$, with P the wetted perimeter, and the gravity force in the x direction is $\gamma A \Delta x \sin \alpha = \gamma A \Delta x S_0$. The net efflux of momentum in the $+x$ direction is $(\rho V^2 A)_x \Delta x$, and the time rate of increase of x momentum within the control volume is $(\rho A V \Delta x)_t$. It is assumed that the lateral inflow enters the control volume with no x momentum. Assembling the terms, we have

$$-\gamma y_x \Delta x A - \tau_0 P \Delta x + \gamma A \Delta x \sin \alpha = (\rho V^2 A)_x \Delta x + (\rho A V \Delta x)_t$$

After expanding, and by dividing through by the mass of the element $\rho A \Delta x$,

$$gy_x + \frac{\tau_0}{\rho R} - g \sin \alpha + 2VV_x + \frac{V^2}{A} A_x + \frac{V}{A} A_t + V_t = 0 \quad (15-1)$$

R is the hydraulic radius A/P .

The continuity equation applied to the control volume of Fig. 15-1 yields

$$\rho q \Delta x - (\rho A V)_x \Delta x = (\rho A \Delta x)_t$$

in which q is the lateral inflow per unit length of channel. By expanding and dividing by $\rho \Delta x$,

$$VA_x + A_t + AV_x = q \quad (15-2)$$

Equation (15-1) may be simplified by multiplying Eq. (15-2) by V/A and subtracting the result from it. Also, if the slope of the energy grade line is introduced, as defined by the Manning or Chezy equation, $\tau_0/\rho R$ may be expressed as gS . This assumes that the

frictional resistance in unsteady flow may be described in the same manner as for steady flow at the same depth and discharge. If, for example, the Manning equation is used,

$$S = \frac{n^2 V^2}{C_m^2 R^{4/3}}$$

in which C_m is an empirical constant equal to 1.486 in English units and equal to 1.0 in SI units, and n is the Manning roughness factor, then

$$gy_x + gS - g \sin \alpha + VV_x + V_t + \frac{V}{A}q = 0 \quad (15-3)$$

Equation (15-2) may be written

$$VTy_x + Ty_t + AV_x - q = 0 \quad (15-4)$$

since

$$A_x = A_y y_x = Ty_x \quad A_t = A_y y_t = Ty_t$$

in which T = top width of prismatic section.

These nonlinear partial differential equations describe the behavior of gradually varying unsteady free surface flows in prismatic channels. Two methods of solution, with appropriate boundary conditions, are described in the next two sections.

15-2 Solution by Method of Characteristics

Equations (15-3) and (15-4) are in a suitable form for transformation by the method of characteristics. Combining, as in Sec. 3.1, yields

$$\left[V_x(V + \lambda A) + V_t \right] + \lambda T \left[y_x \left(V + \frac{g}{\lambda T} \right) + y_t \right] + g(S - S_0) + q \left(\frac{V}{A} - \lambda \right) = 0 \quad (15-5)$$

For the terms within the first pair of brackets to be the total derivative dV/dt ,

$$\frac{dx}{dt} = V + \lambda A$$

and for the terms within the second pair of brackets to be the total derivative dy/dt ,

$$\frac{dx}{dt} = V + \frac{g}{\lambda T}$$

The two equations for dx/dt must be the same; hence

$$V + \lambda A = V + \frac{g}{\lambda T} \quad (15-6)$$

and

$$\lambda = \pm \sqrt{\frac{g}{AT}} \quad (15-7)$$

Therefore,

$$\frac{dx}{dt} = V \pm \sqrt{\frac{gA}{T}} \quad (15-8)$$

For a rectangular cross section, it should be noted that Eq. (15-8) shows the surface-wave propagation velocity to be

$$\frac{dx}{dt} = V \pm \sqrt{gy} \quad (15-9)$$

If the values of λ are introduced into Eq. (15-5) and the last term in Eq. (15-8) is defined by c ,

$$c = \sqrt{\frac{gA}{T}} \quad (15-10)$$

then Eq. (15-5) may be written

$$\frac{dV}{dt} \pm \frac{g}{c} \frac{dy}{dt} + g(S - S_0) + \frac{q}{A}(V \mp c) = 0 \quad (15-11)$$

subject to

$$\frac{dx}{dt} = V \pm c \quad (15-12)$$

No approximations have been made in this transformation from two partial differential equations to the four total differential equations.

If the dependent variables V and y are assumed known at R and S (Fig. 15-2), four equations may be written in terms of four unknowns, V_P , y_P , x_P , and t_P . This involves integration of Eqs. (15-11) and (15-12):

$$C^+ \left\{ V_P - V_R + g \int_{y_R}^{y_P} \frac{1}{c} dy + \int_{t_R}^{t_P} \left[g(S - S_0) + \frac{q}{A}(V - c) \right] dt = 0 \right. \quad (15-13)$$

$$\left. x_P - x_R = \int_{t_R}^{t_P} (V + c) dt \right. \quad (15-14)$$

$$C^- \left\{ V_P - V_S - g \int_{y_S}^{y_P} \frac{1}{c} dy + \int_{t_S}^{t_P} \left[g(S - S_0) + \frac{q}{A}(V + c) \right] dt = 0 \right. \quad (15-15)$$

$$\left. x_P - x_S = \int_{t_S}^{t_P} (V - c) dt \right. \quad (15-16)$$

The equations are paired to emphasize their dependence, and integration must be along the characteristic lines. An approximation is introduced in evaluating the integrals since V , c , A , and S are unknown functions of time in a general transient. Trapezoidal integration produces a set of algebraic equations that yield a stable solution as long as the "Courant" condition^{3,8} is satisfied:

$$\Delta t \leq \frac{\Delta x}{|V| + c} \quad (15-17)$$

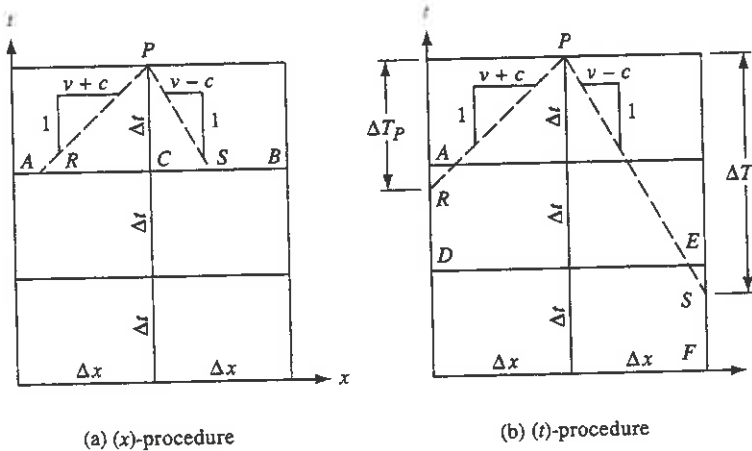


Figure 15-2 Specified-time-interval method.

The resulting equations are nonlinear and an iteration method such as Newton-Raphson is necessary for their solution.

Unfortunately, an interpolation procedure is necessary so that calculations can proceed along characteristic lines. As discussed in Chapter 4, errors are introduced in the interpolation approximation, and these may be particularly damaging to the method depending on the manner of implementation and on the type of problem. An inability to hold steady state and to converge to steady state in the case of nonuniform flow become issues. A check of gross mass conservation over the entire system during the life of the unsteady simulation may show either loss or generation of fluid. Any one of these conditions is rather disconcerting.¹⁵ A time-line interpolation procedure (Fig. 15-2b) that adheres to the Courant condition is utilized herein in favor of the more common distance-line scheme shown in Fig. 15-2a. It provides an improved simulation method for problems involving nonlinear dynamic wave propagation.

If the lateral inflow term is dropped, and with the introduction of Eq. (15-10), the positive-valued Eq. (15-11) may be written

$$\int_R^P dV + \int_R^P \sqrt{gT} \frac{dA}{\sqrt{A}} + \int_R^P g(S - S_0) dt = 0 \quad (15-18)$$

Integration yields

$$V_P - V_R + 4\sqrt{g} \left(\frac{\sqrt{A_P} - \sqrt{A_R}}{\sqrt{T_P} + \sqrt{T_R}} \right) + g \frac{S_P + S_R - 2S_0}{2} (t_P - t_R) = 0 \quad (15-19)$$

$$x_P - x_R = \frac{V_P + c_P + V_R + c_R}{2} (t_P - t_R) \quad (15-20)$$

In the evaluation of the second term in Eq. (15-18) exact integration is used for the area variation while the trapezoidal rule is used for the top-width variation. This is felt to be a reasonable approximation since, in all but the narrowest channels, the top

width is a weaker function of water depth than the area. The trapezoidal rule is used in the last term and in Eq. (15-12). With a similar treatment of the negative-valued equations, the following set of four finite difference equations results.

$$F_P = V_P - V_R + 4\sqrt{g} \frac{\sqrt{A_P} - \sqrt{A_R}}{\sqrt{T_P} + \sqrt{T_R}} + \frac{g}{2} (S_P + S_R - 2S_0) \Delta T_P = 0 \quad (15-21)$$

$$\Delta T_P = \frac{2(x_P - x_R)}{V_P + c_P + V_R + c_R} \quad (15-22)$$

$$F_M = V_P - V_S - 4\sqrt{g} \frac{\sqrt{A_P} - \sqrt{A_S}}{\sqrt{T_P} + \sqrt{T_S}} + \frac{g}{2} (S_P + S_S - 2S_0) \Delta T_M = 0 \quad (15-23)$$

$$\Delta T_M = \frac{2(x_P - x_S)}{V_P - c_P + V_S - c_S} \quad (15-24)$$

A channel is divided into a number of equal reaches of length Δx , and a suitable time interval Δt is selected so that Eq. (15-17) is satisfied. Representative values of V and y must be used in the selection of Δt or, alternatively, at each time interval during the transient Δt may be adjusted so that Eq. (15-17) is always satisfied. The latter technique is recommended herein, so point R remains near point A in Fig. 15-2, at least in one reach.

Points R and S must be located (Fig. 15-3) in accordance with Eqs. (15-22) and (15-24), respectively, before values of the interpolation parameters ζ are available for use in establishing V and y at the points. In addition, it is necessary to retain values of V and y at each section from earlier calculations. A scheme of continuous storage is utilized, as illustrated in Fig. 15-3, for variables V and y at each computational section along the channel. The variable K counts the number of time steps, while the variable KK is used as a pointer to locate the position of values in the vector at the current time step. A vector size for V and y is established, KKM , which must be at least as large as the number of time steps needed to sum up to the maximum possible value of ΔT_M . The pointer KK increases at each time step with the counter K until it exceeds KKM ; then it starts over as illustrated in Fig. 15-3. In this way it always points to the current value for storage of V and y , and other values may be located in the vector in the process of reaching back in time.

Thus an algorithm can be written to locate values of k_2 and k_3 , which are adjacent to point S , Fig. 15-3 with the aid of Eq. (15-24); then ζ can be evaluated to perform an interpolation. A linear interpolation for V_S may be written

$$V_S = V_{k_2} + \zeta (V_{k_3} - V_{k_2}) \quad (15-25)$$

in which $0 \leq \zeta \leq 1$. A similar equation is written for y_S , and a parallel procedure is used to find V_R and y_R with ΔT_P from Eq. (15-22). In the uncommon situation of very high velocity flows, in which the celerity and V are approximately the same size, time-line interpolation becomes impractical for the negative characteristic line as it may become either vertical or close to it. In supercritical flow, which is not considered here, the control of the unsteady flow shifts to the upstream end only, and point S lies to the left of the time line through point P .

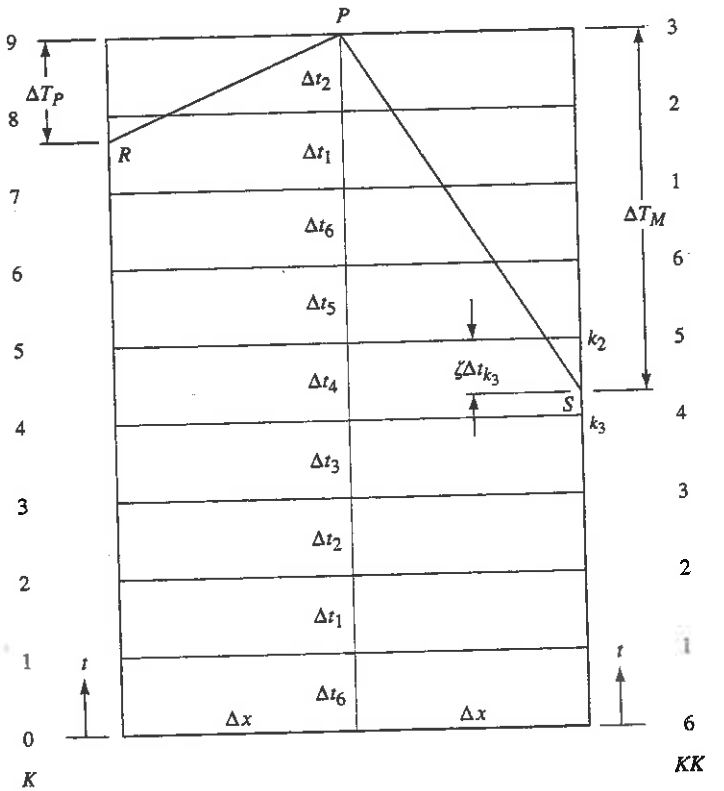


Figure 15-3 Illustration of pointer KK for continuous storage.

With values of V and y determined by interpolation at points R and S , Eqs. (15-21) and (15-23) are solved simultaneously for y_P and V_P . In the program provided in the accompanying disk the Newton-Raphson procedure is used to provide the iterative solution. For the end sections of the channel, Eqs. (15-21) and (15-23), for the downstream and upstream ends, respectively, each provide one equation in two unknowns, V_P and y_P , which, together with a boundary condition, permits the solution to be carried forward.

A continuity balance over the entire system during the life of the transient provides a useful means of assessing the accuracy of the results of a numerical calculation. Although correct results are not assured in procedures that produce a good continuity balance, it is certain that incorrect results are generated by methods that do not satisfy mass conservation. If V_i , and V_f represent the volumes stored in the channel at initial and final times, respectively, and V_{in} , and V_{out} represent the volumetric inflow and outflow during the time t , the continuity balance C_B may be evaluated at any time t after initiation of the numerical procedure.

$$C_B = V_i - V_f + V_{in} - V_{out} \quad (15-26)$$

A nondimensionalized parameter may be defined by dividing by the average volume stored or by the average through-flow volume.

Example 15-1

A trapezoidal channel 1500 m long, 10 m wide, side slopes 0.5 horizontal to 1 vertical, 0.016 Manning roughness, and 0.0002 bottom slope delivers 40 m³/s to the headworks of a hydroelectric scheme, and under normal operation the flow in the channel is uniform. The channel is open to the upstream reservoir and, when the plant is shut down, it is filled with stationary water at reservoir level. With zero initial flow in the system, the discharge is increased linearly to full flow, Q_F , in t_F seconds. Determine the transient conditions in the channel.

A FORTRAN program, OPENMOC.FOR is presented in the disk in the back of this book, to analyze the flow conditions in this channel. The discharge at the downstream end of the channel is given by

$$\begin{aligned} Q &= Q_1 + (Q_F - Q_1) \frac{t}{t_F} & 0 \leq t < t_F \\ Q &= Q_F & t \geq t_F \end{aligned}$$

where Q_1 is the initial flow.

A functional relation is written at the downstream end in place of the C^- compatibility equation

$$F_M = Q - A_P V_P = 0$$

which is solved simultaneously with the C^+ compatibility equation, Eq. (15-21). At the upstream reservoir the energy equation for positive flow provides the relationship

$$F_P = y_P + \frac{V_P^2}{2g}$$

where y_L is the reservoir level above the channel bottom. Minor losses at the channel entrance are neglected. For negative flow $y_P = y_L$. The C^- compatibility equation, Eq. (15-23), is solved simultaneously with the appropriate equation.

Either SI or English units may be used in the program by specifying SI or EN in the first two columns of the last line of input data. The two integers on this line specify the number of reaches in the channel and the number of time-increment integrations between printout of computed results. The program is able to handle prismatic triangular, rectangular, or trapezoidal sections. No provision is made for handling hydraulic bores, so caution should be exercised in rapidly reducing the downstream discharge.

Computer results are given with the program in the disk, and the depth at the downstream end of the channel is shown as a function of time in Fig. 15-4. The consequences of interpolations are evident in the results presented in Fig. 15-4, where data are presented for analyses using different numbers of reaches. The smoothing out of the rapid change in depth at the downstream end is apparent for the small number of reach lengths. In this rapid transient a relatively large number of reach lengths is necessary to assure reasonable accuracy. In channel flows with more gradual transient conditions, satisfactory accuracy can be obtained without resorting to a large number of reach lengths. The continuity balance at 28 minutes expressed as a percentage of the volumetric inflow was -0.26, -0.11, and -0.05 percent for $N = 5, 10$, and 20 , respectively. This is considerably better than can be obtained with distance-line interpolations.

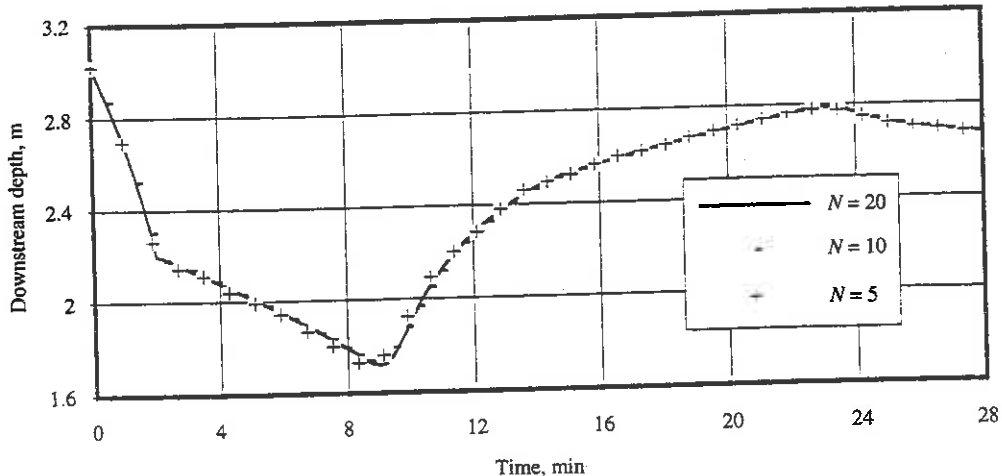


Figure 15-4 Example 15-1, characteristics method.

Use of the characteristics grid method, Sec. 4-5, avoids the need for interpolations and, with the second-order integration, is probably the most accurate numerical procedure. However, it is only useful in simple single channels, as the grid spacing in the xt plane becomes very irregular during large changes in flow and depth.

The characteristics method of specified time intervals has two drawbacks for general application in open channels. The time-step size is limited by the Courant condition, and the reaches must be approximately equal in length to reduce interpolation errors. During slow transients the first condition provides an uneconomical solution, and in modeling natural channels the second condition is restrictive. An implicit procedure, presented in the next section, relaxes both of these constraints.

15-3 Solution by Implicit Method

The implicit procedure offers particular advantages when dealing with slow transients in natural channels. Thus it has been used extensively for flood routing in rivers.^{1,7,8,12} When used with some understanding of its particular attributes it can also be utilized for rapid transients as may be encountered in power canals or pumping station channels. Its use along with other methods and applications have been summarized.¹⁰ The method was first presented in a practical scheme by Preissman,¹² and its use has been advanced by his colleagues at SORGREAH, notably Cunge.^{4,9}

The momentum and continuity equations, Eqs. (15-1) and (15-2), may be written in terms of discharge and depth as the dependent variables. Thus, if lateral inflow is not considered:

$$F_1 = \left(1 - \frac{Q^2 T}{g A^3}\right) \frac{\partial y}{\partial x} + \frac{2Q}{g A^2} \frac{\partial Q}{\partial x} + \frac{1}{g A} \frac{\partial Q}{\partial t} + S - S_0 = 0 \quad (15-27)$$

$$F_2 = T \frac{\partial y}{\partial t} + \frac{\partial Q}{\partial x} = 0 \quad (15-28)$$

Sec. 15-3 Solution by Implicit Method

These partial differential equations are placed in finite difference form for numerical simulation by the implicit method by using the following substitutions. Considering y first, and by referring to Fig. 15-5,

$$\bar{y} = \psi(y'_A + y'_B) + (1 - \psi)(y_A + y_B) \quad (15-29)$$

$$\frac{\partial y}{\partial x} = \frac{\psi(y'_B - y'_A) + (1 - \psi)(y_B - y_A)}{\Delta x} \quad (15-30)$$

$$\frac{\partial y}{\partial t} = \frac{(y'_A + y'_B) - (y_A + y_B)}{2\Delta t} \quad (15-31)$$

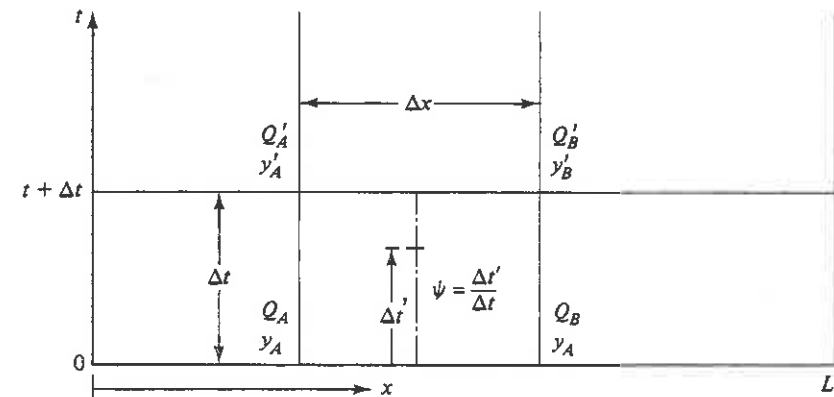


Figure 15-5 Rectangular grid for implicit method.

in which $\psi = \Delta t'/\Delta t =$ a weighting factor. The average values of \bar{A} , \bar{P} , and \bar{T} are evaluated using \bar{y} in Eq. (15-29). A stable numerical solution to Eqs. (15-27) and (15-28) may be obtained by use of values of ψ given by $0.5 < \psi \leq 1$. The solution is generally unstable if $\psi < 0.5$ and is neutrally stable if $\psi = 0.5$.

When the finite difference equivalents presented in Eqs. (15-29) to (15-31) along with a parallel set for the variable Q are used in Eqs. (15-27) and (15-28), the following difference equations result for the grid shown in Fig. 15-5.

$$F_1 = \left(1 - \frac{\bar{Q}^2 \bar{T}}{g \bar{A}^3}\right) [\psi(y'_B - y'_A) + (1 - \psi)(y_B - y_A)] + \frac{2\bar{Q}}{g \bar{A}^2} [\psi(Q'_B - Q'_A) + (1 - \psi)(Q_B - Q_A)] \quad (15-32)$$

$$+ \frac{\Delta x}{\Delta t} \frac{1}{g \bar{A}} \left(\frac{Q'_A + Q'_B}{2} - \frac{Q_A + Q_B}{2} \right) + \frac{n^2 \Delta x \bar{P}^{4/3}}{C_m^2 \bar{A}^{10/3}} \bar{Q} |\bar{Q}| - S_0 \Delta x = 0$$

$$F_2 = \bar{T} \left(\frac{y'_A + y'_B}{2} - \frac{y_A + y_B}{2} \right) \quad (15-33)$$

$$+ \frac{\Delta t}{\Delta x} [\psi(Q'_B - Q'_A) + (1 - \psi)(Q_B - Q_A)] = 0$$

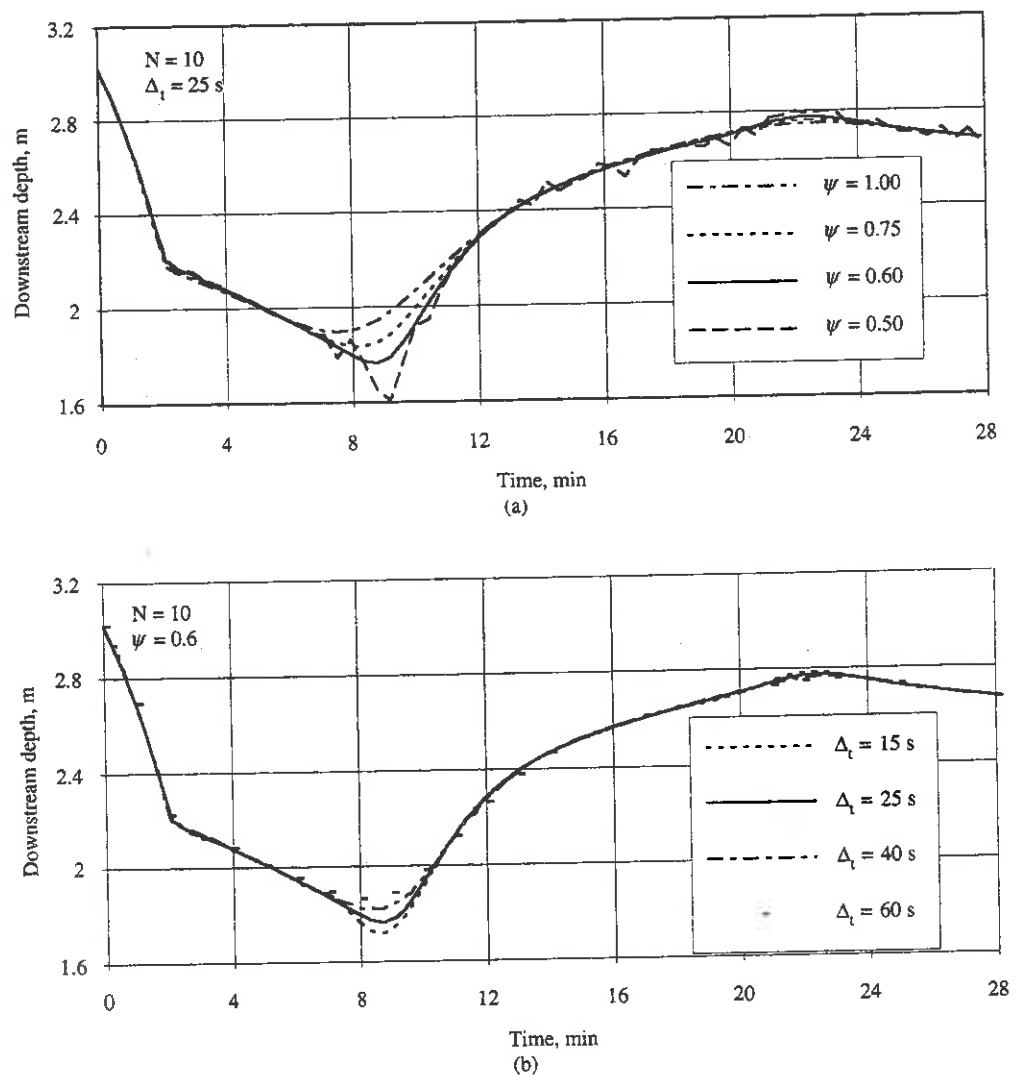


Figure 15-6 Implicit method, initiation of flow.

Equations (15-32) and (15-33) constitute a set of two nonlinear algebraic equations in four independent unknowns, y'_A , y'_B , Q'_A , and Q'_B . The unknowns are common in any two neighboring cells, and a similar pair of equations is written for each of the N cells in the channel. Thus there are $2N$ equations in $2(N + 1)$ unknowns. The boundary condition at each end of the system provides the necessary two additional equations so that a unique solution may be obtained.

Different approaches are possible in finding the solution to the $2(N + 1)$ nonlinear equations. A direct linearization of the equations is possible by writing the variables in terms of the known value plus a change in the value.⁹ Alternatively, the Newton-Raphson procedure may be used to provide a set of linear equations to be solved simultaneously.^{1,13} The iterative solution converges quickly at each time step. The latter approach is used in the implicit program, OPENIMP.FOR, in the disk in the back of this book, and in the following study of the problem posed in Example 15-1. A subroutine must be appended to the program to find the solution to the linearized banded matrix. The subroutine GELB of the IBM System/360 Scientific Subroutine Package⁶ has been used in finding the solution to the linearized banded matrix equation herein.

Figure 15-6 presents results from an implicit method analysis of Example 15-1. In Fig. 15-6a influence of the weighting factor ψ is investigated. Ten reaches were used with a time-step size of 25 s, which is approximately that required by the Courant condition. The modest fluctuations in depth with $\psi = 0.5$ are evident at the one extreme, and the significant numerical damping with $\psi = 1$ is apparent at the other extreme. It appears, for this rapid transient, that a value of $\psi = 0.6$ is appropriate. For other examples, with significant storage and roughness, a value of $\psi = 1$ may be appropriate.¹ The results from the characteristics solution with $N = 20$, Example 15-1, are essentially the same as the results with $\psi = 0.6$.

In Fig. 15-6b the influence of the time-step size is investigated utilizing 10 reaches and $\psi = 0.6$. The larger time steps, although stable, show a dissipative influence just as interpolation errors display in the characteristics method.

Example 15-2

The system described in Example 15-1 is operating at a steady uniform flow of $40 \text{ m}^3/\text{s}$. The plant at the downstream end is shut down in 2 minutes. What channel freeboard is needed to contain the resulting positive surge wave?

Both numerical procedures are used to analyze this problem even though neither is theoretically valid at a steep positive wavefront. A shock-fitting procedure should be utilized at the hydraulic bore, but this becomes extremely complicated from a programming viewpoint since the location of the moving bore is not known in advance. The literature^{4,11} provides some evidence that valid through computations provide reasonable results.

Computed results from the implicit program are shown in the disk. A graph of downstream water level vs. time is shown in Fig. 15-7. The results from both programs show basic agreement. A water surface rise of about 0.9 m above uniform flow is shown. Additional freeboard is required to contain the undular jump that is likely to exist at the wavefront.⁴

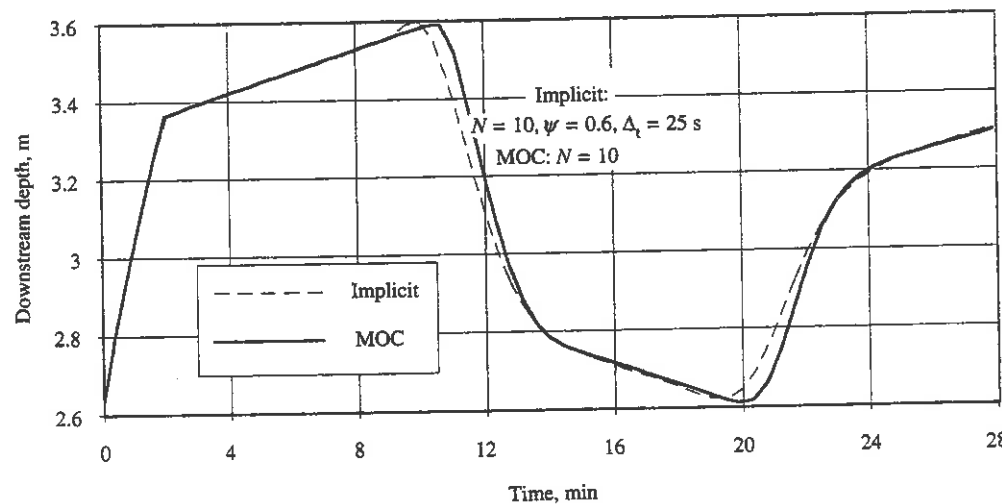


Figure 15-7 Example 15-2, positive surge wave.

15-4 Gate Stroking to Control Unsteady Channel Flow

The valve stroking concepts of Chapter 9 are applied herein to yield predetermined gate motions in open channels to provide desired changes in water-surface profiles. The method begins with a given initial flow and stage along a channel and, through advance calculations, prescribes the operation of the gates or valves, so the final steady flow is established along the channel in a minimum of time or so that neither specified stage variations or limitations on the rate of change of levels are exceeded. Applications may include, among others, the operation of valves that control forebay channels at a pumping station or hydroelectric plant to initiate, alter, or stop the flow, or the operation of control devices in an irrigation canal system.

The procedure for a single channel is similar to the concepts introduced in Sec. 9-2 for valve stroking in specified time. Both dependent variables, depth and discharge, are specified for all time at one end of the channel. Then by use of the method of characteristics, calculations are carried forward in the spatial direction rather than in the conventional time direction used in analysis problems. When the calculations reach the other end of the channel the time variation of the variables are available so that the motion of the control device can be specified.

As discussed in Chapter 9, this "inverse" problem, computing backward in time, is not feasible in highly nonlinear problems in which energy dissipation dominates. Although it has been pointed out⁵ that the inverse calculation becomes virtually impossible in open-channel application the conclusion is not supported in practical channels subject to operating flow controllers. An accurate numerical procedure is necessary, one that does not introduce excess numerical damping, one that reflects energy dissipation as described in the mathematical representation of the physical process, and one that includes the nonlinear convective velocity terms.

Since problems such as irrigation and power canal systems that require regulation and control are primarily inertia dominated, the control calculations function remarkably well. In all situations, once the control calculations are completed, they should be confirmed by a standard analysis of the prescribed control action in the forward time direction to confirm the planned operation. Examples are presented to illustrate simple applications.^{2,14}

Example 15-3

A trapezoidal channel of 4000 ft length delivers water from one reservoir to a second reservoir, both of fixed elevation. Channel properties are $S_0 = 0.0002$; Manning's roughness, $n = 0.015$; bottom width, $B = 10$ ft; and side slopes, 1:1. Gates at each end of the channel are used to control the depth and flow in the channel. Flow is initially steady uniform at a depth, $y_1 = 6$ ft, and discharge $Q_1 = 314.5 \text{ ft}^3/\text{s}$. It is desired to change the flow to steady uniform flow at a depth $y_2 = 4.5$ ft and discharge $Q_2 = 185.2 \text{ ft}^3/\text{s}$.

The stroking solution as it appears in the xt plane is shown in Fig. 15-8. The specified boundary condition at the downstream end of the channel states that the discharge should vary linearly from Q_1 to Q_2 and the depth should vary linearly from y_1 to y_2 . The manner in which the variation of the variables is specified is arbitrary; it is not necessary that the changes be made linearly.

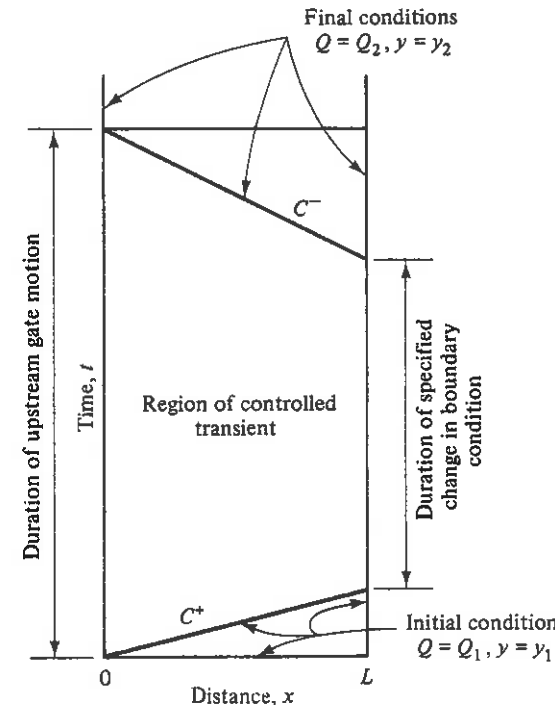


Figure 15-8 Example 15-3.

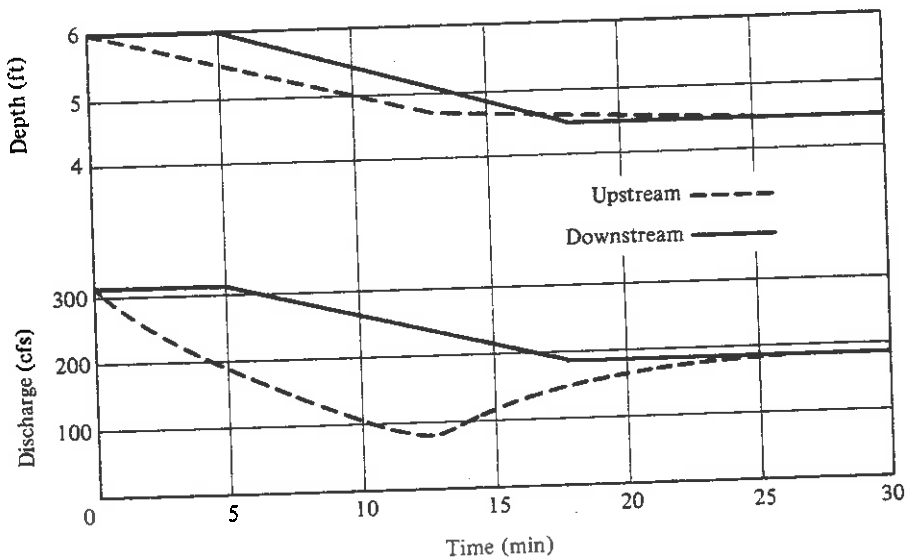


Figure 15-9 Example 15-3, depth and discharge at the boundaries.

For the specified boundary conditions at the downstream end, as shown by the solid lines in Fig. 15-9, there exists a particular solution for the corresponding boundary variations at the upstream end, as indicated by dashed lines, Fig. 15-9. The gate stroking computations show that the total operation time of the upstream gate is 26.3 min and that the initial motion of the upstream control must begin 4.4 min before the downstream gate motion. The downstream gate moves over a period of 13.2 min.

Inasmuch as the water surface elevations on each side of each gate are specified, as well as the discharges, the required gate positions vs. time to accomplish the desired flow alteration can be computed if the gate calibrations are known. The downstream reservoir in the example can easily be visualized as a pumping station forebay in which the flow and elevation could be controlled by valves in the station.

Consideration of the mechanics of the flow in a channel in order to reduce the discharge leads to some important modifications to the concepts of control in Example 15-3. Some of the forward momentum in the channel must be destroyed if the flow rate is to be decreased. The stroking can, therefore, be carried out more effectively by holding the downstream depth constant, or even increasing it either temporarily or permanently. If the flow is to be increased, the reverse would be advised. The next example utilizes this thinking, as well as the concept of maintaining a fixed volume in a canal reach to improve the response time.

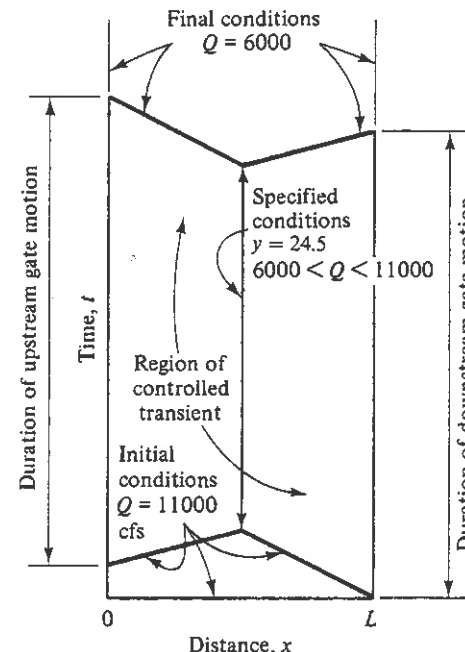


Figure 15-10 Example 15-4.

Example 15-4

A long trapezoidal channel has control gates at each end. Channel physical characteristics are $L = 40,000$ ft, $S_0 = 0.00004$, $n = 0.0162$, $B = 85$ ft, and side slopes are 2 horizontal to 1 vertical. The initial flow in the channel is steady nonuniform at $11,000 \text{ ft}^3/\text{s}$. It is desired to reduce the flow to steady nonuniform flow at $6000 \text{ ft}^3/\text{s}$.

The specified information and the stroking solution are shown in the *xt* diagram of Fig. 15-10. A direct way to consider the stroking solution in this example is to view the analysis as two separate problems, one in the upstream half of the channel with conditions specified at the right end, and the other in the downstream half with identical conditions specified at the left end. The specified values at the common midpoint are: The depth remains constant at 24.5 ft, and the flow is reduced linearly from 11,000 ft³/s to 6000 ft³/s. The constant depth at the midpoint assures an approximate constant volume in the reach. For these specified conditions at the midpoint and a specified duration, there exists a unique solution for the corresponding boundary variations at each channel end.

Figure 15-11a presents one possible solution with a duration of transient of about 70 min. The initial and final water-surface profiles are shown in Fig. 15-11b. Examination of Fig. 15-10 shows that simultaneous gate operation could be achieved by shifting the specified conditions line to the right of the channel midpoint at the beginning of the transient and to the left of the channel midpoint at the end.

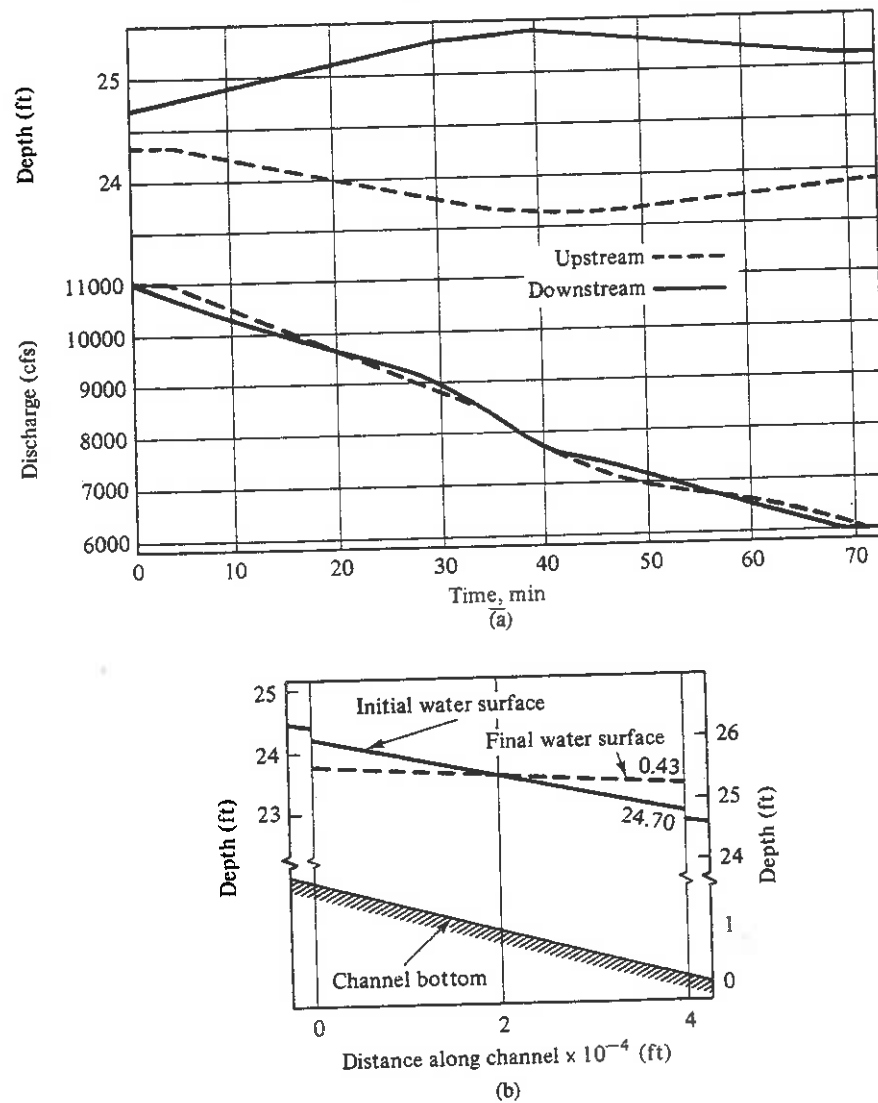


Figure 15-11 Example 15-4, transient conditions in channel.

Gate stroking in a series system of channels and control structures can be visualized by referring to Fig. 15-12. In Fig. 15-12b, the xt diagram for the entire system is shown. Initial conditions are specified below the bottom dashed line and final conditions are desired above the top dashed line. By specifying the depth as a function of time from 1 to 4 at the upstream side of gate A the shaded areas can be calculated; then by specifying the flow as a function of time between points 2 and 3 the gate stroking

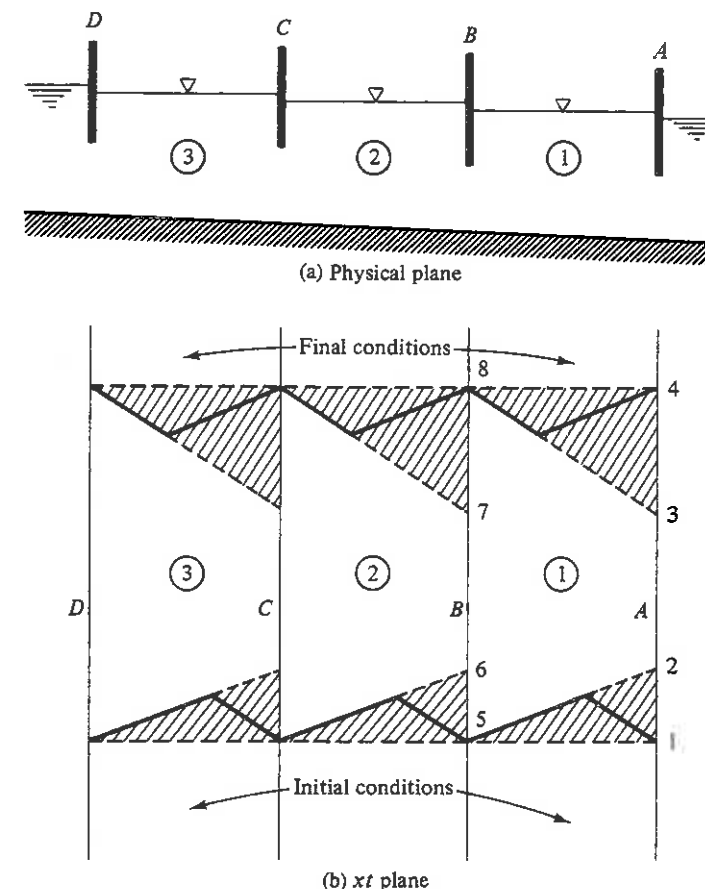


Figure 15-12 Gate stroking in series system.

calculation can be carried out in channel 1 to yield the flow rate at gate B and the depth at the downstream side of the gate. The shaded areas in channel 2 can now be calculated utilizing the known downstream flow variation. This yields the water surface elevation at the upstream side of the gate in regions 5 to 6 and 7 to 8. By specifying the depth variation between 6 and 7, the gate stroking calculation can be completed in channel 2. The same procedure is repeated in channel 3. At the completion of these calculations the discharge at each gate is known as a function of time, as is the depth on each side of each gate. Thus the actual gate position as a function of time can be prescribed to accomplish the desired flow alteration in the system.

The opportunity to impose operating constraints on the system, such as rate of change of depth, is clearly possible. Numerous options are available for specification of variables to yield an optimum operating sequence in complex systems.

Problems

- 15-1. When a unit width of a wide horizontal frictionless channel is considered, the compatibility equations can be written

$$\frac{d(V \pm 2c)}{dt} = 0$$

An estuary level, initially the same as the river outlet level of 1.5 m, drops at a rate of 0.3 m/h for 2 h. The initial velocity is 1 m/s. Neglect the bottom slope and friction and consider a unit width.

- (a) One-half hour after the river level begins to fall, how far upstream will the river level just begin to fall?
 (b) When the river outlet has dropped by 0.6 m what is the velocity at the outlet?
 (c) Determine how long it takes the river level to fall by 0.6 m at a section 1 km upstream from the mouth.

- 15-2. A rectangular channel 20 ft wide and 6 ft deep discharges 2000 ft³/s. The flow is completely stopped by a sudden closure of an upstream gate. Neglect friction and the bottom slope. Determine the depth downstream from the gate after it closes.

- 15-3. A long horizontal frictionless channel is at rest at a depth of 5 m initially. At time zero the depth at the downstream end is lowered linearly to 4 m in 60 s.
 (a) At $t = 40$ s, what is the flow at the downstream end?
 (b) At $t = 40$ s, identify the location where the depth is (i) 5.0 m and (ii) 4.5 m.

- 15-4. The depth of flow at the downstream end of a triangular channel is suddenly reduced from 1.22 m to 1.0 m by opening a gate. The initial conditions in the frictionless horizontal channel are $y_0 = 1.22$ m and $V_0 = 0.61$ m/s. The side slopes of the channel are 1 horizontal to 1 vertical, with $z = 1$.

$$A = zy^2 \quad T = 2zy \quad c = \sqrt{\frac{gy}{2}}$$

- (a) Find the velocity in the channel at the gate after the change has been made.
 (b) Find the location of the disturbed region in the channel 3 min after the adjustment.
 (c) What is the depth and velocity 15 m upstream from the gate 3 min after the adjustment?

- 15-5. A long, horizontal, rectangular, frictionless channel carries a flow of 30 m³/s at a depth of 3 m. The bottom width is 6.1 m. At an intermediate section a flow of 17 m³/s is suddenly withdrawn (and continues to be withdrawn). Visualize withdrawal from a slot in the bottom of the channel. Use the energy equation across the slot and neglect the kinetic energy.

- (a) What is the depth of flow at this section following initiation of this transient?
 (b) What is the flow just upstream from this section?
 (c) What is the flow just downstream from this section?

- 15-6. Develop the downstream boundary condition for Example 15-1. Establish a criterion for the condition if critical depth is reached during the discharge demand.

- 15-7. Alter the program in Example 15-1 to include the forebay size at the downstream boundary.

- 15-8. Outline the procedure to alter the flow from 11,000 to 6000 ft³/s in Example 15-4 by specifying conditions at the upstream end of the channel only. Perform the change (a) by having the downstream end start sooner and end later than upstream and (b) by having "almost simultaneous" gate motions.

References

1. M. Amein, and H. L. Chu, "Implicit Numerical Modeling of Unsteady Flows," *J. Hydraul. Div., ASCE*, Vol. 101, No. HY6, pp. 717-731, June 1975.
2. W. E. Bodley, and E. B. Wylie, "Control of Transients in Series Channel with Gates," *J. Hydraul. Div., ASCE*, Vol. 104, pp. 1395-1407, Oct. 1978.
3. R. K. Courant, K. Friedrichs, and H. Lewy, "Über die partieller differenzen-Gleichungen der mathematischen Physik," *Math. Ann.*, Vol. 100, pp. 32-74, 1928.
4. J. A. Cunge, "Rapidly Varying Flow in Power and Pumping Canals," in K. Mahmood and V. Yevjevich (eds.), *Unsteady Flow in Open Channels*, Vol. 2, Water Resources Publications, Fort Collins, Colo., pp. 539-586, 1975.
5. J. A. Cunge, F. M. Holly, and A. Verwey, *Practical Aspects in Computational Hydraulics*, Pitman, London, 1980.
6. IBM, *System/360 Scientific Subroutine Package (SSP), Version III, Programmer's Manual*, 5th ed., Publication GH20-0205-4, Aug., 1970.
7. C. Lai, "Computation of Transient Flows in Rivers and Estuaries by the Multiple Reach Implicit Method," *U.S. Geol. Survey, Prof. Paper*, 575-B, pp. 228-230, 1967.
8. C. Lai, "Numerical Modeling of Unsteady Open-Channel Flow," Chap. 3, in V. T. Chow and B. C. Yen (eds.), *Advances in Hydroscience*, Vol. 14, Academic Press, New York, pp. 161-333, 1986.
9. J. A. Liggett, and J. A. Cunge, "Numerical Methods of Solution of the Unsteady Flow Equations," in K. Mahmood and V. Yevjevich (eds.), *Unsteady Flow in Open Channels*, Vol. 1, Water Resources Publications, Fort Collins, Colo., 1975.
10. K. Mahmood, and V. Yevjevich (eds.), *Unsteady Flow in Open Channels*, Vols. 1, 2, and 3, Water Resources Publications, Fort Collins, Colo., 1975.
11. C. S. Martin, and F. G. De Fazio, "Open-Channel Surge Simulation by Digital Computer," *J. Hydraul. Div., ASCE*, Vol. 95, No. HY6, pp. 2049-2076, Nov. 1969.
12. A. Preissman, "Propagation des intumescences dans les canaux et les rivières," *Premier Congrès de l'Association Française de Calcul*, Grenoble, France, pp. 433-442, 1960.
13. F. H. Quinn, and E. B. Wylie, "Transient Analysis of the Detroit River by the Implicit Method," *Water Resources Res.*, Vol. 8, No. 6, pp. 1461-1469, Dec. 1972.
14. E. B. Wylie, "Control of Transient Free-Surface Flow," *J. Hydraul. Div., ASCE*, Vol. 95, No. HY1, pp. 347-361, Jan. 1969.
15. E. B. Wylie, "Inaccuracies in the Characteristics Method," *ASCE Proc. Computer and Physical Modeling*, Chicago, pp. 165-176, Aug. 1980.